New Oxidative Transformations towards the Synthesis of Potential Anti-Cancer Heterocyclic Quinone and Bis-Quinone Scaffolds

Darren Conboy

A thesis submitted in partial fulfilment of the requirements of Kingston University for the degree of Doctor of Philosophy

Kingston University London

Faculty of Science, Engineering and Computing

September 2020

Contents

Declaration

I declare that the work included in this thesis is my own work, except where stated otherwise, and has not been previously submitted for a degree to this or any other academic institution.

Darren Conboy

Abstract

This thesis describes new oxidative transformations towards the synthesis of nitrogen-containing heterocyclic quinones.

Chapter 1 provides a review of literature published over the past decade related to heterocyclic systems possessing a central carbocyclic ring fused onto two five-membered nitrogen-containing heterocycles, including imidazobenzimidazoles. The naming of some synthesized fused heterocyclic systems according to IUPAC rules is derived.

Chapter 2 describes the fusion of morpholine and oxetane onto benzimidazole by oxidative cyclization of 3,6-dimethoxy-2-(cycloamino)anilines using hydrogen peroxide with hydroiodic acid. The cyclization serendipitously yielded 1,4,6,9-tetramethoxyphenazine as a by-product, and reaction conditions were optimized to favour phenazine formation. Mechanisms for the HI catalysed reactions *via* a detected nitroso-intermediate are proposed for the oxidative cyclization and the unexpected intermolecular displacement of the oxazine. An aqueous solution of molecular iodine is capable of the same transformations. Oxidative demethylation gave targeted benzimidazolequinones, including without cleavage of the incorporated oxetane.

Chapter 3 reports the synthesis of spirocyclic oxetane-fused imidazobenzimidazoles. Oxone-mediated ring-closures to give imidazobenzimidazoles require acid and the functionalization of 4,6-di(cycloamino)-1,3-phenylenediamines to the anilides. This is in contrast to benzimidazole-forming oxidative cyclizations, which use 2-(cycloamino)anilines and require no acid. New evidence for *N*-oxide and nitroso-intermediates in respective imidazobenzimidazole and benzimidazole forming reactions is provided.

Chapter 4 details the synthesis of the first imidazo[4,5-*f*]benzimidazole iminoquinone, which was found to be inactive against tumour cells, in contrast to the related imidazo[5,4-*f*]benzimidazole isomer.

Chapter 5 discloses an optimized route to alicyclic ring-fused *p*-dimethoxybenzimidazole-*p*-benzimidazolequinone dimers. The dimers possess ambiphilicity, and a selective electrophilic chlorination and bromination at the electron-rich *p*-dimethoxybenzimidazole-CH using respectively NaCl and NaBr with Oxone in HFIP(aq), is described. The benign halide salt-Oxone mix can provide tunable conditions that favour molecular halogen formation allowing one-pot halogenation and quinone formation. In contrast, nucleophilic radical trifluoromethylation occurs selectively at the *p*-benzimidazolequinone-CH with the product subjected to one-pot chlorination and quinone formation.

Acknowledgements

Abbreviations

δ	chemical shift in ppm downfield from TMS
ACN	1,1'-azobis(cyclohexanecarbonitrile)
AIBN	2,2′-azobis(isobutyronitrile)
AMBER	assisted model building with energy refinement
ASAP	atmospheric solids analysis probe
ATR	universal attenuated total reflectance
BINOL	1,1'-bi-2-naphthol
BODIPY	boron-dipyrromethene
br	broad
CAN	cerium(IV) ammonium nitrate
CCDC	Cambridge Crystallographic Data Centre
CL_{int}	intrinsic clearance
CNS	central nervous system
CTAB	cetyltrimethylammonium bromide
CYP450	cytochrome c P450 reductase
d	doublet
DABCO	1,4-diazabicyclo[2.2.2]octane
DBU	1,8-diazabicyclo[5.4.0]undec-7-ene
DCE	1,2-dichloroethane
dd	doublet of doublets
DDQ	2,3-dichloro-5,6-dicyano-1,4-benzoquinone
DEPT	distortionless enhancement by polarization transfer
DMA	dimethylacetamide

DME	dimethyl ether
DMU	dimethyl urea
DTP	Developmental Therapeutics Program
EDG	electron-donating group
EGFR	endothelial growth factor receptor
EI	electron impact
ESI	electrospray ionization
EWG	electron-withdrawing group
FA	Fanconi anaemia
FAAH	fatty acid amide hydrolase
Fc	ferrocene
gem-	*geminal-*
HAS	homolytic aromatic substitution
HDDA	hexadehydro-Diels-Alder
HFIP	hexafluoroisopropanol
His	histidine
HIV	human immunodeficiency virus
HLM	human liver microsomes
hν	light
HRMS	high resolution mass spectrometry
HTIB	hydroxy(tosyloxy)iodobenzene
J	coupling constant
lit	literature
m	multiplet

m-	*meta-*
MAO	monoamine oxidase
m-CPBA	*m*-chloroperoxybenzoic acid
MHz	megahertz
MLM	mouse liver microsomes
μM	micromolar
mM	millimolar
MMC	mitomycin C
M_n	number average molecular weight
MS	mass spectrometry
Ms	methanesulfonyl
MW	microwave
m/z	mass-to-charge ratio
NBDTB	*N*-benzyl DABCO tribromide
NBS	*N*-bromosuccinimide
NCI	National Cancer Institute
NHC	*N*-heterocyclic carbene
NOESY	nuclear overhauser effect spectroscopy
NQO1	NAD(P)H:quinone oxidoreductase 1
NSI	nanospray ionization
o-	*ortho-*
p-	*para-*
PBI	pyrrolo[1,2-*a*]benzimidazolequinone
PDI	polydispersity index

pet.	petroleum
PG	protecting group
PIFA	phenyliodine(III) bis(trifluoroacetate)
PK	pharmacokinetic
PPA	polyphosphoric acid
Py	pyridine
R_f	retention factor
ROS	reactive oxygen species
rt	room temperature
RVC	reticulated vitreous carbon
s	singlet
SAXS	small angle X-ray scattering
S_EAr	electrophilic aromatic substitution
sec	second
SET	single electron transfer
S_NAr	nucleophilic aromatic substitution
SOMO	singly occupied molecular orbital
t	triplet
TBAF	tetrabutylammonium fluoride
TCI	Tokyo Chemical Industry
TD-DFT	time-dependant density functional theory
tert-	*tertiary-*
Tf	triflyl
TFA	trifluoroacetic acid

TFAA	trifluoroacetic anhydride
TFE	trifluoroethanol
THC	tetrahydro-β-carboline
THIQ	tetrahydroisoquinoline
TLC	thin layer chromatography
TOFMS	time-of-flight mass spectrometry
Tol	toluene
Trx	thioredoxin
TrxR	thioredoxin reductase

Index of Novel Compounds Prepared

Chapter 2

p 68

4b, p 68

p 80

12b, p 80

5a, p 70

5b, p 70
CCDC no. 1917885, p 71

6, p 70

4f, p 74
CCDC no. 1917886, p 75

5f, p 80

13b, p 80

1, p 81

2, p 81
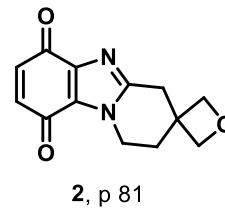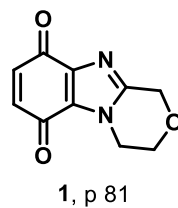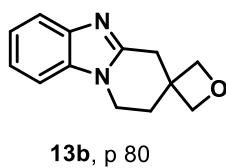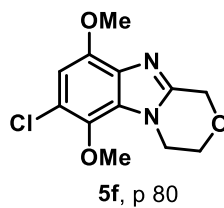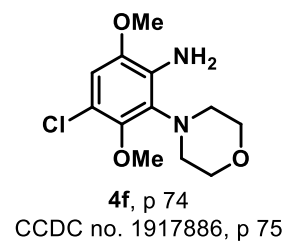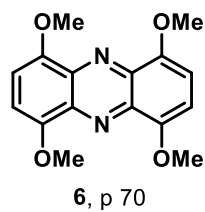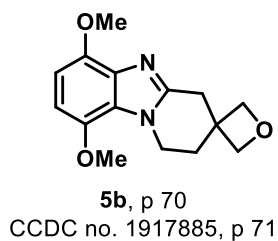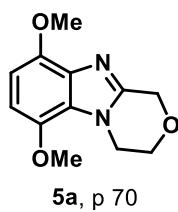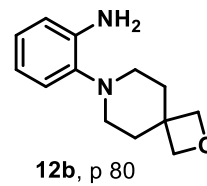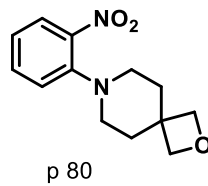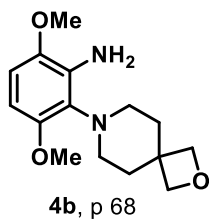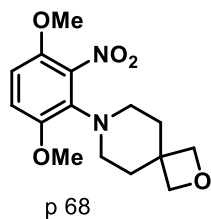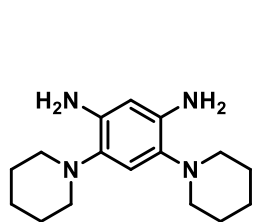
Chapter 3

5, p 115
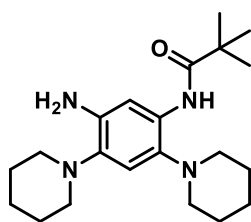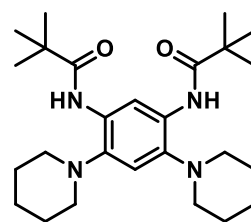
8, p 115

9, p 115
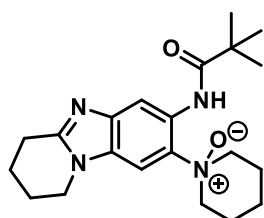
10, p 116
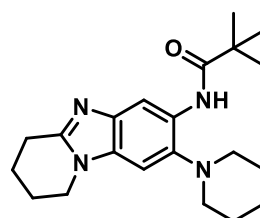
11, p 116
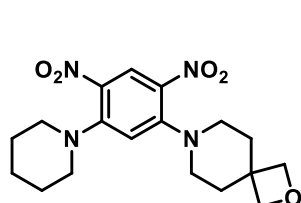
17, p 119
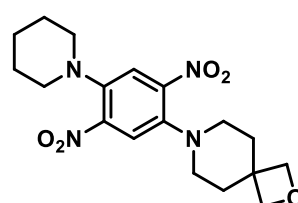
20, p 119
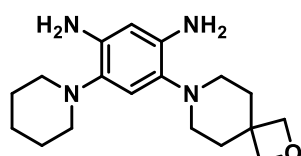
18, p 119
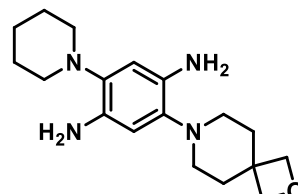
21, p 119
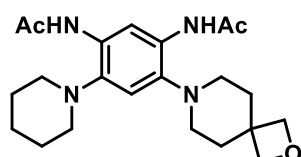
19, p 119
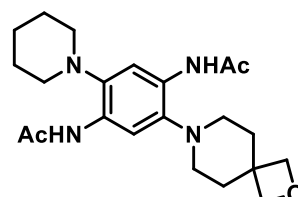
22, p 119
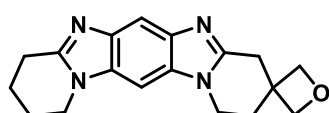
6, p 119
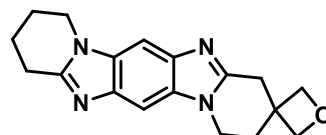
7, p 119

Chapter 4
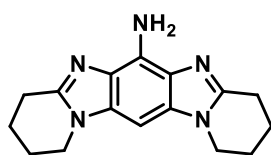
8, p 140
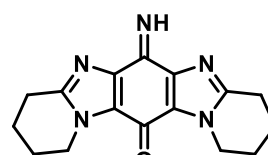
5, p 142
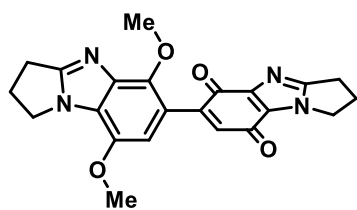
5a, p 175
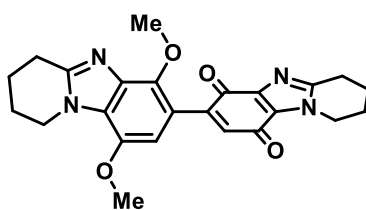
5b, p 178
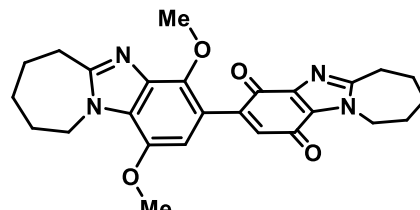
5c, p 178
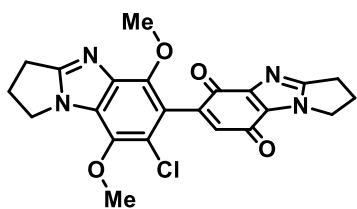
8a, p 180
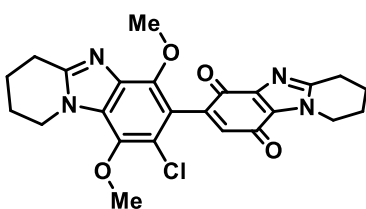
8b, p 184
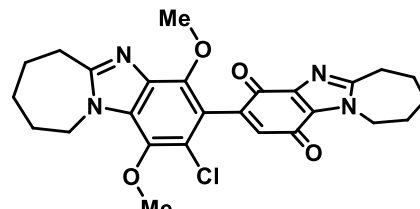
8c, p 184
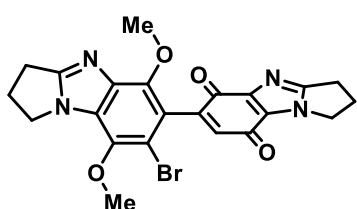
10a, p 184
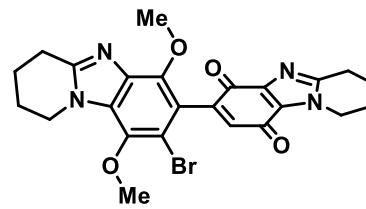
10b, p 184
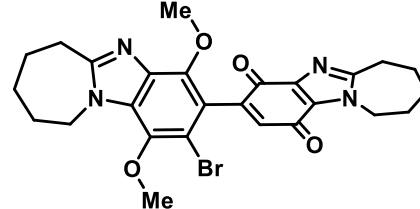
10c, p 184
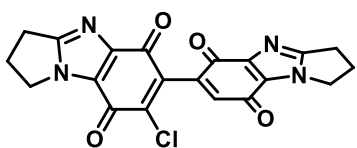
9a, p 184
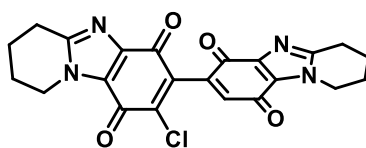
9b, p 184
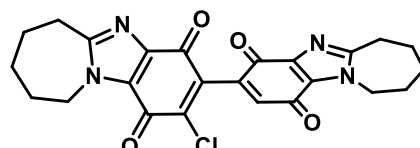
9c, p 184
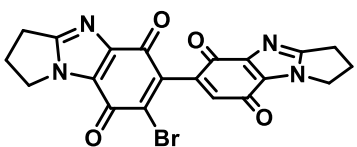
11a, p 184
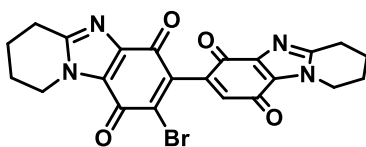
11b, p 184
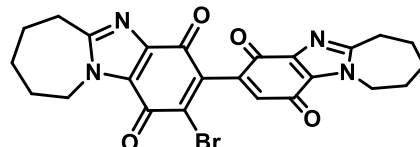
11c, p 184
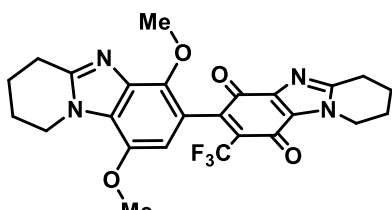
12, p189
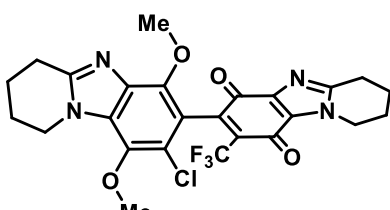
13, p 189
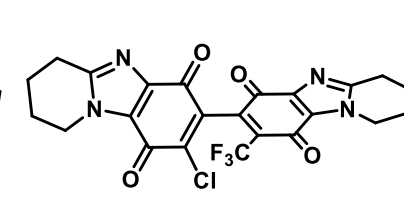
14, p 189

Chapter 1

A Review of the Literature

Tricyclic Heterocyclic Systems: Central 6-Membered Carbocyclic Ring Fused to 5-Membered Heterocycles

Parts of this Chapter are to be published in:

1.1. Central 6-Membered Carbocyclic Ring-Fused onto Two Nitrogen-Containing 5-Membered Heterocycles

1.1.1. Introduction

Tricyclic heterocyclic scaffolds possessing a central 6-membered carbocyclic ring fused onto two 5-membered nitrogen-containing heterocycles are prevalent in medicinal and materials chemistry.[1-4] Imidazobenzimidazoles are a commonly-encountered example, which comprise the core of antitumour bioreductive prodrugs prepared in Chapters 3 and 4 of this thesis. This Chapter reviews literature published in recent years on tricyclic scaffolds containing a central 6-membered carbocyclic ring with fused five-membered nitrogen-containing heterocycles. The heterocycles presented herein vary in the relative orientation of the fused five-membered heterocyclic rings, and are arranged according to the number of heteroatoms in each ring. Sections detail the theoretical and experimental characterization methods, reactions of the heterocyclic systems, methods for their synthesis, and applications. There are numerous reviews published in recent years on certain compound classes in this field, including Hsu's 2015 review on donor-acceptor polymers for organic solar cells,[2] the 2016 review by Hou and co-workers of benzodithiophenes as organic photovoltaic materials,[3] and Bergman's 2018 review on indolocarbazoles.[4]

1.1.2. Theoretical and Experimental Structural Methods

Density functional theory (DFT) was used to provide a mechanistic rationale for the Diels-Alder reaction giving benzodifuroxan systems.[5] 4-Nitrobenzodifuroxan is a weak aromatic, and is considered superelectrophilic with reactivity akin to nitro olefins. The reported ease with which the benzodifuroxan undergoes stepwise Diels-Alder reaction with Danishefsky's diene can be rationalised by initial Michael addition of highly electron-rich diene onto the electrophilic C-5 position (Figure 1.1).
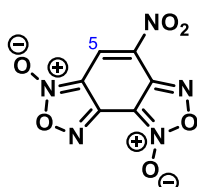
Figure 1.1. 4-Nitrobenzodifuroxan.

AMBER99 molecular mechanics force field24 was used to obtain geometry minimized enzyme-ligand interactions for alicyclic ring-fused imidazo[5,4-*f*]benzimidazole **1** with NAD(P)H:quinone oxidoreductase 1 (NQO1) (Figure 1.2).[6]

Figure 1.2. Imidazobenzimidazole NQO1 substrate.

The X-ray crystal structure of benzoquino-bis-1,2,3-dithiazole revealed sheet-like (or "brick wall") packing, which is optimal for 2D electronic interactions in organic semiconductors (Figure 1.3).[7] Benzoquino-bis-1,2,3-dithiazole is antiaromatic, resulting from its 16π-electron core. The benzoquinone bridge reduces the HOMO-LUMO separation giving ideal semiconductor properties.

Figure 1.3. Antiaromatic benzoquino-bis-1,2,3-dithiazole.

Pyrrolo[3,2-*f*]indole diradical **5** was expected to be more stable than diradical **4** (Figure 1.4), due to the greater steric shielding provided by the benzylic methyl groups, however analysis by EPR spectroscopy indicated that **5** was significantly less persistent than **4**.[8] The decrease in stability was due to the tendency of dimethyl analogue **5** to undergo intramolecular hydrogen-atom abstraction.

Figure 1.4. Pyrroloindole diradicals.

1.1.3. Reactions

1.1.3.1.   Compounds with one heteroatom in each heterocyclic ring

The condensation of pyrrolo[3,2-*e*]indole-4,5-diones with 1,2-diaminobenzene derivatives did not proceed under traditional Brønsted acid-catalysis due to the high electron-density of the tricyclic system, and necessitated the use of BF$_3$•OEt$_2$ in hexafluoroisopropanol (HFIP) under microwave irradiation (Scheme 1.1).[9]

R^1 = H, R^2 = H (23%)
R^1 = H, R^2 = Me (77%)
R^1 = Me, R^2 = Me (43%)
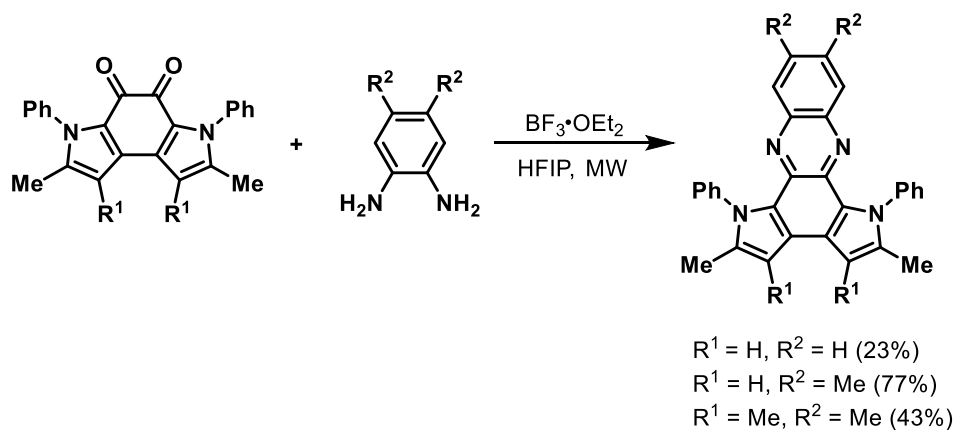
Scheme 1.1. Reaction of pyrroloindole dione with diamines.

Zhu and co-workers utilized B ← N coordinate bonds using either BF$_3$ or BPh$_2$Cl for fine-tuning redox and electrochromic properties of ladder-type molecules consisting of an oxidation-active indolo[3,2-*b*]carbazole core and two reduction-active benzo[*d*]thiazole units (Scheme 1.2).[10]
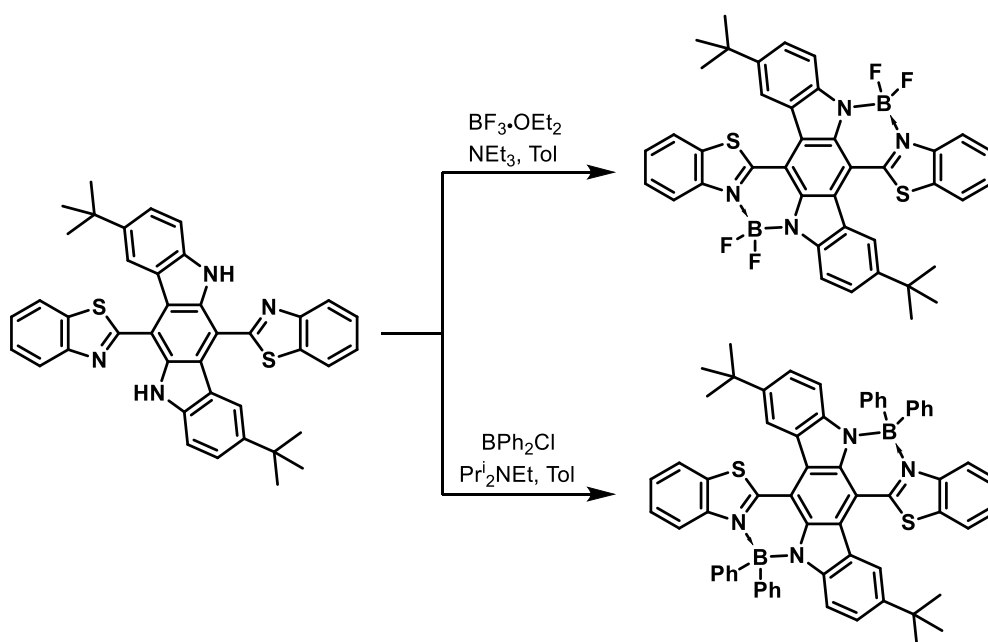
Scheme 1.2. Installing B ← N coordinate bonds.

Reductive cleavage of one or both of the fluoroalkylsulfanyl groups on pyrrolo[2,3-*f*]indole was achieved by varying the equivalents of SmI$_2$ (Scheme 1.3).[11]

R^1 = CH$_2$(CH$_2$)$_5$CH$_3$
R^2 = CH$_2$(CF$_2$)$_7$CF$_3$
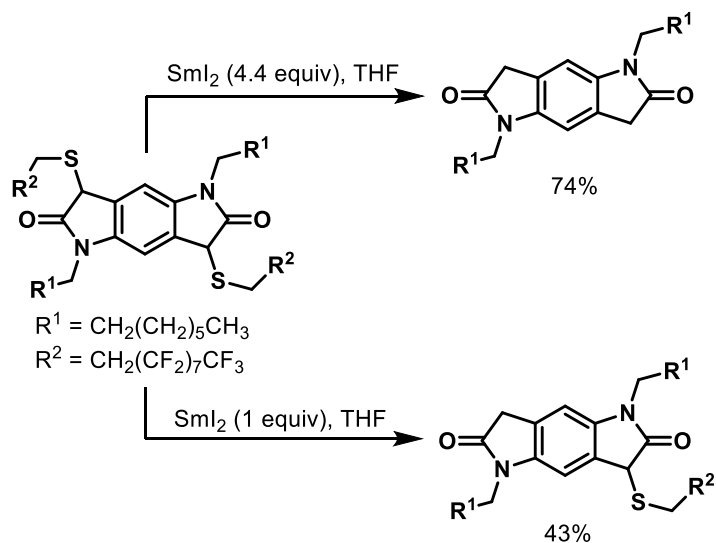
Scheme 1.3. Reductive cleavage of fluoroalkylsulfanyl groups.

1.1.3.2.   Compounds with three heteroatoms arranged 1:2

The dehydrogenation of [1,3]dioxolo[4,5-*f*]indole was achieved using potassium *tert*-butoxide to give the indole (Scheme 1.4).[12] Reduction of a racemic mixture of the 3-ketoindole with Ru-complex occurred stereoselectively to give the 2*R*,3*S*-*cis*-diastereoisomer in excellent yield.[13]

86%

83% yield
>99% ee
>99:1 dr

p-cymene
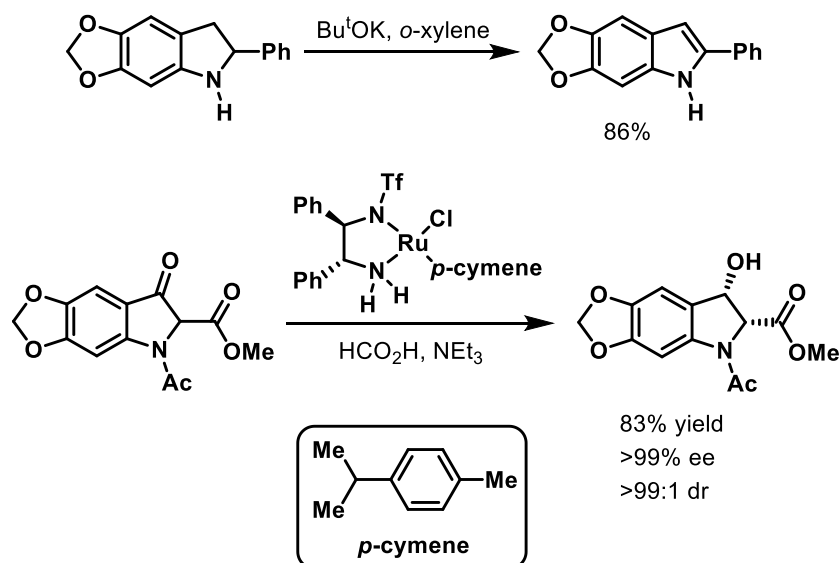
Scheme 1.4. Reactions of [1,3]dioxolo[4,5-*f*]indole.

5

1.1.3.3.   Compounds with four heteroatoms arranged 2:2

Imidazobenzimidazole underwent facile deprotonation to give fluorescent salts (Scheme 1.5).[14] The emission wavelength of the salts is tuneable between 329 and 561 nm by varying the R-group and counterion (X⁻). Reaction of the salts with transition metal complexes yields polymeric *N*-heterocyclic carbene (NHC) heterogeneous catalysts, which have a range of applications including in Suzuki couplings,[15,16] methylation of anilines,[17] and reductive aminations.[18]
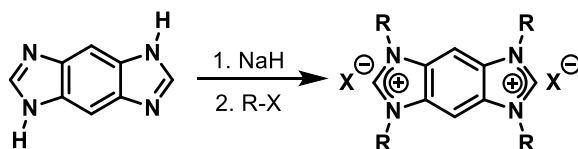
Scheme 1.5. Deprotonation of imidazobenzimidazole to yield tuneable fluorescent salts.

Imidazo[4,5-*f*]benzimidazoles undergo Cu-mediated oxidative polymerization (Scheme 1.6).[19] The M_n and PDI varied greatly depending on the substituents at both imidazole nitrogens with better control (lower polydispersity index (PDI)) achieved upon increasing the length of the *N*-alkyl chain. All polymers had high fluorescence quantum yields with emission spectra in the blue-light region.

63-85% yield
M_n = 22500-44500
PDI = 1.32-2.09
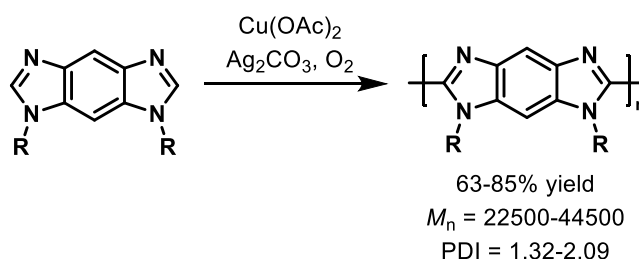
Scheme 1.6. Oxidative polymerization of imidazo[4,5-*f*]benzimidazoles.

Imidazobenzimidazolequinone salts underwent silver-catalyzed retro-Claisen reaction with various alcohols to give the 4-ester-substituted imidazolium salts in near-quantitative yields (Scheme 1.7).[20]

yields >98%
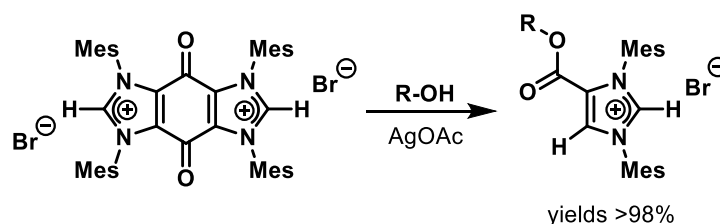
Scheme 1.7. Retro-Claisen reaction of imidazobenzimidazolequinone.

6

Iminoquinones with the diimidazoquinoxaline scaffold based on the natural product Wakayin were synthesized by Frémy oxidation of an imidazobenzimidazole with secondary amine substituent (Scheme 1.8).[21]
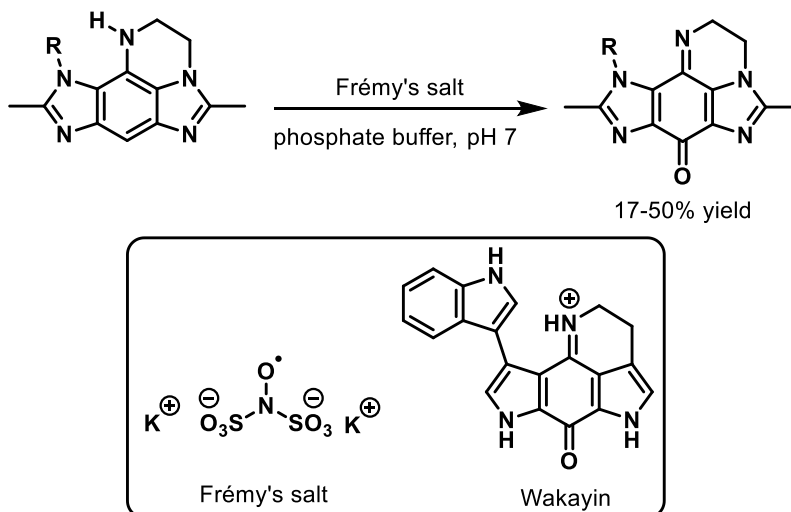
Scheme 1.8. Frémy oxidation to yield Wakayin analogues.

Direct arylation of unsubstituted benzo[1,2-*d*;4,5-*d'*]bisthiazole with various aryl bromides was achieved using a palladium and copper co-catalyst system.[22] Pentafluoroiodobenzene was used for iodination at the same position using SET from potassium *tert*-butoxide (Scheme 1.9).[23]
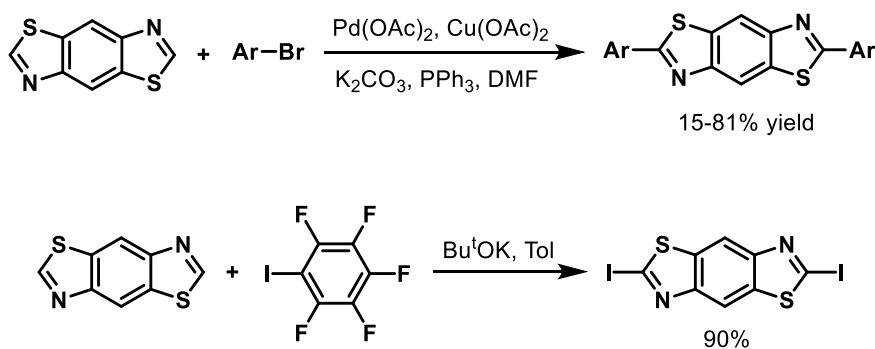
Scheme 1.9. Regioselective arylation and iodination of benzobisthiazole.

1.1.3.4. Compounds with more than four heteroatoms

Benzo[1,2-*d*:3,4-*d'*:5,6-*d''*]tris[1,2,3]triazole underwent complete nitration to yield a highly shock-sensitive explosive (Scheme 1.10).[24] Reaction of the unsubstituted triazole with sodium hypochlorite gave the fully chlorinated derivative, which found application in the oxidation of

alcohols to ketones or aldehydes. It was, however, limited by a lack of solubility in many organic solvents, and ignited spontaneously on contact with DMSO and various amines.
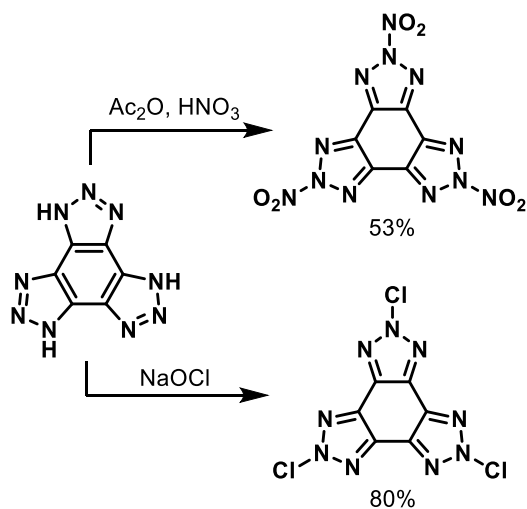
Scheme 1.10. Nitration and chlorination of benzotris[1,2,3]triazole.

The Diels-Alder reaction of 4-nitrobenzodifuroxan with the electron-rich (*E*)-1-methoxy-3-trimethylsilyloxy-buta-1,3-diene (Danishefsky's diene) proceeded in a stepwise manner with initial Michael addition of the diene onto the benzodifuroxan (Scheme 1.11).[5] The zwitterionic intermediate **6** subsequently underwent ring-closure to give a 1:1 mixture of the *exo-* and *endo-*cycloadducts. NMR analysis indicated a gradual disappearance in the signals belonging to the *exo*-diastereomer, and concomitant increase in the *endo*-peaks. The latter underwent slow decomposition to give the stable carbonyl-containing cycloadduct **7**.
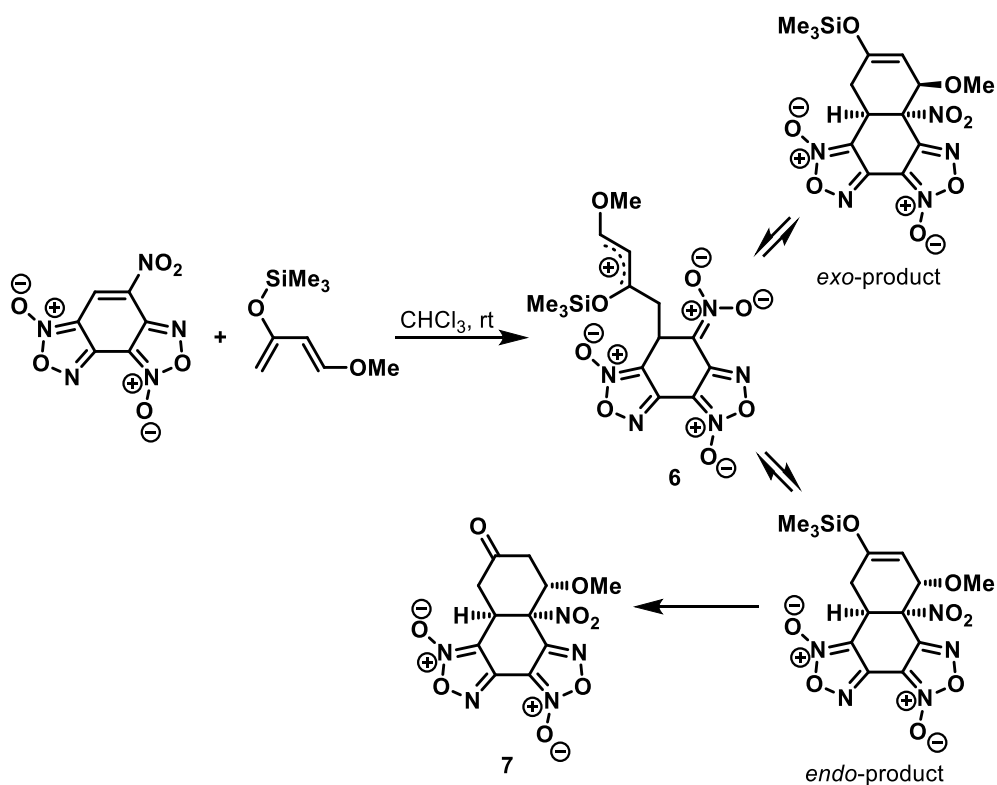
Scheme 1.11. Stepwise Diels-Alder reaction of 4-nitrobenzodifuroxan.

The reaction of [1,3]dithiolo[4,5-*f*]benzothiadiazol-6-imine with dimethyl but-2-ynedioate resulted in ring expansion to the [1,4]dithiino[2,3-*f*]benzothiadiazole (Scheme 1.12).[25] Tetrathiafulvalene-benzothiadiazoles for organic electronics were prepared using a triethyl phosphate mediated coupling of [1,3]dithiolo[4,5-*f*]-2,1,3-benzothiadiazol-6-one with 1,3-dithiole-2-thiones.[26]
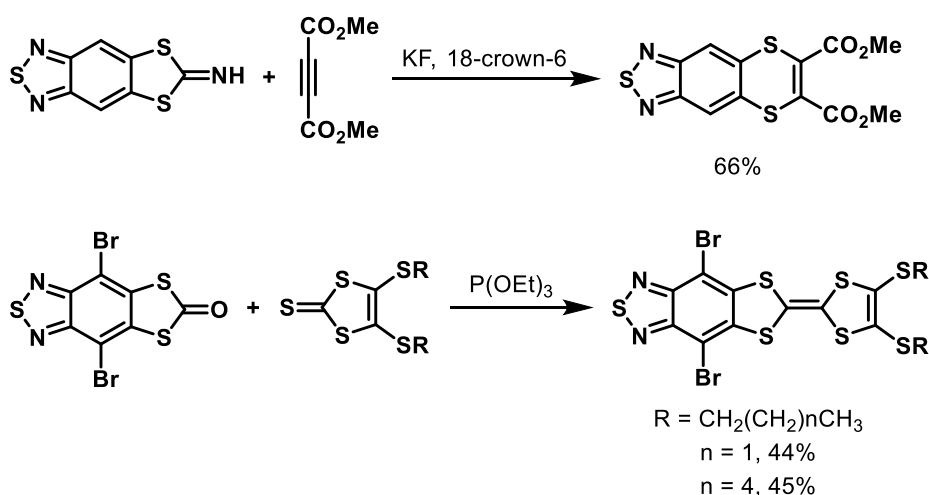
Scheme 1.12. Ring-expansion and coupling of [1,3]dithiolobenzothiadiazole derivatives.

Benzo[1,2-*c*:3,4-*c'*]bis[1,2,5]thiadiazole is photochromic, and exists in the colourless "open form" in the presence of visible-light (Scheme 1.13).[27] Irradiation of with UV-light induces [4+2] cycloaddition to yield the brown "closed form". The reaction is reversible, with the "open form" regenerated on re-exposure to visible-light.

$$\text{open form} \quad \xrightleftharpoons[\text{Vis-light}]{\text{UV-light}} \quad \text{closed form}$$
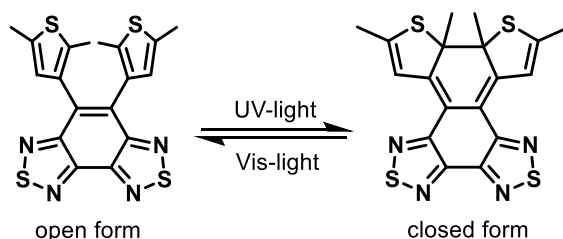
Scheme 1.13. Photochromic benzobis[1,2,5]thiadiazole.

The combination of Br_2 and HBr mediated the regioselective bromination of benzo[1,2-*c*:3,4-*c'*]bis[1,2,5]thiadiazole, and oxidation to the *o*-quinone derivative was mediated by HNO_3 with H_2SO_4 (Scheme 1.14).[28]
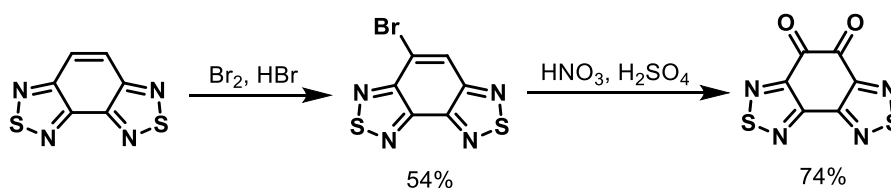
Scheme 1.14. Bromination and oxidation of benzobis[1,2,5]thiadiazole.

Reduction of benzo[1,2-*d*:3,4-*d'*]bis([1,2,3]dithiazolium) dichloride with triphenylstibine generated the 1,2,3-benzodithiazolyl (Herz) radical *in situ*, which underwent dimerization with elimination of sulfur to give bis(dithiazolo)phenazine and dibenzothiadiazepine in respective yields of 42 and 9% (Scheme 1.15).[29]
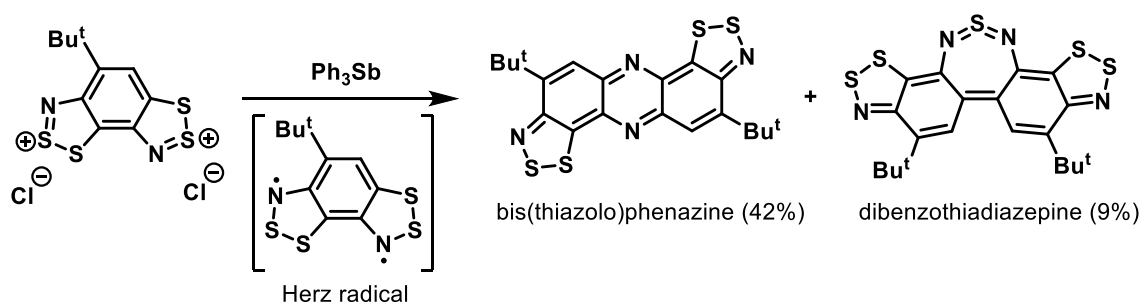
Scheme 1.15. Reductive dimerization of benzobis([1,2,3]dithiazolium) salt.

1.1.4. Synthesis

1.1.4.1. Compounds with one heteroatom in each heterocyclic ring

The hexadehydro-Diels-Alder (HDDA) reaction was popularised by Woods and co-workers as a means of constructing tricyclic scaffolds with a central benzene ring.[30] The HDDA reaction involves initial [4+2] cycloaddition of a 1,3-diyne with an alkyne diynophile to generate a benzyne intermediate, which is trapped intramolecularly with a pendant nucleophile to complete the tricycle (Scheme 1.16). The benzyne can alternatively be trapped by an external diene such as furan to furnish the tricycle.[31]
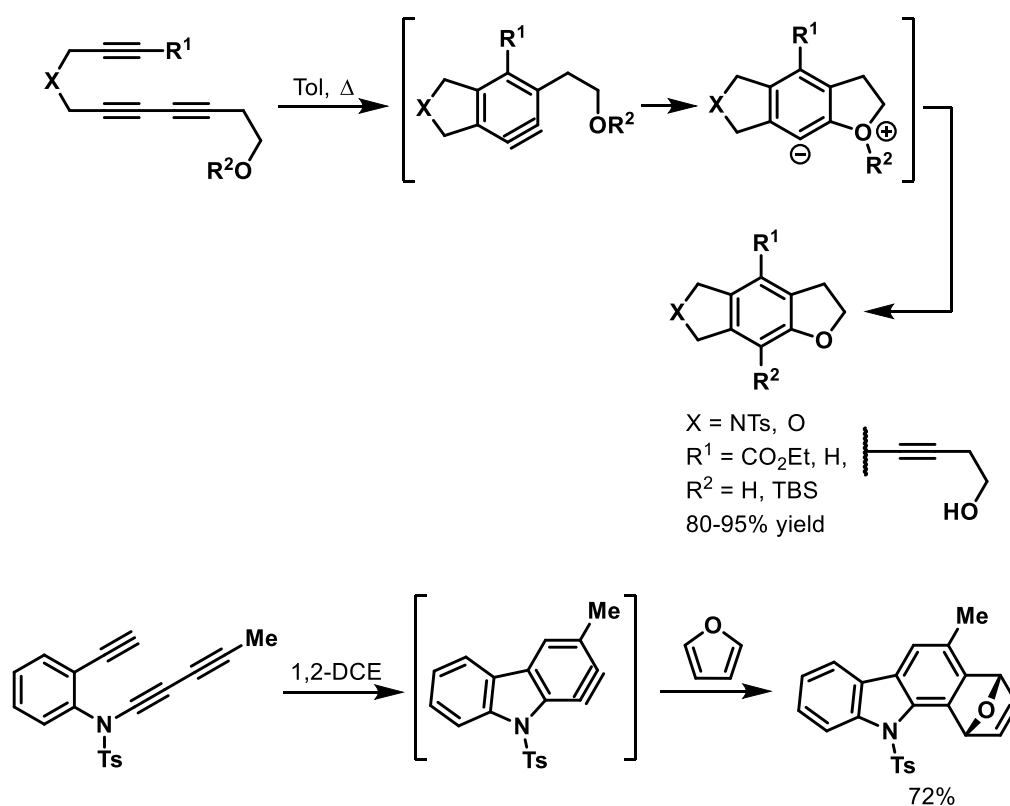
Scheme 1.16. The hexadehydro Diels-Alder reaction.

Wilkinson's catalyst ([RhCl(PPh$_3$)]) induced the [2+2+2] cyclotrimerization of three contiguous alkynes in 25-membered macrocycle to form the benzodipyrrole (Scheme 1.17).[32]
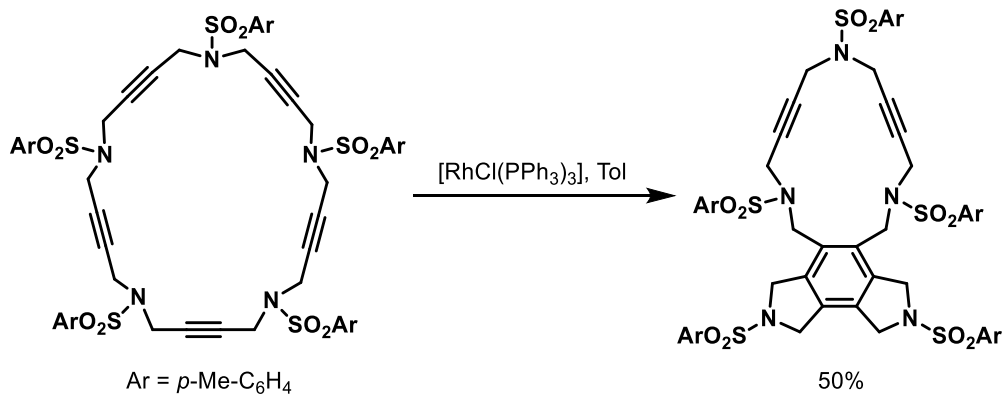
Scheme 1.17. [2+2+2] Cycloaddition to yield benzodipyrrole macrocycle.

A copper-catalyzed formal [2+2+2] cyclization between oximes and maleimides provided access to the benzene ring of fused phthalimides (Scheme 1.18).[33]
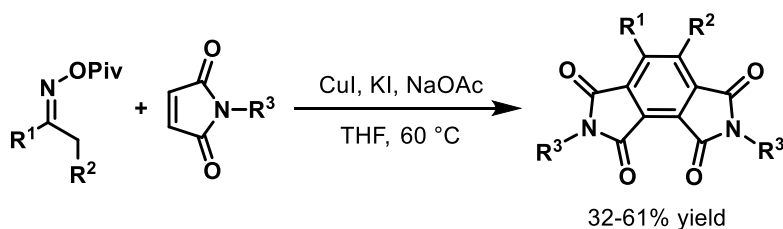
Scheme 1.18. Construction of benzene-fused phthalimides by [2+2+2] cycloaddition.

Pyrrole-fused indoles were obtained *via* copper-catalyzed intramolecular Mannich-type reactions (Scheme 1.19).[34]
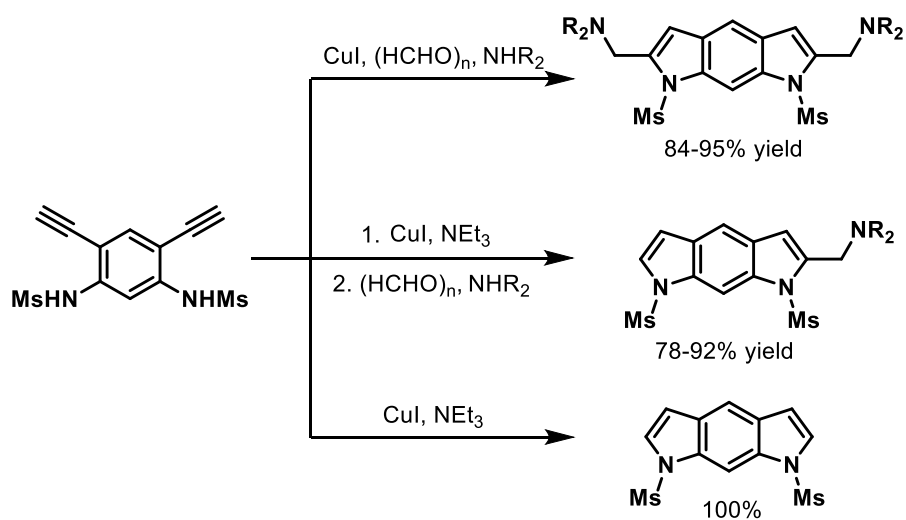
Scheme 1.19. Mannich-reactions towards pyrroloindoles.

Treatment of bis(indolyl)methanes with triethylorthoformate and a catalytic amount of iodine furnished indolo[2,3-*b*]carbazoles (Scheme 1.20).[35] A pyrrole-ring was fused to give pyrrolo[2,3-*b*]carbazoles *via* the CuI and base-mediated reaction of carbazole-2-bromoaldehydes with isocyanoacetates.[36]
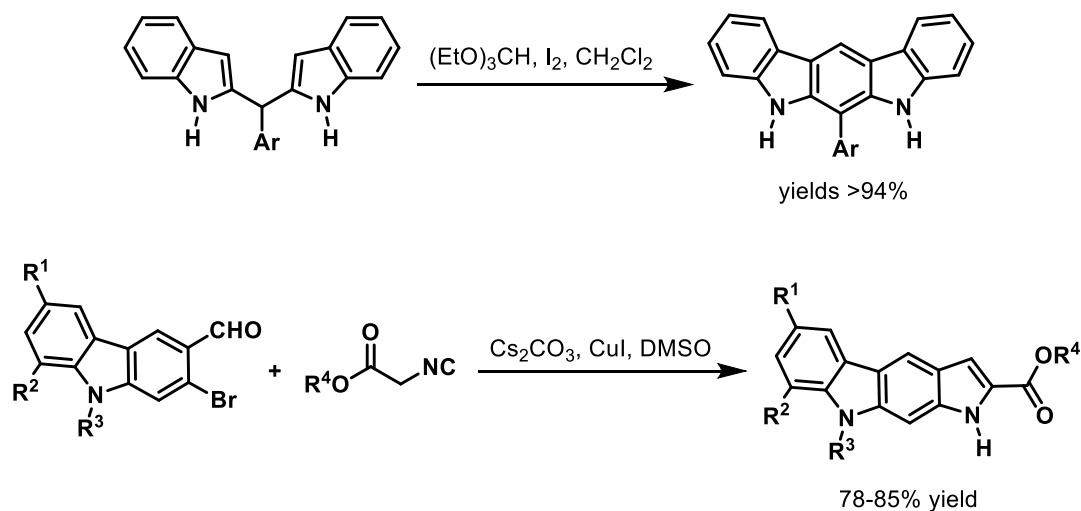
Scheme 1.20. Indolocarbazole synthesis.

Diphenylphosphoric acid catalyzed the benzannulation of (*E*)-2-(2-nitrostyryl)-1*H*-indole with various ketones and aldehydes (Scheme 1.21).[37] Decalin was added to allow the oxidative 6π-electrocyclization to be carried out at 130 °C, while triethyl phosphite reduced the nitro group to a nitroso, facilitating the Cadogan cyclization to construct the pyrrole ring.
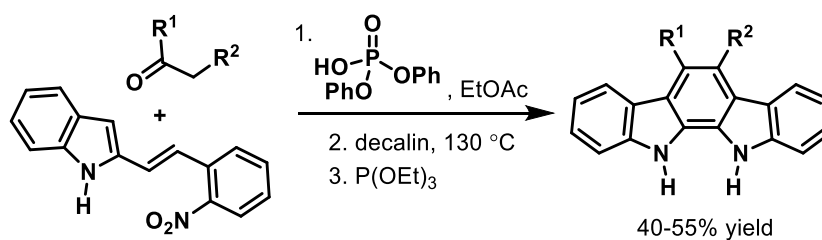
Scheme 1.21. Benzannulation strategy towards indolocarbazole.

Simultaneous pyrrole ring formation in indolo[2,3-*b*]carbazole was achieved by iron-mediated double reductive cyclization of 2,2-(4,6-dinitro-1,3-phenylene)bis(3-hydroxy-5,5-dimethylcyclohex-2-enone) (Scheme 1.22).[38]

13
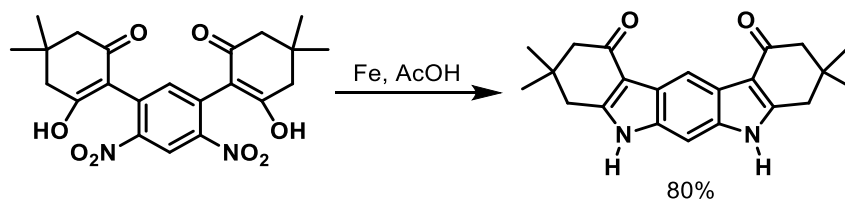
Scheme 1.22. Indolocarbazole synthesis by double reductive cyclization.

Tartaric acid-dimethyl urea (DMU) serves as the solvent and catalyst for Fischer indole synthesis,[39] giving the indolo[2,3-*b*]carbazole (when R = H in **8**) and two diastereomers of pyrazolo[4,3-*a*]carbazole (R = Me in **8**) (Scheme 1.23).[40]
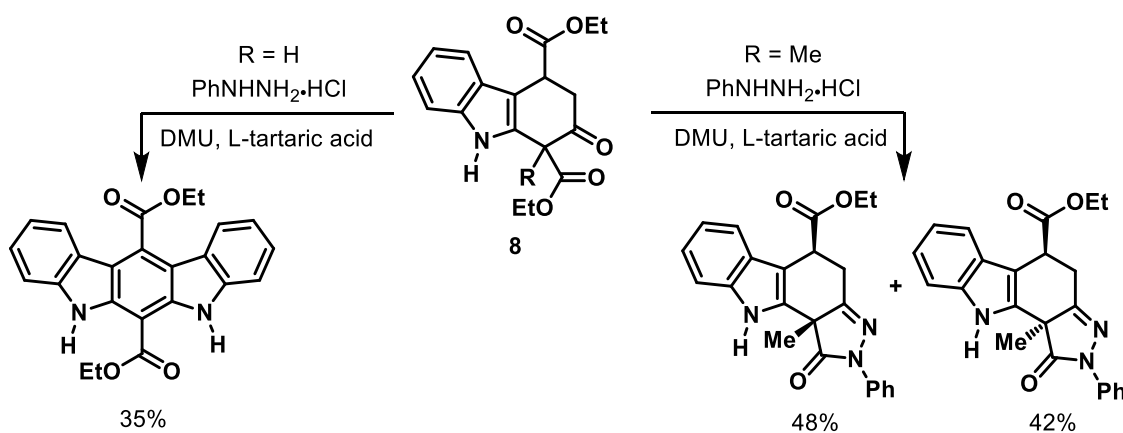
Scheme 1.23. Fischer indole synthesis.

A copper-mediated one-pot double amination, β-elimination, deprotection, and rearomatization of tetrahydroisoquinoline derivative yielded pyrrolo[3,2-*e*]indole, towards the synthesis of PDE-II, a potent DNA-alkylating natural product (Scheme 1.24).[41]
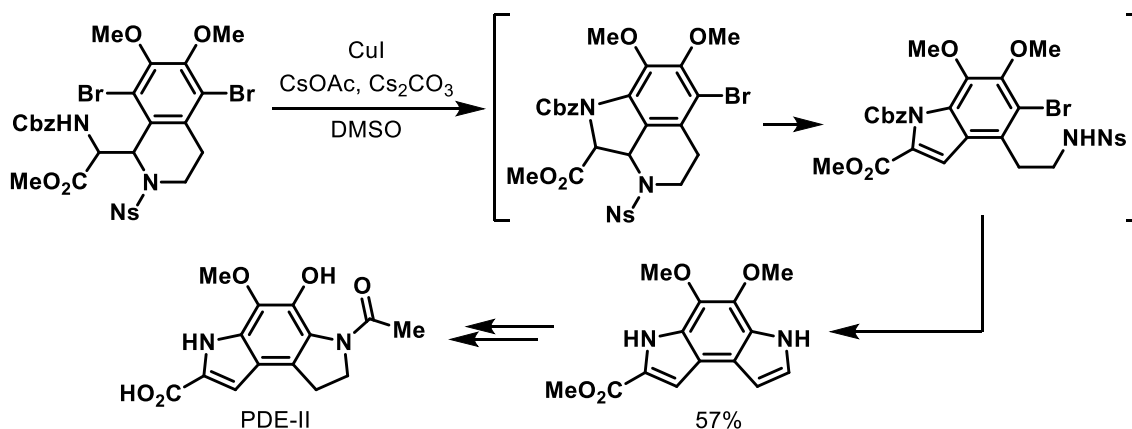
Scheme 1.24. Synthesis of the natural product PDE II.

Bispyrroles formed *in situ* are excellent nucleophiles, which react with maleic anhydride to form pyrrolo[3,2-*e*]indoles (Scheme 1.25).[42]
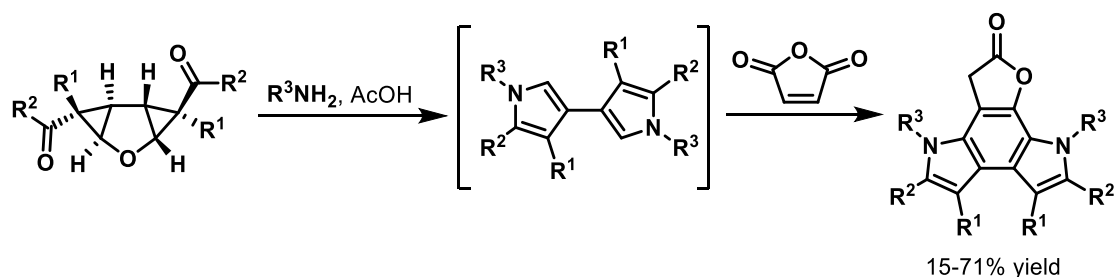
Scheme 1.25. *In situ* generated bispyrroles as nucleophiles.

A palladium-catalyzed carbonylative amidation of 1,2,4,5-tetrabromobenzene was reported to give benzo[1,2-*c*:5,4-*c'*]dipyrrole-1,3,5,7-tetrone (Scheme 1.26).[43]
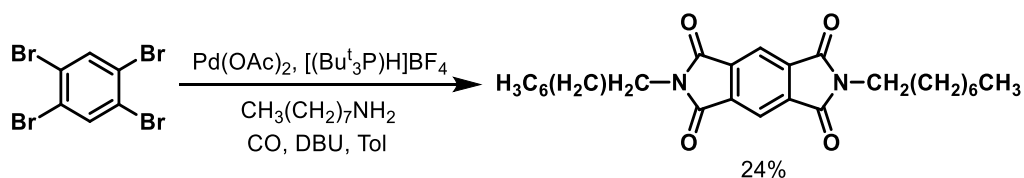
Scheme 1.26. Carbonylative amidation to yield benzodipyrrole.

A Lewis acid-mediated connective Pummerer-type reaction of thiols with bis-glyoxamides was employed to construct the lactam rings of pyrrolo[3,2-*f*]indoles (Scheme 1.27).[11]
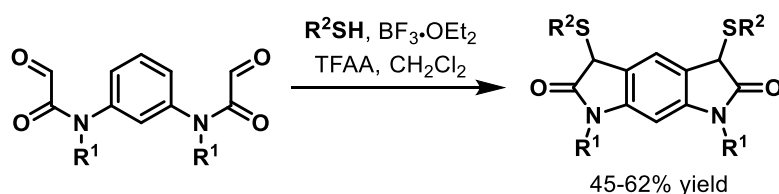
Scheme 1.27. Pyrroloindole synthesis by Pummerer-type reaction.

m-Dinitrobenzene underwent dearomatization with TFA in the presence of *N*-benzyl azomethine ylide, generated *in situ* from the reaction of silylated hemiaminal delivering benzo[1,2-*c*:3,4-*c'*]dipyrrole (Scheme 1.28).[44]

15
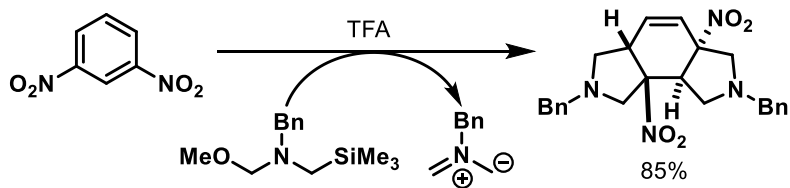
Scheme 1.28. Benzodipyrrole formation using azomethine ylide.

A nosyl-protected amine underwent one-pot Michael addition and Smiles rearrangement to give the pyrrolidine. Reduction induced further cyclization to furnish the pyrrolo[2,3-b]carbazole (Scheme 1.29).[45]

72% (for 2 steps)
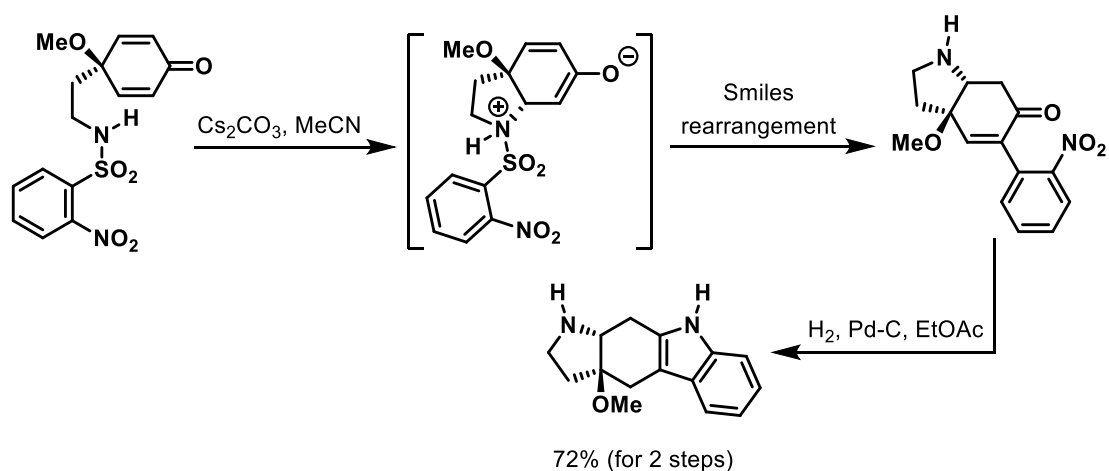
Scheme 1.29. Michael-Smiles rearrangement and reduction to generate pyrrolocarbazole.

The pyrrolo[2,3-*f*]indolequinone scaffold was accessed by reaction of 2,6-dibromobenzoquinone with methyl 3-(methylamino)crotonate (Scheme 1.30).[46] Indolequinones were condensed with β-ketoamines,[47] and ethyl acetoacetate in the presence of cerium (IV) ammonium nitrate (CAN) to fuse the pyrrole ring.[48] Coupling of the amine-substituted indolequinone with 4-hydroxyphenyl acetaldehyde diethyl acetal was the strategy employed to prepare the precursor of pyrrolo[2,3-*f*]indolequinone alkaloids zyzzyanones A-D.[49]

16
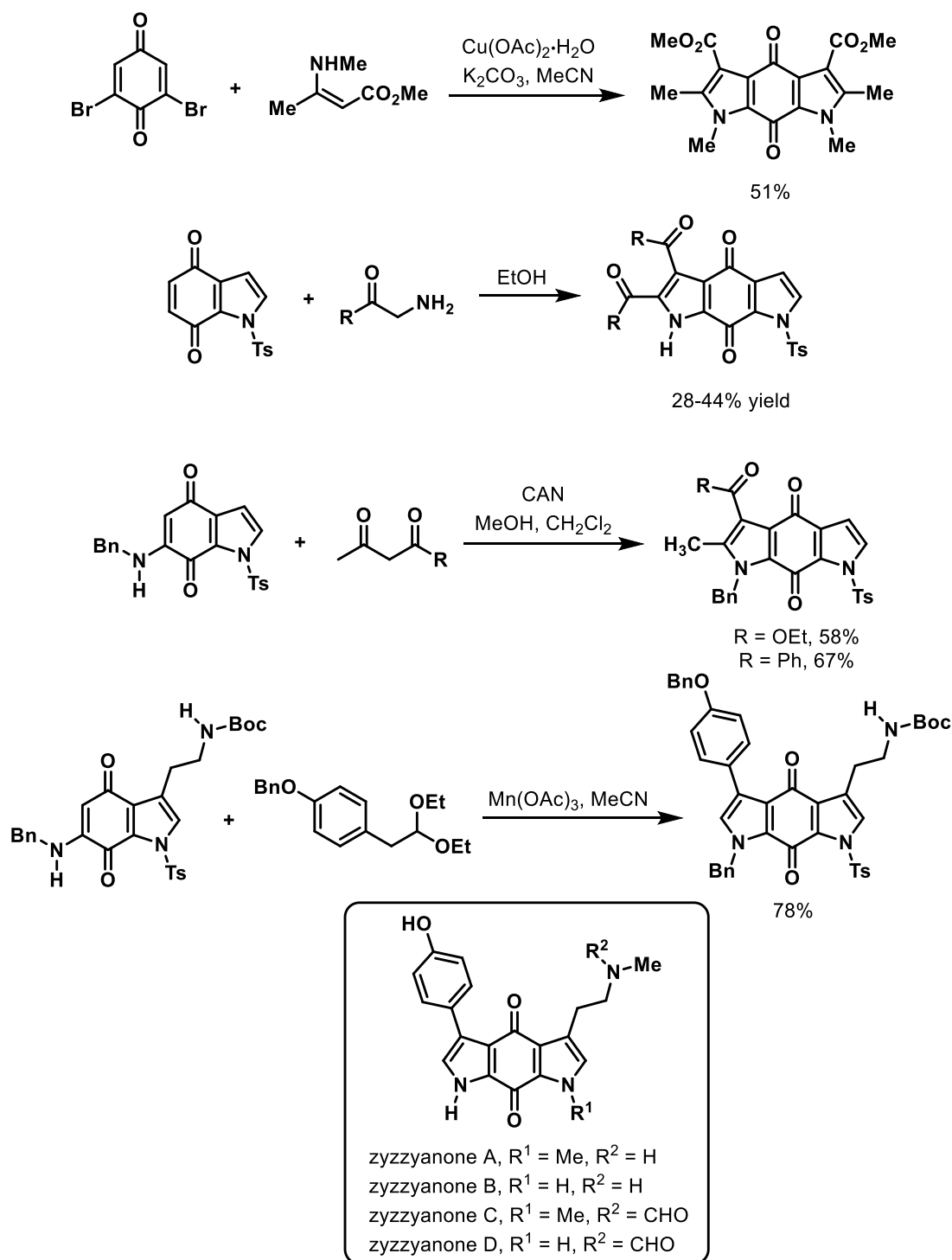
Scheme 1.30. Pyrroloindolequinone synthesis.

The synthesis of the pyrrolo[2,3-*f*]indolequinone natural product terreusinone was reported by Wang and Sperry with hydroamination of *o*-alkynylaniline catalyzed by a cationic gold complex and Frémy oxidation to the quinone (Scheme 1.31).[50]
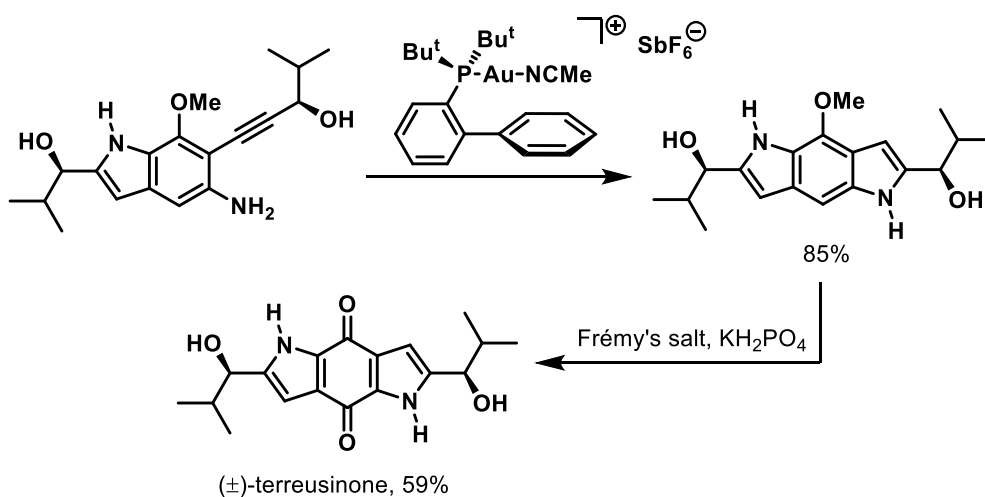
Scheme 1.31. Synthesis of terreusinone.

Furo[3,2-*f*]indoles were prepared *via* ketenimine intermediates in the 1,6-addition of *o*-alkenylaryl isocyanides onto ene-yne-ketones with subsequent cyclization (Scheme 1.32).[51] A formal ZnCl$_2$-catalysed [1+2+3] annulation with methyleneindolinones gave indolo[3,2-*b*]carbazoles towards the synthesis of the indolo[3,2-*b*]carbazole alkaloid malasseziazole C.[52]
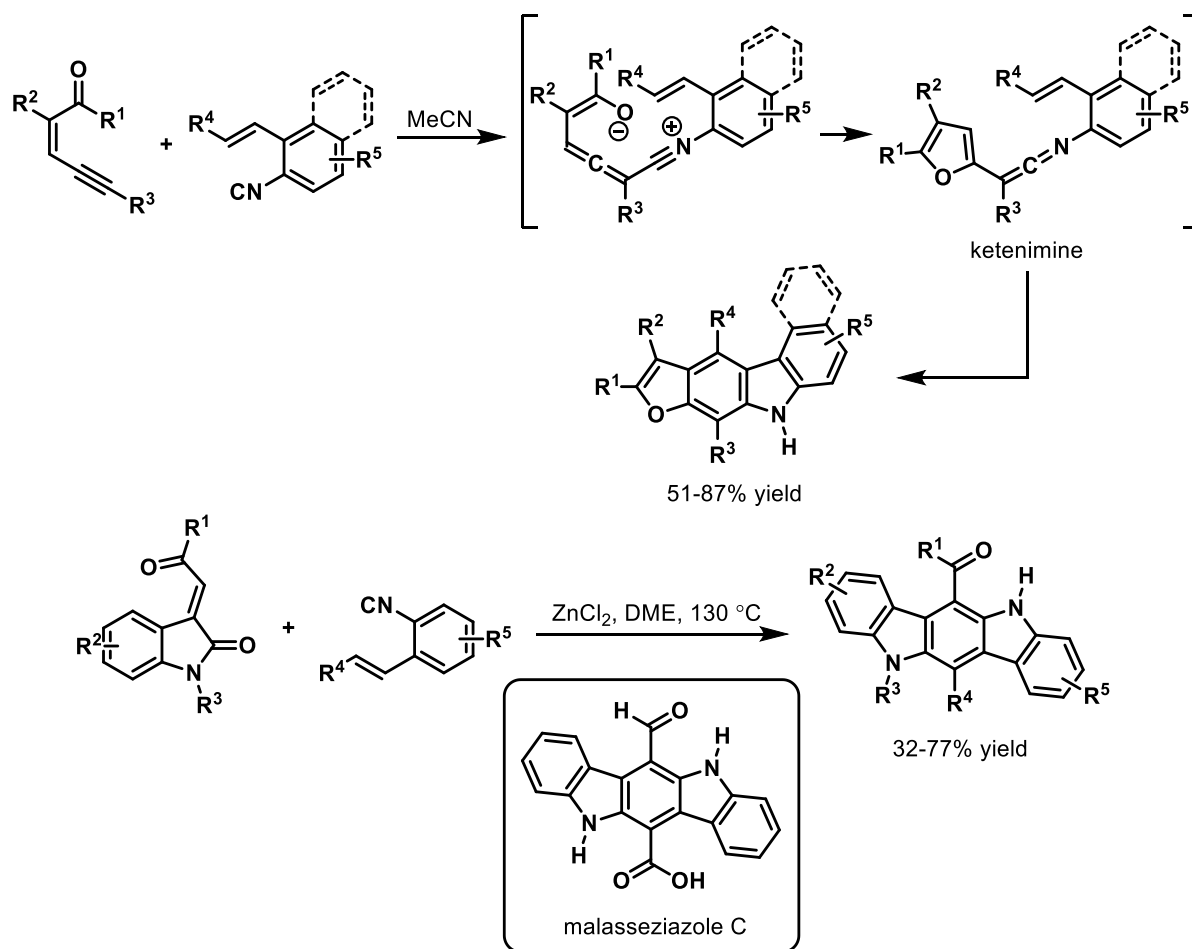
Scheme 1.32. Alkenylaryl isocyanides in the synthesis of furoindoles and indolocarbazoles.

18

2-Pivaloyloxymethylindoles underwent arylation, cyclization and aromatization to give thieno[2,3-*b*]carbazoles, furo[2,3-*b*]carbazoles and pyrrolo[2,3-*b*]carbazoles (Scheme 1.33).[53]
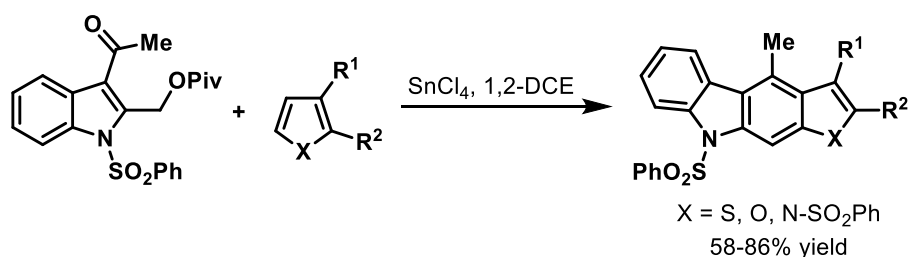
Scheme 1.33. Conversion of pivaloyloxymethylindoles to tricyclic scaffolds.

An In(OTf)$_3$-catalyzed dehydrative cyclization of 2-(1-(benzofuran-2-yl)ethyl)-1-methyl-1*H*-indole-3-carbaldehyde furnished the carbocyclic ring of *N*-methyl benzofuro[2,3-*b*]carbazole (Scheme 1.34).[54] The *N*-phenyl derivative was accessed by palladium-catalyzed dual C-N bond formation in the reaction of aniline with an iodoarene.[55]
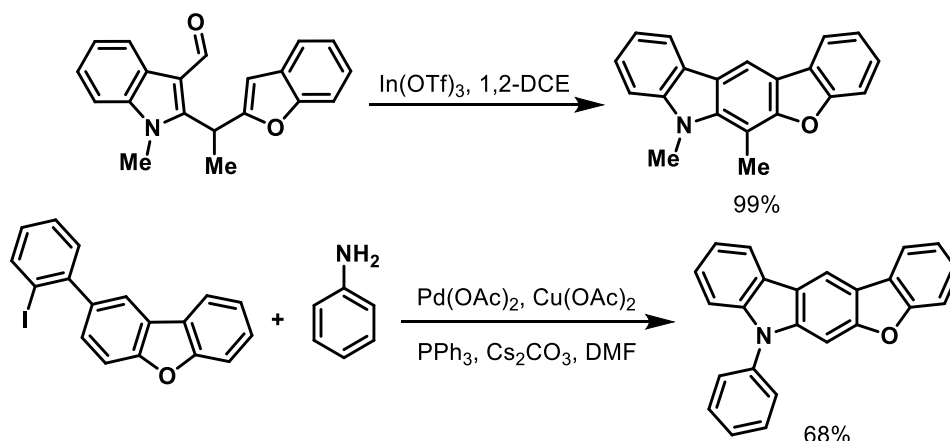
Scheme 1.34. Construction of benzofurocarbazoles.

Ring-rearrangement of a diketopyrrolopyrrole possessing two benzofuryl groups occurred in the presence of trimethylsilyl bromide and hydroxyl(tosyloxy)iodobenzene (HTIB) in HFIP to give furo[2,3-*f*]isoindole-4,7-dione (Scheme 1.35).[56]

19
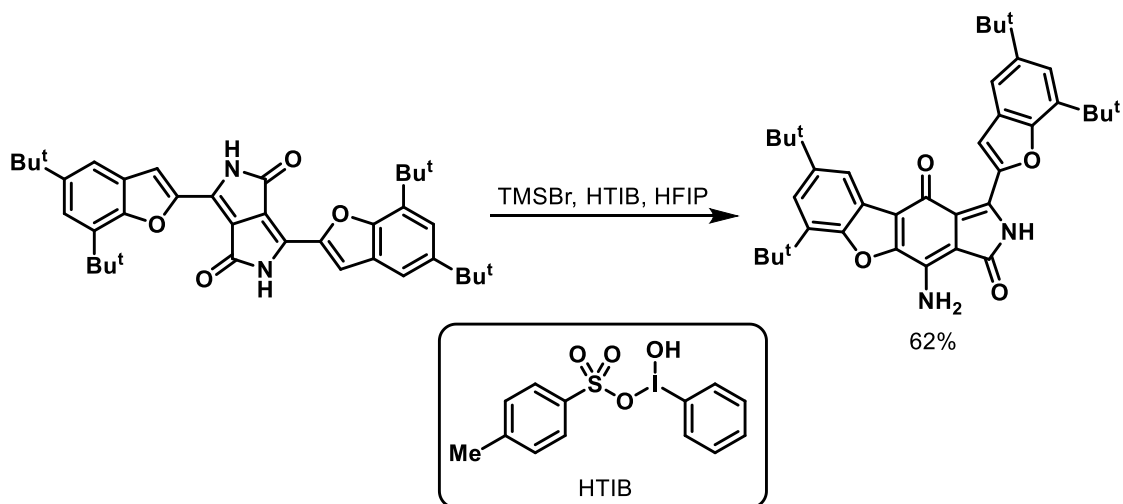
Scheme 1.35. Ring-rearrangement to yield furoisoindole.

AgOAc was employed as the oxidant to induce a cascade intramolecular amination and cyclization of mesylated 2-[cyclopropylidene(furan-3-yl)methyl]-4-methylaniline with chloranil mediated aromatization, and basic deprotection giving the furo[2,3-*c*]carbazole natural product eustifoline-D (Scheme 1.36).[57] Furo[3,2-*a*]carbazole natural product furostifoline was accessed by conversion of aldehyde-substituted indole to the *N*-tosylhydrazone, Rh$_2$(OAc)$_4$-catalysed cyclization of the hydrazone, and Boc-deprotection.[58] The key step in the first total synthesis of furoclausine-B was a palladium(II)-catalyzed oxidative cyclization.[59]
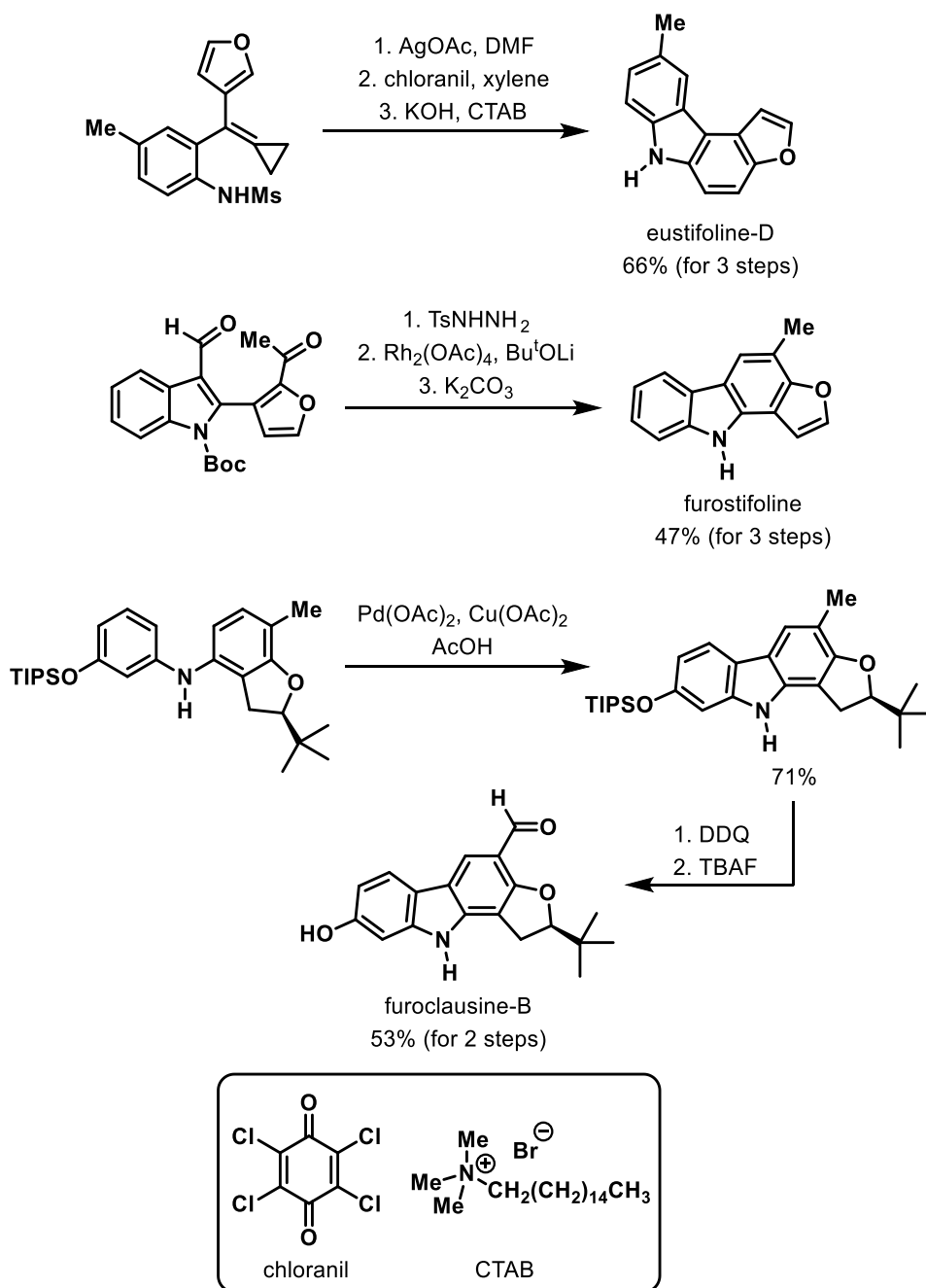
Scheme 1.36. Synthesis of furo[3,2-*a*]carbazole natural products.

Thieno and furo[2,3-*e*]indoles were accessed by intramolecular Cu(OTf)$_2$-catalyzed aromatic substitution of 2-(diazoacetyl)-pyrroles (Scheme 1.37).[60]
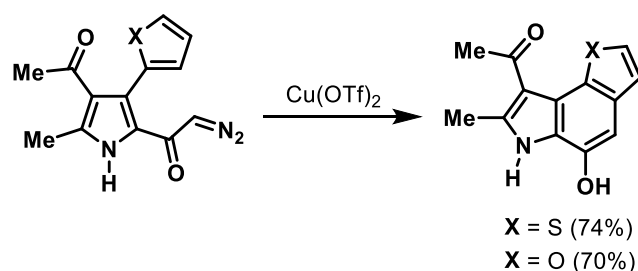
Scheme 1.37. Intramolecular aromatization to furnish thieno and furoindoles.

1.1.4.2. Compounds with three heteroatoms arranged 1:2

A 5-*exo trig* carboiodination onto an acrylamide gave the [1,3]dioxolo[4,5-*f*]indol-6-one as a racemic mixture (Scheme 1.38).[61]
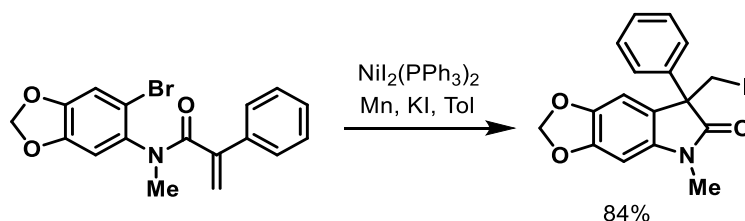
Scheme 1.38. Carboiodination to yield [1,3]dioxoloindole.

1.1.4.3. Compounds with four heteroatoms arranged 1:3

The pyrrole ring of [1,2,5]oxadiazolo[3,4-*g*]indole was constructed by reacting benzo[*c*][1,2,5]oxadiazolone oxime with acetylene under basic conditions (Scheme 1.39).[62]
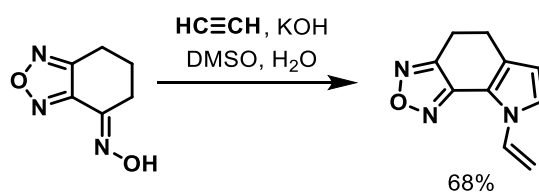
Scheme 1.39. Pyrrole ring formation using acetylene.

The cyclic aryliodonium salt generated in the reaction of 4-(2-iodophenyl)-benzothiadiazole with *m*-CPBA and TfOH, underwent nucleophilic substitution to furnish thiadiazolo[3,4-*c*]carbazole, benzofuro[3,2-*e*]benzothiadiazole, benzothienobenzothiadiazole, and benzoselenobenzothiadiazole (Scheme 1.40).[63]

22
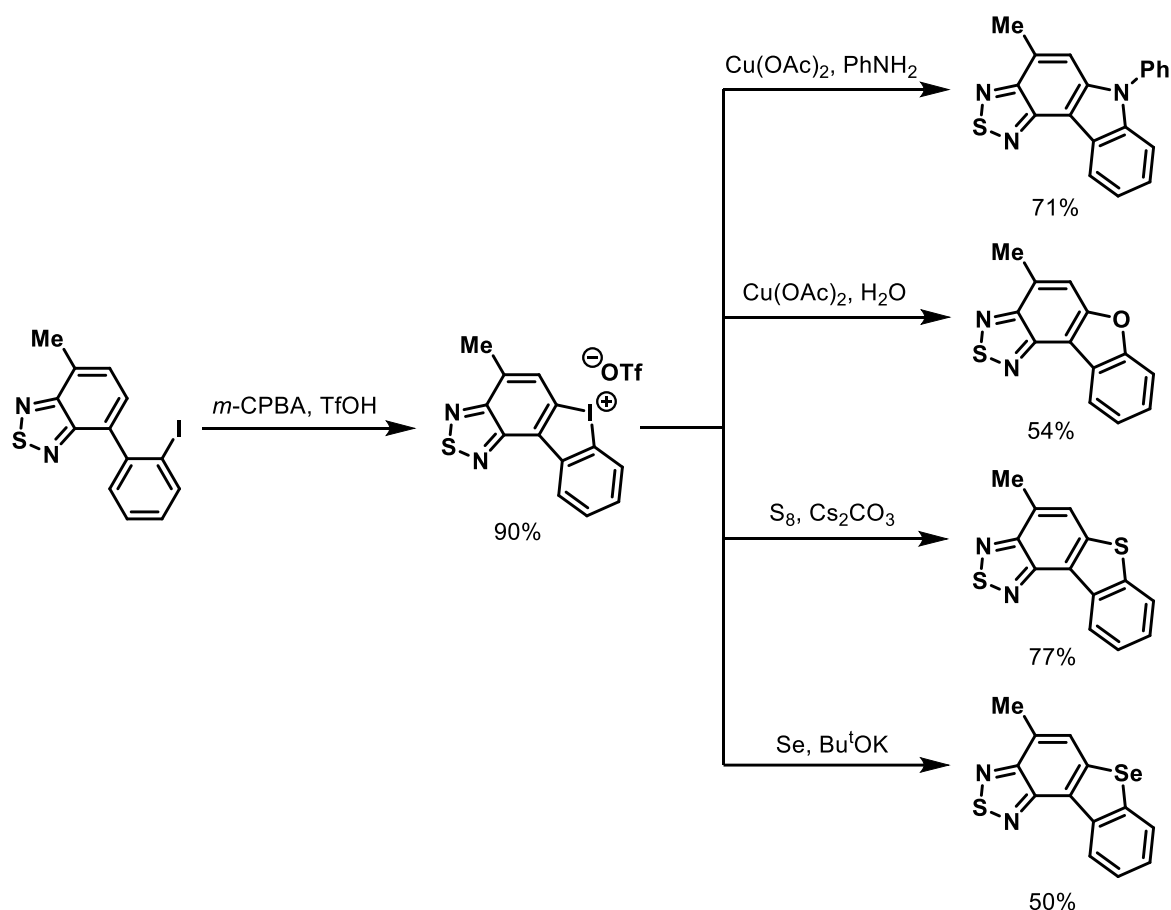
Scheme 1.40. Heterocycle formation *via* iodonium salt.

1.1.4.4. Compounds with four heteroatoms arranged 2:2

Treatment of 1,2,4,5-benzenetetramine tetrahydrochloride with neat benzylic amines gave disubstituted imidazobenzimidazoles (Scheme 1.41).[64]

R = Ph (85%)
R = 3-Py (89%)
R = 2-Py (54%)
R = 3,4,5-OMe-C$_6$H$_2$ (63%)
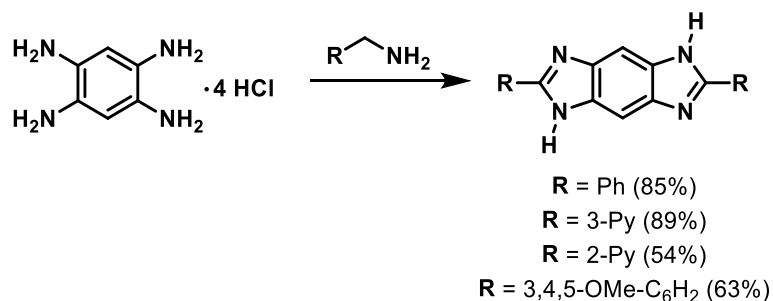
Scheme 1.41. Imidazobenzimidazole formation from benzenetetramine.

Imidazo[4,5-*f*]benzimidazole was furnished in the zinc-mediated reductive ring contraction of zwitterionic tetraphenylhexaazaanthracene (Scheme 1.42).[65] Using fewer equivalents of zinc

powder yielded the stable imidazo[4,5-*g*][1,2,4]benzotriazin-1-yl radical, which underwent complete reductive ring contraction on exposure to a further 2 equivalents of zinc.
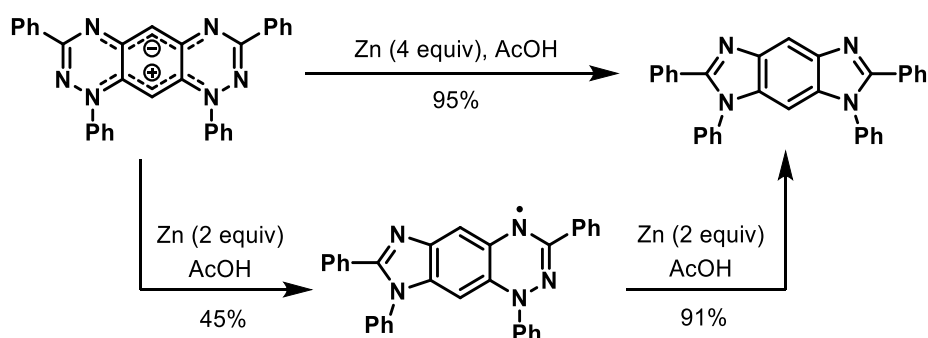
Scheme 1.42. Ring-contraction towards imidazo[4,5-*f*]benzimidazole.

2,6-Disubstituted benzobisoxazoles were prepared by the condensation 2,5-diaminohydroquinone with various orthoesters,[66] and benzobisoxazoles were also reported from resorcinols and nitroalkanes with polyphosphoric acid (PPA) activation (Scheme 1.43).[67]
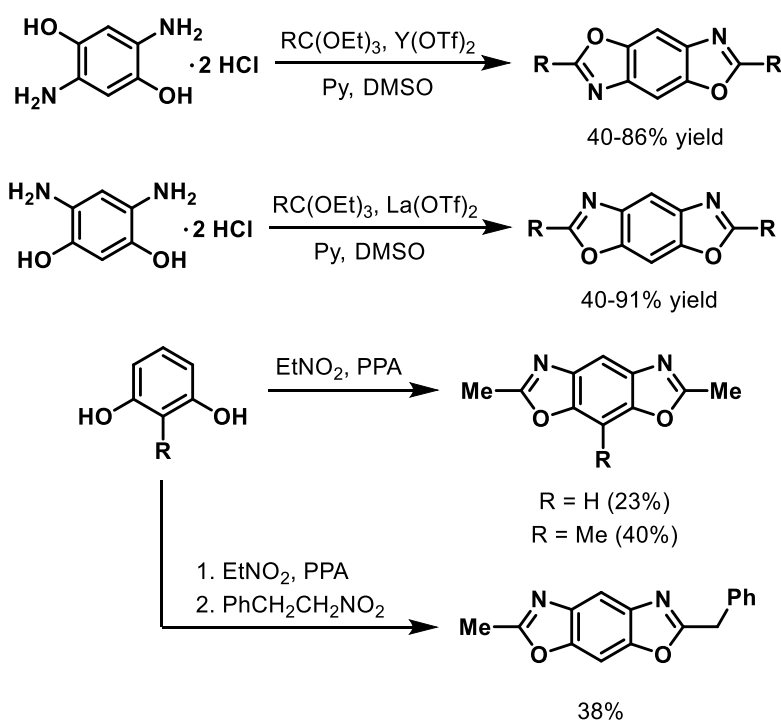
Scheme 1.43. Benzobisoxazole preparation.

Dioxolo[4,5-*f*]benzimidazol-6-one was prepared *via* a DABCO-mediated substitution of carbazate onto 2-iodoaniline with the resulting intermediate undergoing copper-catalyzed intramolecular coupling (Scheme 1.44).[68]
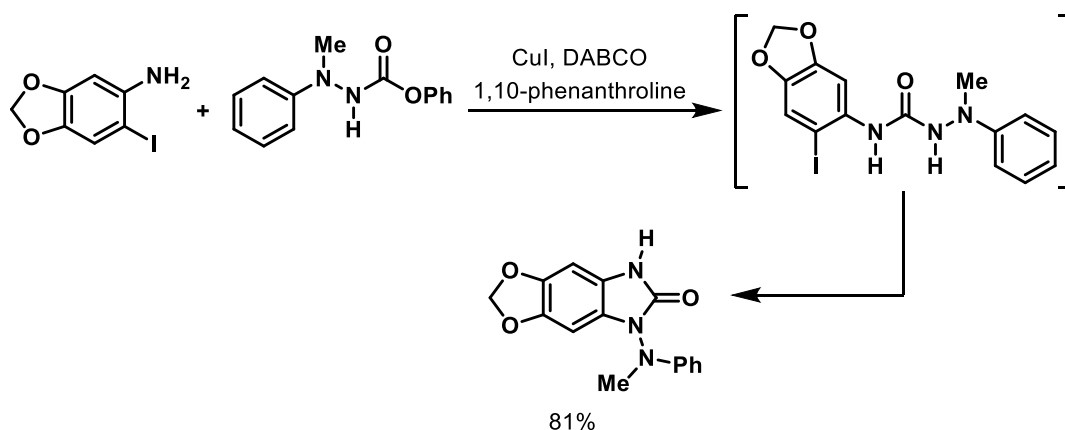
Scheme 1.44. Imidazole ring formation of dioxolobenzimidazole.

N-Benzyl-DABCO tribromide (NBDTB)-mediated the oxidative cyclization of bis(thiobenzanilides) to give a series of benzodithiazoles (Scheme 1.45).[69]
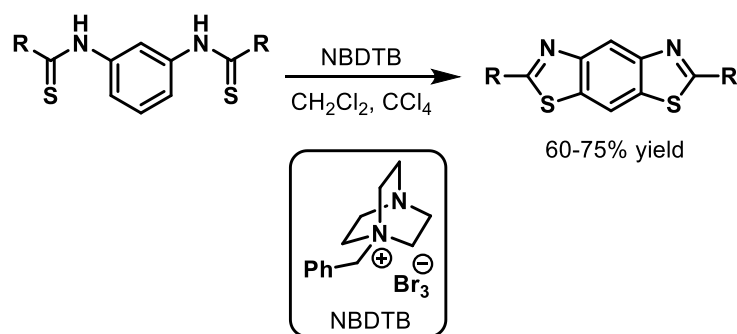
Scheme 1.45. Oxidative cyclization to yield benzodithiazoles.

1.1.4.5.   Compounds with more than four heteroatoms

Treatment of benzothiadiazole-4,5-diamine with aromatic aldehydes in the presence of dipyridine copper chloride as Lewis acid catalyst constructed the imidazole ring of imidazo[*e*]benzothiadiazoles (Scheme 1.46).[70]
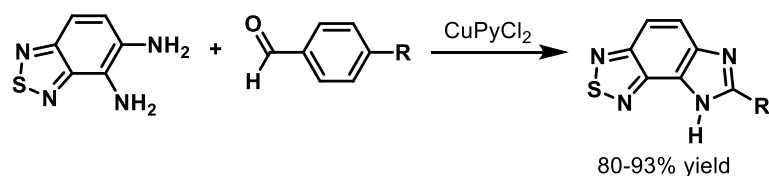
Scheme 1.46. Lewis acid-mediated formation of imidazobenzothiadiazoles.

Benzobis[1,2,3]triazole-4,8-diones were synthesized by [3+2] cycloaddition of aryl azides onto 1,4-benzoquinone generated *in situ* from the *m*-CPBA-mediated oxidation of phenol (Scheme 1.47).[71] 4,8-Dibromobenzobis[1,2,3]triazole was prepared from tetraaminobenzene tetrabromide and nitrous acid,[72] and bisiodotriazoles were reported to undergo intramolecular homocoupling catalyzed by palladacycle **30**.[73]
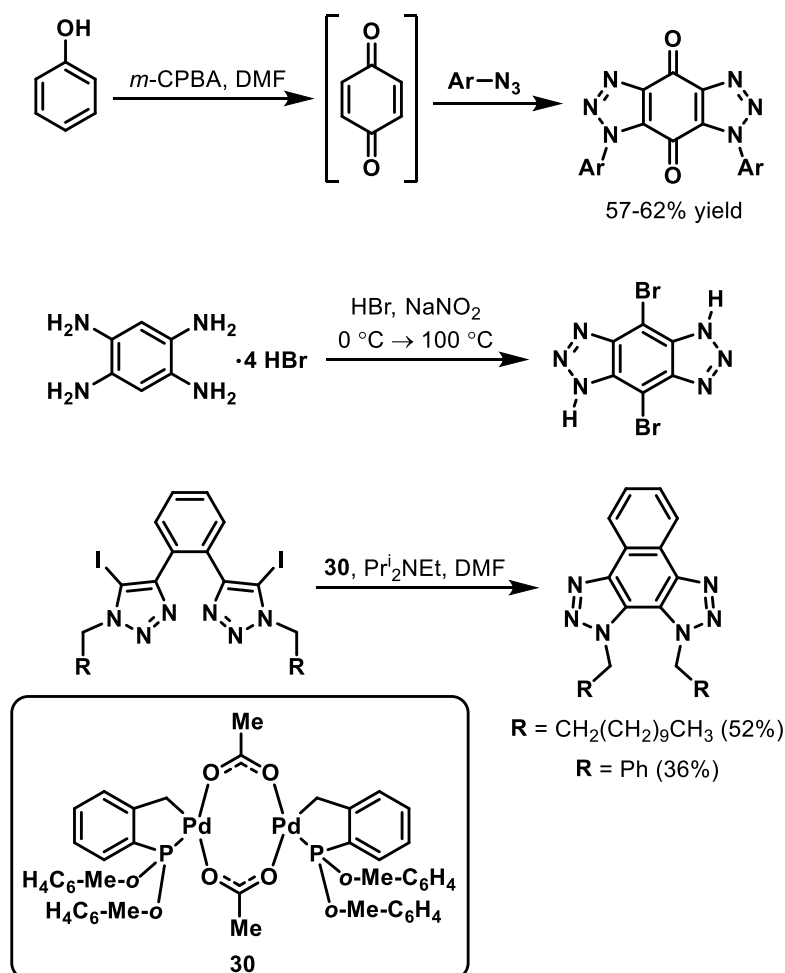
Scheme 1.47. Benzobistriazole formation.

4-Fluorobenzodifuroxan was prepared in two steps starting from 2,4,6-trifluoro-1,3-dinitrobenzene and sodium azide (Scheme 1.48).[74]

Scheme 1.48. Two-step benzodifuroxan synthesis.

Benzyne-fused oxadisilole was generated *in situ* from the desilylation of benzo[1,2-*c*:4,5-*c'*]bisoxadisilole through sequential phenyliodination and fluoride-mediated elimination (Scheme 1.49).[75] The benzyne was trapped *via* 1,3-dipolar cycloaddition of aryl and benzylic azides to yield oxadisilo[3,4-*f*]benzotriazoles. Oxadisilole-fused benzisoxazoles were prepared by trapping the benzyne with aryl nitrile *N*-oxides generated *in situ* from the corresponding oximes.[76]
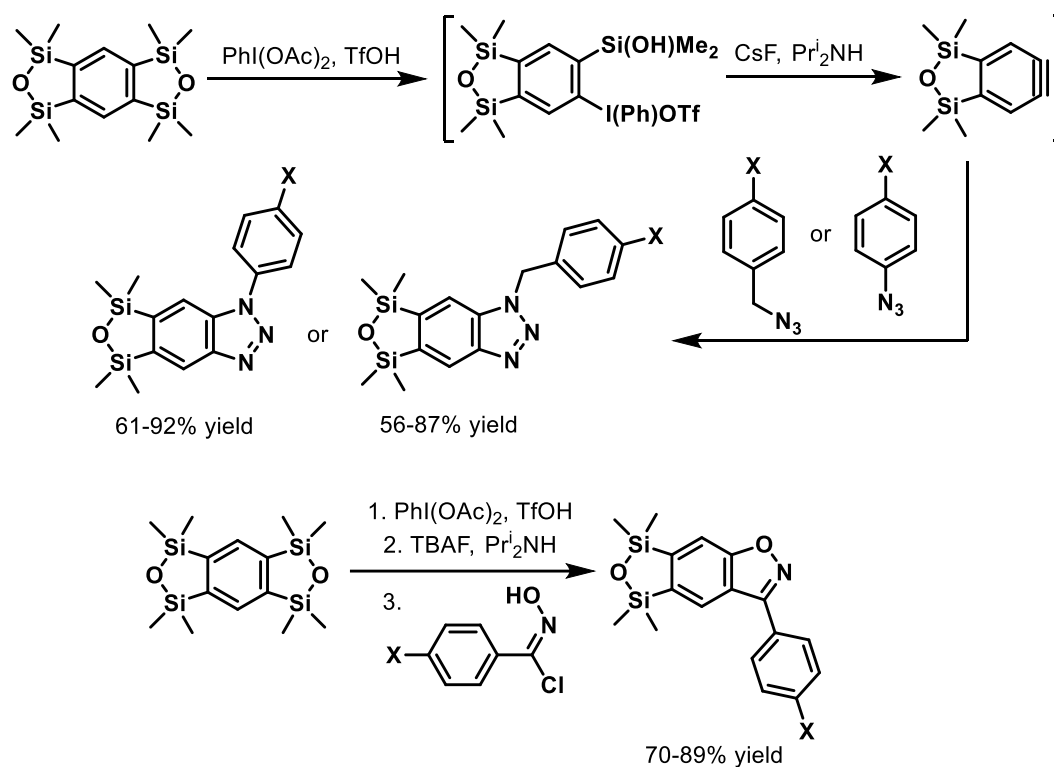
Scheme 1.49. Heterocycle formation *via* benzyne trapping.

1.1.5. Applications

Pyrroloindole-fused BODIPY dye has potential optoelectronic applications given its intense absorption at 629 nm with a broad shoulder band up to 900 nm, compared with the parent BODIPY, which absorbed maximally at 519 nm (Figure 1.5).[77]
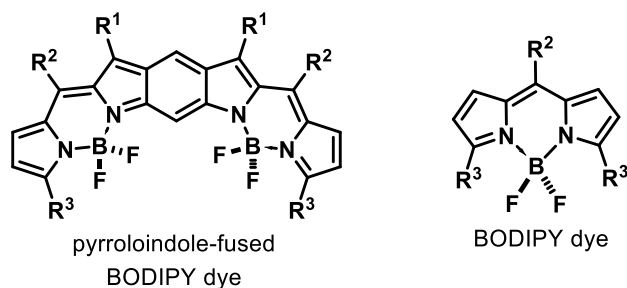
Figure 1.5. BODIPY dyes.

The amide of thiazole-substituted [1,3]thiazolo[4,5-*f*]indole undergoes hydrolysis in the presence of fatty acid amide hydrolase (FAAH) with the resulting carboxylic acid being a substrate of the enzyme firefly luciferase (Figure 1.6).[78] Binding of the acid to luciferase induces luminescence. Application of luciferin amide are in bioluminescent detection of FAAH activity *in vitro* and *in vivo*.
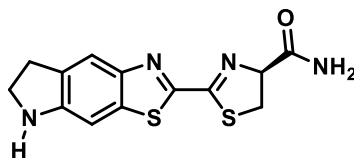
Figure 1.6. Luciferin amide.

1.2. Target Heterocycles: Nomenclature

All compounds prepared in this thesis are named according to the rules determined by IUPAC.[79,80] Naming heterocyclic systems containing two or more fused rings involves three steps:

1.2.1. Construct fusion name
1.2.2. Assign peripheral numbering
1.2.3. Assign indicated hydrogen and hydro positions

1.2.1. Construct the fusion name

The fusion name indicates the position on the molecule in which the rings are annulated. This involves deconstructing the molecule into its constituent carbo- and heterocycles. The heterocycles are ranked according to priority determined by IUPAC. Nitrogen heterocycles always have the highest priority, followed by heterocycles containing the following atoms (arranged in order of priority):

$$O > S > Se > Te > P > As > Sb > Bi > Si > Ge > Sn > Pb > B.$$
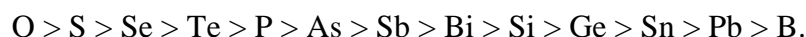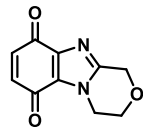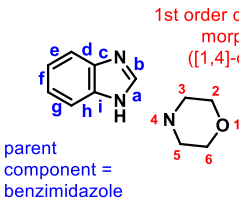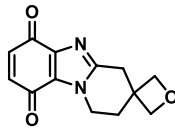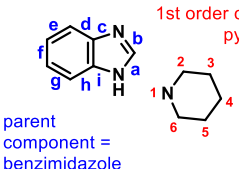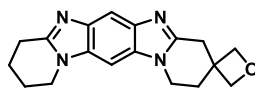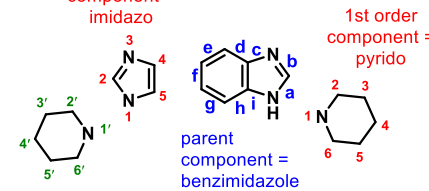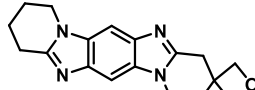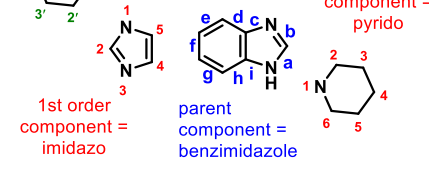
Heterocycles are always ranked higher than carbocycles. The highest priority heterocycle is termed the parent component. Fused to the parent component are the 1st order components, while the 2nd order components are fused to the 1st order components. The bonds on the parent component are assigned lettered locants, starting from the bond adjacent to the heteroatom of highest priority. Priority is assigned according to the above list (except for nitrogen, whose priority lies between Se and Te). Labelling goes in the direction in which the bond adjacent to the next highest heteroatom is given the lowest possible letter. The atoms of the 1st order component are assigned numerical locants, again starting from the heteroatom of highest priority, and going in the direction that results in the heteroatom of next highest priority being assigned the lowest possible number. The atoms of the 2nd order component are labelled with primed numerical locants.
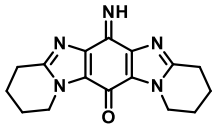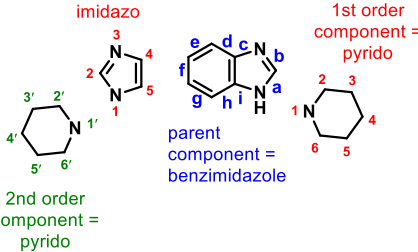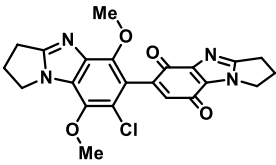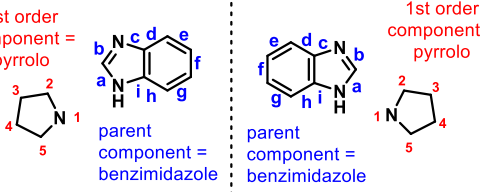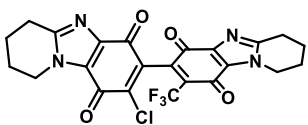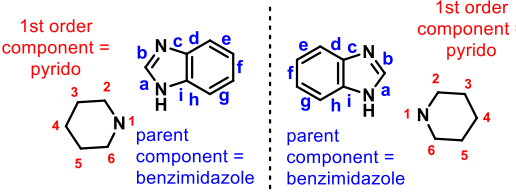
The fusion between the parent and 1st order components are indicated by the numerical locants of the 1st order component, followed by the letter locant of the parent component, cited within square brackets, and separated by a hyphen. The 1st order numerical locants are always cited in the same direction as the letters of the parent component.

The fusion between the 1st and 2nd order components are indicated by the primed numerical locants of the 2nd order, followed by numerical locants of the 1st order component, cited within square brackets and separated by a colon. For the purposes of constructing the fusion name, substituents are disregarded, as are any cyclic components not fused to the rest of the molecule (*e.g.* spirocycles).

Some examples of the construction of fusion names for compounds presented in this thesis are shown in Table 1.1.

Table 1.1. Fusion name construction.

Structure	Components	Fusion Name
		[1,4]oxazino[4,3-*a*] **benzimidazole**
		pyrido[1,2-*a*] **benzimidazole**
		pyrido[1,2-*a*] **pyrido[1',2':1,2]imidazo** **[4,5-*f*]benzimidazole**
		pyrido[1,2-*a*] **pyrido[1',2':1,2]imidazo** **[5,4-*f*]benzimidazole**

(structure)	1st order component = imidazo 3 4 2 N 5 N 1 (imidazo) e d c N b f a g h i N H parent component = benzimidazole 1st order component = pyrido 2 3 1 N 4 6 5 3' 2' 4' N 1' 5' 6' 2nd order component = pyrido	**pyrido[1,2-*a*] pyrido[1',2':1,2]imidazo [4,5-*f*]benzimidazole**
(structure)	1st order component = pyrrolo b N c d e a f N H i h g parent component = benzimidazole 3 2 4 N 1 5 e d c N b f a g h i N H parent component = benzimidazole 1st order component = pyrrolo 2 3 1 N 4 5	**bipyrrolo[1,2-*a*] benzimidazole**
(structure)	1st order component = pyrido b N c d e a f N H i h g parent component = benzimidazole 3 2 4 N 1 5 6 e d c N b f a g h i N H parent component = benzimidazole 1st order component = pyrido 2 3 1 N 4 6 5	**bipyrido[1,2-*a*] benzimidazole**

1.2.2. Assign peripheral numbering

The molecule as a whole is re-numbered, disregarding the locants assigned for the fusion name. The molecule is drawn such that the most possible rings are on the horizontal axis. A horizontal and vertical axis is drawn through the molecule, giving 4 equal quadrants. Numbering begins in the upper right-hand quadrant, on the most anti-clockwise non-fusion atom, and proceeds in a clockwise direction. Fusion carbon atoms are not given a number, instead being assigned the number of the atom before it, with the letter 'a' after it. If more than one orientation is possible, then the following rules are assigned, until the preferred orientation is determined:

(i)   Give low numbers to heteroatoms as a set.
(ii)   Give low numbers to heteroatoms when considered in the order: O > S > Se > Te > N > P > As > Sb > Bi > Si > Ge > Sn > Pb > B.
(iii)   Give low numbers to fusion carbons as a set.
(iv)   Give low numbers to fusion rather than non-fusion atoms of the same heteroelement.

For spirocyclic systems, the two ring systems connected by the spiro atom are numbered independently and in alphabetical order. The atoms of the component starting with the letter earliest in the alphabet are assigned numbers, while atoms of the other component are given primed numbers.

Examples are shown in Figures 1.7 – 1.10.

In the below spirocyclic system, pyrido[1,2-*a*]benzimidazole is connected to oxetane *via* the spiro atom. Alphabetically, oxetane comes before pyrido[1,2-*a*]benzimidazole, so the former component is given numbers, while the latter is assigned primed numbers. Numbering for the oxetane starts from the heteroatom, while the order of numbering for the fused component is determined as above.
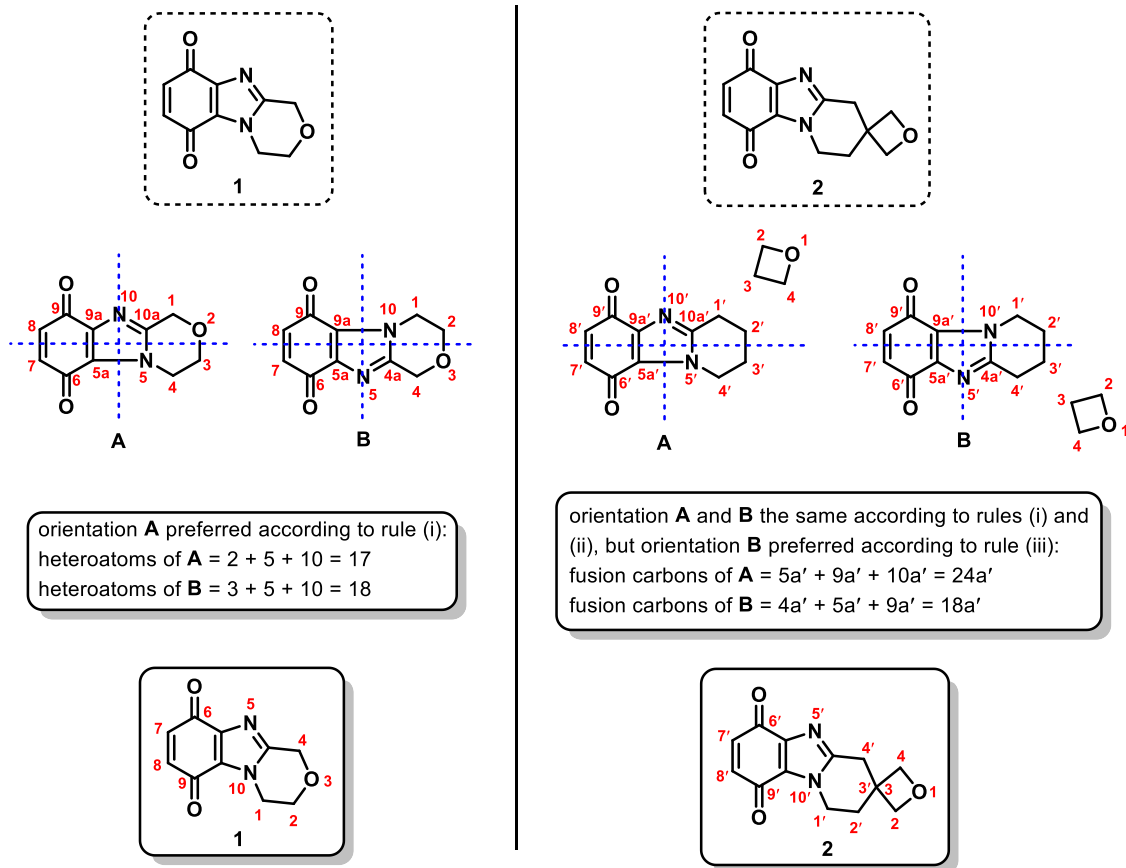
Figure 1.7. Assigning peripheral numbering for benzimidazolequinones **1** and **2** (Chapter 2).
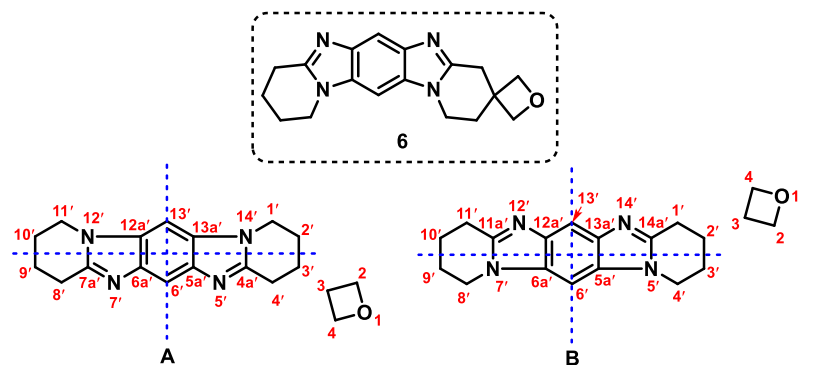
orientation **A** and **B** the same according to rules (i) and (ii), but
orientation **A** preferred according to rule (iii):
fusion carbons of **A** = 4a′ + 5a′ + 6a′ + 7a′ + 12a′ + 13a′ = 47a′
fusion carbons of **B** = 5a′ + 6a′ + 11a′ + 12a′ + 13a′ + 14a′ = 61a′
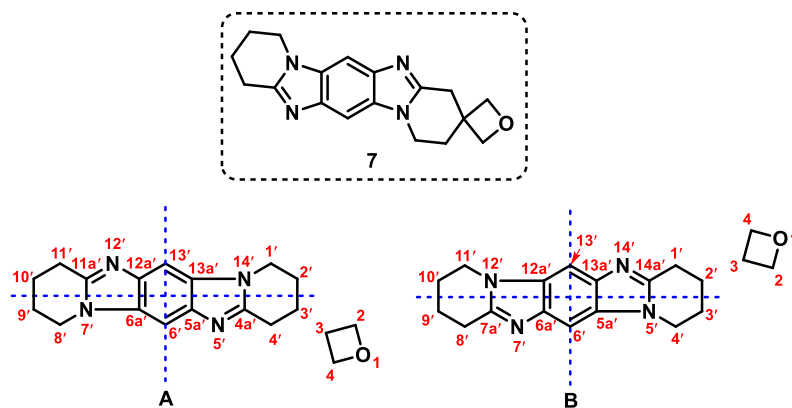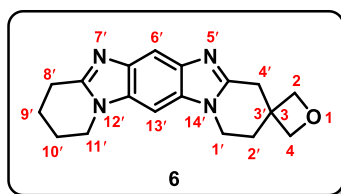
orientation **A** and **B** the same according to rules (i) and (ii), but
orientation **A** preferred according to rule (iii):
fusion carbons of **A** = 4a′ + 5a′ + 6a′ + 11a′ + 12a′ + 13a′ = 51a′
fusion carbons of **B** = 5a′ + 6a′ + 7a′ + 12a′ + 13a′ + 14a′ = 57a′
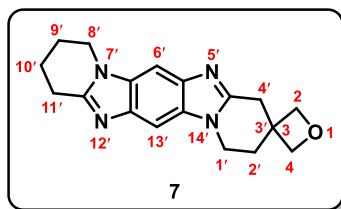
Figure 1.8. Peripheral numbering for imidazobenzimidazoles **6** and **7** (Chapter 3).
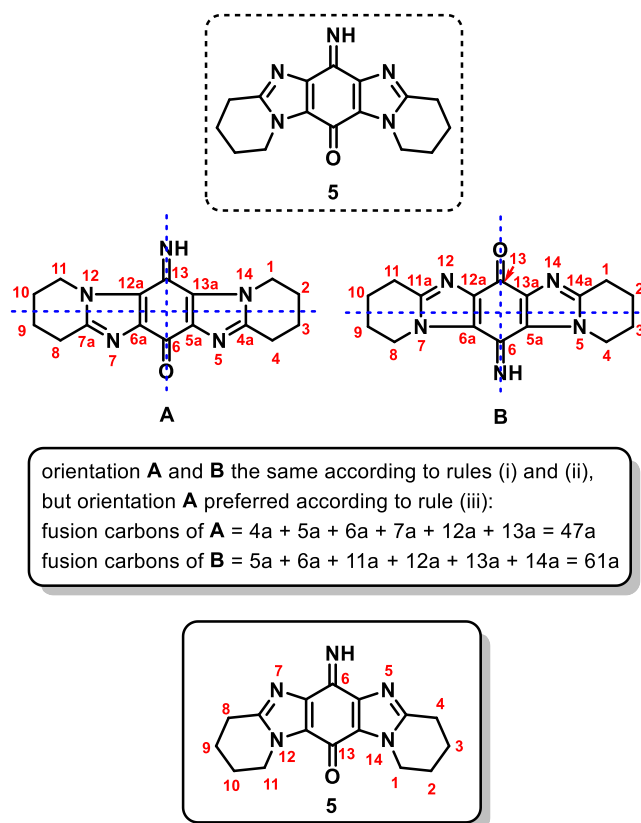
Figure 1.9. Peripheral numbering for iminoquinone **5** (Chapter 4).

The following two dimers are assemblies of two identical parent systems varying only in the degree of saturation and the presence of substituents. The two ring systems connected by the central C-C bond are numbered independently, with the atoms of the higher priority ring system given numerical locants, while the lower priority system is assigned primed numbers. In the *p*-dimethoxybenzimidazole-benzimidazolequinone dimers, the benzimidazolequinone is assigned higher priority than the dimethoxybenzimidazole. For the bis-*p*-quinones, the ring system containing the substituent of highest molecular weight is assigned higher priority (*e.g.*) Cl > CF$_3$ (Cl higher M.W. than C).

orientation **A** and **B** the same according to rules (i) and (ii), but orientation **B** preferred according to rule (iii):
fusion carbons of **A** = 4a′ + 8a′ + 9a′ = 21a′
fusion carbons of **B** = 3a′ + 4a′ + 8a′ = 15a′

orientation **C** and **D** the same according to rules (i) and (ii), but orientation **C** preferred according to rule (iii):
fusion carbons of **C** = 3a + 4a + 8a = 15a
fusion carbons of **D** = 4a + 8a + 9a = 21a

orientation **A** and **B** the same according to rules (i) and (ii), but orientation **B** preferred according to rule (iii):
fusion carbons of **A** = 5a + 9a + 10a = 24a
fusion carbons of **B** = 4a + 5a + 9a = 18a

orientation **C** and **D** the same according to rules (i) and (ii), but orientation **C** preferred according to rule (iii):
fusion carbons of **C** = 4a′ + 5a′ + 9a′ = 18a′
fusion carbons of **D** = 5a′ + 9a′ + 10a′ = 24a′

Figure 1.10. Peripheral numbering for dimers **8a** and **14** (Chapter 5).

36

1.2.3. Assign indicated hydrogen and hydro positions

On the alicyclic rings of the fused systems, the positions where double bonds could potentially exist are designated as hydro positions, while the remaining positions are indicated hydrogens (Figure 1.11). Where multiple orientations of double bonds are possible, that which allows the greatest number of double bonds is selected. Furthermore, where possible, the indicated hydrogen positions are assigned the lowest possible number. Hydro positions are indicated in the compound name by identifying the positions on the molecule where they exist (using the peripheral numbering system), followed by the prefix indicating the number of hydro positions (*e.g.* di-, tetra-, hexa-, octa- etc.; hydro positions always exist in pairs). The indicated hydrogens are denoted by the position in which they exist, followed by an italic *H*.
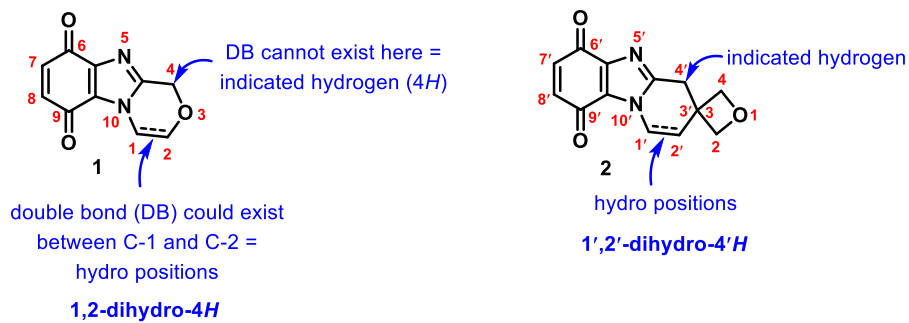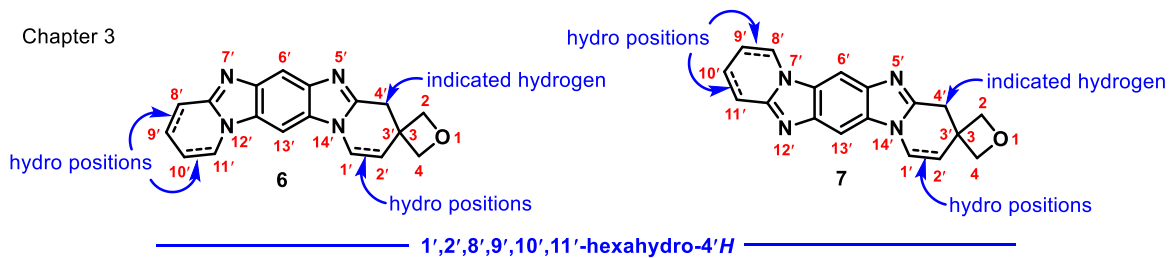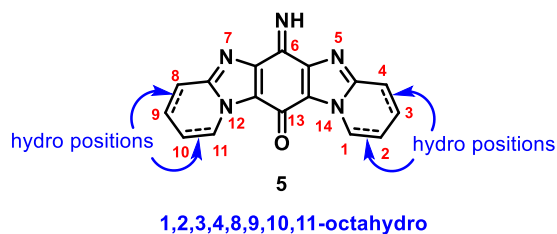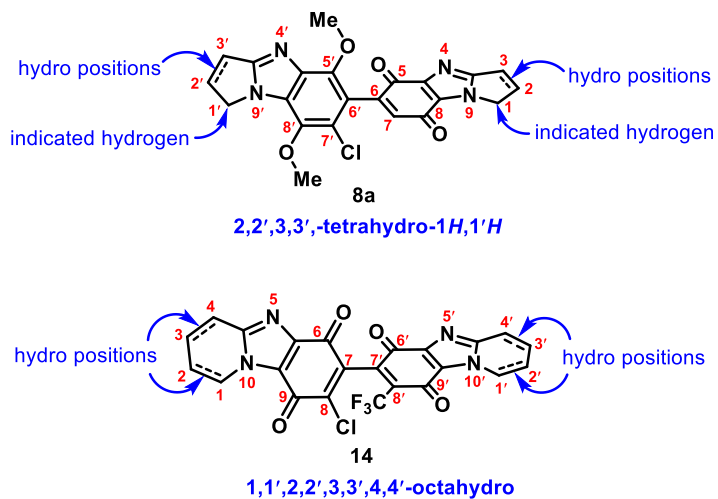
Figure 1.11. Hydro and indicated hydrogen positions.

The compound names are then constructed by first indicating the position of substituents (except for carbonyl groups directly attached to the rings (*e.g.*) quinones, which come at the end of the name). Following the substituent positions are the hydro and indicated hydrogens, and then the fusion name.

Therefore the names of the above compounds are as follows:
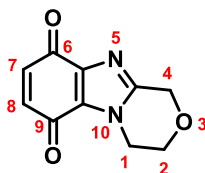
1 (Chapter 2)

3,4-Dihydro-1*H*-[1,4]oxazino[4,3-*a*]benzimidazole-6,9-dione

For spirocyclic systems (such as the below), the word "spiro" comes directly after the indicated hydrogens, followed by the names of the two components connected *via* the spiro atom listed alphabetically, and cited within square brackets. The position of the spiro atom is indicated by the peripheral numbers, and is placed between both components in the compound name.
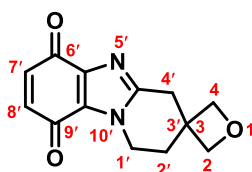
2 (Chapter 2)

1′,2′-Dihydro-4′*H*-spiro[oxetane-3,3′-pyrido[1,2-*a*]benzimidazole]-6′,9′-dione
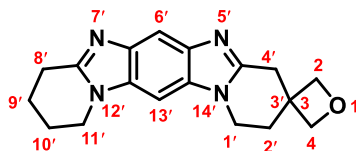
6 (Chapter 3)

1',2',8',9',10',11'-Hexahydro-4'*H*-spiro[oxetane-3,3'-pyrido[1,2-*a*]pyrido[1',2':1,2] imidazo[4,5-*f*]benzimidazole]
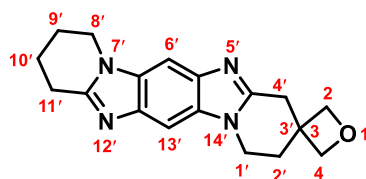
7 (Chapter 3)

1',2',8',9',10',11'-Hexahydro-4'*H*-spiro[oxetane-3,3'-pyrido[1,2-*a*]pyrido[2',1':2,3]imidazo[4,5-*f*]benzimidazole]
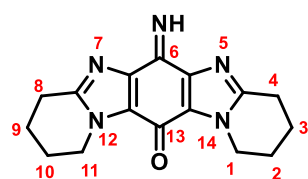
5 (Chapter 4)

6-Imino-1,2,3,4,8,9,10,11-octahydropyrido[1,2-*a*]pyrido[1′,2′:1,2]imidazo[4,5-*f*]benzimidazole-13-one
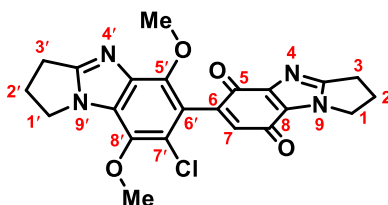
8a (Chapter 5)

7'-Chloro-5',8'-dimethoxy-2,2',3,3'-tetrahydro-1*H*,1'*H*-[6,6'-bipyrrolo[1,2-*a*]benzimidazole]-5,8-dione
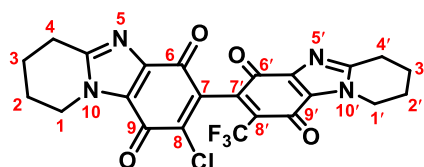
14 (Chapter 5)

8-Chloro-8'-(trifluoromethyl)-1,1',2,2',3,3',4,4'-octahydro[7,7'-bipyrido[1,2-*a*]benzimidazole]-6,6',9,9'-tetrone

1.3. Chapter 1 References

(1)   Graham, A.; Robinson, M. Tricyclic Systems: Central Carbocyclic Ring with Fused Five-Membered Rings. In *Comprehensive Heterocyclic Chemistry III*, Katritzky, A. R. Exec Ed; Ramsden, C. A., Scriven, E. F. V., Taylor, R. J. K., Ed; Jones, R. C. F. Vol. Ed; Elsevier; **2008**; Vol. 10, Chapt. 10.21, pp 1135–1199. https://doi.org/10.1016/B978-008044992-0.00921-4.

(2)   Wu, J.-S.; Cheng, S.-W.; Cheng, Y.-J.; Hsu, C.-S. Donor–Acceptor Conjugated Polymers Based on Multifused Ladder-Type Arenes for Organic Solar Cells. *Chem. Soc. Rev.* **2015**, *44*, 1113–1154. https://doi.org/10.1039/C4CS00250D.

(3)   Yao, H.; Ye, L.; Zhang, H.; Li, S.; Zhang, S.; Hou, J. Molecular Design of Benzodithiophene-Based Organic Photovoltaic Materials. *Chem. Rev.* **2016**, *116*, 7397–7457. https://doi.org/10.1021/acs.chemrev.6b00176.

(4)   Janosik, T.; Rannug, A.; Rannug, U.; Wahlström, N.; Slätt, J.; Bergman, J. Chemistry and Properties of Indolocarbazoles. *Chem. Rev.* **2018**, *118*, 9058–9128. https://doi.org/10.1021/acs.chemrev.8b00186.

(5)   Steglenko, D. V.; Kletsky, M. E.; Kurbatov, S. V.; Tatarov, A. V.; Minkin, V. I.; Goumont, R.; Terrier, F. The Stepwise Diels-Alder Reaction of 4-Nitrobenzodifuroxan with Danishefsky's Diene. *Chem. Eur. J.* **2011**, *17*, 7592–7604. https://doi.org/10.1002/chem.201003695.

(6)   Fagan, V.; Bonham, S.; Carty, M. P.; Saenz-Méndez, P.; Eriksson, L. A.; Aldabbagh, F. COMPARE Analysis of the Toxicity of an Iminoquinone Derivative of the Imidazo[5,4-*f*]benzimidazoles with NAD(P)H:Quinone Oxidoreductase 1 (NQO1) Activity and Computational Docking of Quinones as NQO1 Substrates. *Bioorg. Med. Chem.* **2012**, *20*, 3223–3232. https://doi.org/10.1016/j.bmc.2012.03.063.

(7)   Mailman, A.; Leitch, A. A.; Yong, W.; Steven, E.; Winter, S. M.; Claridge, R. C. M.; Assoud, A.; Tse, J. S.; Desgreniers, S.; Secco, R. A.; Oakley, R. T. The Power of Packing: Metallization of an Organic Semiconductor. *J. Am. Chem. Soc.* **2017**, *139*, 2180–2183. https://doi.org/10.1021/jacs.6b12814.

(8)   Olankitwanit, A.; Rajca, S.; Rajca, A. Aza-*m*-Xylylene Diradical with Increased Steric Protection of the Aminyl Radicals. *J. Org. Chem.* **2015**, *80*, 5035–5044. https://doi.org/10.1021/acs.joc.5b00421.

(9)   Lücht, A.; Jones, P. G.; Werz, D. B. Reactions of 3,3′-Linked Bispyrroles with Carbon Electrophiles. *Eur. J. Org. Chem.* **2019**, 5254-5260. https://doi.org/10.1002/ejoc.201900106.

(10)   Zhu, C.; Ji, X.; You, D.; Chen, T. L.; Mu, A. U.; Barker, K. P.; Klivansky, L. M.; Liu, Y.; Fang, L. Extraordinary Redox Activities in Ladder-Type Conjugated Molecules Enabled by B ← N Coordination-Promoted Delocalization and Hyperconjugation. *J. Am. Chem. Soc.* **2018**, *140*, 18173–18182. https://doi.org/10.1021/jacs.8b11337.

(11)   Miller, M.; Vogel, J. C.; Tsang, W.; Merrit, A.; Procter, D. J. Formation of *N*-Heterocycles by the Reaction of Thiols with Glyoxamides: Exploring a Connective Pummerer-Type Cyclisation. *Org. Biomol. Chem.* **2009**, *7*, 589–597. https://doi.org/10.1039/B816608K.

(12)   Liu, T.; Wu, K.; Wang, L.; Yu, Z. Potassium *tert*-Butoxide-Promoted Acceptorless Dehydrogenation of *N*-Heterocycles. *Adv. Synth. Catal.* **2019**, *361*, 3958–3964. https://doi.org/10.1002/adsc.201900499.

(13)   Luo, Z.; Sun, G.; Zhou, Z.; Liu, G.; Luan, B.; Lin, Y.; Zhang, L.; Wang, Z. Stereogenic *cis*-2-Substituted-*N*-Acetyl-3-Hydroxy-Indolines *via* Ruthenium(II)-Catalyzed Dynamic Kinetic Resolution-Asymmetric Transfer Hydrogenation. *Chem. Commun.* **2018**, *54*, 13503–13506. https://doi.org/10.1039/C8CC07336H.

(14)   Boydston, A. J.; Vu, P. D.; Dykhno, O. L.; Chang, V.; Wyatt, A. R.; Stockett, A. S.; Ritschdorff, E. T.; Shear, J. B.; Bielawski, C. W. Modular Fluorescent Benzobis(Imidazolium) Salts: Syntheses, Photophysical Analyses, and Applications. *J. Am. Chem. Soc.* **2008**, *130*, 3143–3156. https://doi.org/10.1021/ja7102247.

(15)   Karimi, B.; Akhavan, P. F. Main-Chain NHC-Palladium Polymer as a Recyclable Self-Supported Catalyst in the Suzuki–Miyaura Coupling of Aryl Chlorides in Water. *Chem. Commun.* **2009**, *25*, 3750-3752. https://doi.org/10.1039/b902096a.

(16) Karimi, B.; Akhavan, P. F. A Novel Water-Soluble NHC-Pd Polymer: An Efficient and Recyclable Catalyst for the Suzuki Coupling of Aryl Chlorides in Water at Room Temperature. *Chem. Commun.* **2011**, *47*, 7686-7688. https://doi.org/10.1039/c1cc00017a.

(17) Chen, J.; Wu, J.; Tu, T. Sustainable and Selective Monomethylation of Anilines by Methanol with Solid Molecular NHC-Ir Catalysts. *ACS Sustainable Chem. Eng.* **2017**, *5*, 11744–11751. https://doi.org/10.1021/acssuschemeng.7b03246.

(18) Sun, Z.; Chen, J.; Tu, T. NHC-Based Coordination Polymers as Solid Molecular Catalysts for Reductive Amination of Biomass Levulinic Acid. *Green Chem.* **2017**, *19*, 789–794. https://doi.org/10.1039/C6GC02591A.

(19) Huang, Q.; Qin, X.; Li, B.; Lan, J.; Guo, Q.; You, J. Cu-Catalysed Oxidative C–H/C–H Coupling Polymerisation of Benzodiimidazoles: An Efficient Approach to Regioregular Polybenzodiimidazoles for Blue-Emitting Materials. *Chem. Commun.* **2014**, *50*, 13739–13741. https://doi.org/10.1039/C4CC06291D.

(20) Visbal, R.; Laguna, A.; Gimeno, M. C. Highly Efficient Catalysis of Retro-Claisen Reactions: From a Quinone Derivative to Functionalized Imidazolium Salts. *Chem. Eur. J.* **2016**, *22*, 4189–4195. https://doi.org/10.1002/chem.201505095.

(21) Hoang, H.; Huang, X.; Skibo, E. B. Synthesis and *in vitro* Evaluation of Imidazole-Based Wakayin Analogues. *Org. Biomol. Chem.* **2008**, *6*, 3059-3064. https://doi.org/10.1039/b806883f.

(22) Bon, J. L.; Feng, D.; Marder, S. R.; Blakey, S. B. A C–H Functionalization Protocol for the Direct Synthesis of Benzobisthiazole Derivatives. *J. Org. Chem.* **2014**, *79*, 7766–7771. https://doi.org/10.1021/jo501416j.

(23) Shi, Q.; Zhang, S.; Zhang, J.; Oswald, V. F.; Amassian, A.; Marder, S. R.; Blakey, S. B. KO^{t}Bu-Initiated Aryl C–H Iodination: A Powerful Tool for the Synthesis of High Electron Affinity Compounds. *J. Am. Chem. Soc.* **2016**, *138*, 3946–3949. https://doi.org/10.1021/jacs.5b12259.

(24) Thottempudi, V.; Forohor, F.; Parrish, D. A.; Shreeve, J. M. Tris(triazolo)benzene and Its Derivatives: High-Density Energetic Materials. *Angew. Chem. Int. Ed.* **2012**, *51*, 9881–9885. https://doi.org/10.1002/anie.201205134.

(25) Pawliczek, M.; Garve, L. K. B.; Werz, D. B. Exploiting Amphiphilicity: Facile Metal Free Access to Thianthrenes and Related Sulphur Heterocycles. *Chem. Commun.* **2015**, *51*, 9165–9168. https://doi.org/10.1039/C5CC01757B.

(26) Pop, F.; Amacher, A.; Avarvari, N.; Ding, J.; Daku, L. M. L.; Hauser, A.; Koch, M.; Hauser, J.; Liu, S.-X.; Decurtins, S. Tetrathiafulvalene-Benzothiadiazoles as Redox-Tunable Donor-Acceptor Systems: Synthesis and Photophysical Study. *Chem. Eur. J.* **2013**, *19*, 2504–2514. https://doi.org/10.1002/chem.201202742.

(27) Zhu, W.; Yang, Y.; Métivier, R.; Zhang, Q.; Guillot, R.; Xie, Y.; Tian, H.; Nakatani, K. Unprecedented Stability of a Photochromic Bisthienylethene Based on Benzobisthiadiazole as an Ethene Bridge. *Angew. Chem. Int. Ed.* **2011**, *50*, 10986–10990. https://doi.org/10.1002/anie.201105136.

(28) Müller, M.; Koser, S.; Tverskoy, O.; Rominger, F.; Freudenberg, J.; Bunz, U. H. F. Thiadiazolo-Azaacenes. *Chem. Eur. J.* **2019**, *25*, 6082–6086. https://doi.org/10.1002/chem.201900462.

(29) Makarov, A. Yu.; Volkova, Y. M.; Shundrin, L. A.; Dmitriev, A. A.; Irtegova, I. G.; Bagryanskaya, I. Yu.; Shundrina, I. K.; Gritsan, N. P.; Beckmann, J.; Zibarev, A. V. Chemistry of Herz Radicals: A New Way to near-IR Dyes with Multiple Long-Lived and Differently-Coloured Redox States. *Chem. Commun.* **2020**, *56*, 727–730. https://doi.org/10.1039/C9CC08557B.

(30) Hoye, T. R.; Baire, B.; Niu, D.; Willoughby, P. H.; Woods, B. P. The Hexadehydro-Diels–Alder Reaction. *Nature* **2012**, *490*, 208–212. https://doi.org/10.1038/nature11518.

(31) Wang, T.; Hoye, T. R. Hexadehydro-Diels–Alder (HDDA)-Enabled Carbazolyne Chemistry: Single Step, de Novo Construction of the Pyranocarbazole Core of Alkaloids of the *Murraya Koenigii* (Curry Tree) Family. *J. Am. Chem. Soc.* **2016**, *138*, 13870–13873. https://doi.org/10.1021/jacs.6b09628.

(32) Dachs, A.; Torrent, A.; Roglans, A.; Parella, T.; Osuna, S.; Solà, M. Rhodium(I)-Catalysed Intramolecular [2+2+2] Cyclotrimerisations of 15-, 20- and 25-Membered Azamacrocycles: Experimental and Theoretical Mechanistic Studies. *Chem. Eur. J.* **2009**, *15*, 5289–5300. https://doi.org/10.1002/chem.200802548.

(33) Yang, J.; Zhao, B.; Xi, Y.; Sun, S.; Yang, Z.; Ye, Y.; Jiang, K.; Wei, Y. Construction of Benzene Rings by Copper-Catalyzed Cycloaddition Reactions of Oximes and Maleimides: An Access to Fused Phthalimides. *Org. Lett.* **2018**, *20*, 1216–1219. https://doi.org/10.1021/acs.orglett.8b00141.

(34) Suzuki, Y.; Ohta, Y.; Oishi, S.; Fujii, N.; Ohno, H. Efficient Synthesis of Aminomethylated Pyrroloindoles and Dipyrrolopyridines *via* Controlled Copper-Catalyzed Domino Multicomponent Coupling and Bis-Cyclization. *J. Org. Chem.* **2009**, *74*, 4246–4251. https://doi.org/10.1021/jo900681p.

(35) Lafzi, F.; Kilic, H.; Saracoglu, N. Protocols for the Syntheses of 2,2′-Bis(indolyl)arylmethanes, 2-Benzylated Indoles, and 5,7-Dihydroindolo[2,3-*b*]carbazoles. *J. Org. Chem.* **2019**, *84*, 12120–12130. https://doi.org/10.1021/acs.joc.9b02124.

(36) Prakash, K. S.; Nagarajan, R. Copper-Catalyzed Heteroannulation: A Simple Route to the Synthesis of Pyrrolo[2,3-*b*]carbazole and Pyrrolo[2,3-*b*]quinoline Derivatives. *Tetrahedron Lett.* **2015**, *56*, 69–72. https://doi.org/10.1016/j.tetlet.2014.10.070.

(37) Saha, S.; Banerjee, A.; Maji, M. S. Brønsted Acid Catalyzed One-Pot Benzannulation of 2-Alkenylindoles under Aerial Oxidation: A Route to Carbazoles and Indolo[2,3-*a*]carbazole Alkaloids. *Org. Lett.* **2018**, *20*, 6920–6924. https://doi.org/10.1021/acs.orglett.8b03063.

(38) Janreddy, D.; Kavala, V.; Bosco, J. W. J.; Kuo, C.-W.; Yao, C.-F. An Easy Access to Carbazolones and 2,3-Disubstituted Indoles. *Eur. J. Org. Chem.* **2011**, 2360–2365. https://doi.org/10.1002/ejoc.201001357.

(39) Gore, S.; Baskaran, S.; König, B. Fischer Indole Synthesis in Low Melting Mixtures. *Org. Lett.* **2012**, *14*, 4568–4571. https://doi.org/10.1021/ol302034r.

(40) Sakthivel, S.; Balamurugan, R. Annulation of a Highly Functionalized Diazo Building Block with Indoles under Sc(OTf)$_3$/Rh$_2$(OAc)$_4$ Multicatalysis through Michael Addition/Cyclization Sequence. *J. Org. Chem.* **2018**, *83*, 12171–12183. https://doi.org/10.1021/acs.joc.8b02127.

(41) Okano, K.; Mitsuhashi, N.; Tokuyama, H. Total Synthesis of PDE-II by Copper-Mediated Double Amination. *Chem. Commun.* **2010**, *46*, 2641-2643. https://doi.org/10.1039/b926965g.

(42) Kaschel, J.; Schneider, T. F.; Kratzert, D.; Stalke, D.; Werz, D. B. Domino Reactions of Donor-Acceptor-Substituted Cyclopropanes for the Synthesis of 3,3′-Linked Oligopyrroles and Pyrrolo[3,2-*e*]indoles. *Angew. Chem. Int. Ed.* **2012**, *51*, 11153–11156. https://doi.org/10.1002/anie.201205880.

(43) Fuse, S.; Takahashi, R.; Takahashi, T. Facile, One-Step Synthesis of 5-Substituted Thieno[3,4-*c*]pyrrole-4,6-dione by Palladium-Catalyzed Carbonylative Amidation. *Eur. J. Org. Chem.* **2015**, 3430–3434. https://doi.org/10.1002/ejoc.201500273.

(44) Lee, S.; Chataigner, I.; Piettre, S. R. Facile Dearomatization of Nitrobenzene Derivatives and Other Nitroarenes with *N*-Benzyl Azomethine Ylide. *Angew. Chem. Int. Ed.* **2011**, *50*, 472–476. https://doi.org/10.1002/anie.201005779.

(45) Coulibali, S.; Godou, T.; Canesi, S. Use of the Nosyl Group as a Functional Protecting Group in Applications of a Michael/Smiles Tandem Process. *Org. Lett.* **2016**, *18*, 4348–4351. https://doi.org/10.1021/acs.orglett.6b02105.

(46) Inman, M.; Moody, C. J. Copper(II)-Mediated Synthesis of Indolequinones from Bromoquinones and Enamines. *Eur. J. Org. Chem.* **2013**, 2179–2187. https://doi.org/10.1002/ejoc.201201597.

(47) Vanicat, A.; André-Barrès, C.; Delfourne, E. New Reaction of Formation of the Fused Tricyclic Bispyrroloquinone Ring System. *Tetrahedron Lett.* **2017**, *58*, 342–345. https://doi.org/10.1016/j.tetlet.2016.12.030.

(48) Murugesan, S.; Nadkarni, D. H.; Velu, S. E. A Facile Synthesis of Bispyrroloquinone and Bispyrroloiminoquinone Ring System of Marine Alkaloids. *Tetrahedron Lett.* **2009**, *50*, 3074–3076. https://doi.org/10.1016/j.tetlet.2009.04.021.

(49) Nadkarni, D. H.; Murugesan, S.; Velu, S. E. Total Synthesis of Zyzzyanones A–D. *Tetrahedron* **2013**, *69*, 4105–4113. https://doi.org/10.1016/j.tet.2013.03.052.

(50) Wang, C.; Sperry, J. Total Synthesis of the Photoprotecting Dipyrrolobenzoquinone (+)-Terreusinone. *Org. Lett.* **2011**, *13*, 6444–6447. https://doi.org/10.1021/ol2027398.

(51) Hu, Z.; Dong, J.; Li, Z.; Yuan, B.; Wei, R.; Xu, X. Metal-Free Triple Annulation of Ene–Yne–Ketones with Isocyanides: Domino Access to Furan-Fused Heterocycles *via* Furoketenimine. *Org. Lett.* **2018**, *20*, 6750–6754. https://doi.org/10.1021/acs.orglett.8b02870.

(52) Dong, J.; Zhang, D.; Men, Y.; Zhang, X.; Hu, Z.; Xu, X. [1+2+3] Annulation as a General Access to Indolo[3,2-*b*]carbazoles: Synthesis of Malasseziazole C. *Org. Lett.* **2019**, *21*, 166–169. https://doi.org/10.1021/acs.orglett.8b03646.

(53) Saravanan, V.; Mageshwaran, T.; Mohanakrishnan, A. K. Synthesis of Cyclo[*b*]fused Carbazoles *via* SnCl$_4$-Mediated Domino Reaction of 2-Indolylmethylpivalates with Arenes and Heteroarenes. *J. Org. Chem.* **2016**, *81*, 8633–8646. https://doi.org/10.1021/acs.joc.6b01646.

(54) Lee, P.-S.; Yoshikai, N. Aldimine-Directed Branched-Selective Hydroarylation of Styrenes. *Angew. Chem. Int. Ed.* **2013**, *52*, 1240–1244. https://doi.org/10.1002/anie.201207958.

(55) Liu, X.; Sheng, H.; Zhou, Y.; Song, Q. Palladium-Catalyzed C–H Bond Activation for the Assembly of *N*-Aryl Carbazoles with Aromatic Amines as Nitrogen Sources. *Chem. Commun.* **2020**, *56*, 1665–1668. https://doi.org/10.1039/C9CC09493H.

(56) Vakuliuk, O.; Jun, Y. W.; Vygranenko, K.; Clermont, G.; Reo, Y. J.; Blanchard-Desce, M.; Ahn, K. H.; Gryko, D. T. Modified Isoindolediones as Bright Fluorescent Probes for Cell and Tissue Imaging. *Chem. Eur. J.* **2019**, *25*, 13354-13362. https://doi.org/10.1002/chem.201902534.

(57) Fan, X.; Yu, L.-Z.; Wei, Y.; Shi, M. Cascade Amination/Cyclization/Aromatization Process for the Rapid Construction of [2,3-*c*]Dihydrocarbazoles and [2,3-*c*]Carbazoles. *Org. Lett.* **2017**, *19*, 4476–4479. https://doi.org/10.1021/acs.orglett.7b01957.

(58) Xia, Y.; Liu, Z.; Xiao, Q.; Qu, P.; Ge, R.; Zhang, Y.; Wang, J. Rhodium(II)-Catalyzed Cyclization of Bis(*N*-Tosylhydrazone)s: An Efficient Approach towards Polycyclic Aromatic Compounds. *Angew. Chem. Int. Ed.* **2012**, *51*, 5714–5717. https://doi.org/10.1002/anie.201201374.

(59) Spindler, B.; Kataeva, O.; Knölker, H.-J. Enantioselective Total Synthesis and Assignment of the Absolute Configuration of the Furo[3,2-*a*]carbazole Alkaloid Furoclausine-B. *J. Org. Chem.* **2018**, *83*, 15136–15143. https://doi.org/10.1021/acs.joc.8b02426.

(60) Bodunov, V. A.; Galenko, E. E.; Sakharov, P. A.; Novikov, M. S.; Khlebnikov, A. F. Selective Cu-Catalyzed Intramolecular Annulation of 3-Aryl/Heteryl-2-(diazoacetyl)-1*H*-pyrroles: Synthesis of Benzo/Furo/Thieno[*e*]-Fused 1*H*-Indol-7-oles and Their Transformations. *J. Org. Chem.* **2019**, *84*, 10388–10401. https://doi.org/10.1021/acs.joc.9b01573.

(61) Yoon, H.; Marchese, A. D.; Lautens, M. Carboiodination Catalyzed by Nickel. *J. Am. Chem. Soc.* **2018**, *140*, 10950–10954. https://doi.org/10.1021/jacs.8b06966.

(62) Budaev, A. B.; Ivanov, A. V.; Petrova, O. V.; Samsonov, V. A.; Ushakov, I. A.; Tikhonov, A. Ya.; Sobenina, L. N.; Trofimov, B. A. 1,2,5-Oxadiazolo[3,4-*g*]indoles *via* Annelation of 6,7-Dihydrobenzo[*c*][1,2,5]oxadiazol-4(5*H*)-one Oxime with Acetylene. *Mendeleev Commun.* **2019**, *29*, 53–54. https://doi.org/10.1016/j.mencom.2019.01.016.

(63) He, H.; Guo, J.; Sun, W.; Yang, B.; Zhang, F.; Liang, G. Palladium-Catalyzed Direct Mono- or Polyhalogenation of Benzothiadiazole Derivatives. *J. Org. Chem.* **2020**, *85*, 3788–3798. https://doi.org/10.1021/acs.joc.9b03418.

(64) Andeme Edzang, J.; Chen, Z.; Audi, H.; Canard, G.; Siri, O. Transamination at the Crossroad of the One-Pot Synthesis of *N*-Substituted Quinonediimines and C-Substituted Benzobisimidazoles. *Org. Lett.* **2016**, *18*, 5340–5343. https://doi.org/10.1021/acs.orglett.6b02640.

(65) Berezin, A. A.; Koutentis, P. A. Ring Contraction of 1,3-Diphenylbenzo[1,2,4]triazinyl Radicals to 1,2-Diphenylbenzimidazoles. *Org. Biomol. Chem.* **2014**, *12*, 1641–1648. https://doi.org/10.1039/C3OB42130A.

(66) Mike, J. F.; Makowski, A. J.; Jeffries-EL, M. An Efficient Synthesis of 2,6-Disubstituted Benzobisoxazoles: New Building Blocks for Organic Semiconductors. *Org. Lett.* **2008**, *10*, 4915–4918. https://doi.org/10.1021/ol802011y.

(67) Aksenov, N. A.; Aksenov, A. V.; Nadein, O. N.; Aksenov, D. A.; Smirnov, A. N.; Rubin, M. One-Pot Synthesis of Benzoxazoles *via* the Metal-Free *ortho*-C–H Functionalization of Phenols with Nitroalkanes. *RSC Adv.* **2015**, *5*, 71620–71626. https://doi.org/10.1039/C5RA15128G.

(68) An, J.; Alper, H.; Beauchemin, A. M. Copper-Catalyzed Cascade Substitution/Cyclization of *N*-Isocyanates: A Synthesis of 1-Aminobenzimidazolones. *Org. Lett.* **2016**, *18*, 3482–3485. https://doi.org/10.1021/acs.orglett.6b01686.

(69) Hassan, Z.; Langer, P. Mild and Convenient Synthesis of Benzodithiazoles by Oxidative Cyclization of Bis(Thiobenzanilides). *Synlett* **2012**, *23*, 2811–2813. https://doi.org/10.1055/s-0032-1317510.

(70) Madhav, J. V.; Kuarm, B. S.; Rajitha, B. Dipyridine Copper Chloride as a Mild and Efficient Catalyst for the Solid State Synthesis of 2-Substituted Benzimidazoles. *Arkivoc* **2008**, 145–150. http://dx.doi.org/10.3998/ark.5550190.0009.d17.

(71) Chen, P.-F.; Kuo, K.-K.; Vandavasi, J. K.; Boominathan, S. S. K.; Chen, C.-Y.; Wang, J.-J. Metal-Free Cycloaddition to Synthesize Naphtho[2,3-*d*][1,2,3]triazole-4,9-diones. *Org. Biomol. Chem.* **2015**, *13*, 9261–9266. https://doi.org/10.1039/C5OB01322D.

(72) Tam, T. L.; Tan, H. H. R.; Ye, W.; Mhaisalkar, S. G.; Grimsdale, A. C. One-Pot Synthesis of 4,8-Dibromobenzo[1,2-*d*;4,5-*d'*]bistriazole and Synthesis of Its Derivatives as New Units for Conjugated Materials. *Org. Lett.* **2012**, *14*, 532–535. https://doi.org/10.1021/ol2031558.

(73) Juríček, M.; Stout, K.; Kouwer, P. H. J.; Rowan, A. E. Fusing Triazoles: Toward Extending Aromaticity. *Org. Lett.* **2011**, *13*, 3494–3497. https://doi.org/10.1021/ol201290q.

(74) Jovené, C.; Jacquet, M.; Chugunova, E. A.; Kharlamov, S. V.; Goumont, R. Synthesis and 1-Oxide/3-Oxide Interconversion of 4-Substituted Benzodifuroxans: A Thorough NMR and Theoretical Study of the Structure of 4-Fluoro- and 4-Chloro-Benzodifuroxan. *Tetrahedron* **2016**, *72*, 2057–2063. https://doi.org/10.1016/j.tet.2016.03.021.

(75) Lin, Y.; Chen, Y.; Ma, X.; Xu, D.; Cao, W.; Chen, J. Aryne Click Chemistry: Synthesis of Oxadisilole Fused Benzotriazoles or Naphthotriazoles from Arynes and Azides. *Tetrahedron* **2011**, *67*, 856–859. https://doi.org/10.1016/j.tet.2010.12.039.

(76) Ma, X.; Chen, Y.; Zhang, Y.; Xu, D.; Cao, W.; Chen, J. Synthesis and Study of Oxadisilole-Fused Benzisoxazoles or Naphthisoxazoles. *Eur. J. Org. Chem.* **2012**, 1388–1393. https://doi.org/10.1002/ejoc.201101583.

(77) Wakamiya, A.; Murakami, T.; Yamaguchi, S. Benzene-Fused BODIPY and Fully-Fused BODIPY Dimer: Impacts of the Ring-Fusing at the *b* Bond in the BODIPY Skeleton. *Chem. Sci.* **2013**, *4*, 1002–1007. https://doi.org/10.1039/C2SC21768F.

(78) Mofford, D. M.; Adams, S. T.; Reddy, G. S. K. K.; Reddy, G. R.; Miller, S. C. Luciferin Amides Enable *in Vivo* Bioluminescence Detection of Endogenous Fatty Acid Amide Hydrolase Activity. *J. Am. Chem. Soc.* **2015**, *137*, 8684–8687. https://doi.org/10.1021/jacs.5b04357.

(79) Favre, H. A.; Powell, W. H. *Nomenclature of Organic Chemistry*; The Royal Society of Chemistry, 2013.

(80) Rasmussen, S. C. The Nomenclature of Fused-Ring Arenes and Heterocycles: A Guide to an Increasingly Important Dialect of Organic Chemistry. *ChemTexts* **2016**, *2*. https://doi.org/10.1007/s40828-016-0035-3.

Chapter 2

H$_2$O$_2$/HI: Oxidative Cyclizations towards Spirocyclic Oxetane and Morpholine-Fused Benzimidazolequinones, and Serendipitous Synthesis of 1,4,6,9-Tetramethoxyphenazine
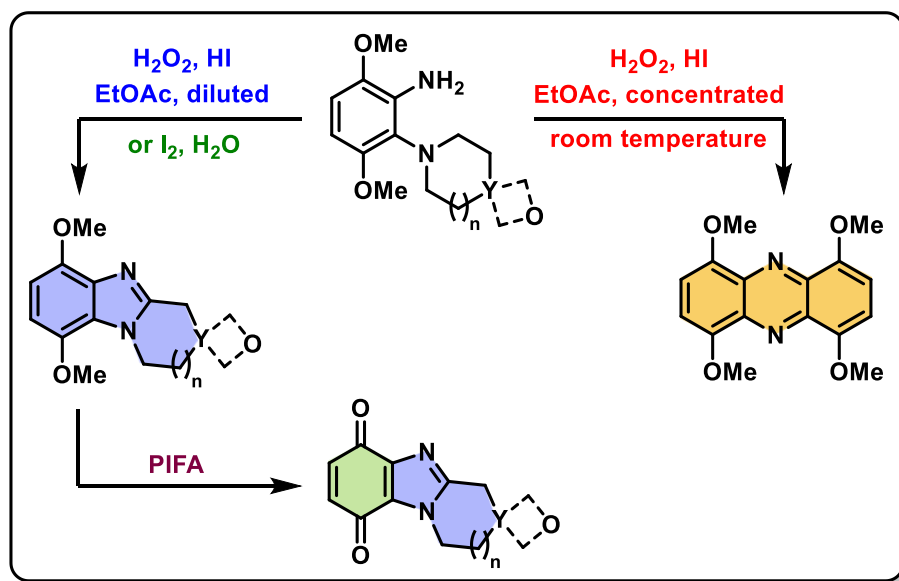
Parts of this Chapter are published in:

2.1. Introduction

2.1.1. Benzimidazolequinone Anti-Tumour Agents

The targeting of enzymes overexpressed in tumours represents a powerful strategy in the development of selective anticancer therapeutics. Reductases such as NAD(P)H cytochrome c P450 reductase (CYP450) and NAD(P)H:quinone oxidoreductase 1 (NQO1) are expressed at elevated concentrations in tumour cells.[1–4] Both enzymes are implicated in the bioreductive activation of the natural product, mitomycin C (MMC),[1] an antitumour prodrug used since the 1970s.[5] CYP450-mediated bioreduction is a single-electron process, which occurs under hypoxic conditions (Scheme 2.1).[4] In the presence of oxygen, the intermediate semiquinone radical anion is reoxidized, with concurrent superoxide formation.[4] In contrast, the two-electron NQO1-mediated bioreduction irreversibly yields a hydroquinone.[3] The unstable electron-rich products of bioreduction possess reactive electrophilic sites at C-1 and C-10, which alkylate tumour cell DNA (Scheme 2.1).[1]
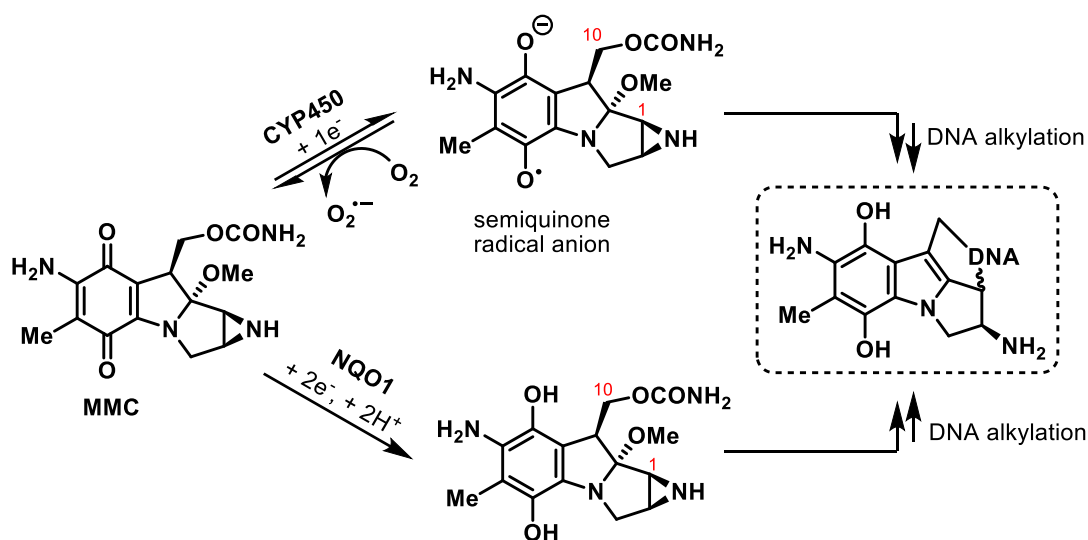
Scheme 2.1. Bioreductive activation of MMC.[1–4]

At its core, MMC is an indolequinone, and Moody and co-workers have extensively explored the development of synthetic analogues,[1] including the cyclopropamitosenes (Figure 2.1).[6–9] The premise for bioactivity was based upon radical ring-opening of the cyclopropane ring upon single-electron bioreduction generating a reactive primary radical, capable of hydrogen atom abstraction from DNA.[1] O'Shaughnessy and Aldabbagh prepared cyclopropane-fused benzimidazolequinones, whose basic nitrogen (highlighted) elicited a lower reduction potential

(–1.052 V, vs. ferrocene, Fc) than that of methoxy-substituted cyclopropamitosenes (–1.395 V, vs. Fc), thus facilitating more facile bioreduction.[10,11]
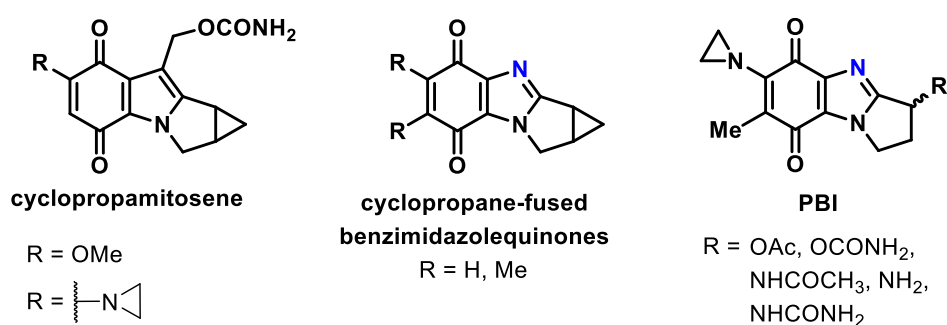
Figure 2.1. Cyclopropamitosenes and related benzimidazolequinones.

The first reports of anti-tumour benzimidazolequinones were by the group of Skibo, who developed the pyrrolo[1,2-*a*]benzimidazolequinones (PBIs; Figure 2.1).[12–19] Evaluation of bioactivity against the 60 cell lines at the National Cancer Institute (NCI) revealed cytotoxicity against CNS, ovarian, renal, breast, colon and non-small cell lung cancer cell lines.[12–19] Bioreduction of the electron-deficient PBIs to the electron-rich hydroquinone derivatives, activates the aziridinyl-ring towards alkylation at the DNA-phosphate backbone, with site-specific hydrogen bonds to A-T and G-C base pair in the major groove of DNA.[20]

Several different anti-tumour benzimidazolequinone scaffolds were developed in the Aldabbagh group. Pyrido[1,2-*a*]benzimidazolequinone possessed nanomolar cytotoxicity under hypoxic conditions with favourable hypoxia cell ratios (Figure 2.2).[21] Adding methyl groups at the 7- and 8-positions was found to decrease cytotoxicity due to inductive electron-donation increasing reductive potential.[21]
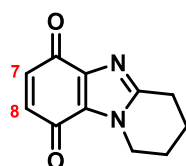
Figure 2.2. Pyrido[1,2-*a*]benzimidazolequinone with nanomolar cytotoxicity.[21]

Increasing the conjugation of the benzimidazolequinone scaffold was investigated as a means of improving cytotoxicity through increasing the stability of reduced hydroquinone intermediates.[22] The phenyl, pyrido and naphthyl-[1,2-*a*] fused benzimidazoles displayed *in vitro* selectivity towards the HeLa and DU-145 cancer cell lines, which overexpress NQO1, compared to the GM00637 normal skin fibroblast cell line (Figure 2.3).[22]

53
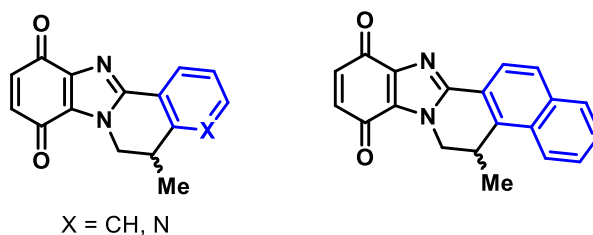
Figure 2.3. Conjugated benzimidazolequinones.[22]

Aldabbagh *et al*. reported benzimidazolequinones to target the FANC repair pathway, which malfunctions in Fanconi Anaemia (FA). The rare genetic childhood disease is characterized by hypersensitivity to cross-linking agents (*e.g.* MMC).[23,24] The scaffolds incorporated an aziridine ring, but unlike MMC there was only one position for alkylation of DNA, thus crosslinking was not possible (Figure 2.4).[23,24] The aziridinyl-substituted benzimidazolequinones displayed nanomolar cytotoxicity against the PD20i FA cell line deficient in FANCD2 protein with expression of FANCD2 correcting hypersenstivity.[23,24] Surprisingly however, non-fused 4,7-dimethoxybenzimidazole with pendant aziridinyl ring also showed hypersensitivity towards the FANCD2 deficient cell line, indicating that bioreduction and crosslinking are unnecessary for the response of aziridines *via* the FANC pathway.[24]
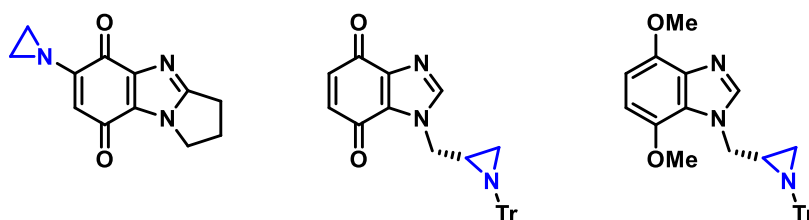
Figure 2.4. Benzimidazole(quinone)s targeted towards FA.[23,24]

Given the cytotoxicity of the aziridine-substituted *p*-dimethoxybenzimidazole, further benzimidazole scaffolds were prepared with both a fused and non-fused aziridine ring (Figure 2.5).[25] Evaluation of compounds revealed 4-8 times greater toxicity towards the MCF-7 and HCC1937 breast cancer cell lines, than the GM00637 normal skin fibroblast cell line. The aziridine ring-fused benzimidazole was less toxic than the non-fused derivative. MMC was also evaluated, and was found to display selective cytotoxicity towards the HCC1937 (BRCA1 deficient) cell line compared to the MCF-7 (BRCA1 expressing) cell line.[25] BRCA1 is a protein responsible for cellular response to DNA crosslinks and BRCA proteins are implicated in the FANC pathway.[25] The lack of specificity of aziridine-substituted benzimidazoles towards the HCC1937 cell line indicates a different mechanism of cytotoxicity compared to MMC. Unlike

MMC, the benzimidazoles cannot undergo crosslinking to DNA since there is only one position for DNA-alkylation.[25]
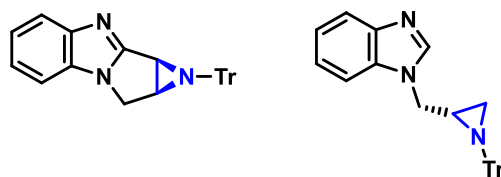
Figure 2.5. Cytotoxic aziridine-functionalized benzimidazoles.[25]

Imidazobenzimidazolequinones, and iminoquinone synthetic precursors have shown specificity towards NQO1.[26–30] Their synthesis and bioactivity will be discussed in more detail in Chapters 3 and 4. Upon establishing the remarkable selectivity of pyrido-fused imidazo[5,4-*f*]benzimidazoleiminoquinone towards cell lines that overexpress NQO1 (Figure 2.6), Fagan and Aldabbagh carried out computational docking.[30] It was deduced that the existing scaffold was not exploiting a possible hydrogen bonding interaction with an available histidine residue (His194) in the active site of NQO1.[30] Therefore, introducing a hydrogen bonding acceptor 4- to 5-bonds away from the reducible (imino)quinone was proposed, as a means of further increasing binding of iminoquinone and quinone imidazobenzimidazole derivatives at the NQO1 active site.[30]
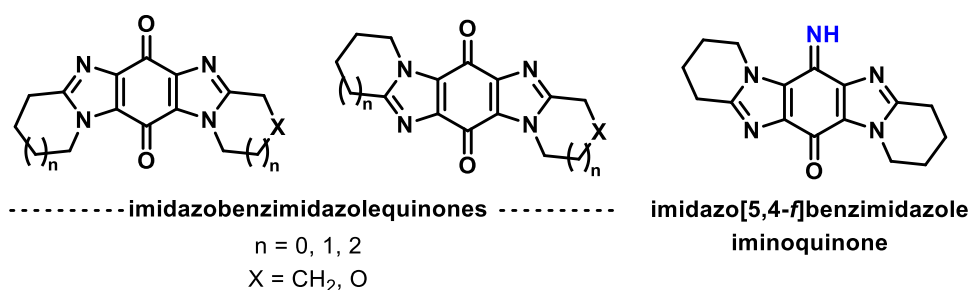
Figure 2.6. Imidazobenzimidazolequinones and iminoquinone.

2.1.2. Oxidative Cyclizations to give Benzimidazole(quinone)s

Benzimidazoles are invaluable scaffolds in medicinal chemistry,[31–33] and are often synthetic precursors of benzimidazolequinones. The oxidative cyclization of *o*-cyclic amine-substituted anilines represents a well-established and powerful strategy for their synthesis. The earliest example published in 1908 by Spiegel and Kaufmann exploited peroxysulfuric acid (Caro's acid) to cyclize 5-nitro-2-(piperidin-1-yl)aniline to the benzimidazole.[34] Over 50 years later, Nair and Adams reported that peroxytrifluoroacetic acid generated *in situ* from the reaction of H_2O_2 with TFA, could be used in place of Caro's acid to mediate the cyclization (Scheme 2.2).[35] The scope included pyrrolo-, pyrido-, morpholino- and azepino-substituted anilines, with the presence of an electron-withdrawing group *para* to the cyclic amine improving the yield of cyclization.[35]

R				
H	81%	58%	73%	91%
Cl	75%	66%	62%	–
Me	86%	60%	61%	–
NO$_2$	72%	95%	76%	–
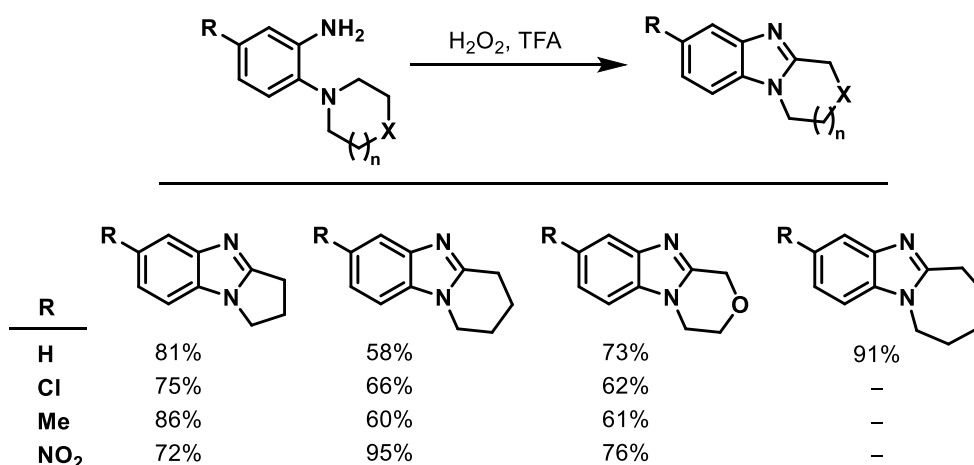
Scheme 2.2. Oxidative cyclization mediated by peroxytrifluoroacetic acid.[35]

The scope of oxidative cyclizations towards ring-fused benzimidazoles was further expanded by Meth-Cohn with Suschitzky, who used H_2O_2 in combination with HCO_2H to generate performic acid *in situ*, which cyclized a range of *o*-cycloamino anilines (Scheme 2.3).[36] The acylated derivatives cyclized with equal efficiency.[36] The same authors later generalized that *tert*-anilines bearing an appropriate *ortho*-substituent (*e.g.* amine, nitroso, azide, anilide) have a tendency to undergo cyclization. Meth-Cohn with Suschitzky termed the tendency for cyclization the "*tert*-amino effect,"[37,38] which has since been exploited to cyclize a wide variety of substrates.[39] Furthermore, the H_2O_2/HCO_2H combination has since been extensively employed in the cyclization of benzimidazoles and imidazobenzimidazoles.[12,13,16,26,27,40]

56
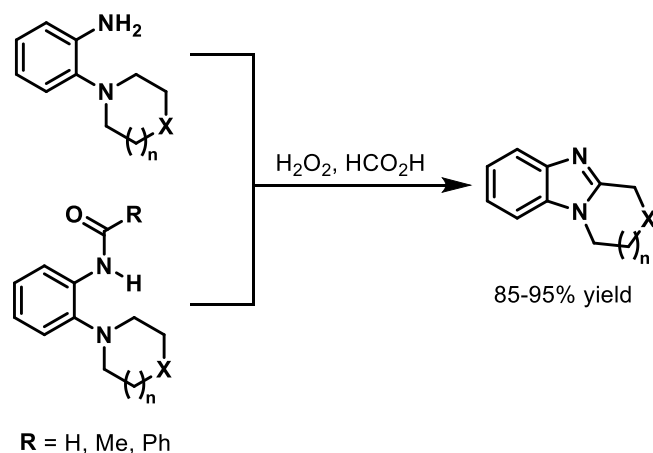
Scheme 2.3. Performic acid-mediated oxidative cyclizations.[36]

The use of hydrogen peroxide as oxidant is advantageous in organic synthesis since it is cheap, of low molecular weight to allow high atom economy, odourless, and eco-friendly.[41] Aldabbagh *et al*. have shown that it can be used independently to cyclize *o*-(pyrrolidin-1-yl)anilines to the pyrrolo[1,2-*a*]benzimidazoles in good yields, without the requirement for organic-aqueous extraction or column chromatography (Table 2.1).[42] Ethyl acetate was used as the reaction solvent, given its status as a green solvent.[43] Azepino- and azocino-substituted anilines also cyclized in good yields.[42] Pyrido-substituted aniline, and 3,6-dimethoxy-2-(cycloamino)anilines bearing an *ortho* six-, seven- or eight-membered alicyclic ring required the addition of a stoichiometric equivalent of the environmentally benign methanesulfonic acid to cyclize.

Table 2.1. Environmentally benign oxidative cyclizations using H_2O_2.[42]

64-93% yield
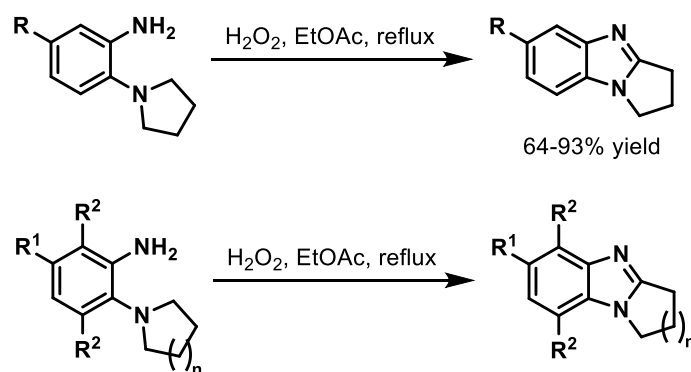
R^1	R^2	n	Yield (%)
OMe	H	1	79
OMe	H	2^a	75
OMe	H	3	65
OMe	H	4	73
H	OMe	1	81
H	OMe	2^a	80
H	OMe	3^a	72
H	OMe	4^a	60

^{a}Methanesulfonic acid (1 equiv) added.

Combining H_2O_2 with hydrohalic acids (HX) is a means of generating the molecular halogens (X_2; Scheme 2.4). The H_2O_2/HX combination initially yields the hypohalous acid (HOX),[44] which in the presence of excess acid, drives the equilibrium towards X_2 formation.[45]

$$(1)\quad H_2O_2 + HX \longrightarrow HOX + H_2O$$
$$(2)\quad HOX + HX \rightleftharpoons X_2 + H_2O$$

Scheme 2.4. The combination of H_2O_2 and HX.

Aldabbagh *et al*. have shown that reacting *o*-cyclic amine substituted anilines with H_2O_2 (10 equiv) and HX (12 equiv; X = Cl, Br) mediates regioselective aromatic halogenation in addition to oxidative cyclization, to yield dihalogenated ring-fused benzimidazoles (Scheme 2.5).[46] Chlorinations proceeded in mostly excellent yields after 20 min, and tolerated the presence of electron-withdrawing and electron-donating R-groups. In most cases column chromatography

was not required. The analogous brominations also proceeded in mostly good yields, with the same disubstitution pattern observed when R = H, indicating the regioselectivity is not dictated by the R-group. The brominations were affected to a greater extent by the electron-density of the ring than the chlorinations, as the trifluoromethyl-substituted substrate did not undergo bromination, while mono-brominated products were obtained for cyano- and fluoro-substituted anilines.[46] Replacing H_2O_2 as the oxidant with commercial bleach resulted in the same transformation as the H_2O_2/HCl combination, with the moderate yield of 56% attributed to the necessity for column chromatography to separate additives in the bleach.[46]
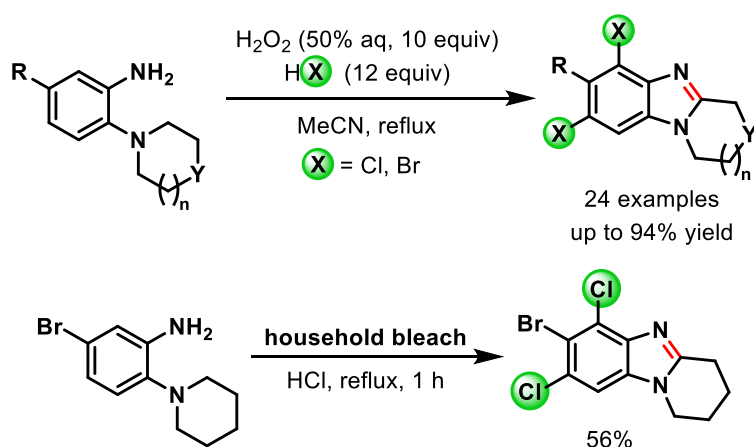
Scheme 2.5. One-pot halogenation and oxidative cyclization using H_2O_2/HX.[46]

When the H_2O_2 and HX (X = Cl, Br) system was applied to 3,6-dimethoxy-2-(cycloamino)anilines, a tuneable one-pot transformation was established (Scheme 2.6).[47] A higher molar amount of H_2O_2 relative to HX resulted in oxidative cyclization and halogenation, while lower amounts of H_2O_2 relative to HX mediated one-pot halogenation, cyclization, and quinone formation, so generating halogenated ring-fused benzimidazolequinones. A larger proportion of the hydrohalic acid relative to hydrogen peroxide favours halogen (X_2) formation (Scheme 2.4), and molecular chlorine and bromine in water were shown to independently mediate the six-electron oxidative transformations to give the halogenated ring-fused benzimidazolequinones (Scheme 2.6).
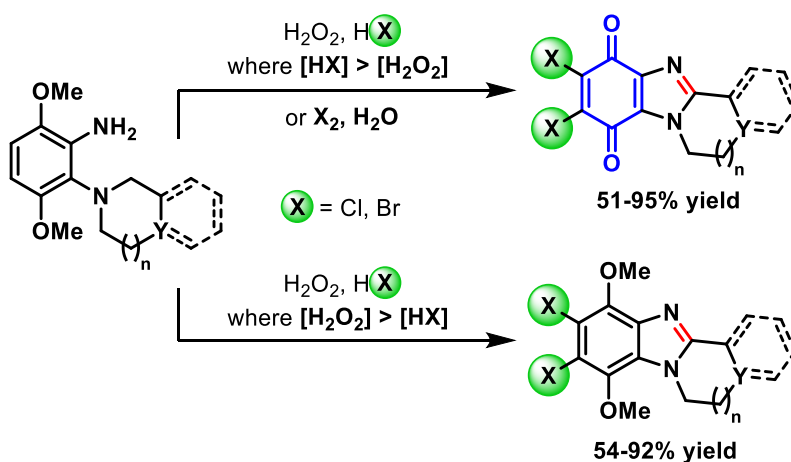
Scheme 2.6. Tuneable H_2O_2/HX-mediated transformations of 3,6-dimethoxy-2-(cycloamino)anilines.[47]

In recent years various miscellaneous oxidative cyclizations have been reported that give ring-fused benzimidazoles. Foss Jr. and co-workers used catalytic quantities of $FeCl_3 \cdot 6H_2O$ to cyclize *o*-cyclic amine substituted anilines to give a wide range of benzimidazoles, including ring-fused derivatives (Scheme 2.7).[48] Tetrahydroisoquinoline (THIQ) substrates bearing various functional groups cyclized in good to excellent yields. However, the reaction did not tolerate the morpholine substrate, which gave only trace amounts of the benzimidazole. The presence of air was found to be necessary to drive the cyclization.
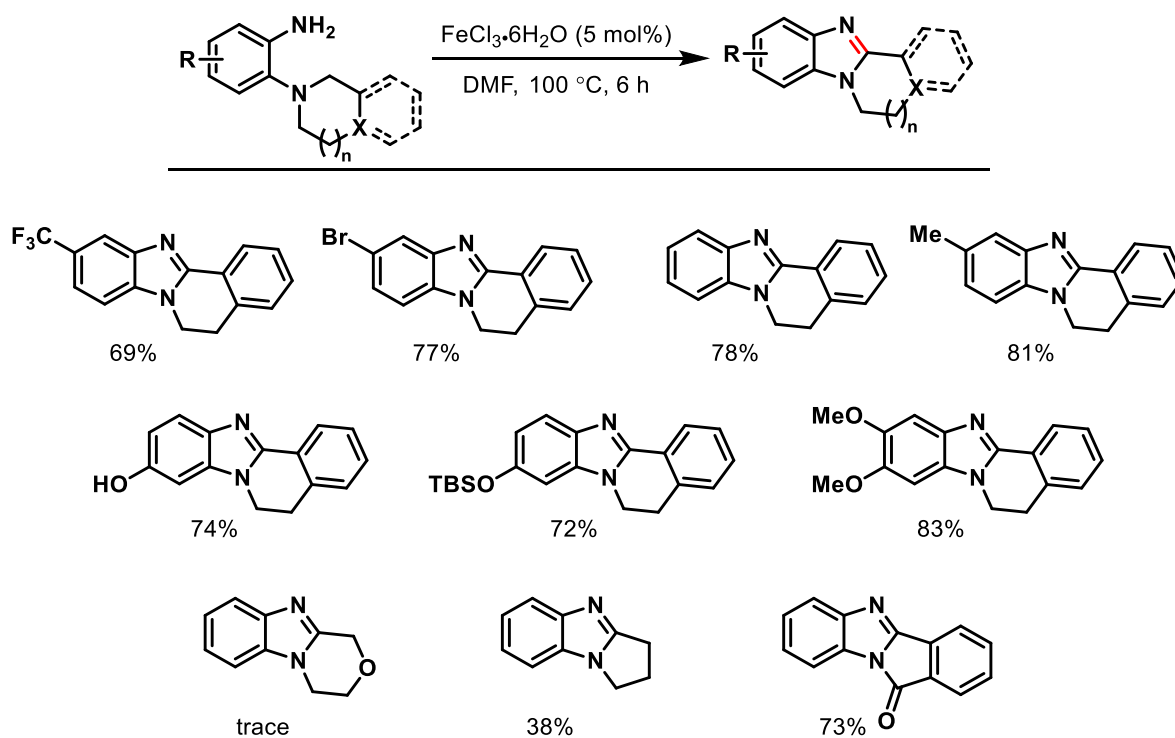
Scheme 2.7. Oxidative cyclization with catalytic FeCl$_3$.[48]

PIFA-mediated the oxidative cyclization of biphenyl-substituted benzimidazoles with symmetrically-substituted benzimidazoles cyclizing in excellent yields. (Scheme 2.8).[49] However a disadvantage of already having the benzimidazole in place is the tendency for the imidazole to undergo tautomerism, which led to the formation of regioisomers for unsymmetrically monosubstituted substrates. The reaction reportedly proceeded *via* PIFA oxidation of the benzimidazole to the nitrenium ion, which undergoes electrophilic substitution onto the neighbouring phenyl ring. Aromatization *via* loss of a proton is likely mediated by a trifluoroacetate ion liberated in the initial PIFA oxidation step.[49]
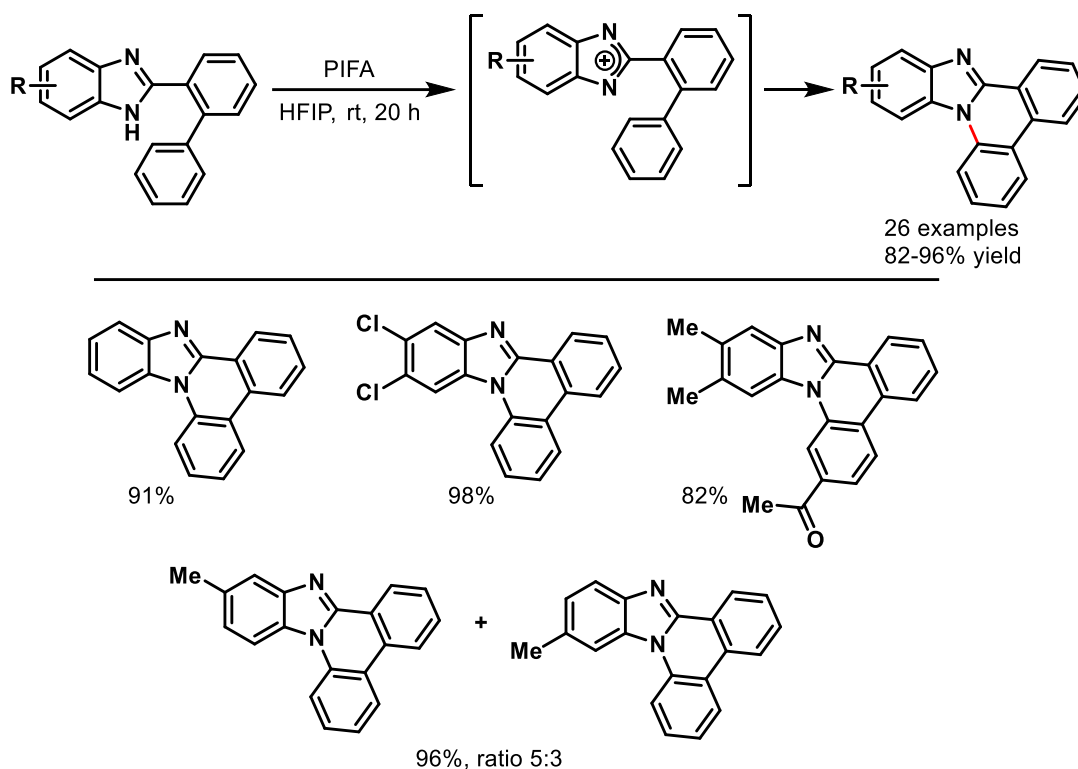
Scheme 2.8. Cyclization *via* PIFA-mediated formation of nitrenium ion.[49]

Electrochemistry has undergone a renaissance in recent years, and has been applied to the synthesis of ring-fused benzimidazoles.[50] Using Reticulated Vitreous Carbon (RVC) as the anode and Pt as the cathode in an undivided cell at a constant current of 10 mA with *n*-Bu$_4$NPF$_6$ as the electrolyte, *o*-cyclic amine substituted anilines underwent oxidative cyclization to yield pyrrolo-, pyrido-, morpholino-, thiomorpholino- and tetrahydroisoquinoline-[1,2-*a*]-fused benzimidazoles (Scheme 2.9). Mostly good to excellent yields were obtained, however the presence of an inductively withdrawing trifluoromethyl group on the aromatic ring diminished the yield somewhat. The morpholine substrate cyclized in a moderate 52% yield, while only trace amounts of the thiomorpholine analogue were obtained. Mechanistically, the *o*-cyclic amine substituted anilines undergo SET oxidation at the anode, with the radical cation undergoing further oxidation to yield the iminium ion on the *tert*-amine. The iminium ion undergoes cyclization as per the *tert*-amino effect, and the system aromatizes *via* further 2-electron anodic oxidation.[50]
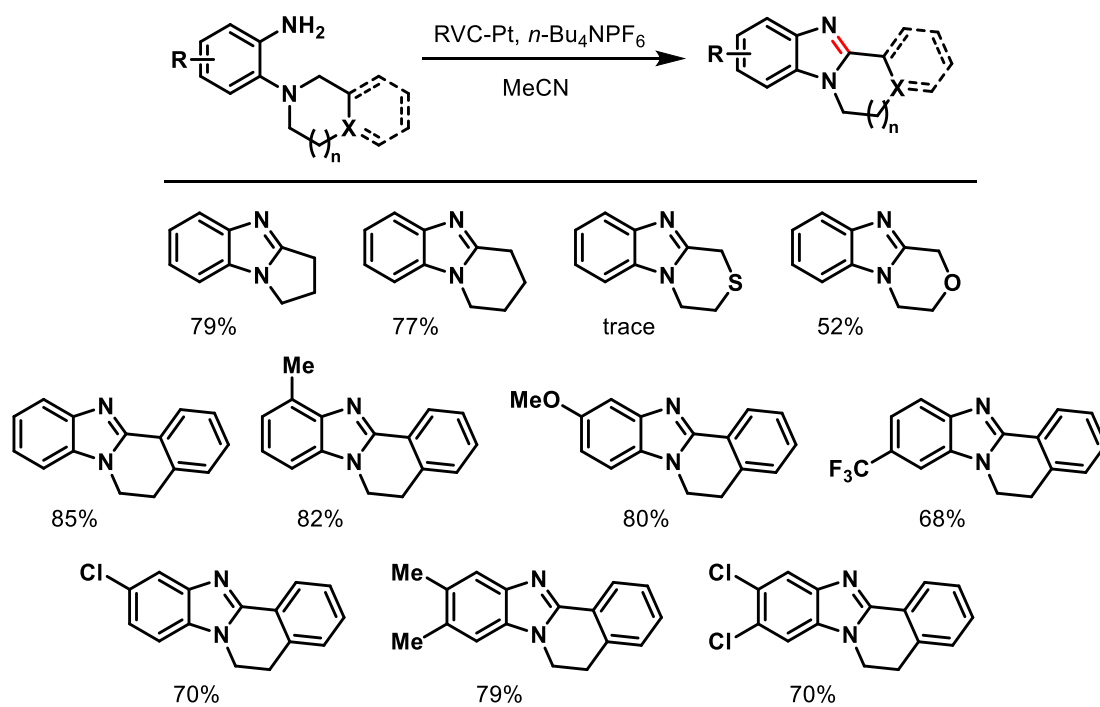
Scheme 2.9. Benzimidazole formation *via* electrochemical oxidation.[50]

2.1.3. Morpholine and Oxetane

Morpholine is a prevalent heterocycle in marketed drugs with some examples shown in Figure 2.7a.[51] Moclobemide is an anti-depressant which reversibly inhibits monoamine oxidase (MAO). Linezolid is an antibiotic, while Gefitinib is an anticancer agent whose mechanism of action is the inhibition of epidermal growth factor receptor (EGFR). Introducing morpholine into bioactive molecules in place of alternative functional groups can have a profound improvement in pharmacokinetic (PK) properties.[52,53] Replacing the piperidine ring on Gleave and co-workers' CB2 agonist with morpholine decreased the clearance rate over 12-fold (Figure 2.7b).[54] Making the same alteration to Wan and co-workers' 11β-hydroxysteroid dehydrogenase type I (11β-HSD1) inhibitor more than doubled its half-life ($t_{1/2}$) in mouse liver microsomes (Figure 2.7b).[55] Morpholine additionally opens up new hydrogen bonding opportunities.[56]
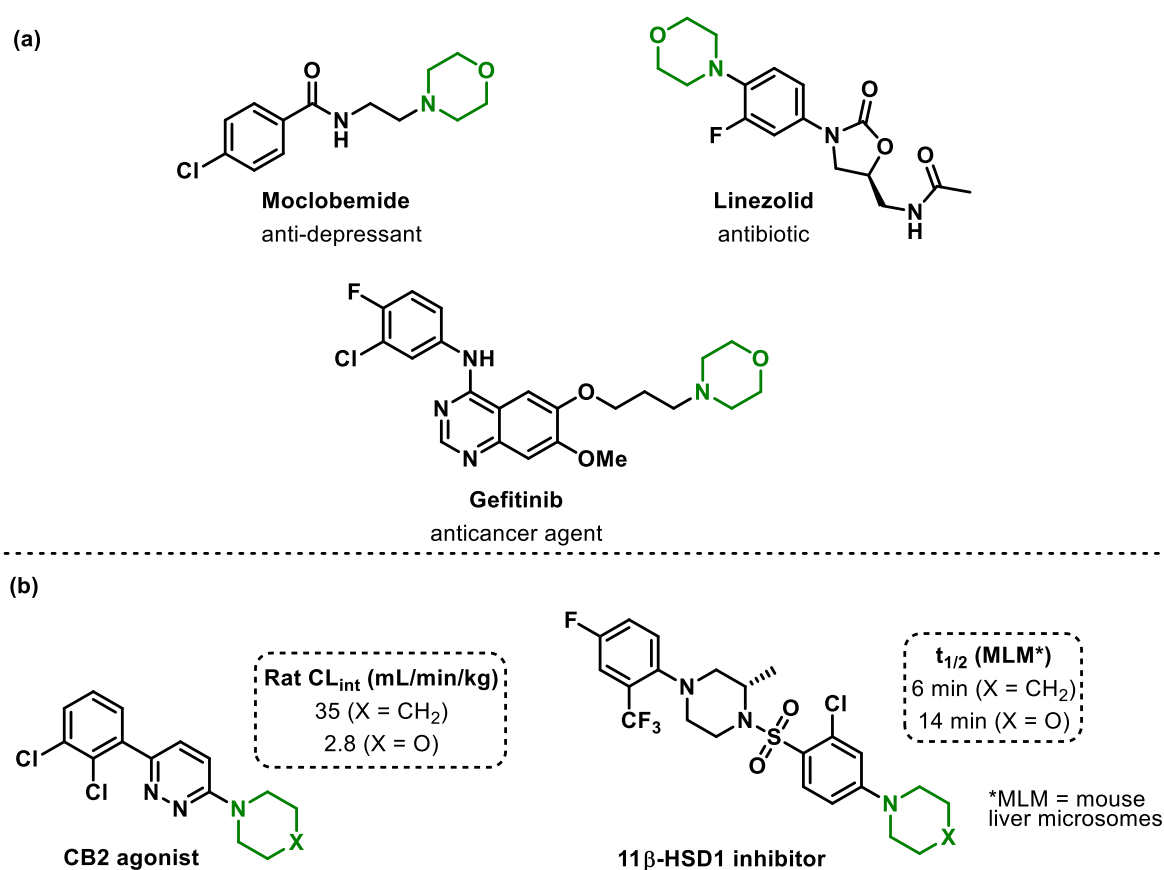
Figure 2.7. (a) Morpholine-containing marketed drugs; (b) Improvement in PK properties on replacing piperidine with morpholine.

Oxetane is a cyclic ether with hydrogen bonding ability similar to that of morpholine, which has emerged as a polar alternative to the *gem*-dimethyl group in medicinal chemistry.[57,58]

Several natural products incorporate oxetane, the most well-known of which is the clinically-used anticancer drug, Paclitaxel (Figure 2.8a).[59] Other examples include Oxetanocin A, which inhibits HIV reverse transcriptase by mimicking adenosine, and Oxetin, an antibacterial agent.[59] Carreira's seminal publications on the robustness of oxetane,[57,60,61] have paved the way for its extensive incorporation into medicinally-active moieties for the purpose of improving their physicochemical properties and PK profiles.[62] Pfizer's γ-secretase inhibitor underwent oxidative metabolism at the cyclohexyl substituent, resulting in poor human liver microsomal (HLM) stability (Scheme 2.8b).[63] Replacement with an oxetane ring resulted in significantly lower rates of oxidative metabolism, with the rate of clearance from HLMs reduced from 176 mL/min/kg to 28.6 mL/min/kg.[63] The instability of thalidomide in human plasma was ameliorated by substituting one of its carbonyl groups with an oxetane ring (Scheme 2.8c).[64]

oxetane

(a)

Paclitaxel (Taxol)
anticancer drug

Oxetanocin A
HIV inhibitor

Oxetin
antibacterial agent

(b)

γ-secretase inhibitor

R	$CL_{int,app}$ (mL/min/kg)[a]
	176
	28.6

[a]Total intrinsic clearance from human liver microsomes

(c)

Thalidomide
unstable in human plasma

Oxetano-thalidomide
stable in human plasma
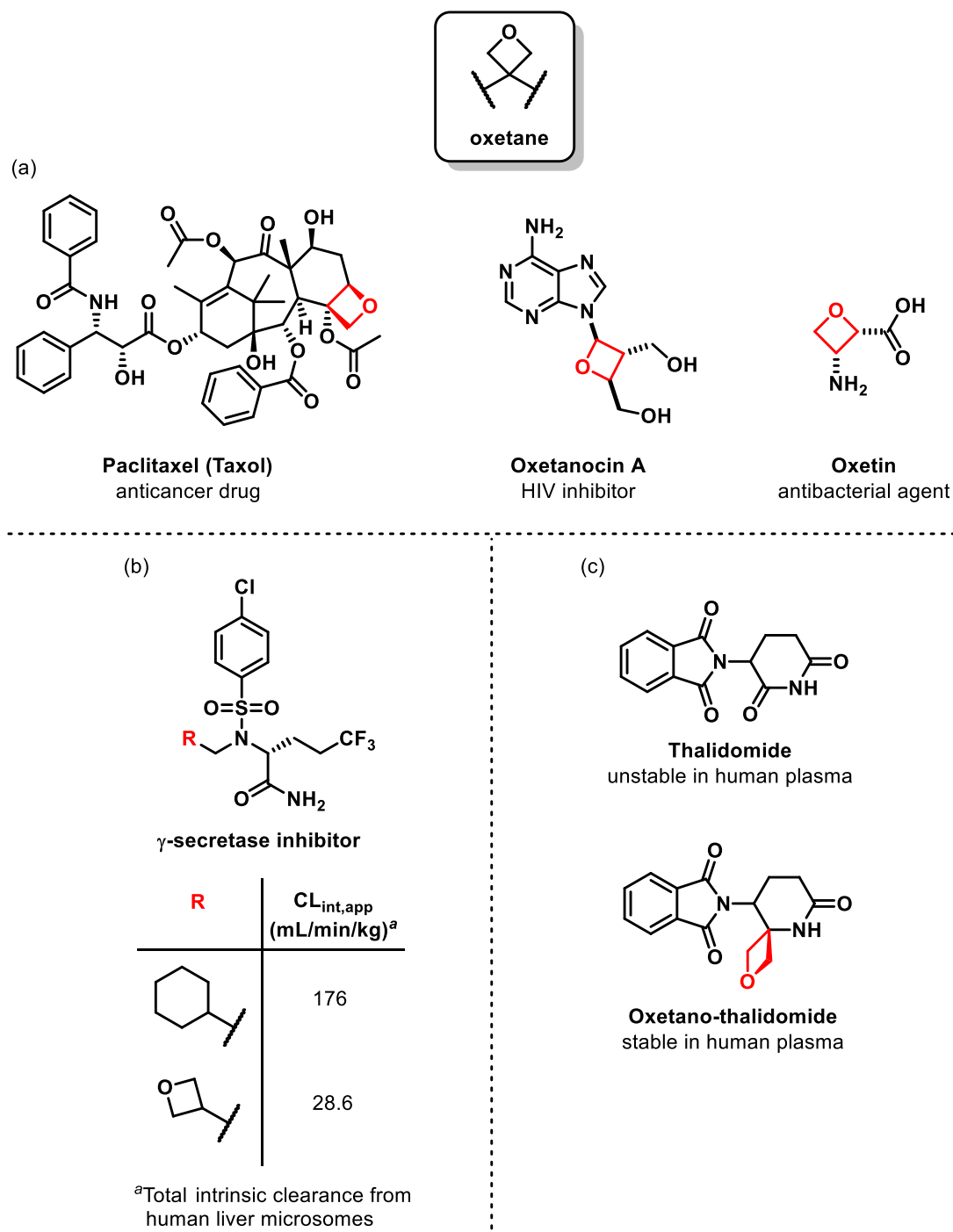
Figure 2.8. (a) Natural products containing oxetane. (b) Effect of oxetane on metabolism of γ-secretase inhibitor. (c) Oxetano-thalidomide derivative of thalidomide.

2.2. Chapter Aims and Objectives

The aims of this chapter are summarised in Scheme 2.10:

- To prepare morpholine- and spirocyclic oxetane ring-fused benzimidazolequinones **1** and **2**. The scaffolds contain a hydrogen bond acceptor (cyclic ether) ideally positioned to interact with the His194 residue in the active site of NQO1.

- To use H_2O_2 with hydroiodic acid (HI) for the synthesis of targets **1** and **2**. The use of HI is preferred over the other hydrohalic acids because the oxidative cyclization is more likely to occur without halogenation, as the electrophilicity of the halogens decreases from $Cl_2 > Br_2 > I_2$.[65]

- To optimize the H_2O_2/HI reaction conditions to favour the formation of the ring-fused *p*-dimethoxybenzimidazole.

- To propose a mechanism for unexpected 1,4,6,9-tetramethoxyphenazine formation.

- To oxidatively demethylate the *p*-dimethoxybenzimidazoles to give the target benzimidazolequinones **1** and **2**.
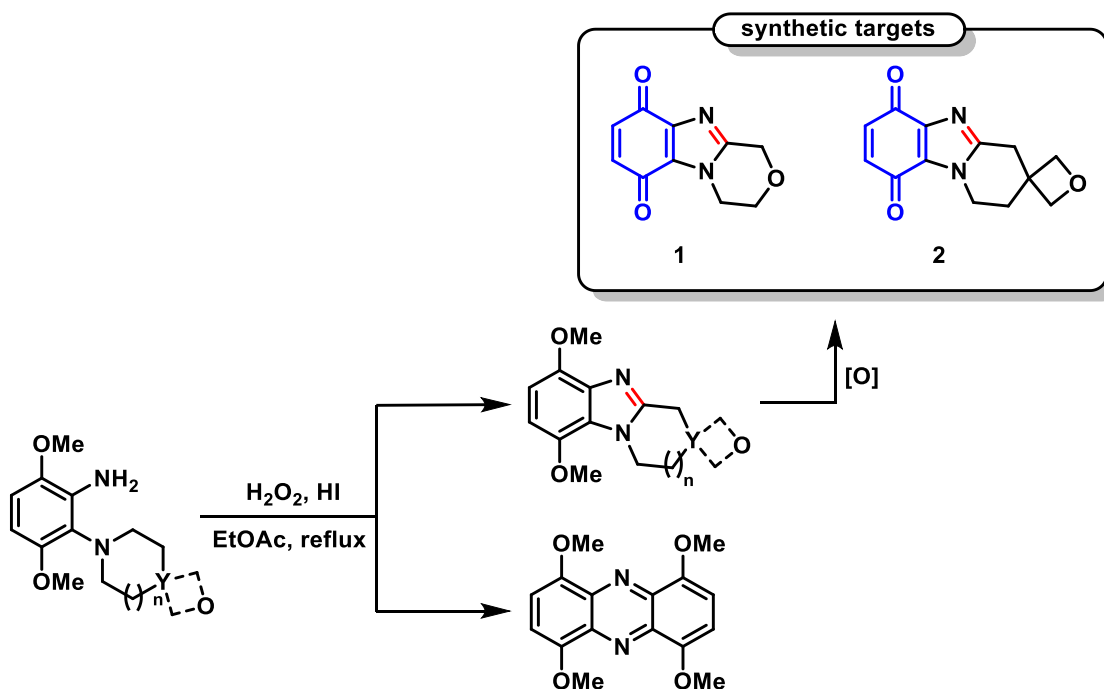
Scheme 2.10. H_2O_2 and HI-mediated transformations of 3,6-dimethoxy-2-(cycloamino)anilines.

2.3. Results and Discussion

2.3.1. Synthesis of Cyclization Substrates

The synthesis of ring-fused benzimidazolequinones **1** and **2** began with nucleophilic aromatic substitution (S$_N$Ar) of morpholine and 2-oxa-7-azaspiro[3.5]nonane onto 1,4-dimethoxy-2,3-dinitrobenzene. The latter spirocyclic oxetane nucleophile was prepared as bis(2-oxa-7-azaspiro[3.5]nonan-7-ium) ethanedioate (**3**) according to the five-step procedure developed by Gurry and Aldabbagh.[66] The condensation of *N*-tosylbis(2-bromoethyl)amine with diethyl malonate yielded *N*-tosyl-piperidine-4,4-diethyl ester, which was subjected to diester reduction followed by ring-closure of the diol.[66] Tosyl deprotection followed by oxalate salt formation furnished the spirocyclic oxetane nucleophile **3**.[66] The substitution of oxalate salt **3** onto 1,4-dimethoxy-2,3-dinitrobenzene proceeded in 68% yield when using K$_2$CO$_3$ (4 equiv) in a 5:1 acetonitrile:water mixture (Scheme 2.11). Reduction of nitrobenzenes with iron powder gave the aniline oxidative cyclization precursors in high yields with 3,6-dimethoxy-2-(2-oxa-7-azaspiro[3.5]nonan-7-yl)aniline (**4b**) formed in 80% yield.
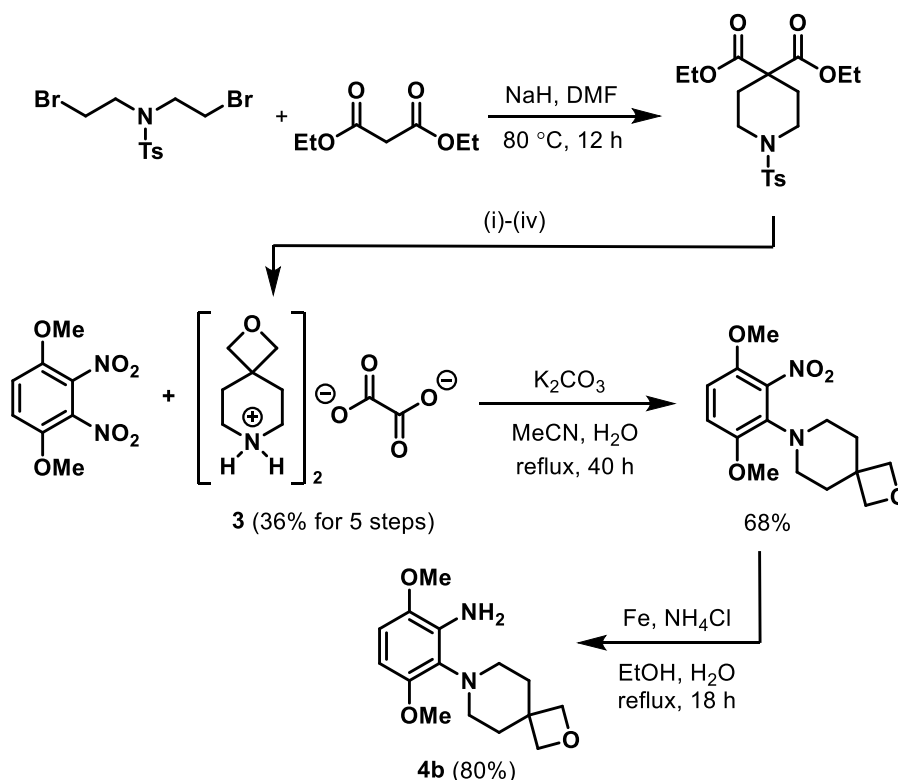
Scheme 2.11. Preparation of bis(2-oxa-7-azaspiro[3.5]nonan-7-ium) ethanedioate (**3**) and 3,6-dimethoxy-2-(2-oxa-7-azaspiro[3.5]nonan-7-yl)aniline (**4b**). (i) LiAlH$_4$, THF, rt, 16 h; (ii) MsCl, *t*-BuOK, THF, rt, 3 h; (iii) Mg,))), MeOH, 1 h.; (iv) (COOH)$_2$, Et$_2$O.

2.3.2. Optimization of H$_2$O$_2$/HI Reaction towards Oxidative Cyclization

With 3,6-dimethoxy-2-(morpholin-4-yl)aniline (**4a**)[47] and spirocyclic oxetane analogue **4b** in hand, the oxidative cyclization using H$_2$O$_2$ and HI was investigated (Table 2.2). In keeping with the principles of green chemistry, ethyl acetate was chosen as the reaction solvent.[42,43] Morpholine **4a** did not undergo any transformation in EtOAc at reflux in the presence of H$_2$O$_2$ (20 equiv) alone. Addition of one stoichiometric equivalent of HI gave, after 1 h, 6,9-dimethoxy-3,4-dihydro-1*H*-[1,4]oxazino[4,3-*a*]benzimidazole (**5a**) in 56% yield along with an unexpected orange precipitate. Spectroscopic data identified the precipitate as 1,4,6,9-tetramethoxyphenazine (**6**) formed in 25% yield. Using less than stoichiometric amounts of HI (0.2 equiv) increased the yield of the desired benzimidazole **5a** to 69%, and less phenazine **6** formed in 19% yield. Using these conditions on substrate **4b** gave spirocyclic oxetane ring fused benzimidazole **5b** in 74% yield with 11% phenazine **6** formed. The X-ray crystal structure of **5b** proved the structural integrity of the oxetane remained intact throughout the reaction (Figure 2.9).

The amount of phenazine **6** (12% yield) was consistent for other six-membered cyclizations, as demonstrated by conversion of 3,6-dimethoxy-2-(piperidin-1-yl)-aniline (**4c**) to give 6,9-dimethoxy-1,2,3,4-tetrahydropyrido[1,2-*a*]benzimidazole (**5c**) in 72% yield (entry 5, Table 2.2). Variation of ring sizes was investigated with the five- and seven-membered cyclizations of 3,6-dimethoxy-(2-pyrrolidin-1-yl)aniline (**4d**) and 2-(azepan-1-yl)-3,6-dimethoxyaniline (**4e**) proceeding in high yield to respectively give 5,8-dimethoxy-2,3-dihydro-1*H*-pyrrolo[1,2-*a*]benzimidazole (**5d**) and 1,4-dimethoxy-7,8,9,10-tetrahydro-6*H*-azepino[1,2-*a*]benzimidazole (**5e**) in 89 and 91% yield. The absence of phenazine **6** from the latter reactions is consistent with previous observations of substrates bearing a six-membered cyclic amine being more difficult to cyclize than those bearing a five- and seven-membered alicyclic ring (Table 2.1).[42] For all reactions, chromatography was not required, with residues triturated in diethyl ether to afford benzimidazoles **5a**−**5e**.

Table 2.2. Yields obtained from H_2O_2 and HI-mediated reactions.[a]
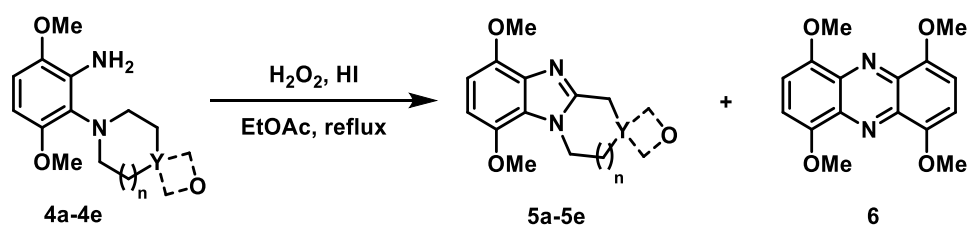
Entry	Aniline	Y	n	HI (mmol)	Time (h)	Yield of 5a-5e (%)[b]	Yield of 6 (%)[b, c]
1	**4a**	O	1	0.0	16	**5a**, 0	0
2	**4a**	O	1	1.0	1	**5a**, 56	25
3	**4a**	O	1	0.2	1	**5a**, 69	19
4	**4b**		1	0.2	1	**5b**, 74	11
5	**4c**	CH_2	1	0.2	1	**5c**, 72	12
6	**4d**	CH_2	0	0.2	1	**5d**, 89	0
7	**4e**	CH_2	2	0.2	1	**5e**, 91	0

[a]Conditions: Aniline (1.0 mmol), H_2O_2 (50% aq.; 20.0 mmol), EtOAc (40 mL). [b]Isolated. [c]Precipitate.
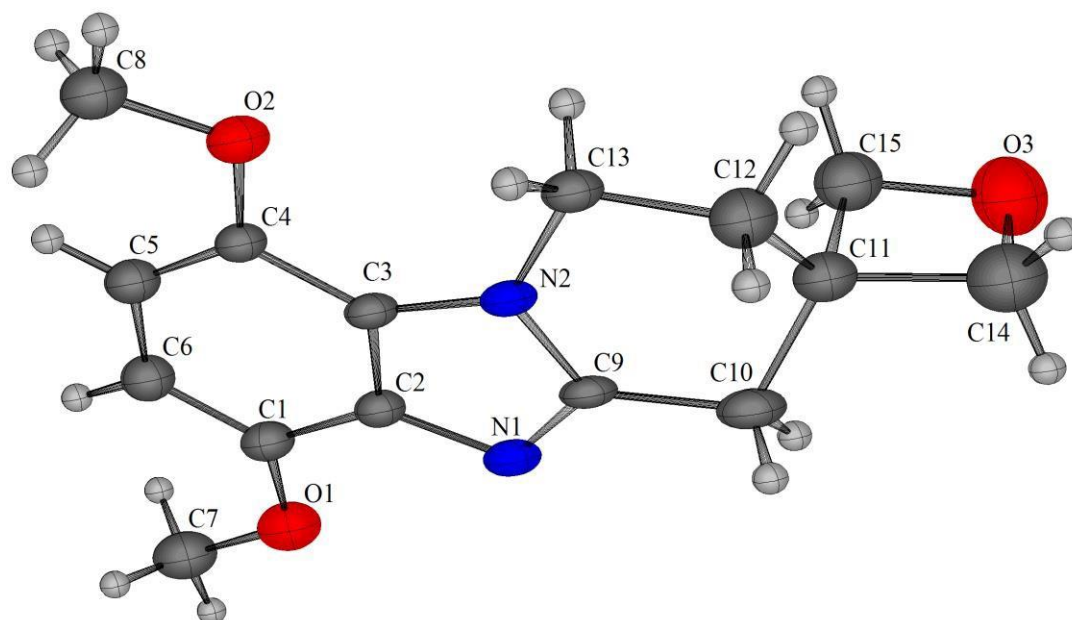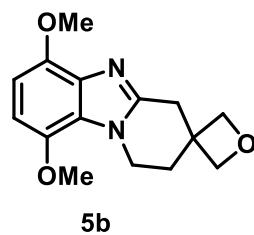
Figure 2.9. Thermal ellipsoid plot for crystal structure of 6',9'-dimethoxy-1',2'-dihydro-4'*H*- spiro[oxetane-3,3'-pyrido[1,2-*a*]benzimidazole] (**5b**; CCDC number 1917885) with 40% probability for non-hydrogen atoms and arbitrary spheres for hydrogen atoms.

2.3.3. Optimization of Phenazine Formation

Phenazine is the scaffold of secondary metabolites from *Pseudomonas* and *Streptomyces* with many natural and unnatural examples having potent biological activity, notably anticancer.[67,68] The oldest synthesis is the Wohl−Aue reaction,[69] which is known to be low-yielding, and reported to give 1,4,6,9-tetramethoxyphenazine (**6**) in 10% yield using potassium hydroxide in benzene (Scheme 2.12).[70] We attempted to improve this condensation of the aniline with nitrobenzene by using potassium *tert*-butoxide as base in toluene,[71] but the yield of **6** remained low, at 34%.

yields: (i) 10%
(ii) 34%
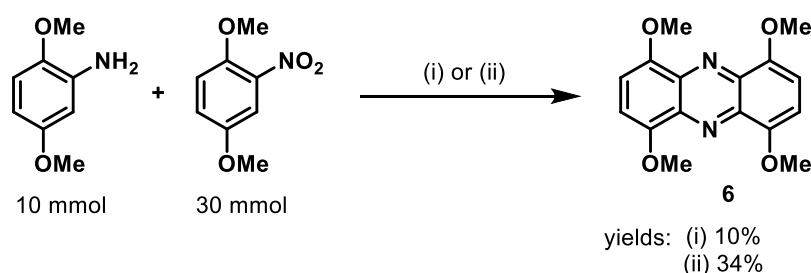
*a*Conditions: (i) KOH (90 mmol), benzene (50 mL), reflux, 5 h.[70]
(ii) *t*-BuOK (40 mmol), Tol (50 mL), reflux, 16 h.

Scheme 2.12. Wohl-Aue reaction.*a*

We established a more facile route to **6** through manipulation of the optimized H_2O_2 and HI-mediated oxidative cyclization conditions for morpholine **4a** (Table 2.3). Given that phenazine **6** formation is an intermolecular reaction, it seemed plausible that the use of more concentrated conditions (less ethyl acetate) would lead to increased yields of **6**. This was indeed the case when reducing the amount of solvent by 4-fold; phenazine **6** became the major product in 47% yield with benzimidazole **5a** formed in 28% yield. The H_2O_2 and HI-mediated cyclization seemed to give the thermodynamic product because the yield of cyclized benzimidazole **5a** became increasingly insignificant (4% then 2%) when reducing the reaction temperature from reflux to 40 °C to room temperature with phenazine **6** isolated in excellent yield of 82%. The requirement for higher temperatures for the cyclization may also be due to the nature of the oxidizing system; although hypoiodous acid (HOI) is formed, the mediating oxidant is unknown.[72,73]

Table 2.3. Optimization of Phenazine Formation[a]
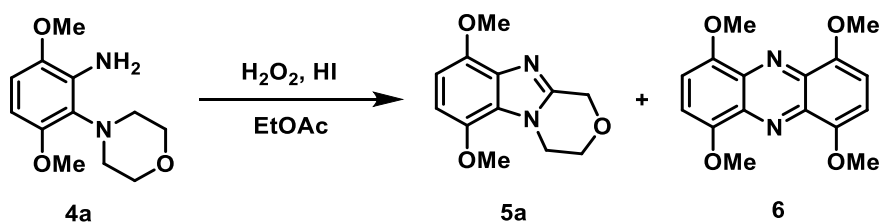
Entry	EtOAc (mL)	Temperature	Time (h)	Yield of **5a** (%)[b]	Yield of **6** (%)[b, c]
1	40	reflux	1	69	19
2	10	reflux	1	28	47
3	10	40 °C	16	4	79
4	10	rt	24	2	82

[a]Conditions: Aniline **4a** (1.0 mmol), H_2O_2 (20.0 mmol, 50% aq.), HI (0.2 mmol). [b]Isolated. [c]Precipitate.

2.3.4. H₂O₂ with Catalytic HCl

Phenazine **6** was not formed when replacing HI (0.2 equiv) with HCl (0.2 equiv) (Scheme 2.13). Under these conditions, mainly recovered **4a** was observed with 4-chloro-3,6-dimethoxy-2-(morpholin-4-yl)aniline (**4f**) formed in 17% yield. The regioselectivity of the chlorination was confirmed by X-ray crystallography, and was likely directed by the primary amine (Figure 2.10). This result can help to retrospectively rationalise the regioselectivity of the diahlogenation in Aldabbagh and Gurry's one-pot reaction, which proceeded *ortho*-and *para*-to the primary amine (Scheme 2.5).[46] The same regioselectivity was observed by Sweeney and Aldabbagh in their tunable H₂O₂/HX transformation, where THIQ-substituted aniline underwent mono-chlorination *para* to the primary amine, prior to oxidative cyclization (Scheme 2.14).[47] The yield of chlorinated aniline **4f** increased to 76% through use of a stoichiometric equivalent of HCl with H₂O₂. The greater reactivity of catalytic amounts of HI relative to HCl reflects the lower pK_a of HI[74] and relative ease of oxidation of iodine,[27] which allows facile breakdown of H₂O₂.[72,73]
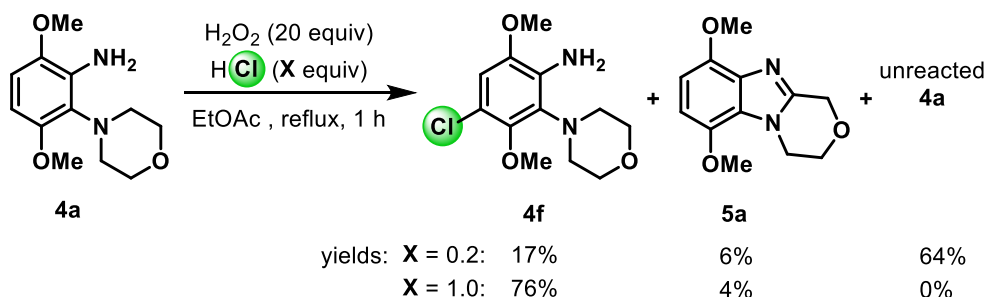
Scheme 2.13. Reactivity of aniline **4a** towards H₂O₂ and HCl.
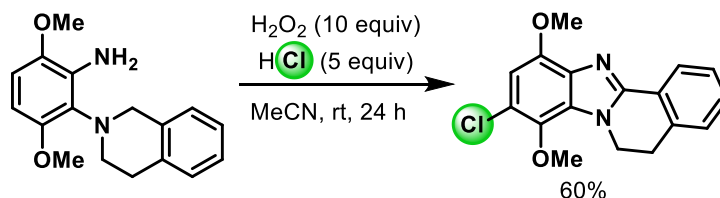
Scheme 2.14. Regioselective chlorination with oxidative demethylation of THIQ-substituted aniline.[47]
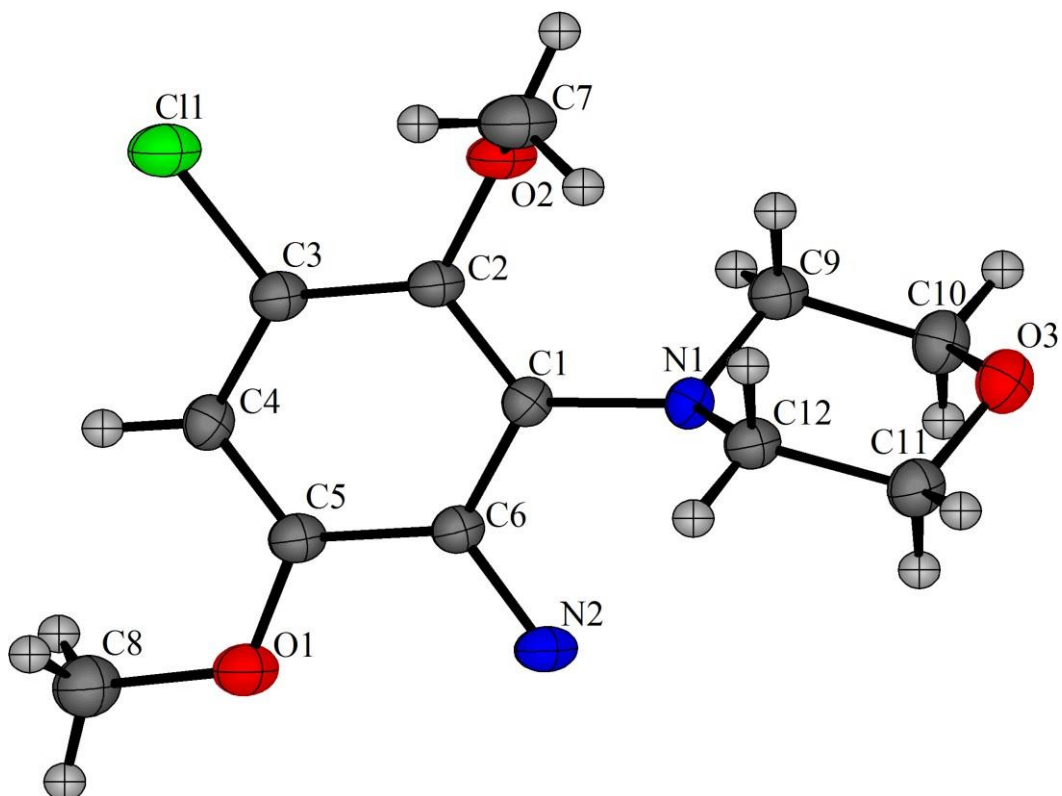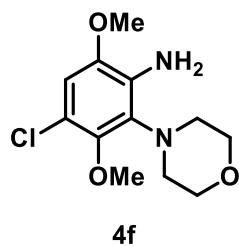
Figure 2.10. Thermal ellipsoid plot for crystal structure of 4-chloro-3,6-dimethoxy-2-(morpholin-4-yl)aniline (**4f**; CCDC number 1917886) with 40% probability for non-hydrogen atoms and arbitrary spheres for hydrogen atoms.

2.3.5. Reactivity of Aqueous I$_2$

Recently, chlorine (50 equiv) and bromine (50 equiv) with water (100 equiv) were established as mediators for six-electron oxidation, converting 3,6-dimethoxy-2-(cycloamino)anilines into cyclized benzimidazolequinones (Scheme 2.6).[47] Molecular iodine is, however, a less powerful oxidizing agent,[75] and using the latter conditions did not give benzimidazolequinones, but mixtures of difficult to separate iodinated aromatics. In the iodine-mediated reactions, ethyl acetate was replaced by acetonitrile because the former solvent is immiscible with water. Using iodine (10 equiv) in 20% aqueous acetonitrile, a 4-electron oxidation occurred in 10 min to give cyclized noniodinated benzimidazoles (Scheme 2.15). Morpholine **4a** and pyrrole **4d** were converted to 6,9-dimethoxy[1,4]oxazino[4,3-*a*]benzimidazole (**5a**) and 5,8-dimethoxypyrrolo[1,2-*a*]benzimidazole (**5d**) in 48 and 92% yield, respectively. Similar to the H$_2$O$_2$ and HI-mediated reaction, the five-membered cyclization was regioselective and did not give phenazine; however, the less favoured morpholine cyclization gave side products, including **6** in 6% yield. Presumably for iodine in water, the concentration of HOI is greater than that in the H$_2$O$_2$ and HI-mediated reactions (in Table 2.2), resulting in intractable iodinated side products.
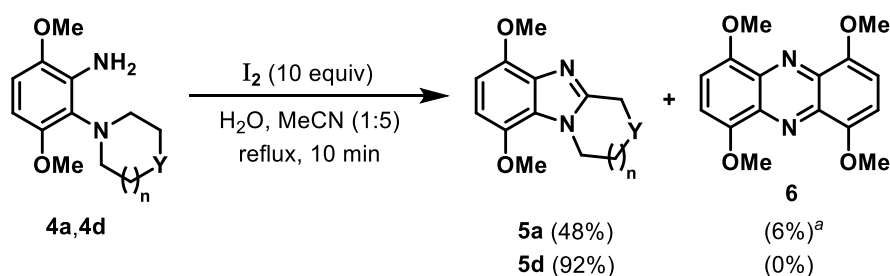
a & an intractable mixture of iodinated benzimidazoles.

Scheme 2.15. Aqueous I$_2$-mediated cyclization and phenazine formation.

2.3.6. Mechanistic Considerations

Common to the oxidative cyclization of *o*-cyclic amine substituted anilines to give benzimidazoles[35,76] and the Wohl−Aue and other phenazine syntheses[67,68,77] is the likelihood of a nitroso-intermediate. Transformations *via* the *N*-oxide of the *tert*-amine of **4a** are unlikely with amine *N*-oxide isolated intermediates only when the primary NH$_2$ is deactivated to an acetamide.[29,78] We were, however, unable to isolate a nitroso intermediate, although encouragingly, GC-MS of the reaction mixture (entry 4, Table 2.3) after 1 h revealed the presence of a peak whose EI-MS fragmentation pattern supported the formation of intermediate **7** (Figure 2.11, Scheme 2.16). The latter GC peak was absent from a control sample of aniline **4a**.
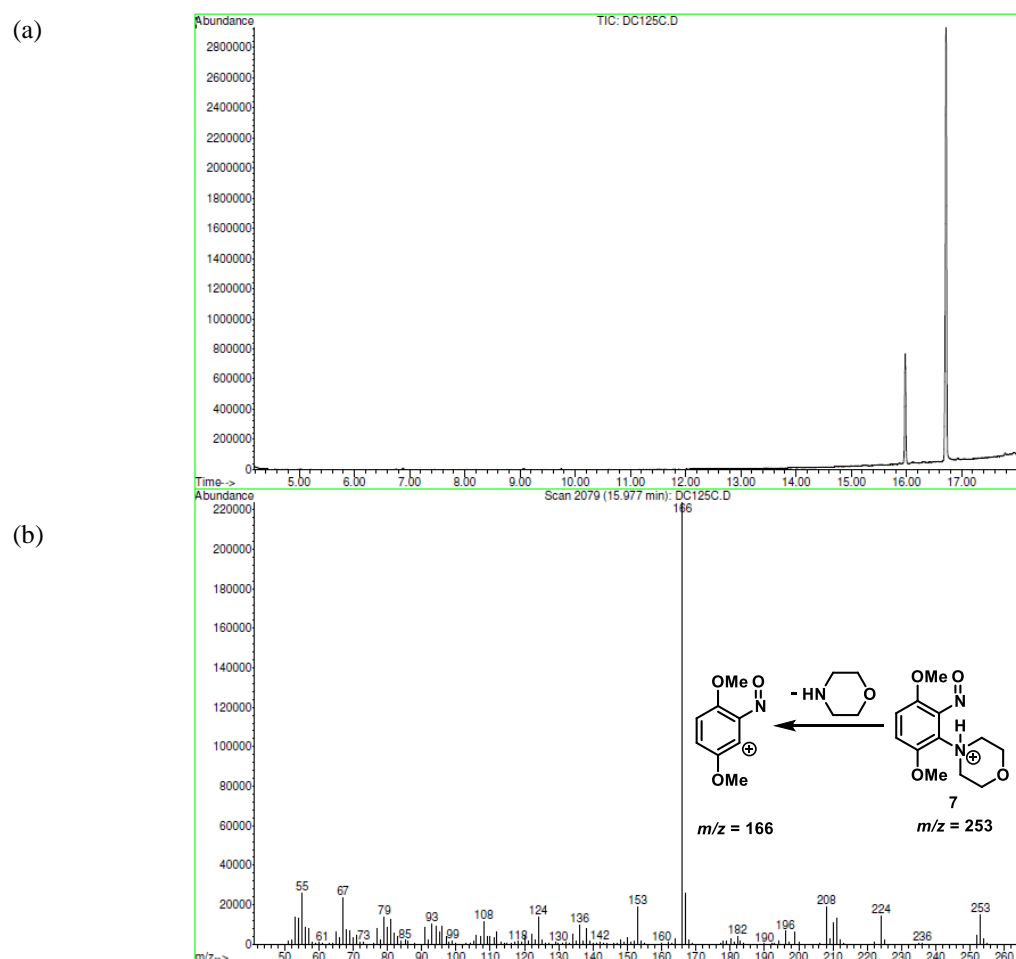
Figure 2.11: GC-MS of the room temperature H$_2$O$_2$ and HI-mediated oxidative cyclization of 3,6-dimethoxy-2-(morpholin-4-yl)aniline (**4a**; Table 2.3, entry 4): (a) GC of the reaction mixture after 1 h, where the peak at 16.7 min is 3,6-dimethoxy-2-(morpholin-4-yl)aniline (**4a**), and the peak at 16.0 min is 4-(3,6-dimethoxy-2-nitrosophenyl)morpholin-4-ium (**7**). (b) EI mass spectrum of the GC peak at 16.0 min.

77

The existence of highly reactive nitroso-intermediate **7** is supported by Meth-Cohn, who also refuted claims of isolations of *o*-nitroso-*tert*-anilines, including the nitrosation of *p*-benzyldimethylaniline, which gave only the nitro-compound.[37] Nitroso **7** should undergo a formal hydride shift as per the *tert*-amino effect to the likely hydroxylamine **8**,[37,76,79,80] which subsequently cyclizes and is oxidized to give benzimidazole **5a** (Scheme 2.16). Literature precedence indicates the requirement for elevated temperatures to drive the hydride shift, which may help to rationalize the greater yields of cyclized benzimidazole at higher temperatures.[38] The unexpected 1,4,6,9-tetramethoxyphenazine (**6**) formation *via* nitroso-intermediate **7** would involve intermolecular reaction of **7** with starting aniline **4a**, resulting in nucleophilic aromatic substitution adduct **10**. The proposed formation of iodide **11** is reminiscent of the Bamberger−Ham reaction for making phenazine-*N*-oxides,[81] where two nitrosobenzenes substituted with *para*-electron-donating (through resonance) groups condense under acidic conditions.[67,68] It is known that HOI reacts with H_2O_2 *via* a reduction to generate additional HI,[72,73] which would favour conversion of **10** to **11**. Further, the yield of phenazine **6** is increased when using a full equivalent of HI (entry 2, Table 2.2). Similar to the conversion of hydroxylamine salts **9** and **11** into products **5a** and **6**, respectively, Nguyen *et al*. also proposed iodide as a direct reductant for removal of oxygen in iodine-catalyzed reductive cyclizations of *o*-nitro-*tert*-anilines to give benzimidazoles.[79]
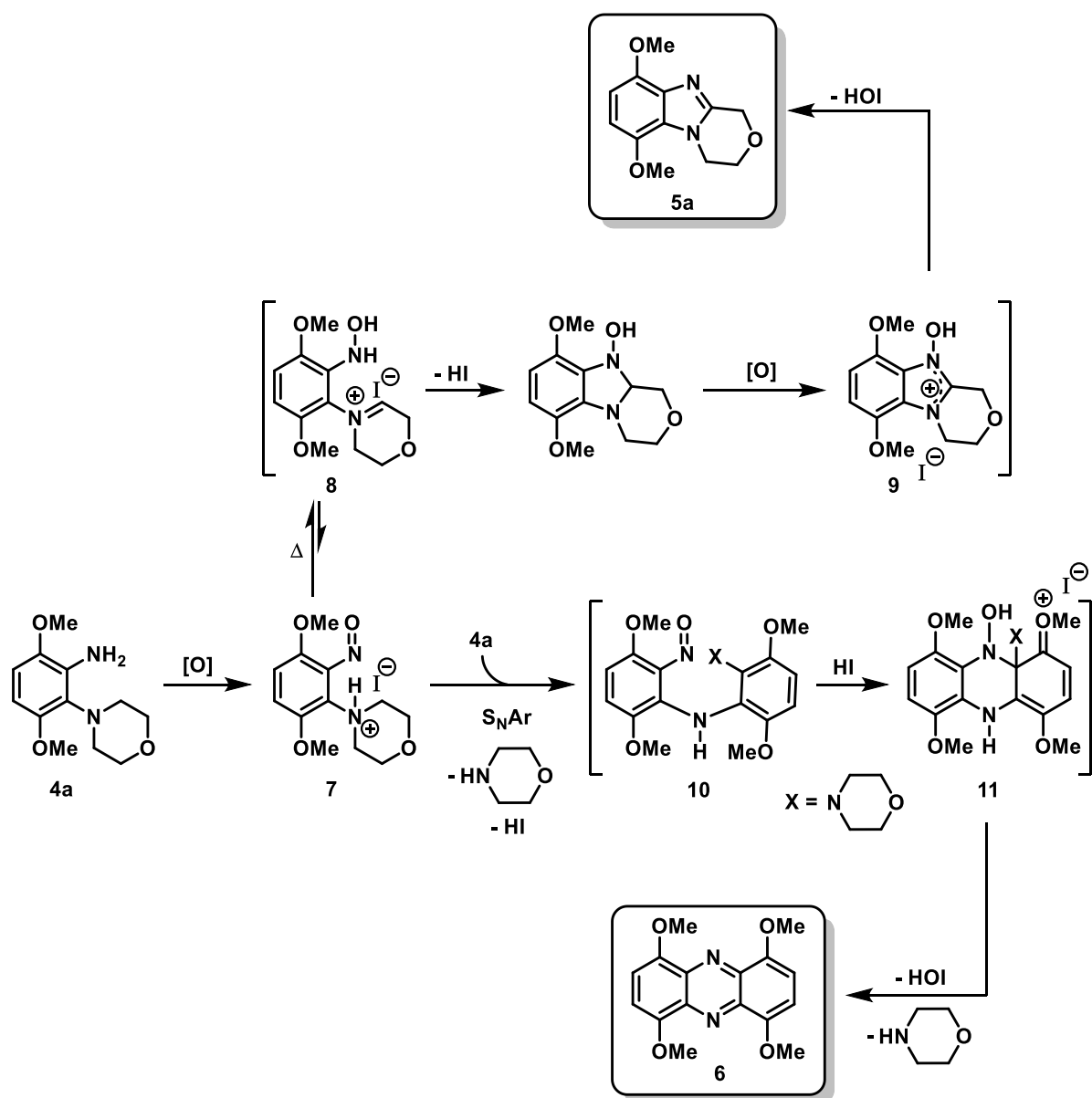
Scheme 2.16. Proposed mechanisms for the H_2O_2 and HI (catalyst) mediated transformations using 3,6-dimethoxy-2-(morpholin-4-yl)aniline (**4a**).

The necessity for the electron-donating (OMe) group in our H_2O_2 and HI-mediated synthesis of phenazine was investigated using 2-(morpholin-4-yl)aniline (**12a**)[46] and 2-(2-oxa-7-azaspiro[3.5]nonan-7-yl)aniline (**12b**), prepared from 1-fluoro-2-nitrobenzene (Scheme 2.17). In both cases, oxidative cyclization adducts (**13a**[79] and **13b**) were exclusively isolated in moderate yields (67 and 70%) after column chromatography with phenazine **14**[82] not observed. The presence of appropriately positioned OMe groups does not, however, guarantee phenazine formation. Surprisingly, chloride **4f** exclusively cyclized to give 7-chloro-6,9-dimethoxy-3,4-dihydro-1*H*-[1,4]oxazino[4,3-*a*]benzimidazole (**5f**) in 79% isolated yield (Scheme 2.17) through use of the H_2O_2 and HI reaction conditions (in Table 2.2), which favored formation of **6**. Presumably, electronic effects of the Cl substituent circumvent the S_NAr step (in Scheme 2.16).
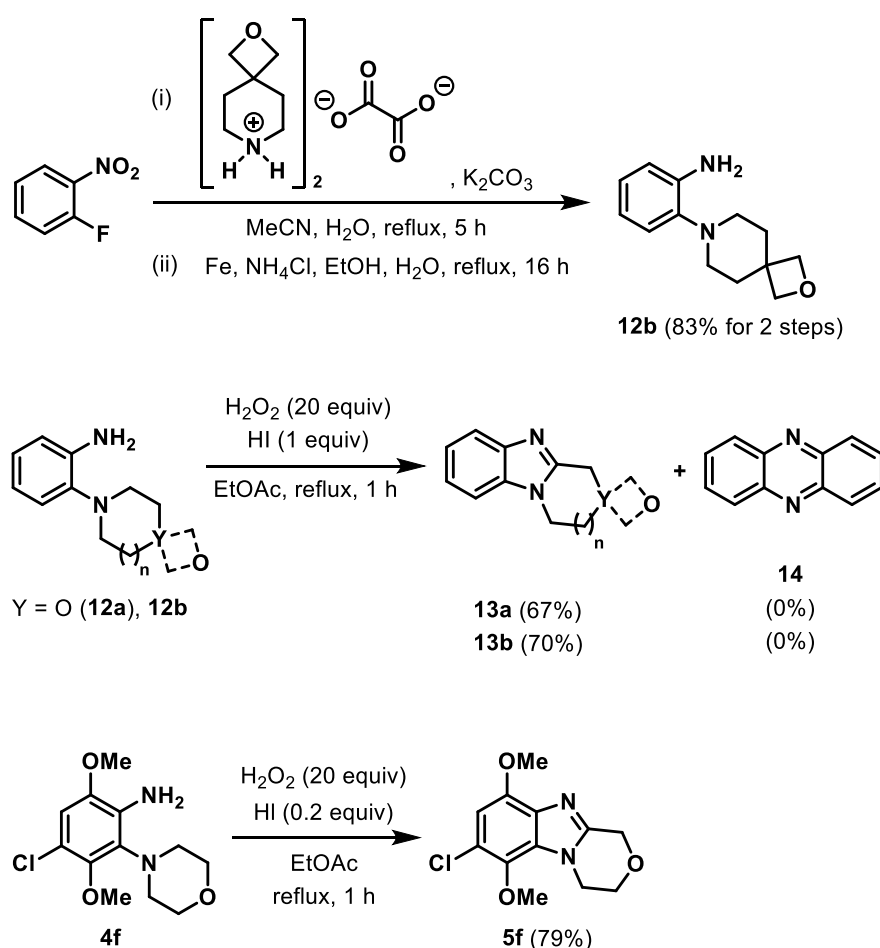
Scheme 2.17. Preparation of 2-(2-oxa-7-azaspiro[3.5]nonan-7-yl)aniline (**12b**) and oxidative cyclizations.

2.3.7. Oxidative Demethylation to the Target Benzimidazolequinones

The hypervalent iodine reagent [bis(trifluoroacetoxy)iodo]benzene (PIFA) in water at room temperature is reported to convert *p*-dimethoxybenzenes to quinones.[83] This mild procedure was used to give target ether-containing ring-fused benzimidazolequinones **1** and **2** in 74 and 78% yield from 6,9-dimethoxy-3,4-dihydro-1*H*-[1,4]oxazino[4,3-*a*]benzimidazole (**5a**) and spirocyclic oxetane ring-fused benzimidazole (**5b**), respectively (Scheme 2.18). Importantly PIFA, unlike other oxidants,[84,85] had no apparent adverse effect on the integrity of the oxetane motif.
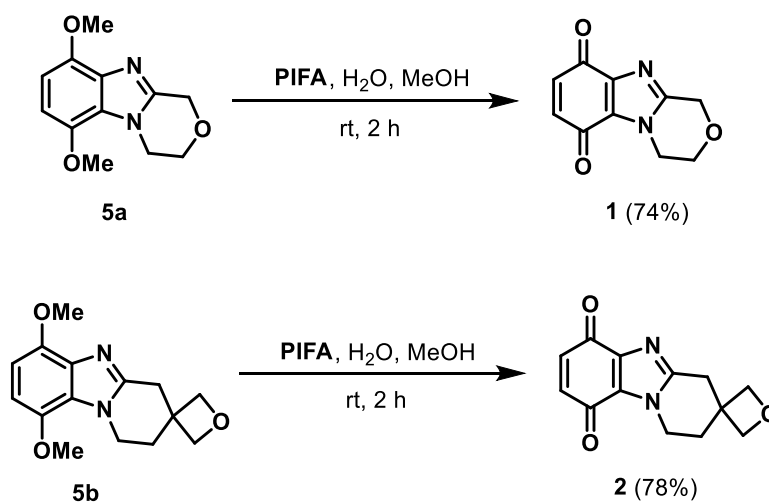
Scheme 2.18. Oxidative demethylation.

2.4. Conclusions

In summary, H_2O_2 and HI-mediated oxidative cyclization of 3,6-dimethoxy-2-(cycloamino)anilines to give the ring-fused benzimidazoles can be tuned alternatively to give 1,4,6,9-tetramethoxyphenazine (**6**) in high yield. Phenazine formation is however not ubiquitous and competes with the six-membered cyclization only with the suitably activated 3,6-dimethoxy-2-(cycloamino)anilines. The detection of nitroso-intermediate **7** has led to a proposed mechanism for this new HI-catalyzed reaction. Oxidative demethylation of the *p*-dimethoxybenzimidazolequinones proceeded smoothly using PIFA, to yield benzimidazolequinones incorporating hydrogen-bonding functionality.

2.5. Future work

The bioactivity of the cyclic ether-substituted benzimidazolequinones will be evaluated. Although phenazines have been extensively studied, the synthesis and biological evaluation of scaffolds incorporating quinone functionality has not been reported. Synthesis of the non-symmetrical phenazine-quinone would likely improve the solubility of the scaffold compared with the fully symmetrical tetramethoxyphenazine (Scheme 2.19), thus making it more attractive from a pharmacological perspective. The proposed scaffold has potential dual bioreductive and intercalating activity, similar to that of the clinically-used topoisomerase II inhibitor, doxorubicin.[86]
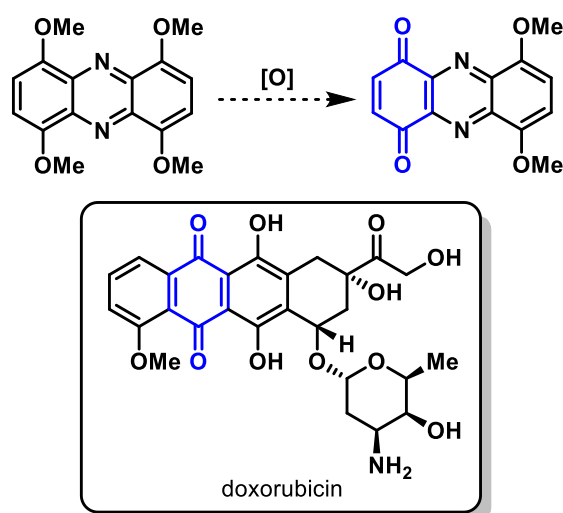
Scheme 2.19. Potential functionalization of 1,4,6,9-tetramethoxyphenazine.

2.6. Experimental Section

2.6.1. Materials

All chemicals were obtained from commercial sources and used without further purification. 1,4-Dimethoxy-2,3-dinitrobenzene was prepared from 1,4-dimethoxybenzene (Sigma-Aldrich, 99% (GC)) and nitric acid (Honeywell Fluka, 64−66%).[87] Bis(2-oxa-7-azaspiro[3.5]nonan-7-ium) ethanedioate was prepared using the procedure described by our group (Scheme 2.11).[66] The preparations of 3,6-dimethoxy-2-(morpholin-4-yl)aniline (**4a**), 3,6-dimethoxy-2-(piperidin-1-yl)aniline (**4c**), 3,6-dimethoxy-2-(pyrrolidin-1-yl)aniline (**4d**), and 2-(azepan-1-yl)-3,6-dimethoxyaniline (**4e**) were previously reported using the S_NAr of morpholine (Alfa Aesar, 99%), piperidine (Sigma-Aldrich, 99%), pyrrolidine (Acros, +99%), and azepane (Fluorochem, >98%), respectively, onto 1,4-dimethoxy-2,3-dinitrobenzene, followed by reduction with iron powder (Alfa Aesar, reduced, 99%).[42,47] 2,5-Dimethoxyaniline was prepared by the reduction of 1,4-dimethoxy-2-nitrobenzene (TCI, >99.0% (GC)) using iron powder.[88] 2-(Morpholin-4-yl)aniline (**12a**)[46] was prepared by the S_NAr of morpholine onto 1-fluoro-2-nitrobenzene (Fluorochem, 99%), followed by reduction with iron powder. H_2O_2 (Honeywell Fluka, 50% *w/v* in water, stabilized), HI (Sigma-Aldrich, 57% *w/v* in water), HCl (Sigma-Aldrich, 37% *w/v* in water), I_2 (VWR, ≥99%, resublimed), PIFA (Sigma-Aldrich, 97%), EtOAc (VWR, 99.9%), pet. ether (Fisher Scientific, 40-60 °C, Extra Pure, SLR), and $MgSO_4$ (Anhydrous, Fisher Scientific, Extra Pure, SLR, Dried) were used as received. Thin layer chromatography (TLC) was performed on TLC silica gel 60 F_{254} plates. Flash column chromatography was carried out on silica gel (Apollo Scientific 60/40−63 μm).

2.6.2. Measurements

Melting Points: Melting points were measured on a Stuart Scientific melting point apparatus SMP1, except for 1,4,6,9-tetramethoxyphenazine (**6**) which was recorded using differential scanning calorimetry (DSC) performed on a Mettler Toledo DSC822 differential scanning calorimeter, using standard aluminum pans.

Gas Chromatography: GC-MS used to detect the formation of nitrosoarene **7** was performed on an Agilent 6890N Series GC system equipped with an Agilent 5973 Inert Mass Selective Detector (EI) and an SGE, 25 m, ID 0.25 mm, FD 0.25 μm column. The carrier gas used was He at a flow rate of 1.3 mL/min. The injector heated to 280 °C and the oven temperature increased from 80 to 280 °C at the rate of 10 °C/min and increased to 320 °C at 40 °C/min.

Infrared (IR) Spectroscopy: IR spectra were recorded using a PerkinElmer Spec 1 with ATR attached.

Nuclear Magnetic Resonance (NMR) Spectroscopy: NMR spectra for compounds **2**, **3**, **4b**, and **5b** were recorded using a Jeol ECX 400 MHz instrument equipped with a DEC AXP 300 computer workstation. NMR spectra for all other compounds were recorded using a Bruker Avance III 400 MHz spectrometer equipped with a 5mm BBFO+, broadband autotune probe and controlled with TopSpin 3.5.7 acquisition software and IconNMR 5.0.7 automation software Copyright © 2017 Bruker BioSpin GmbH. The chemical shifts are in ppm relative to tetramethylsilane. ^{13}C NMR spectra at 100 MHz are with complete proton decoupling. NMR assignments are supported by DEPT-135, ^{1}H−^{1}H DQF COSY and ^{1}H−^{13}C edited HSCQ correlation.

High Resolution Mass Spectrometry (HRMS): HRMS spectra were obtained using ESI time-of-flight mass spectrometer (TOFMS) on a Waters LCT Mass Spectrometry instrument. The precision of all accurate mass measurements was better than 5 ppm.

X-ray Crystallography: A single crystal of **4f** was grown from CH_2Cl_2 at 2 °C, and a single crystal of **5b** was grown by slow evaporation from CH_2Cl_2. Single crystal data were collected using an Oxford Diffraction Xcalibur system operated using the CrysAlisPro software, and the data collection temperature was controlled at 298 K using a Cryojet system from Rigaku Oxford Diffraction. The crystal structures were solved using ShelxT version 2014/55[89] and refined using ShelxL version 2017/1,[90] both of which were operated within the Oscail software package.[91] Crystallographic data for compounds **4f** and **5b** were deposited with the Cambridge Crystallographic Data Centre with deposition numbers CCDC 1917886 and CCDC 1917885, respectively. These data are available free of charge *via* www.ccdc.cam.ac.uk/data_request/cif (or from the Cambridge Crystallographic Data Centre, 12 Union Road, Cambridge CB2 1EZ, U.K.; fax +44 1223 336033; or e-mail deposit@ccdc.cam.ac.uk).

2.6.3. Synthetic Procedures and Characterization

2.6.3.1. Synthesis of 7-(3,6-Dimethoxy-2-nitrophenyl)-2-oxa-7-azaspiro[3.5]nonane
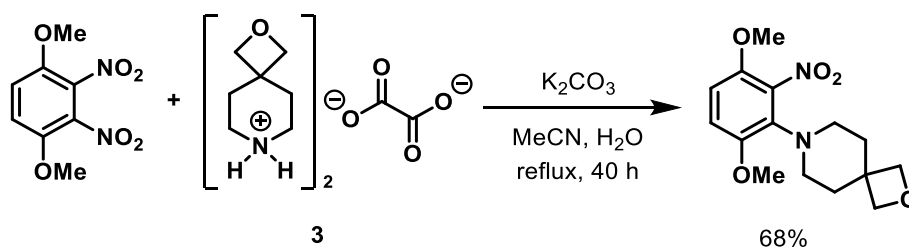
1,4-Dimethoxy-2,3-dinitrobenzene (0.680 g, 2.98 mmol), bis(2-oxa-7-azaspiro[3.5]nonan-7-ium) ethanedioate (**3**) (2.053 g, 5.96 mmol), and K_2CO_3 (1.647 g, 11.92 mmol) in MeCN (30 mL) and H_2O (6 mL) were heated at reflux for 40 h. The mixture was evaporated, dissolved in EtOAc (30 mL), and washed with brine (3 × 20 mL). The organic extract was dried ($MgSO_4$), evaporated, and purified by column chromatography using gradient elution of pet. ether/EtOAc to give the *title compound* (0.624 g, 68%) as a yellow solid; R_f 0.44 (1:1 pet. ether/EtOAc); mp 125−127 °C; ν_{max} (neat, cm^{-1}) 2931, 2861, 2841, 1539 (NO_2), 1495, 1381 (NO_2), 1256, 1094, 1057; ^{1}H NMR (400 MHz, CDCl$_3$) δ: 6.83 (d, J = 9.2 Hz, 1H), 6.74 (d, J = 9.2 Hz, 1H), 4.42 (s, 4H, OCH$_2$), 3.80 (s, 3H, Me), 3.78 (s, 3H, Me), 2.97−2.90 (br.s, 4H), 1.88−1.80 (br.s, 4H); ^{13}C{^{1}H} NMR (100 MHz, CDCl$_3$) δ: 152.7, 144.5, 141.9, 133.9 (all C), 112.9, 109.4 (both CH), 82.1 (OCH$_2$), 56.8, 56.2 (both Me), 47.8 (CH$_2$), 38.4 (C), 35.6 (CH$_2$); HRMS (ESI) *m/z* [M + H]$^+$ Calcd for C$_{15}$H$_{21}$N$_2$O$_5$ 309.1449; Found 309.1450.

2.6.3.2. Synthesis of 3,6-Dimethoxy-2-(2-oxa-7-azaspiro[3.5]nonan-7-yl)aniline (4b)
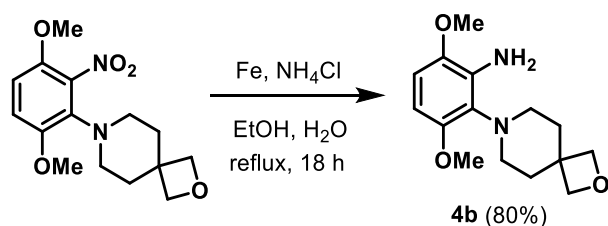
7-(3,6-Dimethoxy-2-nitrophenyl)-2-oxa-7-azaspiro[3.5]nonane (0.616 g, 2.00 mmol), iron powder (0.357 g, 6.40 mmol), and NH_4Cl (55 mg, 1.00 mmol) in EtOH (40 mL) and H_2O (12 mL) were heated at reflux for 18 h. The mixture was filtered through Celite, evaporated, dissolved in EtOAc (80 mL), and washed with brine (2 × 60 mL). The organic extract was dried ($MgSO_4$), evaporated, and purified by column chromatography using gradient elution of pet. ether/EtOAc to give **4b** (0.445 g, 80%) as an off-white solid; R_f 0.33 (3:1 pet. ether/EtOAc); mp 138−140 °C; ν_{max} (neat, cm^{-1}) 3444, 3338, 2989, 2917, 2856, 2830, 1605, 1556, 1490, 1258, 1107; ^{1}H NMR (400 MHz, CDCl$_3$) δ: 6.54 (d, J = 8.8 Hz, 1H), 6.13 (d, J = 8.8 Hz, 1H), 4.56 (s, 2H, OCH$_2$), 4.40 (s, 2H, OCH$_2$), 4.37−4.27 (br.s, disappears with D_2O, 2H, NH$_2$), 3.78 (s, 3H, Me), 3.71 (s, 3H, Me), 3.14 (t, J = 12.1 Hz, 2H), 2.75 (d, J = 11.4 Hz, 2H), 2.13 (d, J = 12.4 Hz, 2H), 1.79−1.66 (m, 2H); ^{13}C{^{1}H} NMR (100 MHz, CDCl$_3$) δ: 153.6, 142.1, 135.4, 126.3 (all C), 107.5, 99.0 (both CH), 82.8, 81.7 (both OCH$_2$), 56.1, 55.5 (both Me), 47.3 (CH$_2$), 38.6 (C), 36.7 (CH$_2$); HRMS (ESI) m/z [M + H]$^+$ Calcd for C$_{15}$H$_{23}$N$_2$O$_3$ 279.1709; Found 279.1701.

2.6.3.3. Synthesis of 7-(2-Nitrophenyl)-2-oxa-7-azaspiro[3.5]nonane

94%
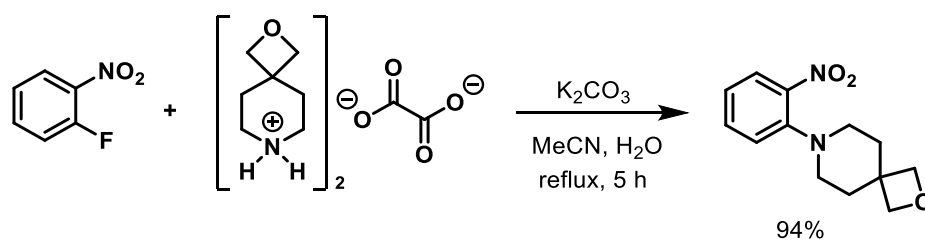
1-Fluoro-2-nitrobenzene (0.296 g, 2.10 mmol), bis(2-oxa-7-azaspiro[3.5]nonan-7-ium) ethanedioate (0.722 g, 2.10 mmol), and K_2CO_3 (1.161 g, 8.40 mmol) in MeCN (20 mL) and H_2O (4 mL) were heated at reflux for 5 h. The mixture was evaporated, dissolved in EtOAc (20 mL), and washed with brine (3 × 20 mL). The organic extract was dried (MgSO$_4$), evaporated, and purified by column chromatography using gradient elution of pet. ether/EtOAc to give the *title compound* (0.489 g, 94%) as an orange solid; R_f 0.38 (3:2 pet. ether/EtOAc); mp 95−96 °C; ν_{max} (neat, cm^{-1}) 2931, 2859, 2814, 1603, 1567, 1519 (NO$_2$), 1488, 1463, 1444, 1384, 1343 (NO$_2$), 1298, 1234, 1167, 1129; ^{1}H NMR (400 MHz, CDCl$_3$) δ: 7.76 (dd, J = 8.1, 1.6 Hz, 1H), 7.48−7.43 (m, 1H), 7.11 (dd, J = 8.3, 1.1 Hz, 1H), 7.05−7.00 (m, 1H), 4.48 (s, 4H, OCH$_2$), 2.95 (t, J = 5.5 Hz, 4H), 2.02 (t, J = 5.5 Hz, 4H); ^{13}C{^{1}H} NMR (100 MHz, CDCl$_3$) δ: 146.3, 143.3 (both C), 133.4, 125.9, 121.7, 121.2 (all CH), 81.6 (OCH$_2$), 49.2 (CH$_2$), 38.3 (C), 34.9 (CH$_2$); HRMS (ESI) m/z [M + H]$^+$ Calcd for C$_{13}$H$_{17}$N$_2$O$_3$ 249.1239; Found 249.1245.

2.6.3.4. Synthesis of 2-(2-Oxa-7-azaspiro[3.5]nonan-7-yl)aniline (12b)

12b (88%)
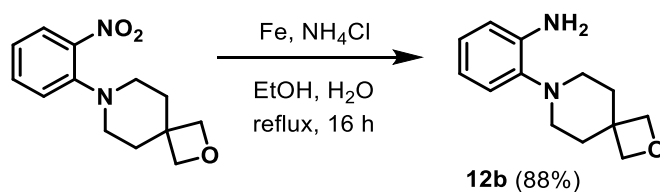
7-(2-Nitrophenyl)-2-oxa-7-azaspiro[3.5]nonane (0.480 g, 1.94 mmol), iron powder (0.347 g, 6.21 mmol), and NH_4Cl (52 mg, 0.97 mmol) in EtOH (30 mL) and H_2O (10 mL) were heated at reflux for 16 h. The mixture was filtered through Celite, evaporated, dissolved in EtOAc (60 mL), and washed with brine (2 × 40 mL). The organic extract was dried ($MgSO_4$), evaporated, and purified by column chromatography using gradient elution of pet. ether/EtOAc to give **12b** (0.372 g, 88%) as a pale brown solid; R_f 0.35 (3:2 pet. ether/EtOAc); mp 137−139 °C; ν_{max} (neat, cm^{-1}) 3408, 3325, 3032, 2914, 2856, 2806, 2740, 2677, 1617, 1501, 1461, 1438, 1425, 1383, 1289, 1211, 1135, 1125; ^{1}H NMR (400 MHz, CDCl$_3$) δ: 6.94−6.86 (m, 2H), 6.74−6.65 (m, 2H), 4.46 (s, 4H, OCH$_2$), 4.02−3.87 (br.s, disappears with D$_2$O, 2H, NH$_2$), 2.89−2.60 (br.s, 4H), 2.06−1.86 (br.s, 4H); ^{13}C{^{1}H} NMR (100 MHz, CDCl$_3$) δ: 141.6, 139.6 (both C), 124.6, 119.8, 118.5, 115.1 (all CH), 81.9 (OCH$_2$), 48.7 (CH$_2$), 38.6 (C), 35.9 (CH$_2$); HRMS (ESI) *m/z* [M + H]$^+$ Calcd for C$_{13}$H$_{19}$N$_2$O 219.1497; Found 219.1487.

2.6.3.5. H_2O_2 and HX-Mediated Transformations

Reaction conditions are given in Table 2.2 and Scheme 2.17 for H_2O_2 and HI, and in Scheme 2.13 for H_2O_2 and HCl. H_2O_2 and HX were sequentially added dropwise to a stirred solution of the anilines (1 mmol) in EtOAc (10 or 40 mL) at the indicated reaction temperatures. For the room temperature reaction of aniline **4a**, the additions of H_2O_2 and HI were done over ice, and the mixture was then allowed to warm to room temperature. At the end of the reaction, the solution was filtered, and the orange precipitate washed with EtOAc (30 mL) to give 1,4,6,9-tetramethoxyphenazine (**6**). The filtrate was washed with Na_2CO_3 (satd., 60 mL) and dried ($MgSO_4$). The organic extract was evaporated, and the residue was triturated from Et_2O to give benzimidazoles **5a−5d**. Azepane **5e** did not require purification. The residues of **4f**, **5f**, **13a**, and **13b** were purified by column chromatography using gradient elution of pet. ether/EtOAc.

4a → 5a (69%) + 6 (19%)

H₂O₂ (20 equiv)
HI (0.2 equiv)
EtOAc (25 mM), reflux
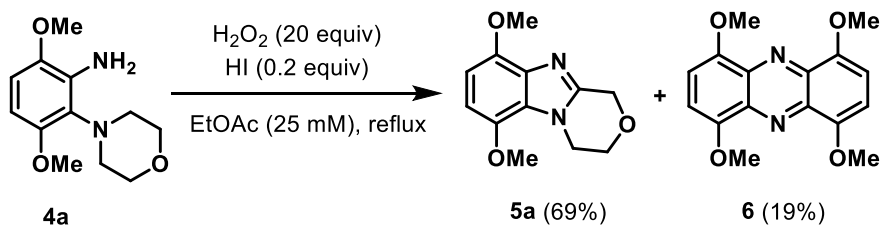
6,9-Dimethoxy-3,4-dihydro-1*H*-[1,4]oxazino[4,3-*a*]benzimidazole (5a). (0.161 g, 69%, Table 2.2, entry 3); pale brown solid; mp 109−111 °C; v_{max} (neat, cm⁻¹) 2929, 2827, 1523, 1475, 1440, 1426, 1402, 1316, 1259, 1227, 1193, 1165, 1119, 1103, 1084; ¹H NMR (400 MHz, CDCl₃) δ: 6.45 (ABq, *J* = 8.6 Hz, 2H), 4.92 (s, 2H, 1-CH₂), 4.41 (t, *J* = 5.2 Hz, 2H), 4.03 (t, *J* = 5.2 Hz, 2H), 3.87 (s, 3H, Me), 3.79 (s, 3H, Me); ¹³C{¹H} NMR (100 MHz, CDCl₃) δ: 146.3, 145.8, 141.8, 134.4, 125.0 (all C), 102.8, 102.0 (both CH), 65.5 (1-CH₂), 64.3 (CH₂), 55.9, 55.8 (both Me), 44.9 (CH₂); HRMS (ESI) *m/z* [M + H]⁺ Calcd for $C_{12}H_{15}N_2O_3$ 235.1083; Found 235.1081

1,4,6,9-tetramethoxyphenazine (6) (29 mg, 19%); orange solid; mp (DSC) onset 351.2 °C, peak max 355.9 °C (lit m.p.[26] > 360 °C); v_{max} (neat, cm⁻¹) 3075, 3010, 2900, 2833, 1177, 1622, 1492, 1456, 1445, 1437, 1322, 1266, 1248, 1197, 1157, 1127, 1109; ¹H NMR (400 MHz, CDCl₃) δ: 6.97 (s, 4H), 4.09 (s, 12H, Me); ¹³C{¹H} NMR (100 MHz, CDCl₃) δ: 148.8, 135.6 (both C), 106.0 (CH), 56.1 (Me); HRMS (ESI) *m/z* [M + H]⁺ Calcd for $C_{16}H_{17}N_2O_4$ 301.1188; Found 301.1179.
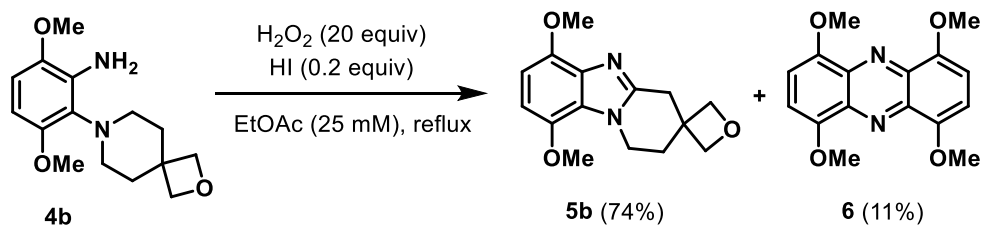
6′,9′-Dimethoxy-1′,2′-dihydro-4′*H*-spiro[oxetane-3,3′-pyrido[1,2-*a*]benzimidazole] **(5b).** (0.203 g, 74%); off-white solid; mp 166−167 °C; ν_{max} (neat, cm^{-1}) 3004, 2931, 2865, 2837, 1810, 1606, 1523, 1441, 1260, 1223, 1100, 1082; ^{1}H NMR (400 MHz, CDCl$_3$) δ: 6.47 (s, 2H), 4.53 (ABq, *J* = 6.1 Hz, 4H, OCH$_2$), 4.45 (t, *J* = 6.3 Hz, 2H, 1′-CH$_2$), 3.92 (s, 3H, Me), 3.83 (s, 3H, Me), 3.32 (s, 2H, 4′-CH$_2$), 2.34 (t, *J* = 6.3 Hz, 2H, 2′-CH$_2$); ^{13}C{^{1}H} NMR (100 MHz, CDCl$_3$) δ: 148.2, 145.6, 141.8, 135.0, 125.3 (all C), 102.6, 101.8 (both CH), 80.8 (OCH$_2$), 55.93, 55.89 (both Me), 41.7 (1′-CH$_2$), 37.7 (C), 35.0 (4′-CH$_2$), 31.3 (2′-CH$_2$); HRMS (ESI) *m/z* [M + H]$^+$ Calcd for C$_{15}$H$_{19}$N$_2$O$_3$ 275.1396; Found 275.1380,

1,4,6,9-Tetramethoxyphenazine (6) (17 mg, 11%).
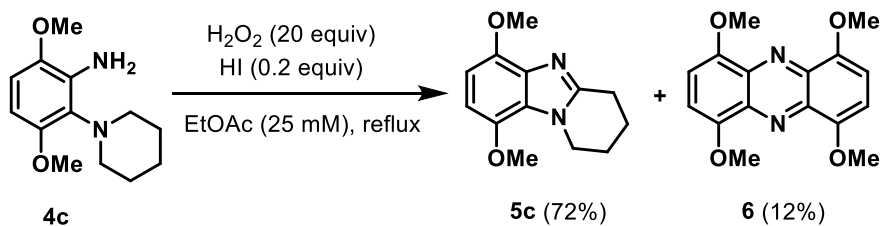
6,9-Dimethoxy-1,2,3,4-tetrahydropyrido[1,2-*a*]benzimidazole (5c). (0.167 g, 72%); brown solid; spectral data and melting point were consistent with the literature.[42]

1,4,6,9-Tetramethoxyphenazine (6) (18 mg, 12%).
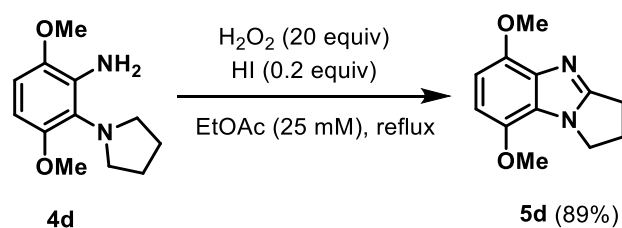
5,8-Dimethoxy-2,3-dihydro-1*H*-pyrrolo[1,2-*a*]benzimidazole (5d). (0.194 g, 89%); off-white solid; spectral data and melting point were consistent with the literature.[42]
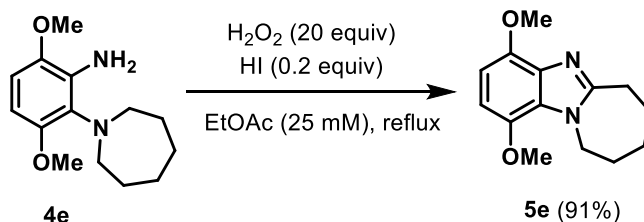
1,4-Dimethoxy-7,8,9,10-tetrahydro-6*H*-azepino[1,2-*a*]benzimidazole (5e). (0.224 g, 91%); brown oil; spectral data were consistent with the literature.[42]

92
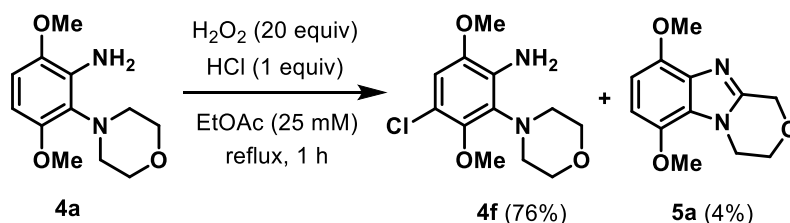
4-Chloro-3,6-dimethoxy-2-(morpholin-4-yl)aniline (4f). (0.207 g, 76%); R_f 0.51 (1:1 pet. ether/EtOAc); pale brown solid; mp 149−151 °C; ν_{max} (neat, cm^{-1}) 3434, 3335, 2960, 2909, 2881, 2843, 1596, 1549, 1480, 1456, 1445, 1419, 1261, 1177, 1153, 1041; ^{1}H NMR (400 MHz, CDCl$_3$) δ: 6.65 (s, 1H), 3.98−3.88 (br.s, 2H), 3.87 (s, 3H, Me), 3.81 (s, 3H, Me), 3.78−3.63 (br.s, 2H), 3.52−3.35 (br.s, 2H), 2.87−2.68 (br.s, 2H), NH$_2$ is absent; ^{13}C{^{1}H} NMR (100 MHz, CDCl$_3$) δ: 148.9, 143.6, 133.7, 130.5, 114.8 (all C), 109.3 (CH), 68.4 (2 x CH$_2$), 61.8, 56.0, (both Me), 51.0 (2 x CH$_2$); HRMS (ESI) m/z [M + H]$^+$ Calcd for C$_{12}$H$_{18}$N$_2$O$_3$Cl 273.1006; Found 273.1012

6,9-Dimethoxy-3,4-dihydro-1H-[1,4]oxazino[4,3-a]benzimidazole (5a) (9 mg, 4%); R_f 0.35 (EtOAc).
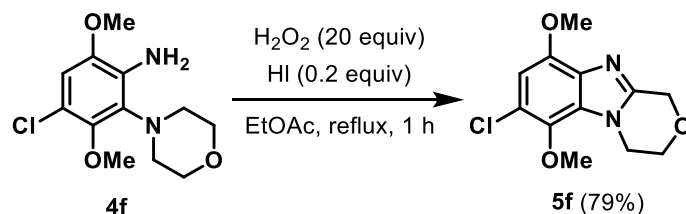
7-Chloro-6,9-dimethoxy-3,4-dihydro-1H-[1,4]oxazino[4,3-a]benzimidazole (5f). (0.212 g, 79%); R_f 0.43 (EtOAc); brown solid; mp 144−146 °C; ν_{max} (neat, cm^{-1}) 2931, 2836, 2359, 1605, 1508, 1473, 1428, 1399, 1309, 1212, 1153, 1111, 1070; ^{1}H NMR (400 MHz, CDCl$_3$) δ: 6.64 (s, 1H), 5.00 (s, 2H, 1-CH$_2$), 4.44 (t, J = 5.2 Hz, 2H), 4.17 (t, J = 5.2 Hz, 2H), 3.96 (s, 3H, Me), 3.94 (s, 3H, Me); ^{13}C{^{1}H} NMR (100 MHz, CDCl$_3$) δ: 147.7, 147.0, 136.7, 133.4, 128.5, 120.5 (all C), 104.8 (CH), 65.5, 64.1 (CH$_2$), 62.5, 56.1 (both Me), 44.2 (CH$_2$); HRMS (ESI) m/z [M + H]$^+$ Calcd for C$_{12}$H$_{14}$N$_2$O$_3$Cl 269.0693; Found 269.0685.
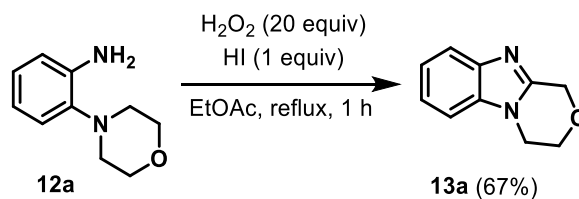
3,4-Dihydro-1*H*-[1,4]oxazino[4,3-*a*]benzimidazole (13a). (0.117 g, 67%); pale brown solid; R_f 0.21 (EtOAc); spectral data and melting point were consistent with the literature.[79]
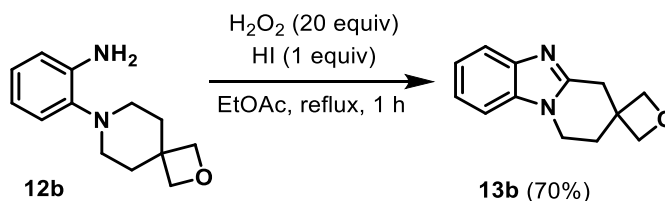
1′,2′-Dihydro-4′*H*-spiro[oxetane-3,3′-pyrido[1,2-*a*]benzimidazole] (13b). (0.149 g, 70%); off-white solid; R_f 0.23 (1:10 MeOH/EtOAc); mp 141−143 °C; ν_{max} (neat, cm^{-1}) 3052, 2936, 2864, 1668, 1616, 1516, 1485, 1457, 1417, 1371, 1344, 1319, 1283, 1228, 1161; ^{1}H NMR (400 MHz, CDCl$_3$) δ: 7.73−7.67 (m, 1H), 7.33−7.28 (m, 1H), 7.28−7.22 (m, 2H), 4.59 (ABq, J = 6.2 Hz, 4H, OCH$_2$), 4.14 (t, J = 6.3 Hz, 2H, 1′-CH$_2$), 3.40 (s, 2H, 4′-CH$_2$), 2.47 (t, J = 6.3 Hz, 2H, 2′-CH$_2$); ^{13}C{^{1}H} NMR (100 MHz, CDCl$_3$) δ: 149.5, 143.2, 134.3 (all C), 122.4, 122.2, 119.2, 108.9 (all CH), 80.6 (OCH$_2$), 38.8 (1′-CH$_2$), 38.0 (C), 34.9 (4′-CH$_2$), 30.7 (2′-CH$_2$); HRMS (ESI) *m/z* [M + H]$^+$ C$_{13}$H$_{15}$N$_2$O Calcd for 215.1184; Found 215.1180.

94

2.6.3.6. Modified Wohl−Aue Reaction

6 (34%)
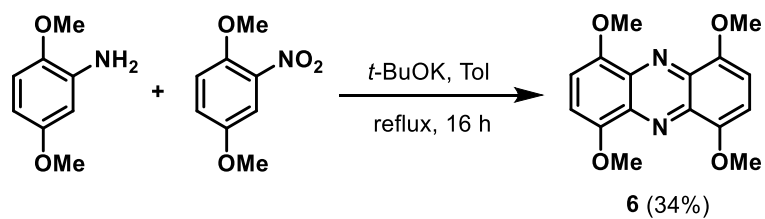
Reaction conditions are given in Scheme 2.12. At the end of the reaction, the mixture was filtered, and the precipitate washed with water (30 mL) to give **6** (1.02 g, 34%) as an orange solid. Spectral data and melting point of phenazine **6** were consistent with the above.

2.6.3.7. Aqueous I$_2$-Mediated Transformations

Anilines (1.00 mmol) in MeCN (10 mL) and H$_2$O (2 mL) were heated to reflux. I$_2$ (10.00 mmol) was added, and the mixture was stirred at reflux for 10 min. The mixture was filtered, and the precipitate was washed with water (20 mL) to give phenazine **6**. The filtrate was washed with Na$_2$CO$_3$ (satd., 20 mL) and Na$_2$S$_2$O$_3$ (1 M, 20 mL), and the organic extract was dried (MgSO$_4$) and evaporated to dryness. Benzimidazole **5d** did not require purification. The residue of benzimidazole **5a** was purified by column chromatography using gradient elution of pet. ether/EtOAc.
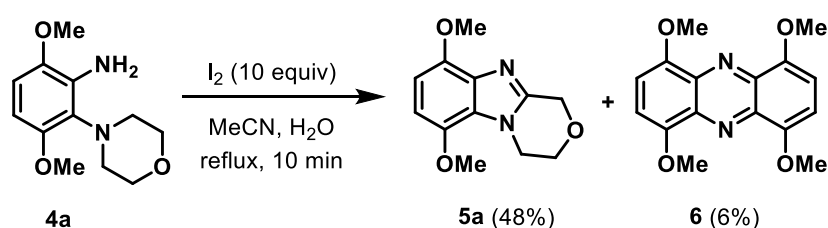
6,9-Dimethoxy-3,4-dihydro-1*H*-[1,4]oxazino[4,3-*a*]benzimidazole (5a). (0.112 g, 48%); R_f 0.35 (EtOAc); spectral data and melting point was consistent with the above.

1,4,6,9-Tetramethoxyphenazine (6) (9 mg, 6%). spectral data and melting point was consistent with the above.
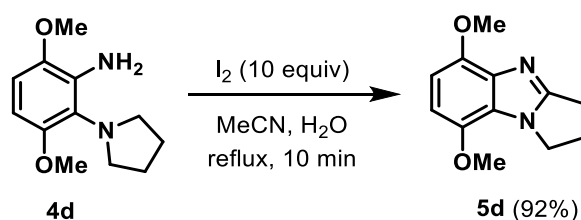
5,8-Dimethoxy-2,3-dihydro-1*H*-pyrrolo[1,2-*a*]benzimidazole (5d). (0.201 g, 92%); off-white solid; spectral data and melting point were consistent with the literature.[42]

2.6.3.8. General Procedure for the Synthesis of Quinones 1 and 2

Benzimidazole (0.26 mmol) and PIFA (0.447 g, 1.04 mmol) in H_2O (29 mL) and MeOH (0.75 mL) were stirred at room temperature for 2 h. The mixture was extracted with CH_2Cl_2 (3 × 40 mL). The organic extracts were dried (MgSO$_4$), evaporated, and purified by column chromatography using gradient elution of pet. ether/EtOAc and EtOAc/MeOH.
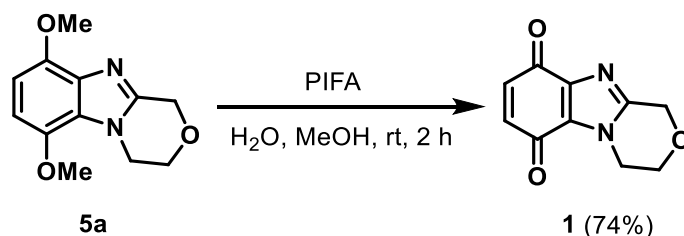
3,4-Dihydro-1*H*-[1,4]oxazino[4,3-*a*]benzimidazole-6,9-dione (1). (39 mg, 74%); yellow solid; R_f 0.41 (EtOAc); mp (decomp. >165 °C); ν_{max} (neat, cm^{-1}) 2924, 1664 (C=O), 1584, 1531, 1475, 1436, 1379, 1345, 1317, 1289, 1225, 1202, 1112, 1095, 1066; ^{1}H NMR (400 MHz, CDCl$_3$) δ: 6.68 (ABq, J = 10.4 Hz, 2H), 4.99 (s, 2H, 1-CH$_2$), 4.44 (t, J = 5.2 Hz, 2H), 4.14 (t, J = 5.2 Hz, 2H); ^{13}C{^{1}H} NMR (100 MHz, CDCl$_3$) δ: 180.9, 178.1 (both C=O), 148.0, 141.2 (both C), 136.6, 135.8 (both CH), 130.1 (C), 65.0 (1-CH$_2$), 63.3, 44.7 (both CH$_2$); HRMS (ESI) *m/z* [M + H]$^+$ C$_{10}$H$_9$N$_2$O$_3$ Calcd for 205.0613; Found 205.0623.
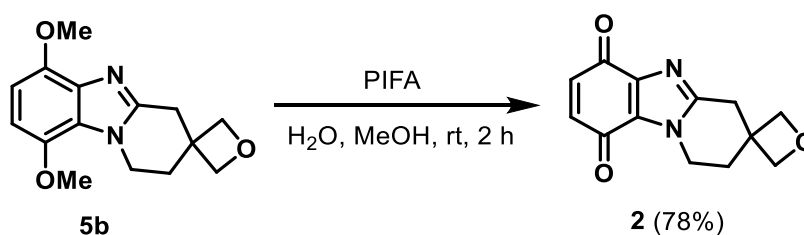
1′,2′-Dihydro-4′*H*-spiro[oxetane-3,3′-pyrido[1,2-*a*]benzimidazole]-6′,9′-dione (2). (49 mg, 78%); yellow oil; R_f 0.44 (1:10 MeOH/EtOAc); ν_{max} (neat, cm^{-1}) 2929, 1661 (C=O), 1510, 1487, 1446, 1350, 1270, 1202, 1132; ^{1}H NMR (400 MHz, CDCl$_3$) δ: 6.62 (ABq, J = 10.4 Hz, 2H), 4.56 (ABq, J = 6.2 Hz, 4H, OCH$_2$), 4.38 (t, J = 6.2 Hz, 2H, 1′-CH$_2$), 3.32 (s, 2H, 4′-CH$_2$), 2.38 (t, J = 6.2 Hz, 2H, 2′-CH$_2$); ^{13}C{^{1}H} NMR (100 MHz, CDCl$_3$) δ: 181.1, 178.2 (both C=O), 151.9, 149.9 (both C), 136.5, 136.0 (both CH), 130.2 (C), 80.5 (OCH$_2$), 41.7 (1′-CH$_2$), 37.2 (C), 34.4 (4′-CH$_2$), 30.4 (2′-CH$_2$); HRMS (ESI) *m/z* [M + H]$^+$ C$_{13}$H$_{13}$N$_2$O$_3$ Calcd for 245.0926; Found 245.0923.

2.7.   Chapter 2 References

(1)   Colucci, M. A.; Couch, G. D.; Moody, C. J. Natural and Synthetic Quinones and Their Reduction by the Quinone Reductase Enzyme NQO1: From Synthetic Organic Chemistry to Compounds with Anticancer Potential. *Org. Biomol. Chem.* **2008**, *6*, 637–656. https://doi.org/10.1039/b715270a.

(2)   Chen, Y.; Hu, L. Design of Anticancer Prodrugs for Reductive Activation. *Med. Res. Rev.* **2009**, *29*, 29–64. https://doi.org/10.1002/med.20137.

(3)   Zhang, K.; Chen, D.; Ma, K.; Wu, X.; Hao, H.; Jiang, S. NAD(P)H:Quinone Oxidoreductase 1 (NQO1) as a Therapeutic and Diagnostic Target in Cancer. *J. Med. Chem.* **2018**, *61*, 6983–7003. https://doi.org/10.1021/acs.jmedchem.8b00124.

(4)   Sharma, A.; Arambula, J. F.; Koo, S.; Kumar, R.; Singh, H.; Sessler, J. L.; Kim, J. S. Hypoxia-Targeted Drug Delivery. *Chem. Soc. Rev.* **2019**, *48*, 771–813. https://doi.org/10.1039/c8cs00304a.

(5)   Crooke, S. T.; Bradner, W. T. Mitomycin C: A Review. *Cancer Treat. Rev.* **1976**, *3*, 121–139. https://doi.org/10.1016/S0305-7372(76)80019-9.

(6)   Jones, G. B.; Moody, C. J. Structurally Modified Antitumour Agents. Synthesis of a Cyclopropamitosene. *J. Chem. Soc. Chem. Commun.* **1989**, 186–187. https://doi.org/10.1039/C39890000186.

(7)   Jones, G. B.; Moody, C. J. Structurally Modified Antitumour Agents. Part 2. Total Synthesis of a Cyclopropamitosene. *J. Chem. Soc. Perkin Trans. 1* **1989**, 2455–2462. https://doi.org/10.1039/P19890002455.

(8)   Cotterill, A. S.; Hartopp, P.; Jones, G. B.; Moody, C. J.; Norton, C. L.; O'Sullivan, N.; Swann, E. Cyclopropamitosenes, Novel Bioreductive Anticancer Agents. Synthesis of 7-Methoxycyclopropamitosene and Related Indolequinones. *Tetrahedron* **1994**, *50*, 7657–7674. https://doi.org/https://doi.org/10.1016/S0040-4020(01)90492-2.

(9)   Moody, C. J.; O'Sullivan, N.; Stratford, I. J.; Stephens, M. A.; Workman, P.; Bailey, S. M.; Lewis, A. Cyclopropamitosenes: Novel Bioreductive Anticancer Agents-Mechanism of Action and Enzymic Reduction. *Anticancer Drugs* **1994**, *5*, 367—372.

(10) O'Shaughnessy, J.; Cunningham, D.; Kavanagh, P.; Leech, D.; McArdle, P.; Aldabbagh, F. Synthesis of Benzimidazolequinone Analogue of Cyclopropamitosene Antitumor Agents. *Synlett* **2004**, 2382–2384. https://doi.org/10.1055/s-2004-831341.

(11) O'Shaughnessy, J.; Aldabbagh, F. Synthesis of Pyrrolo- and Pyrido-[1,2-*a*]Benzimidazolequinone Anti-Tumor Agents Containing a Fused Cyclopropane Ring. *Synthesis* **2005**, 1069–1076. https://doi.org/10.1055/s-2005-861832.

(12) Islam, I.; Skibo, E. B. Synthesis and Physical Studies of Azamitosene and Iminoazamitosene Reductive Alkylating Agents. Iminoquinone Hydrolytic Stability, Syn/Anti Isomerization, and Electrochemistry. *J. Org. Chem.* **1990**, *55*, 3195–3205. https://doi.org/10.1021/jo00297a040.

(13) Islam, I.; Skibo, E. B.; Dorr, R. T.; Alberts, D. S. Structure-Activity Studies of Antitumor Agents Based on Pyrrolo[1,2-*a*]benzimidazoles: New Reductive Alkylating DNA Cleaving Agents. *J. Med. Chem.* **1991**, *34*, 2954–2961. https://doi.org/10.1021/jm00114a003.

(14) Skibo, E. B.; Schulz, W. G. Pyrrolo[1,2-*a*]benzimidazole-Based Aziridinyl Quinones. A New Class of DNA Cleaving Agent Exhibiting G and A Base Specificity. *J. Med. Chem.* **1993**, *36*, 3050–3055. https://doi.org/10.1021/jm00073a002.

(15) Schulz, W. G.; Islam, I.; Skibo, E. B. Pyrrolo[1,2-*a*]benzimidazole-Based Quinones and Iminoquinones. The Role of the 3-Substituent on Cytotoxicity. *J. Med. Chem.* **1995**, *38*, 109–118. https://doi.org/10.1021/jm00001a016.

(16) Zhou, R.; Skibo, E. B. Chemistry of the Pyrrolo[1,2-*a*]benzimidazole Antitumor Agents: Influence of the 7-Substituent on the Ability to Alkylate DNA and Inhibit Topoisomerase II. *J. Med. Chem.* **1996**, *39*, 4321–4331. https://doi.org/10.1021/jm960064d.

(17) Skibo, E. B.; Gordon, S.; Bess, L.; Boruah, R.; Heileman, M. J. Studies of Pyrrolo[1,2-*a*]benzimidazolequinone DT-Diaphorase Substrate Activity, Topoisomerase II Inhibition Activity, and DNA Reductive Alkylation. *J. Med. Chem.* **1997**, *40*, 1327–1339. https://doi.org/10.1021/jm960546p.

(18)   Craigo, W. A.; LeSueur, B. W.; Skibo, E. B. Design of Highly Active Analogues of the Pyrrolo[1,2-*a*]benzimidazole Antitumor Agents. *J. Med. Chem.* **1999**, *42*, 3324–3333. https://doi.org/10.1021/jm990029h.

(19)   Huang, X.; Suleman, A.; Skibo, E. B. Rational Design of Pyrrolo[1,2-*a*]benzimidazole-Based Antitumor Agents Targeting the DNA Major Groove. *Bioorg. Chem.* **2000**, *28*, 324–337. https://doi.org/10.1006/bioo.2000.1183.

(20)   Schulz, W. G.; Nieman, R. A.; Skibo, E. B. Evidence for DNA Phosphate Backbone Alkylation and Cleavage by Pyrrolo[1,2-*a*]benzimidazoles: Small Molecules Capable of Causing Base-Pair-Specific Phosphodiester Bond Hydrolysis. *Proc. Natl. Acad. Sci. U. S. A.* **1995**, *92*, 11854–11858. https://doi.org/10.1073/pnas.92.25.11854.

(21)   Lynch, M.; Hehir, S.; Kavanagh, P.; Leech, D.; O'Shaughnessy, J.; Carty, M. P.; Aldabbagh, F. Synthesis by Radical Cyclization and Cytotoxicity of Highly Potent Bioreductive Alicyclic Ring Fused [1,2-*a*]benzimidazolequinones. *Chem. Eur. J.* **2007**, *13*, 3218–3226. https://doi.org/10.1002/chem.200601450.

(22)   Moriarty, E.; Carr, M.; Bonham, S.; Carty, M. P.; Aldabbagh, F. Synthesis and Toxicity towards Normal and Cancer Cell Lines of Benzimidazolequinones Containing Fused Aromatic Rings and 2-Aromatic Ring Substituents. *Eur. J. Med. Chem.* **2010**, *45*, 3762–3769. https://doi.org/10.1016/j.ejmech.2010.05.025.

(23)   O'Donovan, L.; Carty, M. P.; Aldabbagh, F. First Synthesis of *N*-[(Aziridin-2-Yl)Methyl]Benzimidazolequinone and Analysis of Toxicity towards Normal and Fanconi Anemia Cells. *Chem. Commun.* **2008**, 5592-5594. https://doi.org/10.1039/b814706j.

(24)   Fahey, K.; O'Donovan, L.; Carr, M.; Carty, M. P.; Aldabbagh, F. The Influence of the Aziridinyl Substituent of Benzimidazoles and Benzimidazolequinones on Toxicity towards Normal and Fanconi Anaemia Cells. *Eur. J. Med. Chem.* **2010**, *45*, 1873–1879. https://doi.org/10.1016/j.ejmech.2010.01.026.

(25) Bonham, S.; O'Donovan, L.; Carty, M. P.; Aldabbagh, F. First Synthesis of an Aziridinyl Fused Pyrrolo[1,2-*a*]benzimidazole and Toxicity Evaluation towards Normal and Breast Cancer Cell Lines. *Org. Biomol. Chem.* **2011**, *9*, 6700–6706. https://doi.org/10.1039/c1ob05694h.

(26) Schulz, W. G.; Skibo, E. B. Inhibitors of Topoisomerase II Based on the Benzodiimidazole and Dipyrroloimidazobenzimidazole Ring Systems: Controlling DT-Diaphorase Reductive Inactivation with Steric Bulk. *J. Med. Chem.* **2000**, *43*, 629–638. https://doi.org/10.1021/jm990210q.

(27) Suleman, A.; Skibo, E. B. A Comprehensive Study of the Active Site Residues of DT-Diaphorase: Rational Design of Benzimidazolediones as DT-Diaphorase Substrates. *J. Med. Chem.* **2002**, *45*, 1211–1220. https://doi.org/10.1021/jm0104365.

(28) Fagan, V.; Bonham, S.; Carty, M. P.; Aldabbagh, F. One-Pot Double Intramolecular Homolytic Aromatic Substitution Routes to Dialicyclic Ring Fused Imidazobenzimidazolequinones and Preliminary Analysis of Anticancer Activity. *Org. Biomol. Chem.* **2010**, *8*, 3149–3156. https://doi.org/10.1039/c003511d.

(29) Fagan, V.; Bonham, S.; McArdle, P.; Carty, M. P.; Aldabbagh, F. Synthesis and Toxicity of New Ring-Fused Imidazo[5,4-*f*]benzimidazolequinones and Mechanism Using Amine *N*-Oxide Cyclizations. *Eur. J. Org. Chem.* **2012**, 1967–1975. https://doi.org/10.1002/ejoc.201101687.

(30) Fagan, V.; Bonham, S.; Carty, M. P.; Saenz-Méndez, P.; Eriksson, L. A.; Aldabbagh, F. COMPARE Analysis of the Toxicity of an Iminoquinone Derivative of the Imidazo[5,4-*f*]benzimidazoles with NAD(P)H:Quinone Oxidoreductase 1 (NQO1) Activity and Computational Docking of Quinones as NQO1 Substrates. *Bioorg. Med. Chem.* **2012**, *20*, 3223–3232. https://doi.org/10.1016/j.bmc.2012.03.063.

(31) Welsch, M. E.; Snyder, S. A.; Stockwell, B. R. Privileged Scaffolds for Library Design and Drug Discovery. *Curr. Opin. Chem. Biol.* **2010**, *14*, 347–361. https://doi.org/10.1016/j.cbpa.2010.02.018.

(32) Keri, R. S.; Hiremathad, A.; Budagumpi, S.; Nagaraja, B. M. Comprehensive Review in Current Developments of Benzimidazole-Based Medicinal Chemistry. *Chem. Biol. Drug Des.* **2015**, *86*, 799–845. https://doi.org/10.1111/cbdd.12462.

(33) Manna, S. K.; Das, T.; Samanta, S. Polycyclic Benzimidazole: Synthesis and Photophysical Properties. *ChemistrySelect* **2019**, *4*, 8781–8790. https://doi.org/10.1002/slct.201901941.

(34) Spiegel, L.; Kaufmann, H. Über Die Reduktion Des Dinitrophenyl-Piperidins. *Ber. Dtsch. Chem. Ges.* **1908**, *41*, 679–685. https://doi.org/10.1002/cber.190804101129.

(35) Nair, M. D.; Adams, R. Benzimidazole Syntheses by Oxidative Cyclization with Peroxytrifluoroacetic Acid. *J. Am. Chem. Soc.* **1961**, *83*, 3518–3521. https://doi.org/10.1021/ja01477a038.

(36) Meth-Cohn, O.; Suschitzky, H. 893. Syntheses of Heterocyclic Compounds. Part IV. Oxidative Cyclisation of Aromatic Amines and Their *N*-Acyl Derivatives. *J. Chem. Soc.* **1963**, 4666–4669. https://doi.org/10.1039/JR9630004666.

(37) Meth-Cohn, O.; Suschitzky, H. Heterocycles by Ring Closure of *ortho*-Substituted *t*-Anilines (The *t*-Amino Effect). *Adv. Heterocycl. Chem.* **1972**, *14*, 211–278. https://doi.org/10.1016/S0065-2725(08)60954-X.

(38) Meth-Cohn, O. The *t*-Amino Effect: Heterocycles Formed by Ring Closure of *ortho*-Substituted *t*-Anilines. *Adv. Heterocycl. Chem.* **1996**, *65*, 1–37.

(39) Platonova, A. Y.; Glukhareva, T. V.; Zimovets, O. A.; Morzherin, Y. Y. *tert*-Amino Effect: The Meth-Cohn and Reinhoudt Reactions. *Chem. Heterocycl. Compd.* **2013**, *49*, 357–385. https://doi.org/10.1007/s10593-013-1257-6.

(40) Fahey, K.; Aldabbagh, F. Synthesis of Seven- and Eight-Membered [1,2-*a*] Alicyclic Ring-Fused Benzimidazoles and 3-Aziridinylazepino[1,2-*a*]benzimidazolequinone as a Potential Antitumour Agent. *Tetrahedron Lett.* **2008**, *49*, 5235–5237. https://doi.org/10.1016/j.tetlet.2008.06.121.

(41)   Ranganathan, S.; Sieber, V. Recent Advances in the Direct Synthesis of Hydrogen Peroxide Using Chemical Catalysis – A Review. *Catalysts* **2018**, *8*, 379. https://doi.org/10.3390/catal8090379.

(42)   Sweeney, M.; Gurry, M.; Keane, L. A. J.; Aldabbagh, F. Greener Synthesis Using Hydrogen Peroxide in Ethyl Acetate of Alicyclic Ring-Fused Benzimidazoles and Anti-Tumour Benzimidazolequinones. *Tetrahedron Lett.* **2017**, *58*, 3565–3567. https://doi.org/10.1016/j.tetlet.2017.07.102.

(43)   Alder, C. M.; Hayler, J. D.; Henderson, R. K.; Redman, A. M.; Shukla, L.; Shuster, L. E.; Sneddon, H. F. Updating and Further Expanding GSK's Solvent Sustainability Guide. *Green Chem.* **2016**, *18*, 3879–3890. https://doi.org/10.1039/c6gc00611f.

(44)   Ben-Daniel, R.; De Visser, S. P.; Shaik, S.; Neumann, R. Electrophilic Aromatic Chlorination and Haloperoxidation of Chloride Catalyzed by Polyfluorinated Alcohols: A New Manifestation of Template Catalysis. *J. Am. Chem. Soc.* **2003**, *125*, 12116–12117. https://doi.org/10.1021/ja0364524.

(45)   Eigen, M.; Kustin, K. The Kinetics of Halogen Hydrolysis. *J. Am. Chem. Soc.* **1962**, *84*, 1355–1361. https://doi.org/10.1021/ja00867a005.

(46)   Gurry, M.; Sweeney, M.; McArdle, P.; Aldabbagh, F. One-Pot Hydrogen Peroxide and Hydrohalic Acid Induced Ring Closure and Selective Aromatic Halogenation to Give New Ring-Fused Benzimidazoles. *Org. Lett.* **2015**, *17*, 2856–2859. https://doi.org/10.1021/acs.orglett.5b01317.

(47)   Sweeney, M.; Keane, L. A. J.; Gurry, M.; McArdle, P.; Aldabbagh, F. One-Pot Synthesis of Dihalogenated Ring-Fused Benzimidazolequinones from 3,6-Dimethoxy-2-(cycloamino)anilines Using Hydrogen Peroxide and Hydrohalic Acid. *Org. Lett.* **2018**, *20*, 6970–6974. https://doi.org/10.1021/acs.orglett.8b03135.

(48)   Thapa, P.; Palacios, P. M.; Tran, T.; Pierce, B. S.; Foss, F. W. 1,2-Disubstituted Benzimidazoles by the Iron Catalyzed Cross-Dehydrogenative Coupling of Isomeric *o*-Phenylenediamine Substrates. *J. Org. Chem.* **2020**, *85*, 1991–2009. https://doi.org/10.1021/acs.joc.9b02714.

(49)   Bera, S. K.; Alam, M. T.; Mal, P. C-N Coupling *via* Antiaromatic Endocyclic Nitrenium Ions. *J. Org. Chem.* **2019**, *84*, 12009–12020. https://doi.org/10.1021/acs.joc.9b01921.

(50)   Li, Q. Y.; Cheng, S. Y.; Tang, H. T.; Pan, Y. M. Synthesis of Rutaecarpine Alkaloids: *via* an Electrochemical Cross Dehydrogenation Coupling Reaction. *Green Chem.* **2019**, *21*, 5517–5520. https://doi.org/10.1039/c9gc03028j.

(51)   Vitaku, E.; Smith, D. T.; Njardarson, J. T. Analysis of the Structural Diversity, Substitution Patterns, and Frequency of Nitrogen Heterocycles among U.S. FDA Approved Pharmaceuticals. *J. Med. Chem.* **2014**, *57*, 10257–10274. https://doi.org/10.1021/jm501100b.

(52)   St. Jean, D. J.; Fotsch, C. Mitigating Heterocycle Metabolism in Drug Discovery. *J. Med. Chem.* **2012**, *55*, 6002–6020. https://doi.org/10.1021/jm300343m.

(53)   Arshad, F.; Khan, M. F.; Akhtar, W.; Alam, M. M.; Nainwal, L. M.; Kaushik, S. K.; Akhter, M.; Parvez, S.; Hasan, S. M.; Shaquiuzzaman, M. Revealing Quinquennial Anticancer Journey of Morpholine: A SAR Based Review. *Eur. J. Med. Chem.* **2019**, *167*, 324–356. https://doi.org/10.1016/j.ejmech.2019.02.015.

(54)   Gleave, R. J.; Beswick, P. J.; Brown, A. J.; Giblin, G. M. P.; Goldsmith, P.; Haslam, C. P.; Mitchell, W. L.; Nicholson, N. H.; Page, L. W.; Patel, S.; *et al*. Synthesis and Evaluation of 3-Amino-6-Aryl-Pyridazines as Selective CB2 Agonists for the Treatment of Inflammatory Pain. *Bioorg. Med. Chem. Lett.* **2010**, *20*, 465–468. https://doi.org/10.1016/j.bmcl.2009.11.117.

(55)   Wan, Z. K.; Chenail, E.; Xiang, J.; Li, H. Q.; Ipek, M.; Bard, J.; Svenson, K.; Mansour, T. S.; Xu, X.; Tian, X.; *et al*. Efficacious 11β-Hydroxysteroid Dehydrogenase Type I Inhibitors in the Diet-Induced Obesity Mouse Model. *J. Med. Chem.* **2009**, *52*, 5449–5461. https://doi.org/10.1021/jm900639u.

(56)   Tzara, A.; Xanthopoulos, D.; Kourounakis, A. P. Morpholine As a Scaffold in Medicinal Chemistry: An Update on Synthetic Strategies. *ChemMedChem* **2020**, *15*, 392–403. https://doi.org/10.1002/cmdc.201900682.

(57)   Wuitschik, G.; Carreira, E. M.; Wagner, B.; Fischer, H.; Parrilla, I.; Schuler, F.; Rogers-Evans, M.; Müller, K. Oxetanes in Drug Discovery: Structural and Synthetic Insights. *J. Med. Chem.* **2010**, *53*, 3227–3246. https://doi.org/10.1021/jm9018788.

(58)   Bull, J. A.; Croft, R. A.; Davis, O. A.; Doran, R.; Morgan, K. F. Oxetanes: Recent Advances in Synthesis, Reactivity, and Medicinal Chemistry. *Chem. Rev.* **2016**, *116*, 12150–12233. https://doi.org/10.1021/acs.chemrev.6b00274.

(59)   Burkhard, J. A.; Wuitschik, G.; Rogers-Evans, M.; Müller, K.; Carreira, E. M. Oxetanes as Versatile Elements in Drug Discovery and Synthesis. *Angew. Chem. Int. Ed.* **2010**, *49*, 9052–9067. https://doi.org/10.1002/anie.200907155.

(60)   Wuitschik, G.; Rogers-Evans, M.; Müller, K.; Fischer, H.; Wagner, B.; Schuler, F.; Polonchuk, L.; Carreira, E. M. Oxetanes as Promising Modules in Drug Discovery. *Angew. Chem. Int. Ed.* **2006**, *45*, 7736–7739. https://doi.org/10.1002/anie.200602343.

(61)   Wuitschik, G.; Rogers-Evans, M.; Buckl, A.; Bernasconi, M.; Märki, M.; Godel, T.; Fischer, H.; Wagner, B.; Parrilla, I.; Schuler, F.; *et al*. Spirocyclic Oxetanes: Synthesis and Properties. *Angew. Chem. Int. Ed.* **2008**, *47*, 4512–4515. https://doi.org/10.1002/anie.200800450.

(62)   Toselli, F.; Fredenwall, M.; Svensson, P.; Li, X. Q.; Johansson, A.; Weidolf, L.; Hayes, M. A. Hip to Be Square: Oxetanes as Design Elements to Alter Metabolic Pathways. *J. Med. Chem.* **2019**, *62*, 7383–7399. https://doi.org/10.1021/acs.jmedchem.9b00030.

(63)   Stepan, A. F.; Karki, K.; McDonald, W. S.; Dorff, P. H.; Dutra, J. K.; Dirico, K. J.; Won, A.; Subramanyam, C.; Efremov, I. V.; O'Donnell, C. J.; *et al*. Metabolism-Directed Design of Oxetane-Containing Arylsulfonamide Derivatives as γ-Secretase Inhibitors. *J. Med. Chem.* **2011**, *54*, 7772–7783. https://doi.org/10.1021/jm200893p.

(64)   Burkhard, J. A.; Wuitschik, G.; Plancher, J. M.; Rogers-Evans, M.; Carreira, E. M. Synthesis and Stability of Oxetane Analogs of Thalidomide and Lenalidomide. *Org. Lett.* **2013**, *15*, 4312–4315. https://doi.org/10.1021/ol401705a.

(65)   Parr, R. G.; Szentpály, L. V.; Liu, S. Electrophilicity Index. *J. Am. Chem. Soc.* **1999**, *121*, 1922–1924. https://doi.org/10.1021/ja983494x.

(66)   Gurry, M.; McArdle, P.; Aldabbagh, F. Synthesis of a Spirocyclic Oxetane-Fused Benzimidazole. *Molecules* **2015**, *20*, 13864–13874. https://doi.org/10.3390/molecules200813864.

(67)   Laursen, J. B.; Nielsen, J. Phenazine Natural Products: Biosynthesis, Synthetic Analogues, and Biological Activity. *Chem. Rev.* **2004**, *104*, 1663–1685. https://doi.org/10.1021/cr020473j.

(68)   Guttenberger, N.; Blankenfeldt, W.; Breinbauer, R. Recent Developments in the Isolation, Biological Function, Biosynthesis, and Synthesis of Phenazine Natural Products. *Bioorg. Med. Chem.* **2017**, *25*, 6149–6166. https://doi.org/10.1016/j.bmc.2017.01.002.

(69)   Wohl, A.; Aue, W. Ueber Die Einwirkung von Nitrobenzol Auf Anilin Bei Gegenwart von Alkali. *Ber. Dtsch. Chem. Ges.* **1901**, *34*, 2442–2450. https://doi.org/10.1002/cber.190103402183.

(70)   Sugimoto, A.; Kato, S.; Inoue, H.; Imoto, E. Studies on Organic Semiconductors. XVIII. Photoconductivity of Heteroaromatic Compounds and Their Substituted Derivatives. *Bull. Chem. Soc. Jpn.* **1976**, *49*, 337–338. https://doi.org/10.1246/bcsj.49.337.

(71)   Wrõbel, Z.; Stachowska, K.; Kwast, A. Phenazines and Their *N*-Oxides as Products of Cyclization of *N*-Aryl-2-Nitrosoanilines-Disproof of the Reported Homolytic Cross-Coupling Process Leading to Benzo[*c*]Cinnoline Oxides. *Eur. J. Org. Chem.* **2014**, 7721–7725. https://doi.org/10.1002/ejoc.201402624.

(72)   Bray, W. C.; Liebhafsky, H. A. Reactions Involving Hydrogen Peroxide, Iodine and Iodate Ion. I. Introduction. *J. Am. Chem. Soc.* **1931**, *53*, 38–44. https://doi.org/10.1021/ja01352a006.

(73)   Schmitz, G. Iodine Oxidation by Hydrogen Peroxide in Acidic Solutions, Bray-Liebhafsky Reaction and Other Related Reactions. *Phys. Chem. Chem. Phys.* **2010**, *12*, 6605–6615. https://doi.org/10.1039/b927432d.

(74)   Trummal, A.; Lipping, L.; Kaljurand, I.; Koppel, I. A.; Leito, I. Acidity of Strong Acids in Water and Dimethyl Sulfoxide. *J. Phys. Chem. A* **2016**, *120*, 3663–3669. https://doi.org/10.1021/acs.jpca.6b02253.

(75) Isse, A. A.; Lin, C. Y.; Coote, M. L.; Gennaro, A. Estimation of Standard Reduction Potentials of Halogen Atoms and Alkyl Halides. *J. Phys. Chem. B* **2011**, *115*, 678–684. https://doi.org/10.1021/jp109613t.

(76) Purkait, A.; Roy, S. K.; Srivastava, H. K.; Jana, C. K. Metal-Free Sequential C(sp^2)-H/OH and C(sp^3)-H Aminations of Nitrosoarenes and *N*-Heterocycles to Ring-Fused Imidazoles. *Org. Lett.* **2017**, *19*, 2540–2543. https://doi.org/10.1021/acs.orglett.7b00832.

(77) Kwast, A.; Stachowska, K.; Trawczyński, A.; Wróbel, Z. *N*-Aryl-2-Nitrosoanilines as Intermediates in the Synthesis of Substituted Phenazines from Nitroarenes. *Tetrahedron Lett.* **2011**, *52*, 6484–6488. https://doi.org/10.1016/j.tetlet.2011.09.113.

(78) Meth-Cohn, O. Mechanism of Formation of Benzimidazoles by Oxidation of O-Acylamino-*NN*-Dialkylanilines with Peroxy-Acids. *J. Chem. Soc. C* **1971**, 1356–1357. https://doi.org/10.1039/J39710001356.

(79) Nguyen, T. B.; Ermolenko, L.; Al-Mourabit, A. Formic Acid as a Sustainable and Complementary Reductant: An Approach to Fused Benzimidazoles by Molecular Iodine-Catalyzed Reductive Redox Cyclization of *o*-Nitro-*t*-anilines. *Green Chem.* **2016**, *18*, 2966–2970. https://doi.org/10.1039/c6gc00902f.

(80) Ogata, Y.; Sawaki, Y.; Mibae, J.; Morimoto, T. Kinetics of the Autoxidation of Phenylhydroxylamines to Azoxybenzenes in Methanol. *J. Am. Chem. Soc.* **1964**, *86*, 3854–3858. https://doi.org/10.1021/ja01072a051.

(81) Bamberger, E.; Ham, W. Über Das Verhalten Einiger Parasubstituierter Nitrosobenzole Gegen Konz. Schwefelsäure. *Justus Liebigs Ann. Chem.* **1911**, *382*, 82–128. https://doi.org/10.1002/jlac.19113820105.

(82) Seth, K.; Raha Roy, S.; Chakraborti, A. K. Synchronous Double C-N Bond Formation *via* C-H Activation for a Novel Synthetic Route to Phenazine. *Chem. Commun.* **2016**, *52*, 922–925. https://doi.org/10.1039/c5cc08640j.

(83) Tohma, H.; Morioka, H.; Harayama, Y.; Hashizume, M.; Kita, Y. Novel and Efficient Synthesis of *p*-Quinones in Water *via* Oxidative Demethylation of Phenol Ethers Using Hypervalent Iodine(III) Reagents. *Tetrahedron Lett.* **2001**, *42*, 6899–6902. https://doi.org/10.1016/S0040-4039(01)01407-1.

(84) Nair, V.; Rajan, R.; Mohanan, K.; Sheeba, V. Cerium(IV) Ammonium Nitrate-Mediated Oxidative Rearrangement of Cyclobutanes and Oxetanes. *Tetrahedron Lett.* **2003**, *44*, 4585–4588. https://doi.org/10.1016/S0040-4039(03)00978-X.

(85) Loman, J. J.; Carnaghan, E. R.; Hamlin, T. A.; Ovian, J. M.; Kelly, C. B.; Mercadante, M. A.; Leadbeater, N. E. A Combined Computational and Experimental Investigation of the Oxidative Ring-Opening of Cyclic Ethers by Oxoammonium Cations. *Org. Biomol. Chem.* **2016**, *14*, 3883–3888. https://doi.org/10.1039/c6ob00347h.

(86) Thorn, C. F.; Oshiro, C.; Marsh, S.; Hernandez-Boussard, T.; McLeod, H.; Klein, T. E.; Altman, R. B. Doxorubicin Pathways: Pharmacodynamics and Adverse Effects. *Pharmacogenet. Genomics* **2011**, *21*, 440–446. https://doi.org/10.1097/FPC.0b013e32833ffb56.

(87) Hammershøj, P.; Reenberg, T. K.; Pittelkow, M.; Nielsen, C. B.; Hammerich, O.; Christensen, J. B. Synthesis and Properties of 2,3-Dialkynyl-1,4-benzoquinones. *Eur. J. Org. Chem.* **2006**, 2786–2794. https://doi.org/10.1002/ejoc.200600081.

(88) Wang, G. T.; Zhao, X.; Li, Z. T. Hydrogen Bonded Arylamide-Linked Cholesteryl Dimesogenic Liquid Crystals: A Study of the Length and Side Chain Effects. *Tetrahedron* **2011**, *67*, 48–57. https://doi.org/10.1016/j.tet.2010.11.046.

(89) Sheldrick, G. M. SHELXT - Integrated Space-Group and Crystal-Structure Determination. *Acta Crystallogr., Sect. A: Found. Adv.* **2015**, *71*, 3–8. https://doi.org/10.1107/S2053273314026370.

(90) Sheldrick, G. M. Crystal Structure Refinement with SHELXL. *Acta Crystallogr., Sect. C: Struct. Chem.* **2015**, *71*, 3–8. https://doi.org/10.1107/S2053229614024218.

(91) McArdle, P. Oscail, a Program Package for Small-Molecule Single-Crystal Crystallography with Crystal Morphology Prediction and Molecular Modelling. *J. Appl. Crystallogr.* **2017**, *50*, 320–326. https://doi.org/10.1107/S1600576716018446.

Chapter 3

The Reactivity of Oxone towards 4,6-Di(cycloamino)-1,3-phenylenediamines: Synthesis of Spirocyclic Oxetane Ring-Fused Imidazobenzimidazoles
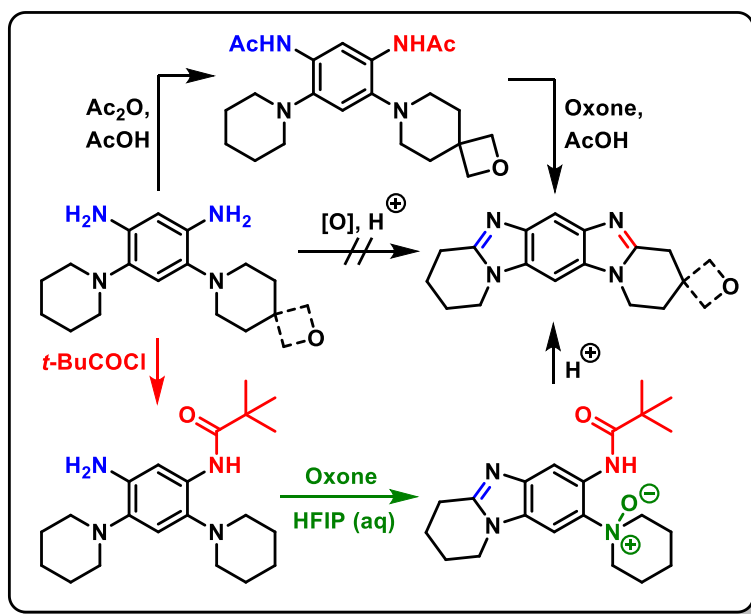
Parts of this chapter have been published in:

3.1. Introduction

Imidazobenzimidazoles are heterocycles that exist in a [4,5-*f*] and [5,4-*f*] arrangement.[1–5] The Skibo group first recognised the potential of the imidazo[4,5-*f*]benzimidazole scaffolds as precursors of pyrrolo- and pyrido-fused imidazobenzimidazolequinone anti-tumour agents.[1,2] Their method of synthesizing the imidazobenzimidazoles was based upon Meth-Cohn's double annulation of *o-tert*-aminoacetanilides using *in situ* generated performic acid (Scheme 3.1). Meth-Cohn reportedly isolated pyrido-fused imidazo[4,5-*f*]benzimidazole in 74% yield.[6] However Skibo achieved a poorer yield of 31%, with the pyrrolo-fused scaffold isolated in 10% yield.[1,2]

imidazo[4,5-*f*]benzimidazoles

n = 1 (10%)
n = 2 (31%[a] or 74%[b])

[a]Skibo et al.[2]
[b]Meth-Cohn et al.[6]

imidazobenzimidazolequinones
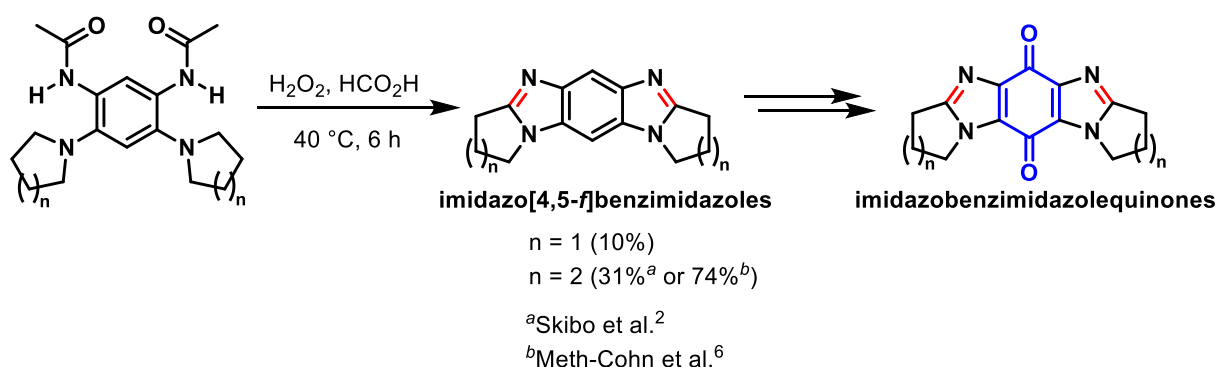
Scheme 3.1. Double annulations using H_2O_2/HCO_2H.

Fagan and Aldabbagh improved yields of imidazo[4,5-*f*] and [5,4-*f*]benzimidazoles by employing an intramolecular homolytic aromatic substitution (HAS) strategy (Scheme 3.2).[3] *N*-Alkyl phenylselenides of imidazo[4,5-*f*]benzimidazole and imidazo[5,4-*f*]benzimidazole underwent ring-closure mediated by Bu_3SnH and 1,1'-azobis(cyclohexanecarbonitrile) (ACN) to give the pyrrolo-, pyrido- and azepino-fused adducts. Greater than full equivalents of azo-initiator were required to support a non-chain mechanism with air and sunlight exposure helping the oxidative aromatization. Camphorsulfonic acid or acetic anhydride were added to activate the imidazole towards the nucleophilic alkyl radical in more difficult five and seven-membered cyclizations.
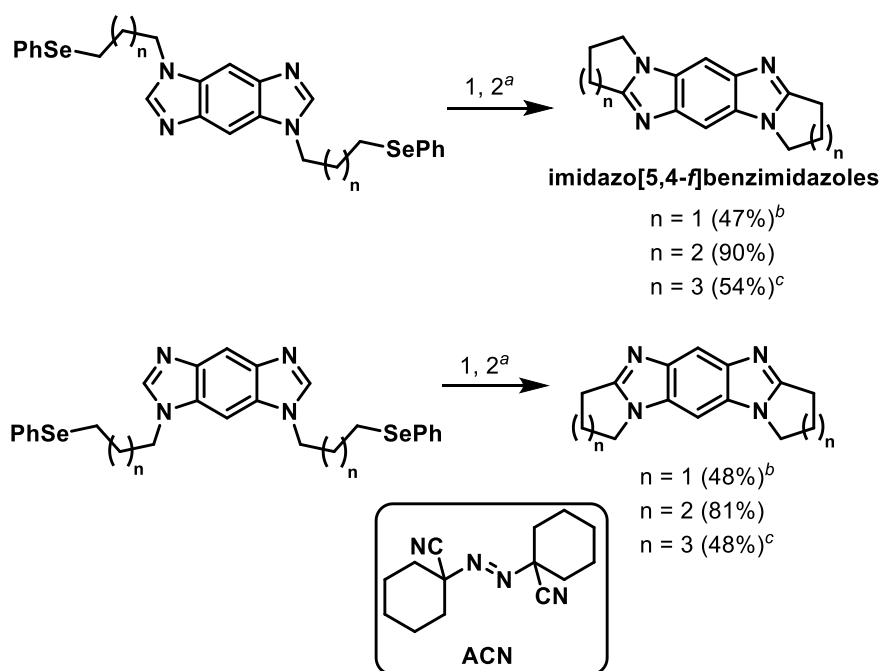
Scheme 3.2. Double intramolecular HAS for imidazobenzimidazole synthesis. [a]1. Bu₃SnH (5 equiv), ACN (5 equiv), slow addition. 2. Sunlight or hν (350 nm). [b]Camphorsulfonic acid added. [c]Ac₂O added.[3]

It was later reported by Fagan and Aldabbagh that Oxone with HCO_2H cyclized *o-tert*-aminoacetanilides to the imidazo[5,4-*f*]benzimidazoles,[4] in better yields than those reported by Skibo for the formation of [4,5-*f*] scaffolds (Scheme 3.3). The fundamental advantage of using the Oxone protocol over radical cyclization methods (in Scheme 3.2),[3] is the ability to synthesize imidazobenzimidazoles (*e.g.* **1**) containing two different fused rings (Scheme 3.3).[4] The Oxone/HCO_2H method was applied by Gurry and Aldabbagh to cyclize spirocyclic oxetane-substituted *o-tert*-aminoacetanilide **2** to the ring-fused benzimidazole, whose structure was confirmed by X-ray crystallography.[7] As indicated in Chapter 2, introducing a hydrogen bond-acceptor such as spirocyclic oxetane into heterocyclic quinone scaffolds is a potential strategy for improving binding affinity towards NAD(P)H:quinone oxidoreductase 1, (NQO1).[8] For cyclization, acid has to be present, and *m*-CPBA in acetone gave the diamine *N*-oxide **3**, as the sole product. Treatment of diamine-*N*-oxide **3** with formic acid in the absence of an external oxidant gave ring-fused benzimidazole **4**, and a mechanism for oxidative cyclization through the internal conjugated system by the second *N*-oxide residue of **3** was provided (Scheme 3.3).
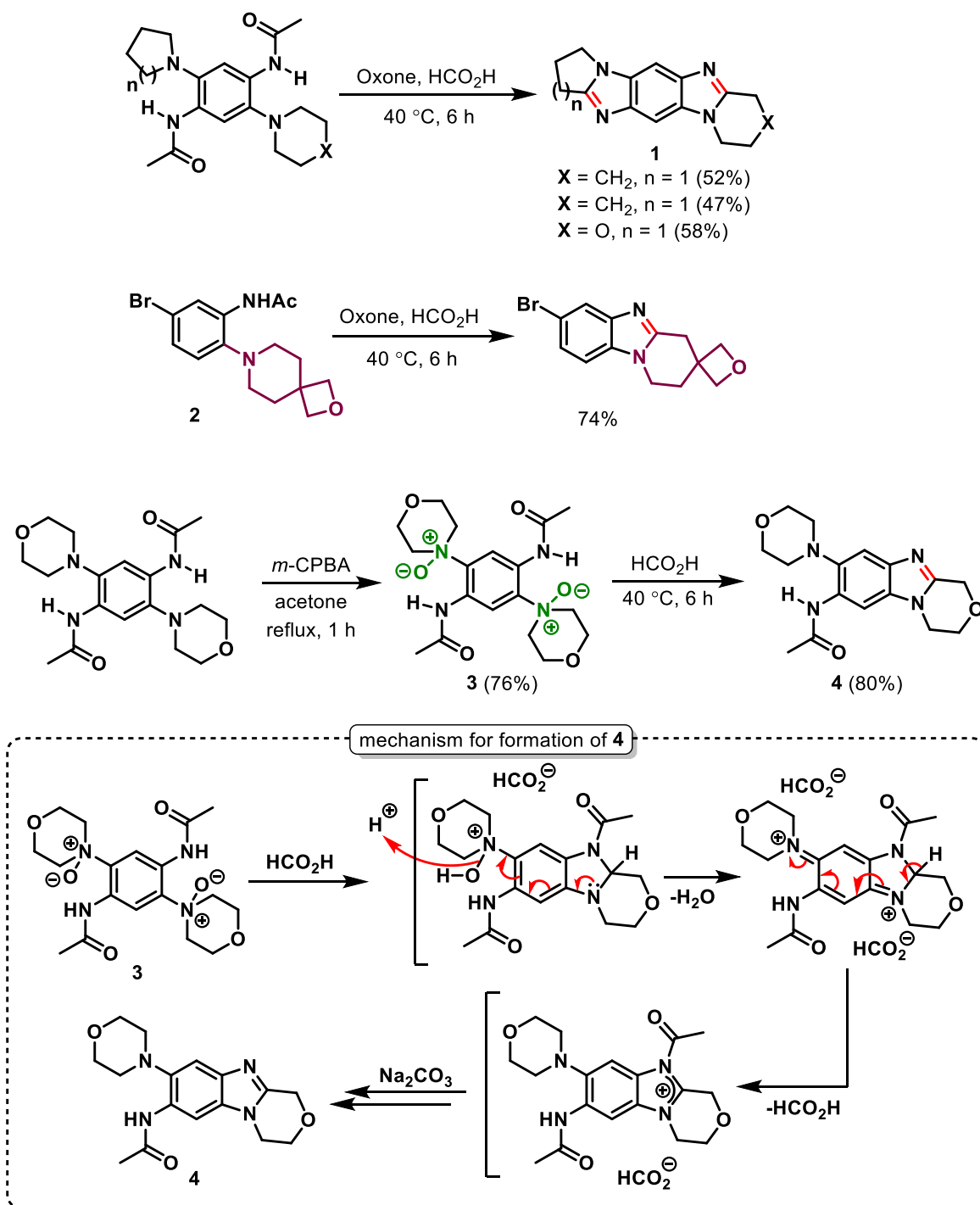
Scheme 3.3. Oxone-mediated oxidative cyclizations and evidence of diamine *N*-oxide intermediate.[4]

The use of Oxone for the preparation of these fanciful imidazobenzimidazole scaffolds is reminiscent of early work by Spiegel and Kaufmann, who utilized Caro's acid (peroxysulfuric acid) to cyclize 5-nitro-2-(piperidin-1-yl)aniline to give benzimidazole (Scheme 3.4).[9] The cyclization was reported not to proceed in the absence of the electron-withdrawing nitro-group.
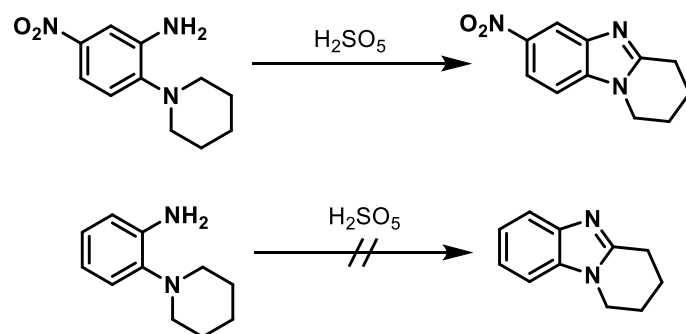
Scheme 3.4. Oxidative cyclization using Caro's acid.[9]

3.2.   Chapter Aims and Objectives

In this Chapter we first aim to examine the reactivity of Oxone towards 4,6-di(piperidin-1-yl)-1,3-phenylenediamine (**5**) (Scheme 3.5). Although numerous reports detail the oxidative cyclization of *o*-cyclic amine substituted anilines,[6,9–14] there is no literature precedence for cyclization of the aryl diamine analogues. Our aim is to decrease the electron-density of the system by acylating one of the primary amines in order to assess the outcome of reacting the amino-acetanilide under oxidative conditions. The mechanistic studies are part of attempts to optimize the cyclization conditions that give spirocyclic oxetane ring-fused imidazobenzimidazoles **6** and **7**.
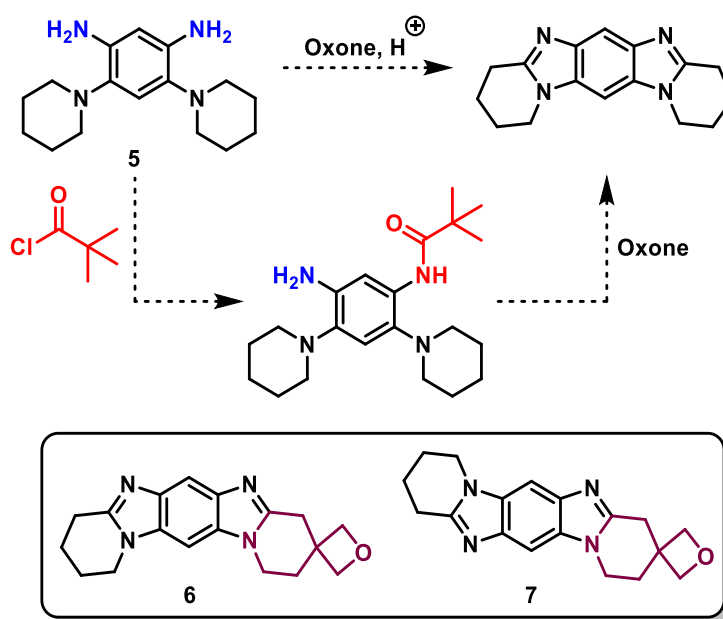
Scheme 3.5. Chapter 3 targets.

3.3. Results and Discussion

Diamine **5** was prepared by S$_N$Ar of piperidine onto 1,5-difluoro-2,4-dinitrobenzene in the presence of NaHCO$_3$,[2] followed by reduction *via* catalytic hydrogenation (Scheme 3.6).
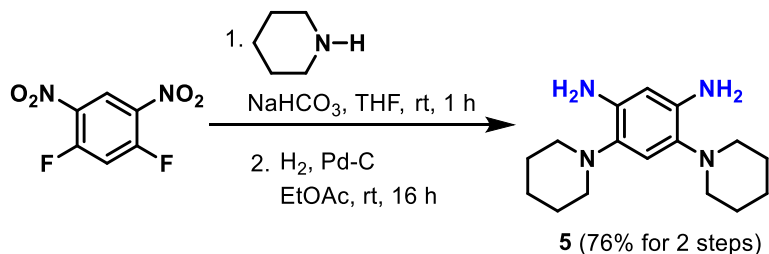
Scheme 3.6. Preparation of 4,6-di(piperidin-1-yl)-1,3-phenylenediamine.

Treating diamine **5** with Oxone in acid did not give imidazo[4,5-*f*]benzimidazole, but led to intractable mixtures (Scheme 3.7). This is in line with our findings in Scheme 3.3,[4] where decreasing the electron-density by acetylating at the primary amines of **5** was necessary.
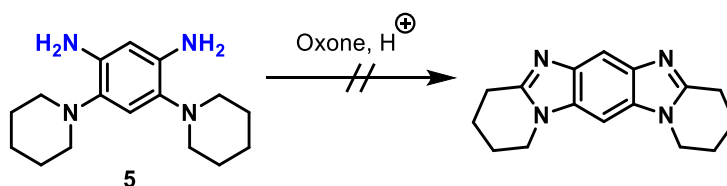
Scheme 3.7. 4,6-Di(cycloamino)-1,3-phenylenediamines do not undergo oxidative cyclization.

This led us to investigate the effect of Oxone on the mono-anilide derivative of **5**. Slow addition of sterically hindered pivaloyl chloride was necessary in order to minimize reaction at both amines of **5**, which gave the desired *N*-[5-amino-2,4-di(piperidin-1-yl)phenyl]-2,2-dimethylpropanamide (**8**) and *N,N′*-[4,6-di(piperidin-1-yl)-1,3-phenylene]bis(2,2-dimethylpropanamide) (**9**) in 61 and 14% yield respectively (Scheme 3.8).
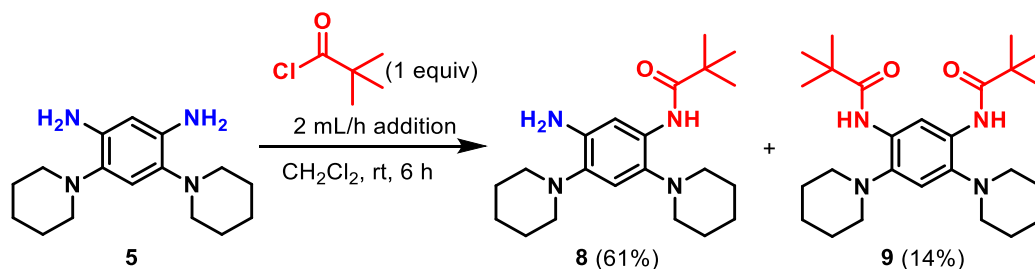
Scheme 3.8. Functionalizing 4,6-di(piperidin-1-yl)-1,3-phenylenediamine (**5**) with pivaloyl chloride.

Reaction of amine-anilide **8** with Oxone in a 10% aqueous solution of hexafluoroisopropanol (HFIP) gave the intriguing adduct **10** in 58% yield, resulting from cyclization and *N*-oxide formation at the amine and anilide parts respectively (Scheme 3.9). Mono-cyclized adduct **11** was also formed in 29% yield due to insufficient oxidation to **10**. The amide singlet is shifted to 14 ppm in the ^{1}H-NMR spectrum of **10** (Figure 3.1), consistent with strong hydrogen bonding to the *N*-oxide, a trait observed for related *N*-oxides, including diacetamide **3**.[4] In contrast, the amide-NH of **11** appears at 9.3 ppm, in the same region as the amide protons of **8** and **9**. The use of HFIP as reaction solvent enabled the solvation of hydrogen-bonding acceptors, including **10** and/or intermediates.[15]
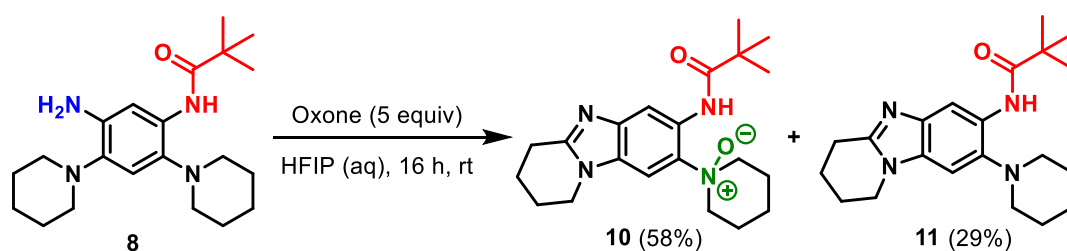
Scheme 3.9. Reaction of amine-anilide with Oxone.
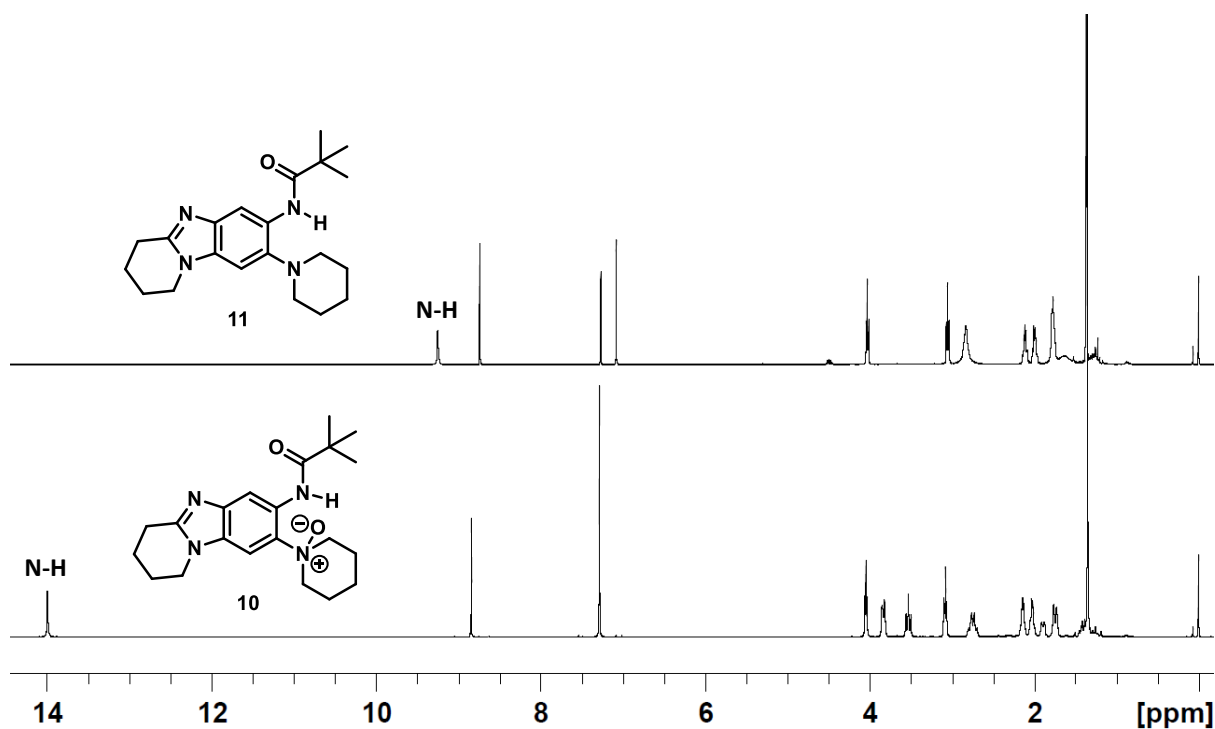
Figure 3.1. Overlaid ^{1}H NMR spectra (CDCl$_3$) of *N*-oxide **10** and benzimidazole-anilide **11**.

Treating **10** with methanesulfonic acid (MsOH) gave the imidazo[4,5-*f*]benzimidazole **12** in 42%,[3,16] and benzimidazole-anilide **11** in 44% yield (Scheme 3.10), in which presumably the *N*-oxide part of **10** allowed oxidative aromatization, similar to the mechanism in Scheme 3.3.[4]
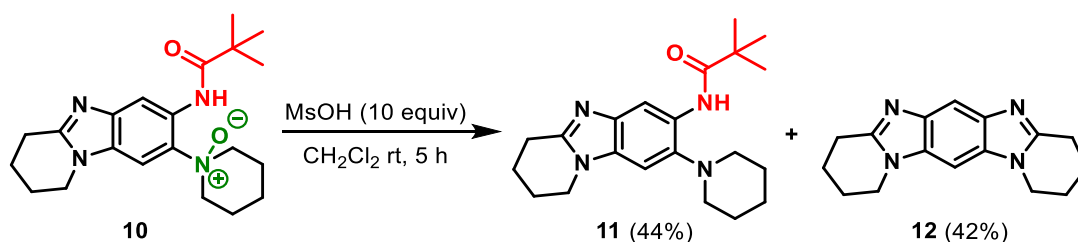
Scheme 3.10. Ring-closure of *N*-oxide.

The formation of **10** from the reaction of amine-anilide **8** with Oxone highlights the difference in mechanism for oxidative cyclization of 2-(cycloamino)anilines and 2-(cycloamino)anilides (Scheme 3.9). Literature advocates a nitroso intermediate for the formation of benzimidazoles from 2-(cycloamino)anilines,[10,14,17,18] although the *o*-nitroso-*tert*-aniline has never been isolated. In Chapter 2 of this thesis, we observed the 4-(2-nitrosophenyl)morpholine intermediate by GC-MS from the oxidative cyclization to the ring-fused benzimidazole, which under certain conditions underwent displacement of oxazine to give 1,4,6,9-tetramethoxyphenazine.[14] Evidence for the *o*-nitroso-*tert*-aniline intermediate **14** is now provided from the reaction of 2-(morpholin-4-yl)aniline (**13**) with Oxone in a CH_2Cl_2:H_2O mixture under N_2 (Scheme 3.11). Quenching this reaction at short times of 30 s and 2 min gave mostly 4-(2-nitrophenyl)morpholine (**16**), which indicates formation of intermediate **14** and advantageous air-oxidation. After 18 and 40 h, it is apparent from the ^{1}H NMR spectra that the morpholine signals at 3.06 and 3.85 ppm for 4-(2-nitrophenyl)morpholine (**16**) have been replaced by those for benzimidazole **15** at 4.20 and 5.05 ppm.
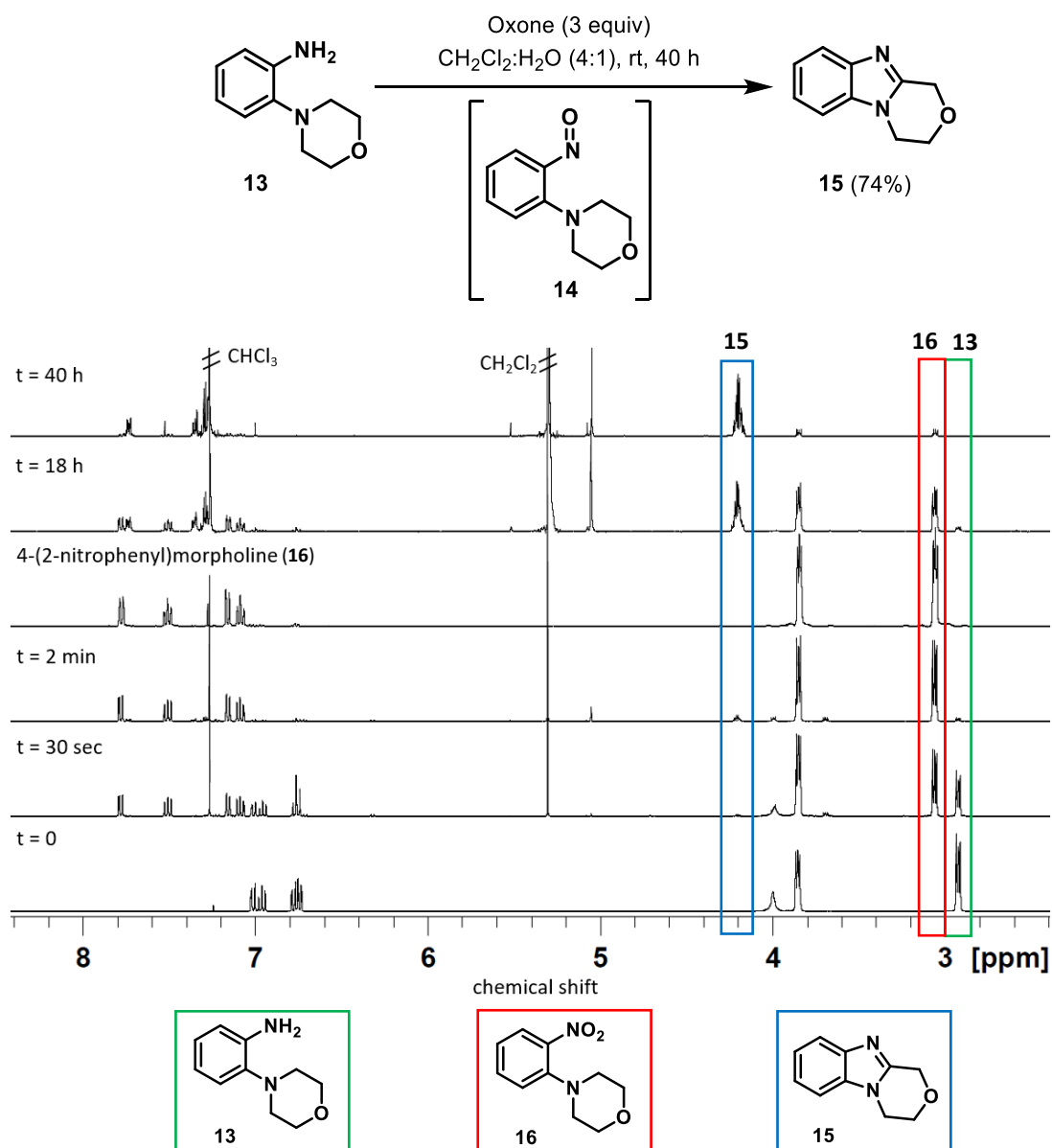
Scheme 3.11. ^{1}H NMR reaction monitoring (CDCl$_3$), providing evidence for the *o*-nitroso-*tert*-aniline intermediate **14**.

The above mechanistic work clarified the requirement for diacetamides **19** and **22** for the respective formation of imidazobenzimidazoles **6** and **7**, negating direct oxidative cyclizations from phenylenediamines **18** and **21** (Scheme 3.12). Syntheses began by nucleophilic aromatic substitution (S$_N$Ar) onto 1,5-difluoro-2,4-dinitrobenzene and 1,4-difluoro-2,5-dinitrobenzene with bis(2-oxa-7-azaspiro[3.5]nonan-7-ium) ethanedioate, followed by S$_N$Ar with the stronger nucleophile, piperidine to give the respective unsymmetrically substituted dinitrobenzenes **17** and **20** in 79 and 85% yield. Hydrogenation to the phenylenediamines **18** and **21** occurred in 91 and 88% yield, and reaction with acetic anhydride gave the cyclization precursors **19** and **22** in 84 and 86% yield respectively. Oxidative cyclizations of **19** and **22** with Oxone (6 equiv)

in acetic acid gave imidazo[4,5-*f*]benzimidazole **6** and imidazo[5,4-*f*]benzimidazole **7** in 55 and 49% yield respectively, representing cumulative yields of ≥70% for each ring closure.
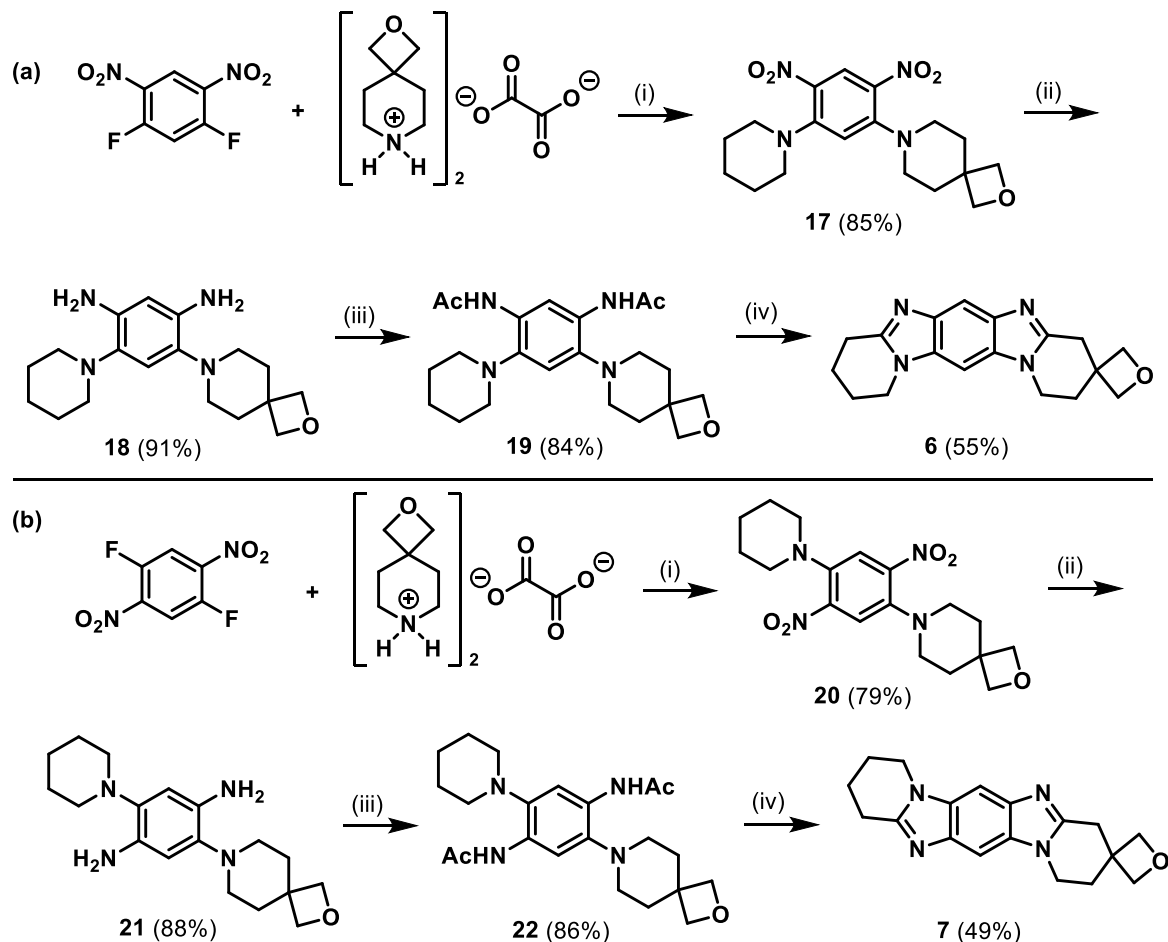
Scheme 3.12. Synthesis of (a) imidazo[4,5-*f*]benzimidazole **6** and (b) imidazo[5,4-*f*]benzimidazole **7**: (i) NaHCO₃, MeCN (aq), rt, 16 h; piperidine, rt, 1 h; (ii) H₂ (balloon), Pd-C, EtOAc, rt, 18 h; (iii) Ac₂O (10 equiv), AcOH, 80 °C, 30 min; (iv) Oxone (6 equiv), AcOH, 40 °C, 7 h.

3.4. Conclusions

This chapter demonstrates the necessity for converting 4,6-di(cycloamino)-1,3-phenylenediamines to anilide/acetamide prior to imidazobenzimidazole formation. New evidence is presented for nitroso and *N*-oxide intermediates in the respective oxidative cyclizations of 2-(cycloamino)anilines and 2-(cycloamino)anilides. Oxetane is incorporated into ring-fused imidazobenzimidazoles for the first time, with Oxone in acetic acid allowing the formation of both [4,5-*f*] and [5,4-*f*] isomers.

3.5. Future Work

Future work should complete the overall oxidation of the aromatic part of **6** and **7** to give the iminoquinone NQO1 substrates (Scheme 3.13). This would follow the procedure to be described in Chapter 4, which involves initial aromatic nitration, followed by reduction of the nitroarene to the aniline, and oxidation using Frémy's salt to yield the iminoquinone. The initial nitration step would likely induce oxetane ring-opening, given the requirements for concentrated HNO$_3$ and H$_2$SO$_4$.[19] It may be necessary to use milder nitrating conditions which circumvent the requirements for concentrated acids, such as Olah's nitronium tetrafluoroborate (NO$_2$BF$_4$).[20–22]
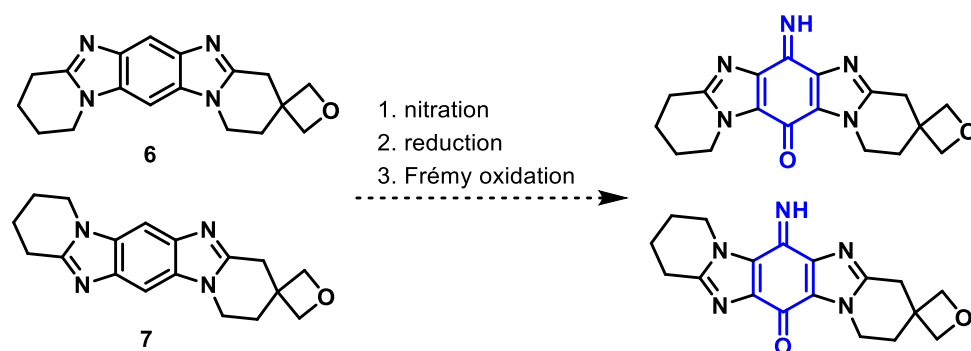
Scheme 3.13. Proposed formation of spirocyclic oxetane-fused imidazobenzimidazole iminoquinones.

3.6. Experimental Section

3.6.1. Materials

Pd-C (Sigma Aldrich, 5% wt. loading), EtOAc (VWR, 99.9%), pet. ether (Fisher Scientific, 40-60°C, Extra Pure, SLR), pivaloyl chloride (Sigma Aldrich, 99%), Oxone (Sigma Aldrich, $KHSO_5 \bullet 0.5KHSO_4 \bullet 0.5K_2SO_4$), HFIP (Fluorochem, 99%), $NaHCO_3$ (Fisher Scientific, ≥99.7%), 1,5-difluoro-2,4-dinitrobenzene (Sigma Aldrich, 97%), MeCN (Fisher Scientific, HPLC grade), piperidine (ACROS OrganicsTM, 99%), AcOH (Fisher Scientific, glacial), Ac_2O (ACROS OrganicsTM, 99+%), MsOH (Fluorochem, >98%), Na_2CO_3 (Fisher Scientific, 99.5%), D_2O (Fluorochem, >99.9%), and $MgSO_4$ (Anhydrous, Fisher Scientific, Extra Pure, SLR, Dried) were used as received. CH_2Cl_2 (Fisher Scientific, 99.8%) was distilled over CaH_2 (ACROS OrganicsTM, ca. 93%, extra pure, 0-2 mm grain size) prior to use. 1,1'-(4,6-Dinitro-1,3-phenylene)dipiperidine was prepared (1.198 g, 92%) by modifying the reported procedure,[2] by reacting piperidine (2.50 mL, 29.00 mmol) and $NaHCO_3$ (1.600 g, 19.50 mmol) with 1,5-difluoro-2,4-dinitrobenzene (0.800 g, 3.90 mmol) in THF (30 mL) at room temperature for 1 h. The synthesis of 4-(2-nitrophenyl)morpholine (**16**) (1.042 g, 83%) was achieved by S_NAr of morpholine (1.56 ml, 18.09 mmol, Alfa Aesar, 99%) onto 1-fluoro-2-nitrobenzene (0.850 g, 6.03 mmol, Fluorochem, 99%) in the absence of solvent at 110 °C for 1 h. 2-(Morpholin-4-yl)aniline (**13**)[11] was obtained in 91% yield, through reduction of **16** with iron powder, according to our previously reported method.[7,12–14] The Aldabbagh group has previously described the synthesis of bis(2-oxa-7-azaspiro[3.5]nonan-7-ium) ethanedioate,[7] and 1,4-difluoro-2,5-dinitrobenzene.[4] All reactions (apart from those using aqueous solutions) were carried out under an inert nitrogen atmosphere. Thin Layer Chromatography (TLC) was carried out on TLC silica gel 60 F_{254} plates, and preparative TLC was done on TLC Silica Gel 60 F_{254} glass plates. Flash column chromatography was carried out on silica gel (Apollo Scientific 60/40−63 µm).

3.6.2. Measurements

Melting points were measured on a Stuart Scientific melting point apparatus SMP1. IR spectra were recorded using a PerkinElmer Spec 1 with ATR attached. NMR spectra were recorded using a Bruker Avance III 400 MHz spectrometer equipped with a 5mm BBFO+, broadband autotune probe and controlled with TopSpin 3.5.7 acquisition software and IconNMR 5.0.7 automation software Copyright © 2017 Bruker BioSpin GmbH. Chemical shifts are in ppm, relative to tetramethylsilane. ^{1}H NMR NH amide and amine assignments were verified by D_2O

exchange experiments. ^{13}C NMR spectra are at 100 MHz with complete proton decoupling and assignments supported by DEPT-135. NMR assignments for synthetic targets **6** and **7** used data of reported spirocyclic oxetane ring-fused compounds.[7,14] HRMS spectra of compounds **6**, **7**, **17**, **19**, **20** and **22** were obtained at the National University of Ireland Galway, using an ESI time-of-flight mass spectrometer (TOFMS) on a Waters LCT Mass Spectrometry instrument. HRMS spectra of all other compounds were obtained at the National Mass Spectrometry Facility at Swansea University using a Waters Xevo G2-S mass spectrometer with an Atmospheric Solids Analysis Probe (ASAP) or Thermo Scientific LTQ Orbitrap XL instrument with Nanospray Ionization (NSI). The precision of all accurate mass measurements was better than 5 ppm.

3.6.3. Synthetic Procedures and Characterization

3.6.3.1. Synthesis of 4,6-Di(piperidin-1-yl)benzene-1,3-diamine (5)

5
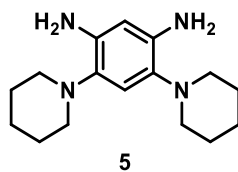
1,1'-(4,6-Dinitro-1,3-phenylene)dipiperidine (0.750 g, 2.25 mmol), and Pd-C (75 mg) in EtOAc (50 mL) were stirred under H_2 at room temperature for 24 h. The mixture was filtered through Celite and evaporated to dryness. The residue was purified by column chromatography using gradient elution of pet. ether and EtOAc to give **5** (0.512 g, 83%) as a brown solid; R_f 0.32 (2:1 pet. ether:EtOAc); mp 172-174 °C; ν_{max} (neat, cm^{-1}) 3378, 3264, 2946, 2923, 2844, 2799, 2742, 1626, 1518, 1466, 1441, 1382, 1339, 1296, 1273, 1257, 1242, 1214, 1201, 1149, 1129, 1111, 1037, 1029; ^{1}H NMR (400 MHz, CDCl$_3$) δ: 6.69 (s, 1H), 6.11 (s, 1H), 4.00-3.31 (br.s, 4H, NH$_2$), 2.85-2.55 (br.s, 8H), 1.64-1.55 (m, 8H), 1.54-1.36 (br.s, 4H); ^{13}C{^{1}H} NMR (100 MHz, CDCl$_3$) δ: 138.6, 132.5 (both C), 112.6, 102.1 (both CH), 53.6, 27.1, 24.4 (all CH$_2$); HRMS (ASAP) *m/z* [M+H]$^+$ found 275.2234, C$_{16}$H$_{27}$N$_4$ requires 275.2236.

3.6.3.2. Anilide Formation
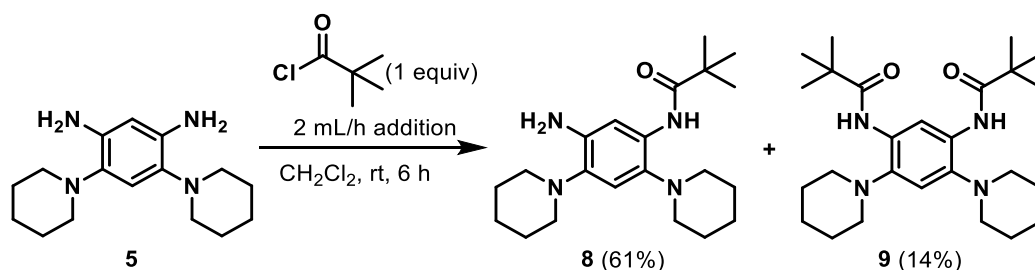
Pivaloyl chloride (45 µL, 0.37 mmol) in CH_2Cl_2 (8 mL) was added *via* syringe pump at a rate of 2 mL/h to diamine **5** (0.103 g, 0.37 mmol) in CH_2Cl_2 (8 mL). The mixture was stirred for a further 2 h at room temperature. H_2O (20 mL) was added, and the mixture was extracted with CH_2Cl_2 (2 x 20 mL). The combined organic extracts were dried ($MgSO_4$), evaporated and purified by column chromatography using gradient elution of pet. ether and EtOAc.

***N*-[5-Amino-2,4-di(piperidin-1-yl)phenyl]-2,2-dimethylpropanamide (8).** (81 mg, 61%); pale brown solid; R_f 0.44 (7:3 pet. ether:EtOAc); mp 149-151 °C; ν_{max} (neat, cm^{-1}) 3423, 3333, 2931, 2851, 2801, 2739, 2360, 1669 (C=O), 1618, 1593, 1519, 1480, 1435, 1377, 1364, 1321, 1272, 1235, 1206, 1193, 1150, 1121, 1110, 1063, 1035, 1029; ^{1}H NMR (400 MHz, CDCl$_3$) δ: 9.13 (s, 1H, NH), 7.92 (s, 1H), 6.85 (s, 1H), 4.05-3.82 (br.s, 2H, NH$_2$), 2.90-2.62 (m, 8H), 1.75-1.64 (m, 8H), 1.63-1.47 (br.s, 4H), 1.31 (s, 9H, Me); ^{13}C{^{1}H} NMR (100 MHz, CDCl$_3$) δ: 176.2 (C=O), 138.9, 135.7, 133.8, 130.5 (all C), 112.4, 105.5 (both CH), 54.3, 53.0 (both CH$_2$), 40.0 (C), 27.8 (Me), 27.3, 26.9, 24.4, 24.1 (all CH$_2$); HRMS (ASAP) *m/z* [M+H]$^+$ found 359.2809, C$_{21}$H$_{35}$N$_4$O requires 359.2811.

***N,N'*-[4,6-Di(piperidin-1-yl)-1,3-phenylene]bis(2,2-dimethylpropanamide) (9).** (22 mg, 14%); brown solid; R_f 0.37 (pet. ether:EtOAc); mp 236-237 °C; ν_{max} (neat, cm^{-1}) 3344, 2949, 2930, 2917, 2849, 1682 (C=O), 1596, 1519, 1480, 1448, 1428, 1393, 1377, 1362, 1356, 1340, 1309, 1269, 1219, 1190, 1162, 1150, 1103, 1063, 1027; ^{1}H NMR (400 MHz, CDCl$_3$) δ: 9.36 (s, 1H), 8.77 (s, 1H, NH), 6.95 (s, 1H), 2.74 (t, *J* = 5.2 Hz, 8H), 1.75-1.68 (m, 8H), 1.62-1.55 (m, 4H), 1.30 (s, 18H, Me); ^{13}C{^{1}H} NMR (100 MHz, CDCl$_3$) δ: 175.6 (C=O), 138.0, 130.8 (both C), 112.4, 110.7 (both CH), 53.9 (CH$_2$), 39.9 (C), 27.8 (Me), 27.1, 24.1 (CH$_2$); HRMS (ASAP) *m/z* [M+H]$^+$ found 443.3384, C$_{26}$H$_{43}$N$_4$O$_2$ requires 443.3386.

3.6.3.3. Reaction of Amine-Anilide 8 with Oxone (in the Absence of Acid)
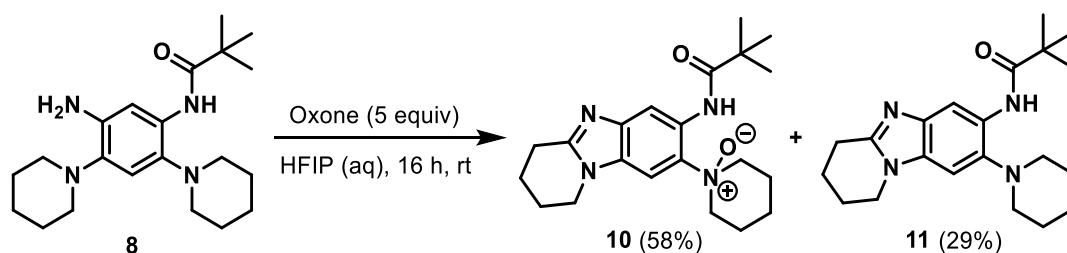
Oxone (0.277 g, 0.90 mmol) was added to amine-anilide **8** (65 mg, 0.18 mmol) in HFIP (3.6 mL, 10% aq.) and stirred at room temperature for 16 h. H_2O (10 mL) was added, and the mixture extracted with CH_2Cl_2 (2 x 10 mL). The organic extracts were dried ($MgSO_4$), evaporated and purified by column chromatography using gradient elution of CH_2Cl_2 and MeOH.

2,2-Dimethyl-*N*-[8-(1-oxidopiperidin-1-yl)-1,2,3,4-tetrahydropyrido[1,2-*a*]benzimidazol-7-yl]propenamide (10). (39 mg, 58%); pale brown solid; R_f 0.26 (9:1 CH_2Cl_2:MeOH); mp (decomp. >161 °C); ν_{max} (neat, cm^{-1}) 2952, 2927, 2866, 1652 (C=O), 1594, 1497, 1474, 1430, 1417, 1366, 1327, 1273, 1199, 1148, 1011; ^{1}H NMR (400 MHz, CDCl$_3$) δ: 13.99 (s, 1H, NH), 8.84 (s, 1H), 7.29 (s, 1H), 4.05 (t, *J* = 6.0 Hz, 2H), 3.84 (d, *J* = 10.7 Hz, 2H), 3.59-3.47 (m, 2H), 3.08 (t, *J* = 6.3 Hz, 2H), 2.80-2.70 (m, 2H), 2.17-2.11 (m, 2H), 2.05-2.01 (m, 2H), 1.89 (d, *J* = 13.0 Hz, 1H), 1.75 (d, *J* = 13.6 Hz, 2H), 1.48-1.37 (m, 1H), 1.35 (s, 9H, Me); ^{13}C{^{1}H} NMR (100 MHz, CDCl$_3$) δ: 176.9 (C=O), 154.1, 142.7, 137.6, 130.6, 129.1 (all C), 114.0, 98.2 (both CH), 66.5, 42.5 (both CH$_2$), 40.0 (C), 27.8 (Me), 25.5, 22.5, 21.9, 20.9, 20.5 (all CH$_2$); HRMS (ASAP) *m/z* [M+H]$^+$ found 371.2447, C$_{21}$H$_{31}$N$_4$O$_2$ requires 371.2447, *m/z* 372 (25%), 371 (M+1, 100%), 356 (16%), 355 (M-16, 73%), 354 (26%), 353 (M-18, 97%), 269 (M-102, 28%).

2,2-Dimethyl-*N*-[8-(piperidin-1-yl)-1,2,3,4-tetrahydropyrido[1,2-*a*]benzimidazol-7-yl]propenamide (11). (19 mg, 29%); brown solid; R_f 0.44 (9:1 CH_2Cl_2:MeOH); mp 171-173 °C; ν_{max} (neat, cm^{-1}) 3340, 2935, 2863, 2809, 1667 (C=O), 1589, 1511, 1473, 1440, 1418, 1365, 1322, 1268, 1242, 1194, 1146, 1136, 1064, 1034; ^{1}H NMR (400 MHz, CDCl$_3$) δ: 9.25 (s, 1H, NH), 8.74 (s, 1H), 7.08 (s, 1H), 4.03 (t, *J* = 6.1 Hz, 2H), 3.05 (t, *J* = 6.4 Hz, 2H), 2.96-2.67 (br.s, 4H), 2.16-2.06 (m, 2H), 2.05-1.95 (m, 2H), 1.84-1.54 (m, 6H), 1.36 (s, 9H, Me); ^{13}C{^{1}H} NMR (100 MHz, CDCl$_3$) δ: 176.0 (C=O), 151.7, 139.7, 139.1, 130.2, 129.8 (all C), 109.0, 101.0 (both CH), 54.7, 42.4 (both CH$_2$), 40.1 (C), 27.9 (Me), 27.2, 25.3, 24.1, 22.7, 20.7 (all CH$_2$); HRMS (ASAP) *m/z* [M+H]$^+$ found 355.2495, C$_{21}$H$_{31}$N$_4$O requires 355.2498.

3.6.3.4. Ring-Closure with Acid
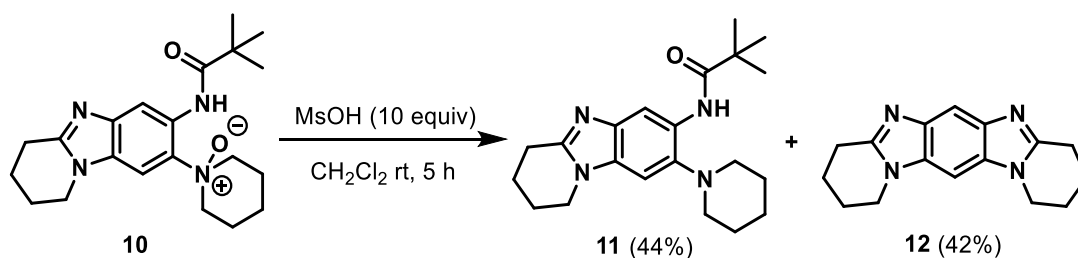
MsOH (0.05 mL, 0.77 mmol) was added to a solution of *N*-oxide **10** (28 mg, 0.08 mmol) in CH_2Cl_2 (0.8 mL) and stirred at room temperature for 5 h. Na_2CO_3 (satd., 2 mL) was added, and the mixture extracted with CH_2Cl_2 (3 x 2 mL). The organic extracts were dried ($MgSO_4$), evaporated and purified by preparative TLC.

2,2-Dimethyl-*N*-[8-(piperidin-1-yl)-1,2,3,4-tetrahydropyrido[1,2-*a*]benzimidazol-7-yl]propenamide (11). (12 mg, 44%); R_f 0.44 (9:1 CH_2Cl_2:MeOH); spectral data and melting point consistent with the above.

1,2,3,4,8,9,10,11-Octahydropyrido[1,2-*a*]pyrido[1',2':1,2]imidazo[4,5-*f*]benzimidazole (12).[3,16] (8 mg, 42%); off-white solid; R_f 0.20 (9:1 CH_2Cl_2:MeOH); mp (decomp. >261 °C); lit. mp[3] (decomp. 266-270 °C); ^{1}H NMR (400 MHz, $CDCl_3$) δ: 7.95 (d, *J* = 0.8 Hz, 1H), 7.04 (d, *J* = 0.8 Hz, 1H), 4.09 (t, *J* = 6.1 Hz, 4H), 3.11 (t, *J* = 6.4 Hz, 4H), 2.20-2.13 (m, 4H), 2.07-2.00 (m, 4H).

3.6.3.5.   Reaction of Aniline 13 with Oxone
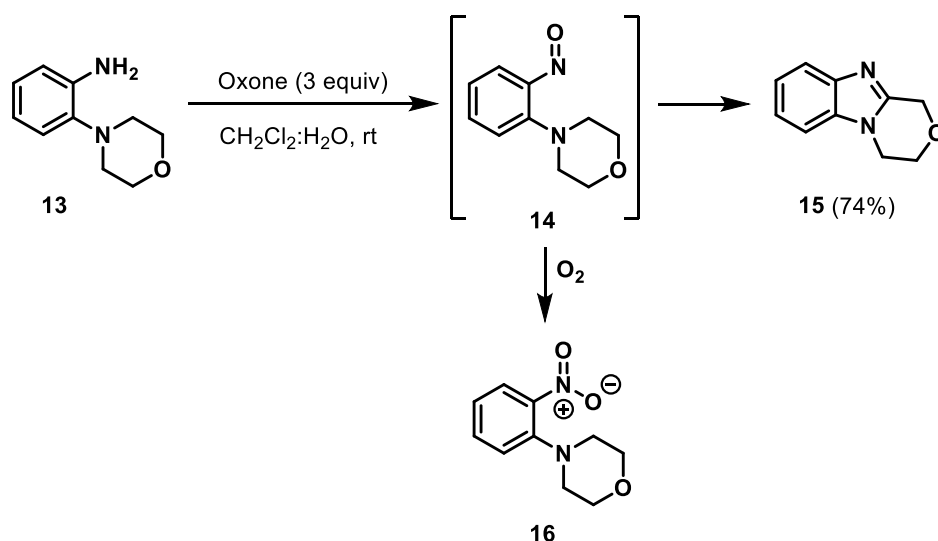
Aniline **13** (0.356 g, 2.00 mmol) and Oxone (1.846 g, 6.01 mmol) in CH_2Cl_2 (4 mL) and H_2O (1 mL) were rapidly stirred at rt. Aliquots (0.2 mL) were taken at the times shown in Scheme 3.11, quenched with water (0.5 mL), and extracted with $CDCl_3$ (0.8 mL) for ^1H NMR analysis. After 2 min, nitrobenzene **16** was the apparent major product. ^1H NMR (400 MHz, $CDCl_3$) δ: 7.78 (dd, $J = 8.1$, 1.6 Hz, 1H), 7.53-7.48 (m, 1H), 7.16 (dd, $J = 8.3$, 1.2 Hz, 1H), 7.11-7.06 (m, 1H), 3.85 (t, $J = 4.6$ Hz, 4H), 3.06 (t, $J = 4.6$ Hz, 4H).

The reaction under the same conditions was stirred for 40 h. H_2O (5 mL) was added, and the mixture extracted with CH_2Cl_2 (2 x 6 mL). The organic extracts were dried ($MgSO_4$), evaporated and purified by column chromatography using gradient elution of pet. ether and EtOAc to give 3,4-dihydro-1*H*-[1,4]oxazino[4,3-*a*]benzimidazole (**15**) (0.259 g, 74%) as a pale brown solid; R_f 0.21 (EtOAc); mp 123-125 °C; lit. mp[10] 129-130 °C; ^1H NMR (400 MHz, $CDCl_3$) δ: 7.76-7.72 (m, 1H), 7.37-7.32 (m, 1H), 7.31-7.27 (m, 2H), 5.05 (s, 2H), 4.24-4.16 (m, 4H). Spectral data and melting point were consistent with reported.[23]

3.6.3.6. Procedure for the Synthesis of Nitrobenzenes 17 and 20

Bis(2-oxa-7-azaspiro[3.5]nonan-7-ium) ethanedioate (0.540 g, 1.57 mmol), NaHCO$_3$ (1.020 g, 12.48 mmol) and 1,5-difluoro-2,4-dinitrobenzene or 1,4-difluoro-2,5-dinitrobenzene (0.636 g, 3.12 mmol) in MeCN (40 ml) and H$_2$O (4 ml) were stirred at room temperature for 16 h. Piperidine (3.00 ml, 30.42 mmol) was added to the mixture and stirred for a further 1 h. The mixture was evaporated, EtOAc (50 mL) added, washed with brine (3 x 50 mL), dried (MgSO$_4$), and evaporated to dryness. The residue was purified by column chromatography using gradient elution of pet. ether and EtOAc.

17
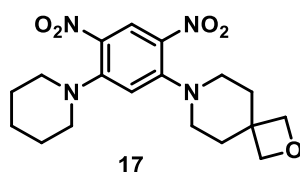
1-(2,4-Dinitro-5-piperidin-1-ylphenyl)-2-oxa-7-azaspiro[3.5]nonane (17). (0.993 g, 85%); yellow solid; R_f 0.32 (1:1 pet. ether:EtOAc); mp 156-157 °C; ν_{max} (neat, cm^{-1}) 2941, 2855, 1600, 1555, 1489 (NO$_2$), 1441, 1326 (NO$_2$), 1299, 1254; ^{1}H NMR (400 MHz, CDCl$_3$) δ: 8.66 (s, 1H), 6.25 (s, 1H), 4.48 (s, 4H, OCH$_2$), 3.12 (t, J = 5.3 Hz, 4H), 3.04 (t, J = 5.5 Hz, 4H), 2.06 (t, J = 5.5 Hz, 4H), 1.76-1.69 (m, 4H), 1.69-1.62 (m, 2H); ^{13}C{^{1}H} NMR (100 MHz, CDCl$_3$) δ: 150.8, 131.1, 130.6 (all C), 130.0, 107.4 (both CH), 81.4 (OCH$_2$), 52.3, 48.6 (both CH$_2$), 38.5 (C), 34.4, 25.5, 23.9 (all CH$_2$); HRMS (ESI) m/z [M+H]$^+$ found 377.1813, C$_{18}$H$_{25}$N$_4$O$_5$ requires 377.1825.

20
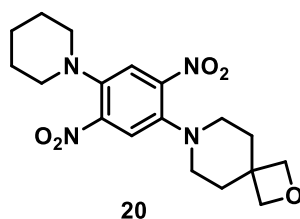
1-(2,5-Dinitro-4-piperidin-1-ylphenyl)-2-oxa-7-azaspiro[3.5]nonane (20). (0.926 g, 79%); red-brown solid; R_f 0.49 (4:1 pet. ether:EtOAc); mp 148-149 °C; ν_{max} (neat, cm^{-1}) 2929, 2859, 2810, 1533, 1495 (NO$_2$), 1466, 1445, 1410, 1385, 1346 (NO$_2$), 1324 (NO$_2$), 1272, 1236, 1225, 1209, 1131, 1042; ^{1}H NMR (400 MHz, CDCl$_3$) δ: 7.45 (s, 1H), 7.41 (s, 1H), 4.45 (s, 4H, OCH$_2$), 2.95 (t, J = 5.3 Hz, 4H), 2.87 (t, J = 5.5 Hz, 4H), 1.99 (t, J = 5.5 Hz, 4H), 1.71-1.65 (m, 4H), 1.60-1.53 (m, 2H); ^{13}C{^{1}H} NMR (100 MHz, CDCl$_3$) δ: 146.8, 144.9, 141.8, 139.5 (all C), 119.3, 118.1 (both CH), 81.6 (OCH$_2$), 53.1, 49.8 (both CH$_2$), 38.2 (C), 34.9, 25.9, 23.8 (all CH$_2$); HRMS (ESI) m/z [M+H]$^+$ found 377.1818, C$_{18}$H$_{25}$N$_4$O$_5$ requires 377.1825.

3.6.3.7. Procedure for the Synthesis of Diamines 18 and 21

Dinitrobenzene **17** or **20** (0.500 g, 1.33 mmol), and Pd-C (50 mg) in EtOAc (50 mL) were stirred under H_2 (balloon) at room temperature for 16 h. The mixture was filtered through Celite and evaporated to dryness.

18
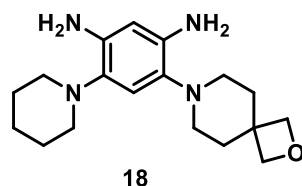
4-(2-Oxa-7-azaspiro[3.5]nonan-7-yl)-6-(piperidin-1-yl)benzene-1,3-diamine (18). (0.381 g, 91%); brown solid; mp 187-188 °C; ν_{max} (neat, cm^{-1}) 3372, 3264, 2951, 2920, 2848, 2740, 1626, 1519, 1468, 1442, 1380, 1296, 1278, 1257, 1246, 1215, 1149, 1132, 1113, 1036, 1026; ^{1}H NMR (400 MHz, CDCl$_3$) δ: 6.60 (s, 1H), 6.07 (s, 1H), 4.40 (s, 4H, OCH$_2$), 3.78-3.64 (br.s, 4H, NH$_2$), 2.81-2.41 (br.s, 8H), 2.02-1.79 (br.s, 4H), 1.64-1.53 (m, 4H), 1.52-1.36 (br.s, 2H); ^{13}C{^{1}H} NMR (100 MHz, CDCl$_3$) δ: 138.9, 138.5, 132.5, 131.2 (all C), 112.4, 102.1 (both CH), 82.1 (OCH$_2$), 53.6, 49.6 (both CH$_2$), 38.5 (C), 36.1, 27.1, 24.4 (all CH$_2$); HRMS (NSI) *m/z* [M+H]$^+$ found 317.2342, C$_{18}$H$_{29}$N$_4$O requires 317.2336.

21
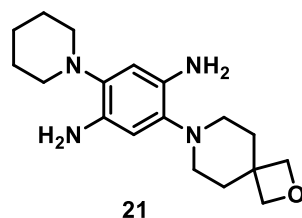
2-(2-Oxa-7-azaspiro[3.5]nonan-7-yl)-5-(piperidin-1-yl)benzene-1,4-diamine (21). (0.369 g, 88%); grey solid; mp 197-199 °C; ν_{max} (neat, cm^{-1}) 3386, 3302, 3273, 3162, 2924, 2855, 2800, 2739, 1585, 1511, 1462, 1450, 1432, 1342, 1301, 1246, 1200, 1111, 1033; ^{1}H NMR (400 MHz, CDCl$_3$) δ: 6.40 (s, 1H), 6.35 (s, 1H), 4.40 (s, 4H, OCH$_2$), 3.64-3.40 (br.s, 4H, NH$_2$), 2.78-2.54 (m, 8H), 1.96-1.84 (br.s, 4H), 1.65-1.56 (m, 4H), 1.53-1.40 (br.s, 2H); ^{13}C{^{1}H} NMR (100 MHz, CDCl$_3$) δ: 137.7, 136.1, 133.5, 133.3 (all C), 108.1, 107.8 (both CH), 82.0 (OCH$_2$), 53.0, 49.0 (both CH$_2$), 38.5 (C), 35.9, 26.9, 24.4 (all CH$_2$); HRMS (NSI) *m/z* [M+H]$^+$ found 317.2339, C$_{18}$H$_{29}$N$_4$O requires 317.2336.

3.6.3.8. Procedure for the Synthesis of Diacetamides 19 and 22

Diamine **18** or **21** (0.354 g, 1.12 mmol) in Ac_2O (1.06 mL, 11.20 mmol) and AcOH (30 mL) was stirred at 80 °C for 30 min. The mixture was evaporated, $NaHCO_3$ (5%, 100 mL) added and stirred for 1 h. The precipitate was collected, washed with water, dried, and recrystallized from EtOAc.

19
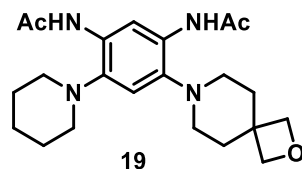
***N,N'*-[4-(2-oxa-7-azaspiro[3.5]nonan-7-yl)-6-piperidin-1-yl-1,3-phenylene]diacetamide (19).** (0.375 g, 84%); white solid; mp 226-228 °C; v_{max} (neat, cm^{-1}) 3291, 2935, 2856, 2797, 2735, 1728, 1672 (C=O), 1659, 1589, 1524, 1491, 1420, 1378, 1368, 1289, 1276, 1256, 1232, 1218, 1196, 1158, 1136, 1122, 1112, 1066, 1032; ^{1}H NMR (400 MHz, $CDCl_3$) δ: 8.98 (s, 1H), 8.19 (s, 1H, NH), 8.07 (s, 1H, NH), 6.76 (s, 1H), 4.43 (s, 4H, OCH_2), 2.71-2.58 (m, 8H), 2.13-2.06 (m, 6H, Me), 2.00-1.90 (br.s, 4H), 1.68-1.60 (m, 4H), 1.55-1.46 (br.s, 2H); $^{13}C\{^1H\}$ NMR (100 MHz, $CDCl_3$) δ: 167.5 (C=O), 138.6, 137.4, 130.3, 129.8 (all C), 112.0 (2 x CH), 81.7 (OCH_2), 53.8, 49.9 (both CH_2), 38.3 (C), 35.8, 26.9 (both CH_2), 24.8 (Me), 24.0 (CH_2); HRMS (ESI) *m/z* [M-H]$^-$ found 399.2397, $C_{22}H_{31}N_4O_3$ requires 399.2396.

22
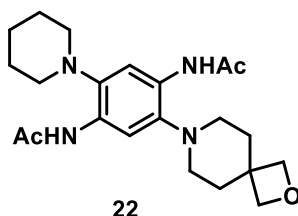
***N,N'*-[2-(2-oxa-7-azaspiro[3.5]nonan-7-yl)-5-(piperidin-1-yl)-1,4-phenylene]diacetamide (22).** (0.386 g, 86%); pale brown solid; mp 221-222 °C; v_{max} (neat, cm^{-1}) 3362, 3286, 2941, 2869, 2808, 1672 (C=O), 1527, 1477, 1417, 1367, 1296, 1239, 1220, 1195, 1108, 1062; ^{1}H NMR (400 MHz, $CDCl_3$) δ: 8.44 (s, 1H, NH), 8.33 (s, 1H, NH), 8.16 (s, 1H), 8.11 (s, 1H), 4.42 (s, 4H, OCH_2), 2.71 (t, *J* = 5.1 Hz, 4H), 2.66 (t, *J* = 5.1 Hz, 4H), 2.11 (s, 3H, Me), 2.10 (s, 3H, Me), 2.01-1.87 (br.s, 4H), 1.68-1.59 (m, 4H), 1.57-1.46 (br.s, 2H); $^{13}C\{^1H\}$ NMR (100 MHz, $CDCl_3$) δ: 168.0, 167.9 (both C=O), 139.3, 137.7, 129.4, 129.3 (all C), 112.0, 111.6 (both CH), 81.7 (OCH_2), 53.7, 49.9 (both CH_2), 38.3 (C), 35.9, 27.0 (both CH_2), 24.9 (Me), 24.0 (CH_2); HRMS (ESI) *m/z* [M+H]$^+$ found 401.2536, $C_{22}H_{33}N_4O_3$ requires 401.2553.

3.6.3.9. Procedure for the Synthesis of Imidazobenzimidazoles 6 and 7

Diacetamide **19** or **22** (50 mg, 0.13 mmol) and Oxone (0.250 g, 0.81 mmol) in AcOH (5 mL) were stirred at 40 °C for 7 h. The mixture was evaporated, H_2O (10 mL) added, neutralized with solid Na_2CO_3, and extracted with CH_2Cl_2 (3 x 5 mL). The organic extracts were dried ($MgSO_4$), evaporated and recrystallized from EtOAc.
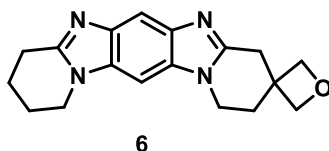
6

1',2',8',9',10',11'-Hexahydro-4'*H*-spiro[oxetane-3,3'-pyrido[1,2-*a*]pyrido[1',2':1,2]imidazo[4,5-*f*]benzimidazole] (6). (22 mg, 55%); brown solid; mp (decomp. >279 °C); ν_{max} (neat, cm^{-1}) 3386, 2946, 2892, 1661, 1526, 1484, 1432, 1420, 1369, 1312, 1254, 1196, 1159, 1136, 1098; ^1H NMR (400 MHz, CDCl$_3$) δ: 7.90 (d, J = 0.9 Hz, 1H, 16-H), 6.99 (d, J = 0.9 Hz, 1H, 9-H), 4.54 (s, 4H, 3,5-CH$_2$), 4.08 (t, J = 6.3 Hz, 2H, 7-CH$_2$), 4.03 (t, J = 6.1 Hz, 2H, 11-CH$_2$), 3.34 (s, 2H, 1-CH$_2$), 3.05 (t, J = 6.4 Hz, 2H), 2.43 (t, J = 6.3 Hz, 2H), 2.14-2.06 (m, 2H), 2.01-1.94 (m, 2H); $^{13}C\{^1H\}$ NMR (100 MHz, CDCl$_3$) δ: 152.1, 149.5, 140.1, 140.0, 132.2, 131.6 (all C), 107.6 (16-CH), 87.3 (9-CH), 80.7 (3,5-CH$_2$), 42.6, 38.9 (7,11-CH$_2$), 38.0 (C), 35.0 (1-CH$_2$), 30.8, 25.7, 22.7, 20.8 (all CH$_2$); HRMS (ESI) *m/z* [M+H]$^+$ found 309.1720, C$_{18}$H$_{21}$N$_4$O requires 309.1715.
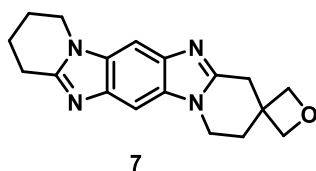
7

1',2',8',9',10',11'-Hexahydro-4'*H*-spiro[oxetane-3,3'-pyrido[1,2-*a*]pyrido[2',1':2,3]imidazo[4,5-*f*]benzimidazole] (7). (20 mg, 49%); orange solid; mp (decomp. >297 °C); ν_{max} (neat, cm^{-1}) 2926, 2856, 1533, 1488, 1449, 1418, 1362, 1279, 1240, 1192, 1166, 1135, 1093; ^1H NMR (400 MHz, CDCl$_3$) δ: 7.53 (d, J = 0.8 Hz, 1H), 7.52 (d, J = 0.8 Hz, 1H), 4.64 (ABq, J = 6.2 Hz, 4H, 3,5-CH$_2$), 4.21 (t, J = 6.3 Hz, 2H, 7-CH$_2$), 4.16 (t, J = 6.1 Hz, 2H, 14-CH$_2$), 3.44 (s, 2H, 1-CH$_2$), 3.14 (t, J = 6.4 Hz, 2H), 2.52 (t, J = 6.3 Hz, 2H), 2.24-2.17 (m, 2H), 2.10-2.04 (m, 2H); $^{13}C\{^1H\}$ NMR (100 MHz, CDCl$_3$), 152.6, 150.0, 139.90, 139.85, 132.5, 132.0 (all C), 97.2, 97.0 (both CH), 80.8 (3,5-CH$_2$), 42.6, 38.9 (7,14-CH$_2$), 38.0 (C), 35.2 (1-CH$_2$), 30.8, 25.7, 22.7, 20.8 (all CH$_2$); HRMS (ESI) *m/z* [M+H]$^+$ found 309.1721, C$_{18}$H$_{21}$N$_4$O requires 309.1715.

3.7. Chapter 3 References

(1)   Schulz, W. G.; Skibo, E. B. Inhibitors of Topoisomerase II Based on the Benzodiimidazole and Dipyrroloimidazobenzimidazole Ring Systems: Controlling DT-Diaphorase Reductive Inactivation with Steric Bulk. *J. Med. Chem.* **2000**, *43*, 629–638. https://doi.org/10.1021/jm990210q.

(2)   Suleman, A.; Skibo, E. B. A Comprehensive Study of the Active Site Residues of DT-Diaphorase: Rational Design of Benzimidazolediones as DT-Diaphorase Substrates. *J. Med. Chem.* **2002**, *45*, 1211–1220. https://doi.org/10.1021/jm0104365.

(3)   Fagan, V.; Bonham, S.; Carty, M. P.; Aldabbagh, F. One-Pot Double Intramolecular Homolytic Aromatic Substitution Routes to Dialicyclic Ring Fused Imidazobenzimidazolequinones and Preliminary Analysis of Anticancer Activity. *Org. Biomol. Chem.* **2010**, *8*, 3149–3156. https://doi.org/10.1039/c003511d.

(4)   Fagan, V.; Bonham, S.; McArdle, P.; Carty, M. P.; Aldabbagh, F. Synthesis and Toxicity of New Ring-Fused Imidazo[5,4-*f*]benzimidazolequinones and Mechanism Using Amine *N*-Oxide Cyclizations. *Eur. J. Org. Chem.* **2012**, 1967–1975. https://doi.org/10.1002/ejoc.201101687.

(5)   Fagan, V.; Bonham, S.; Carty, M. P.; Saenz-Méndez, P.; Eriksson, L. A.; Aldabbagh, F. COMPARE Analysis of the Toxicity of an Iminoquinone Derivative of the Imidazo[5,4-*f*]benzimidazoles with NAD(P)H:Quinone Oxidoreductase 1 (NQO1) Activity and Computational Docking of Quinones as NQO1 Substrates. *Bioorg. Med. Chem.* **2012**, *20*, 3223–3232. https://doi.org/10.1016/j.bmc.2012.03.063.

(6)   Meth-Cohn, O.; Suschitzky, H. 893. Syntheses of Heterocyclic Compounds. Part IV. Oxidative Cyclisation of Aromatic Amines and Their *N*-Acyl Derivatives. *J. Chem. Soc.* **1963**, 4666–4669. https://doi.org/10.1039/JR9630004666.

(7)   Gurry, M.; McArdle, P.; Aldabbagh, F. Synthesis of a Spirocyclic Oxetane-Fused Benzimidazole. *Molecules* **2015**, *20*, 13864–13874. https://doi.org/10.3390/molecules200813864.

(8)   Zhang, K.; Chen, D.; Ma, K.; Wu, X.; Hao, H.; Jiang, S. NAD(P)H:Quinone Oxidoreductase 1 (NQO1) as a Therapeutic and Diagnostic Target in Cancer. *J. Med. Chem.* **2018**, *61*, 6983–7003. https://doi.org/10.1021/acs.jmedchem.8b00124.

(9)   Spiegel, L.; Kaufmann, H. Über Die Reduktion Des Dinitrophenyl-Piperidins. *Ber. Dtsch. Chem. Ges.* **1908**, *41*, 679–685. https://doi.org/10.1002/cber.190804101129.

(10)   Nair, M. D.; Adams, R. Benzimidazole Syntheses by Oxidative Cyclization with Peroxytrifluoroacetic Acid. *J. Am. Chem. Soc.* **1961**, *83*, 3518–3521. https://doi.org/10.1021/ja01477a038.

(11)   Gurry, M.; Sweeney, M.; McArdle, P.; Aldabbagh, F. One-Pot Hydrogen Peroxide and Hydrohalic Acid Induced Ring Closure and Selective Aromatic Halogenation to Give New Ring-Fused Benzimidazoles. *Org. Lett.* **2015**, *17*, 2856–2859. https://doi.org/10.1021/acs.orglett.5b01317.

(12)   Sweeney, M.; Gurry, M.; Keane, L. A. J.; Aldabbagh, F. Greener Synthesis Using Hydrogen Peroxide in Ethyl Acetate of Alicyclic Ring-Fused Benzimidazoles and Anti-Tumour Benzimidazolequinones. *Tetrahedron Lett.* **2017**, *58*, 3565–3567. https://doi.org/10.1016/j.tetlet.2017.07.102.

(13)   Sweeney, M.; Keane, L. A. J.; Gurry, M.; McArdle, P.; Aldabbagh, F. One-Pot Synthesis of Dihalogenated Ring-Fused Benzimidazolequinones from 3,6-Dimethoxy-2-(cycloamino)anilines Using Hydrogen Peroxide and Hydrohalic Acid. *Org. Lett.* **2018**, *20*, 6970–6974. https://doi.org/10.1021/acs.orglett.8b03135.

(14)   Conboy, D.; Mirallai, S. I.; Craig, A.; McArdle, P.; Al-Kinani, A. A.; Barton, S.; Aldabbagh, F. Incorporating Morpholine and Oxetane into Benzimidazolequinone Antitumor Agents: The Discovery of 1,4,6,9-Tetramethoxyphenazine from Hydrogen Peroxide and Hydroiodic Acid-Mediated Oxidative Cyclizations. *J. Org. Chem.* **2019**, *84*, 9811–9818. https://doi.org/10.1021/acs.joc.9b01427.

(15)   Colomer, I.; Chamberlain, A. E. R.; Haughey, M. B.; Donohoe, T. J. Hexafluoroisopropanol as a Highly Versatile Solvent. *Nat. Rev. Chem.* **2017**, *1*, 0088. https://doi.org/10.1038/s41570-017-0088.

(16)   Conboy, D.; Aldabbagh, F. 6-Imino-1,2,3,4,8,9,10,11-Octahydropyrido[1,2-*a*]pyrido[1′,2′:1,2]imidazo[4,5-*f*]benzimidazole-13-one: Synthesis and Cytotoxicity Evaluation. *Molbank* **2020**, M1118. https://doi.org/10.3390/M1118.

(17) Meth-Cohn, O.; Suschitzky, H. Heterocycles by Ring Closure of *ortho*-Substituted *t*-Anilines (The *t*-Amino Effect). *Adv. Heterocycl. Chem.* **1972**, *14*, 211–278. https://doi.org/10.1016/S0065-2725(08)60954-X.

(18) Purkait, A.; Roy, S. K.; Srivastava, H. K.; Jana, C. K. Metal-Free Sequential C(sp^2)-H/OH and C(sp^3)-H Aminations of Nitrosoarenes and N-Heterocycles to Ring-Fused Imidazoles. *Org. Lett.* **2017**, *19*, 2540–2543. https://doi.org/10.1021/acs.orglett.7b00832.

(19) Hylands, K. A.; Moodie, R. B. The Reaction of 3-Substituted Oxetanes with Nitric Acid in Dichloromethane. *J. Chem. Soc. Perkin Trans. 2* **1997**, 709–714. https://doi.org/10.1039/a607257g.

(20) Kuhn, S. J.; Olah, G. A. Aromatic Substitution. VII. Friedel-Crafts Type Nitration of Aromatics. *J. Am. Chem. Soc.* **1961**, *83*, 4564–4571. https://doi.org/10.1021/ja01483a016.

(21) Olah, G. A.; Kuhn, S. J.; Flood, S. H. Aromatic Substitution. IX. Nitronium Tetrafluoroborate Nitration of Halobenzenes in Tetramethylene Sulfone Solution. *J. Am. Chem. Soc.* **1961**, *83*, 4581–4585. https://doi.org/10.1021/ja01483a018.

(22) Olah, G. A.; Narang, S. C.; Olah, J. A.; Lammertsma, K. Recent Aspects of Nitration: New Preparative Methods and Mechanistic Studies (A Review). *Proc. Natl. Acad. Sci. U.S.A.* **1982**, *79*, 4487–4494. https://doi.org/10.1073/pnas.79.14.4487.

(23) Nguyen, T. B.; Ermolenko, L.; Al-Mourabit, A. Formic Acid as a Sustainable and Complementary Reductant: An Approach to Fused Benzimidazoles by Molecular Iodine-Catalyzed Reductive Redox Cyclization of *o*-Nitro-*t*-anilines. *Green Chem.* **2016**, *18*, 2966–2970. https://doi.org/10.1039/c6gc00902f.

Chapter 4

Synthesis and Cytotoxicity Evaluation of an Imidazo[4,5-*f*]benzimidazole Iminoquinone
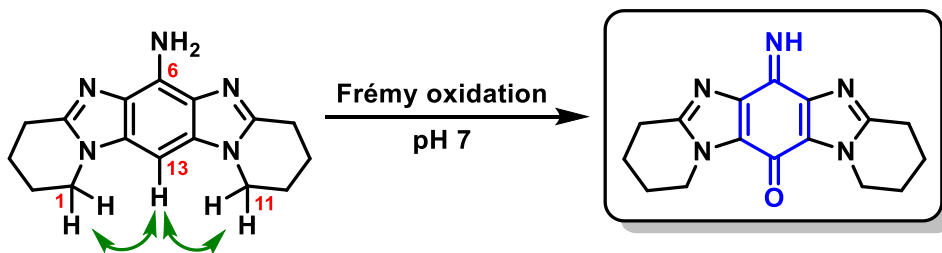
Parts of this Chapter are published in:

4.1. Introduction

Iminoquinone comprises the core of a plethora of natural products, many of which possess potent and varied bioactivities.[1–13] The first of these to be reported, discorhabdin C, was isolated from the *Latrunculia* sponge, and found to possess highly potent cytotoxicity against L1210 lymphocytic leukemia cells (Figure 4.1).[1] Tsitsikammamine C was more recently isolated from the *Zyzzya* marine sponge, and exhibited low-nanomolar toxicity against the *Plasmodium* parasites which cause malaria, including the chloroquine-resistant strain.[4] Makaluvamines, including makaluvamine A and C, were isolated from the same sponge, and found to inhibit topoisomerase II.[7]
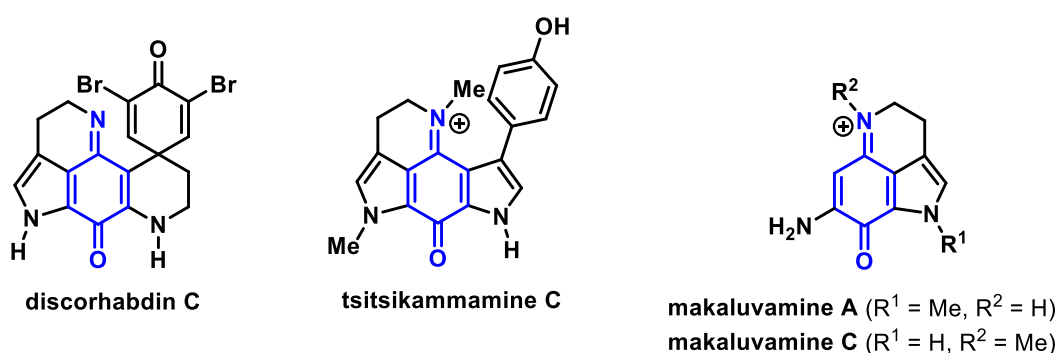
Figure 4.1. Some iminoquinone natural products.

Mitomycin C (MMC) was introduced in Chapter 2 as a naturally occurring antitumour prodrug, and in 1990 the Skibo group reported the synthesis of iminoazamitosenes, which are benzimidazole iminoquinone derivatives of MMC (Figure 4.2).[14] It was previously established that the iminoquinone derivative of the chemotherapy drug daunorubicin, possessed lower oxygen toxicity than the parent drug, which reduced cardiotoxicity.[15] The iminoazamitosenes derivatives of MMC displayed lower toxicity,[14] and are surprisingly stable over a broad pH range due to hydrogen bonding between the imino N-H and the adjacent amide. Below pH 4, hydrolysis of the iminoquinone to the quinone occurred. The reduced form of the iminoazamitosene was found to undergo reoxidation over 100 times slower than the quinone derivative, which correlates with significantly lower generation of reactive oxygen species (ROS), thus reducing potentially undesired oxygen toxicity.[14]
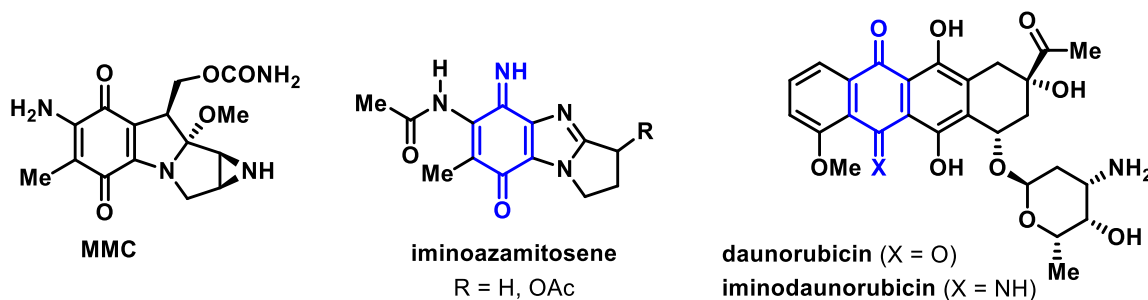
Figure 4.2. Anticancer drugs and their iminoquinone derivatives.

In addition to the iminoazamitosenes, the Skibo group reported the synthesis and anti-tumour activity for five- and six-membered ring-fused imidazo[4,5-*f*]benzimidazolequinones (*e.g.*, **1**, Figure 4.3).[16,17] Computational docking showed that **1** is an excellent substrate of NQO1, with phenylalanine and tryptophan residues intercalating the quinone substrate.[17] Fagan and Aldabbagh provided synthetic routes to enable efficient access to both 4,5-*f* and 5,4-*f* imidazobenzimidazolequinones, which have been discussed in Chapter 3.[18–20]
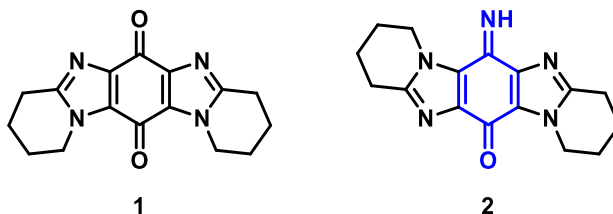
Figure 4.3. Imidazo[4,5-*f*]benzimidazolequinone and imidazo[5,4-*f*]benzimidazole iminoquinone.

Iminoquinone **2** was unexpectedly isolated on the way to the imidazo[5,4-*f*]benzimidazolequinone (Figure 4.3),[18] and found to have exceptional and variable cytotoxicity against the 60 human cell lines of the developmental therapeutics program (DTP) at the National Cancer Institute (NCI).[20] Notable selectivity to the DU-145 prostate cancer cell line which overexpresses NQO1, was observed. Given its promising cytotoxicity, iminoquinone **2** underwent COMPARE analysis, which is an algorithm that ranks the correlation in growth inhibition pattern to known molecular targets in the NCI database, with quantification of the similarity given by the Pearson correlation coefficient.[21,22] Iminoquinone **2** had a moderate correlation of 0.51 to NQO1, which compares favourably to that of MMC (0.43) (Figure 4.4).[20] COMPARE analysis also ranks the similarity in growth inhibition to the other ~43,000 synthetic compounds in the NCI database.[21,22] The two highest correlations of iminoquinone **2** were to compounds **3** and **4**, with respective correlation coefficients of 0.87 and 0.77.[20] The

two latter compounds also correlated strongly to NQO1 with compound **3** possessing the second highest correlation of all synthetic compounds in the NCI database.[20] Notably, compounds **2**, **3** and **4** have two common structural features, the iminoquinone motif, and planar π-stacking capability. It appears that the two latter properties are important in developing NQO1 specific substrates.

	2	**MMC**	**3**	**4**
correlation to **2**:	–	–	0.87	0.77
correlation to NQO1:	0.51	0.43	0.64	0.47
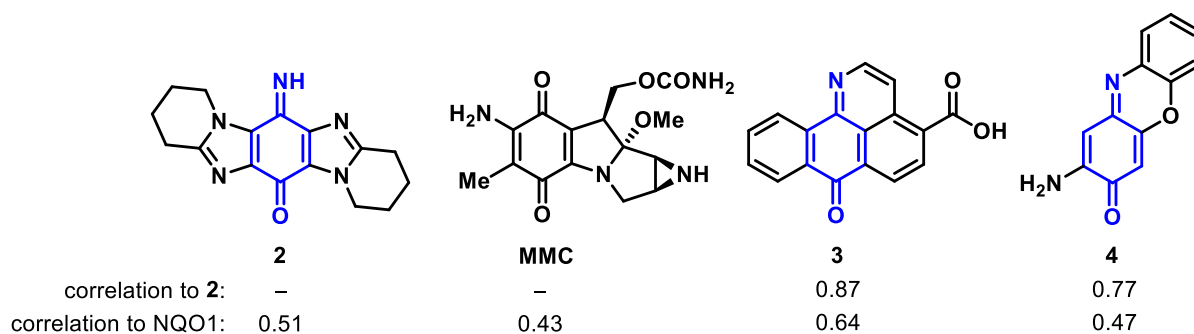
Figure 4.4. Results of COMPARE analysis for iminoquinone **2**.[20]

Further iminoquinones investigated by Aldabbagh *et al*. were the benzotriazinones, which exhibited promising cytotoxicity profiles upon analysis at the NCI (Figure 4.5).[23] COMPARE analysis of both the 3-phenyl and 3-trifluoromethyl derivatives revealed very strong respective correlations of 0.84 and 0.79 to pleurotin. Pleurotin is an antibacterial, antifungal and anticancer agent, whose primary mechanism of action is the inhibition of thioredoxin reductase (TrxR).[24] TrxR reduces the thioredoxin (Trx) protein to its active form, which allows the latter to mediate key cellular processes such as cellular proliferation, apoptosis inhibition and angiogenesis.[25] Trx protein is overexpressed in a number of cancers, and the inhibition of TrxR has been proposed as a potential strategy for anticancer drugs.[23] Given the correlation of the benzotriazinones to the known TrxR inhibitor pleurotin, further analysis by way of TrxR inhibition assays were done on the former heterocycles.[23] Both benzotriazinones were found to inhibit TrxR, although the mechanism was different to pleurotin; the latter is an irreversible inhibitor, while both benzotriazinones reversibly inhibited TrxR.[23]

benzotriazinones ———— pleurotin
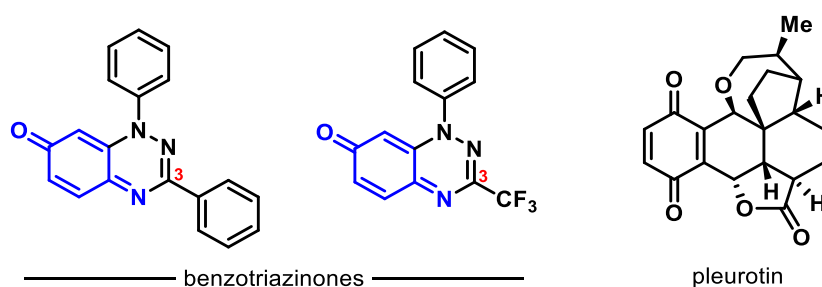
Figure 4.5. Benzotriazinones very strongly correlated to pleurotin.[23]

4.2. Chapter Aims and Objectives

Given the selective and variable cytotoxicity of imidazo[5,4-*f*]benzimidazole iminoquinone **2**,[20] and the potential of imidazo[4,5-*f*]benzimidazolequinone **1** to act as an NQO1 substrate,[17] it seems plausible that imidazo[4,5-*f*]benzimidazole iminoquinone **5** would be a potent antitumour cytotoxin, with selectivity towards NQO1 (Figure 4.6). No examples exist in the literature of imidazo[4,5-*f*]benzimidazole iminoquinones. The synthesis of iminoquinone **5** will be established herein; as will its cytotoxicity against the 60 cell lines at the NCI.
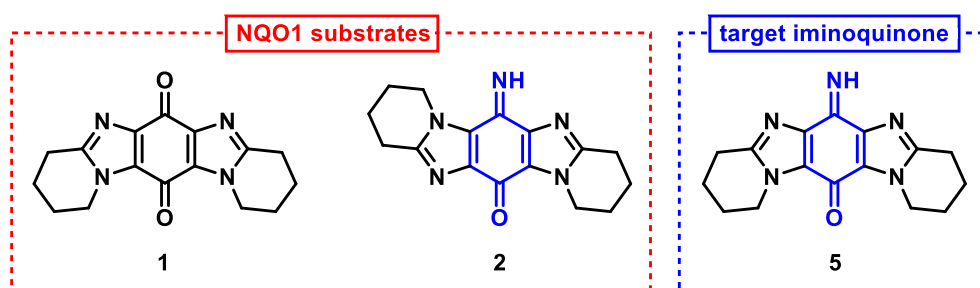
Figure 4.6. Rational drug design: targeting of iminoquinone **5** based on reported NAD(P)H:quinone oxidoreductase 1 (NQO1) substrates.

4.3. Results and Discussion

4.3.1. Synthesis

A similar procedure described in Chapter 3 for the preparation of spirocyclic oxetane-fused imidazobenzimidazoles was followed for the synthesis of 1,2,3,4,8,9,10,11-octahydropyrido[1,2-*a*]pyrido[1',2':1,2]imidazo[4,5-*f*]benzimidazole (**6**) (Scheme 4.1). The sequential S$_N$Ar of piperidine onto 1,5-difluoro-2,4-dinitrobenzene, catalytic hydrogenation, acetylation and Oxone-mediated oxidative cyclization furnished imidazo[4,5-*f*]benzimidazole **6** in an overall yield of 51%. Nitric and sulfuric acid (1:1 mixture) were used in the nitration of **6** to give 6-nitroimidazo[4,5-*f*]benzimidazole **7** in a 54% yield, alongside trace amounts of the 13-nitro and dinitro isomers, which were discarded after column chromatography. Atmospheric-pressure catalytic hydrogenation gave the novel aromatic amine 1,2,3,4,8,9,10,11-octahydropyrido[1,2-*a*]pyrido[1',2':1,2]imidazo[4,5-*f*]benzimidazol-6-amine (**8**), in an almost quantitative yield of 96%. The regioselectivity of the nitration/reduction to give **8** was determined from the 2D NOESY through-space ^{1}H-^{1}H dipolar interactions of the aromatic 13-H to 1-CH$_2$ and 11-CH$_2$ of **8** (Figure 4.7).
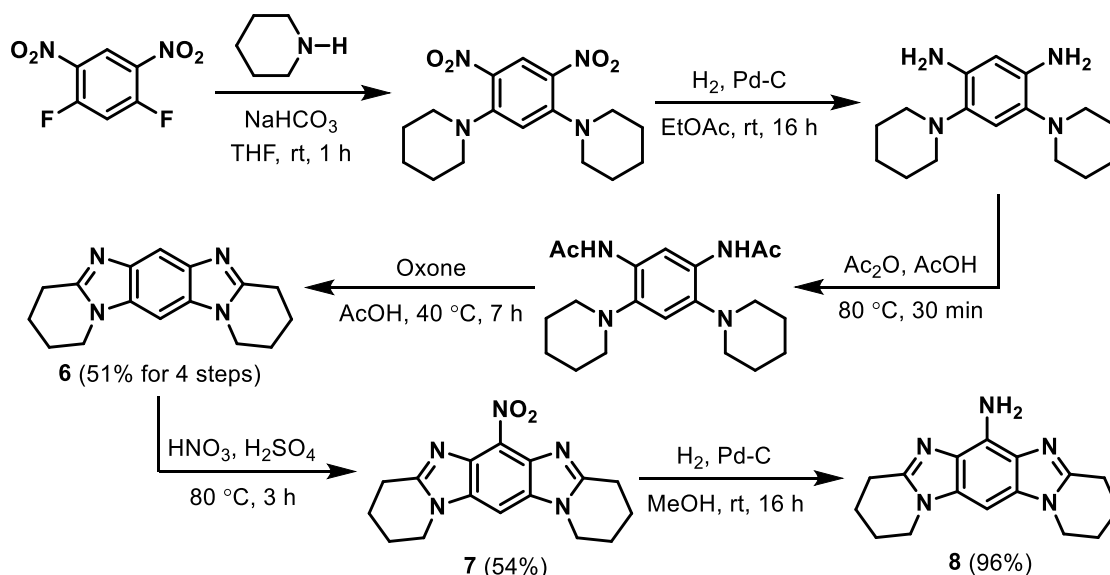
Scheme 4.1. Synthesis of imidazo[4,5-*f*]benzimidazole(imino)quinone **3**.
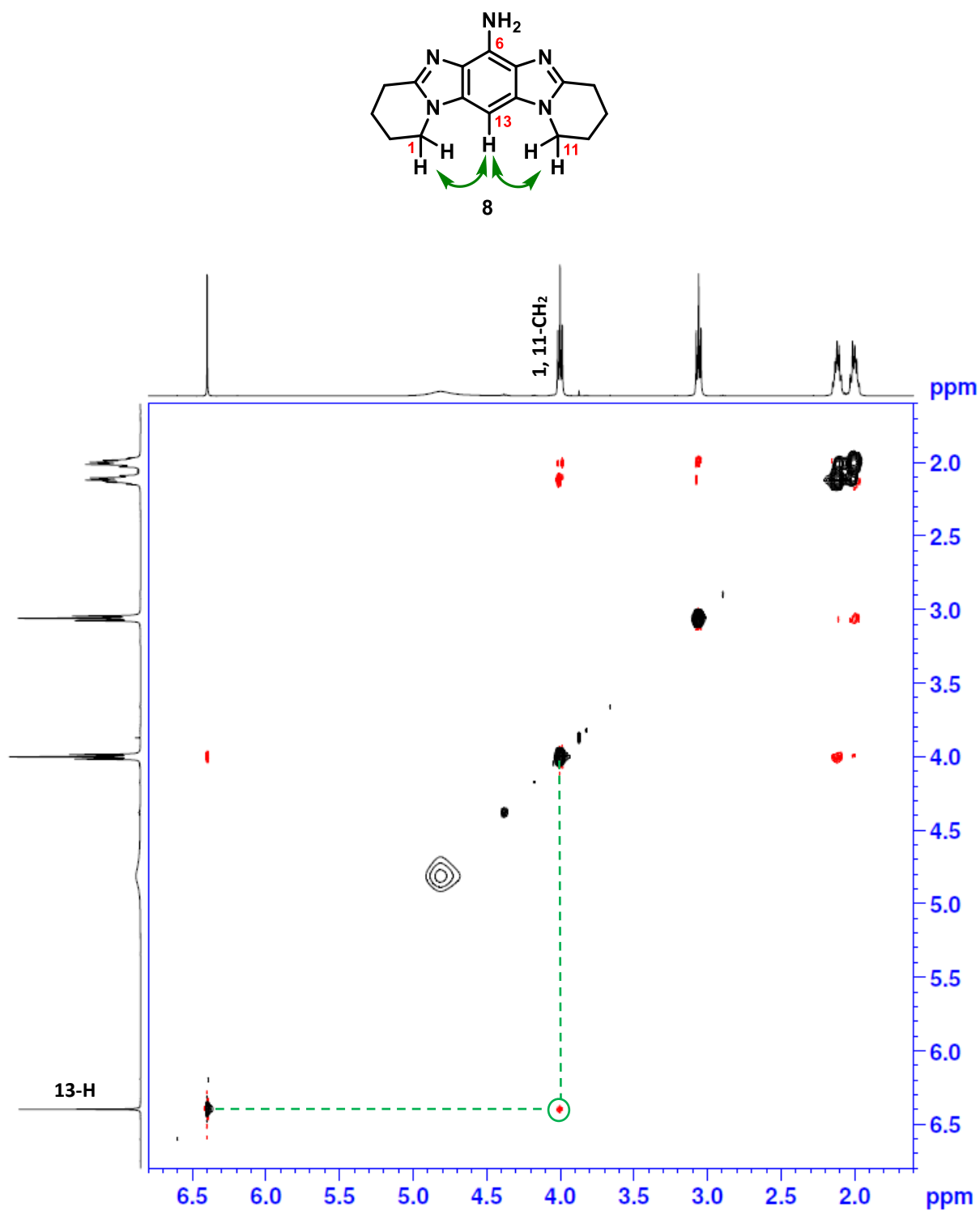
Figure 4.7. 2D NOESY spectrum (CDCl₃) of aromatic amine **8**, with highlighted through-space ^1H-^1H dipolar interactions.

Iminoquinone **2** was previously obtained by Frémy salt ($K_2NO(SO_3)_2$) oxidation of the aromatic amine precursor at pH 4.[18] Under the same buffered conditions, amine **8** gave only the undesired quinone **1** in 81% yield, as a result of acidic hydrolysis (Scheme 4.2). Carrying out the Frémy oxidation at neutral pH however, formed the desired iminoquinone **5** in 61% yield, along with quinone **1**, separated by column chromatography in 8% yield. For isolated **5**, the triplet at 4.31 ppm in the ^{1}H NMR, and the peaks at 151.3, 142.4 and 130.2 ppm in the ^{13}C NMR arise from the presence of minor quantities of quinone **1**,[18] which formed upon acidic hydrolysis of the iminoquinone on silica gel using 'conventional' column chromatography (Figure 4.8). Deactivating the silica with triethylamine prior to elution gave spectroscopically pure compound **5**, in an improved yield of 67%, along with quinone **1** in a 6% yield. The imine group of **5** was observed, with N-*H* at ~11 ppm in the ^{1}H NMR spectrum, and *C*=N at 157 ppm in the ^{13}C NMR spectrum, in accordance with reported data for iminoquinone **2**.[18]
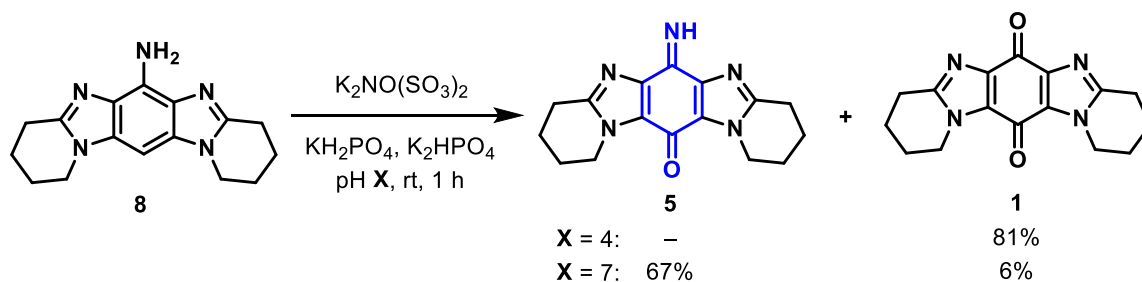
Scheme 4.2. Frémy oxidation.
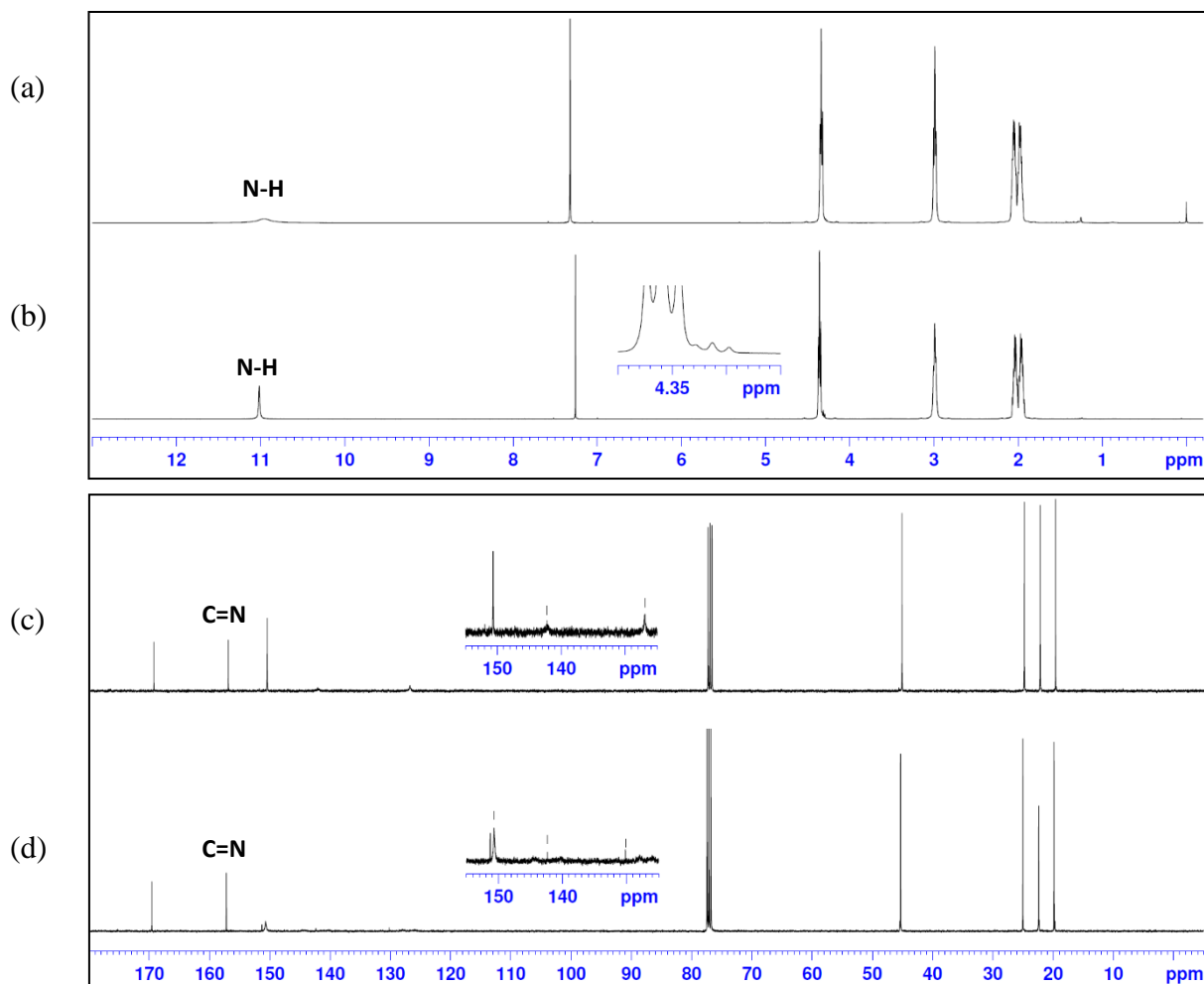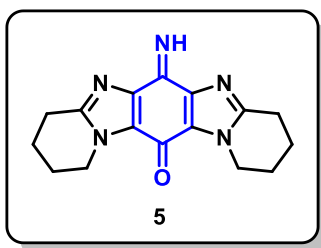
Figure 4.8. Overlaid NMR spectra (CDCl₃) of iminoquinone **5**. (a) ^{1}H NMR spectrum after purification on silica deactivated with NEt₃. (b) ^{1}H NMR spectrum after purification on silica gel. (c) ^{13}C NMR spectrum after purification on silica deactivated with NEt₃. (d) ^{13}C NMR spectrum after purification on silica gel.

4.3.2. Cytotoxicity

The cytotoxicity of iminoquinone **5** was evaluated against the 60-cancer cell line panel at the NCI.[16,20,22] The one-dose graph in Figure 4.10 shows the growth percentage of each cancer cell line when treated with a 10 μM dose of iminoquinone **5** relative to untreated cells. A positive value indicates cell growth, while a negative value indicates growth inhibition. Overall negligible cytotoxicity (growth inhibition) was observed for iminoquinone **5**. This is in contrast to isomeric iminoquinone **2**, which displayed significant cytotoxicity against several solid tumour cell lines,[20] and was selected for subsequent five-dose testing. Given the low toxicity, no further biochemical assays or computational docking studies were carried out on iminoquinone **5**. The lack of bioactivity observed for iminoquinone **5** is likely a result of the active site of NQO1 placing spatial and geometric constraints on potential substrates. Although pyrido-fused imidazo[5,4-*f*]benzimidazole iminoquinone **2** exhibited promising bioactivity, the azepino-fused analogue **9** previously showed negligible cytotoxicity upon one-dose testing at the NCI (Figure 4.9).[20]
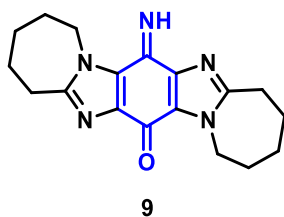
Figure 4.9. Azepino-fused imidazo[5,4-*f*]benzimidazole iminoquinone.[20]

144

Developmental Therapeutics Program
One Dose Mean Graph

NSC: D-813574 / 1   Conc: 1.00E-5 Molar   Test Date: Mar 18, 2019
Experiment ID: 1903OS80   Report Date: Apr 04, 2019

Panel/Cell Line	Growth Percent
Leukemia	
CCRF-CEM	94.06
HL-60(TB)	99.59
K-562	94.98
MOLT-4	98.65
RPMI-8226	94.49
SR	88.84
Non-Small Cell Lung Cancer	
A549/ATCC	99.79
EKVX	98.35
HOP-62	104.26
HOP-92	112.26
NCI-H226	105.34
NCI-H23	97.92
NCI-H322M	102.53
NCI-H460	96.68
NCI-H522	89.70
Colon Cancer	
COLO 205	107.35
HCC-2998	119.57
HCT-116	102.51
HCT-15	94.75
HT29	110.37
KM12	97.67
SW-620	101.40
CNS Cancer	
SF-268	93.41
SF-295	99.45
SF-539	97.96
SNB-19	102.15
SNB-75	101.93
U251	96.92
Melanoma	
LOX IMVI	92.15
MALME-3M	71.58
M14	99.47
MDA-MB-435	104.82
SK-MEL-2	105.57
SK-MEL-28	110.98
SK-MEL-5	94.42
UACC-257	101.65
UACC-62	98.93
Ovarian Cancer	
IGROV1	100.32
OVCAR-3	92.33
OVCAR-4	84.20
OVCAR-5	105.18
OVCAR-8	97.60
NCI/ADR-RES	105.53
SK-OV-3	110.06
Renal Cancer	
786-0	93.34
A498	92.55
ACHN	99.95
CAKI-1	90.28
RXF 393	107.24
SN12C	97.90
TK-10	103.12
UO-31	87.48
Prostate Cancer	
PC-3	101.78
DU-145	99.77
Breast Cancer	
MCF7	87.34
MDA-MB-231/ATCC	97.91
HS 578T	111.87
BT-549	105.01
T-47D	100.09
MDA-MB-468	93.67
Mean	99.12
Delta	27.54
Range	47.99

Mean Growth Percent - Growth Percent

150 100 50 0 -50 -100 -150

Figure 4.10. One dose data for iminoquinone **5**.

145

4.4. Conclusions

The first synthesis of an iminoquinone based on the imidazo[4,5-*f*]benzimidazole scaffold has been achieved in 7 steps. The key step was a Frémy oxidation at neutral pH, with oxidation at pH 4 resulting in acidic hydrolysis to the quinone. One-dose testing at the NCI revealed negligible cytotoxicity, in contrast to the bioactive imidazo[5,4-*f*]benzimidazole iminoquinone. It is thus apparent that planar, iminoquinone scaffolds are not ubiquitously good substrates of NQO1.

4.5. Experimental Section

4.5.1. Materials

Piperidine (Sigma Aldrich, 99%), $NaHCO_3$ (Fisher Scientific, ≥99.7%), 1,5-difluoro-2,4-dinitrobenzene (Sigma Aldrich, 97%), Pd-C (Sigma Aldrich, 10 wt% loading), EtOAc (VWR, 99.9%), Ac_2O (ACROS Organics™, 99+%), AcOH (VWR, glacial), Oxone (Sigma Aldrich, $KHSO_5$•$0.5KHSO_4$•$0.5K_2SO_4$), Na_2CO_3 (Fisher Scientific, 99.5%), $MgSO_4$ (Anhydrous, Fisher Scientific, Extra Pure, SLR, Dried), CH_2Cl_2 (Fisher Scientific, 99.8%), HNO_3 (Fisher Scientific, 70%), H_2SO_4 (Fisher Scientific, ≥95%), MeOH (VWR, ≥99.8%) and potassium nitrosodisulfonate (Sigma Aldrich) were used as received. THF was freshly distilled over Na and benzophenone prior to use. Thin layer chromatography (TLC) was performed on TLC silica gel 60 F_{254} plates. Flash column chromatography was carried out on silica gel (Apollo Scientific 60/40−63 μm), and deactivated by making a slurry using Et_3N in EtOAc (2% *v/v*), for the purification of compound **5**.

4.5.2. Measurements

Melting points were measured on a Stuart Scientific melting point apparatus SMP1. IR spectra were recorded using a PerkinElmer Spec 1 with ATR attached. NMR spectra were recorded using a Bruker Avance III 400 MHz spectrometer equipped with a 5mm BBFO+, broadband autotune probe and controlled with TopSpin 3.5.7 acquisition software and IconNMR 5.0.7 automation software Copyright © 2017 Bruker BioSpin GmbH. The chemical shifts are in ppm, relative to tetramethylsilane. ^{13}C NMR spectra at 100 MHz are with complete proton decoupling. NMR assignments are supported by DEPT-135. The HRMS spectrum of iminoquinone **5** was obtained at the National University of Ireland Galway, using an ESI time-of-flight mass spectrometer (TOFMS) on a Waters LCT Mass Spectrometry instrument, while the HRMS spectrum of aromatic amine **8** was obtained at the National Mass Spectrometry Facility at Swansea University using a Waters Xevo G2-S mass spectrometer with an atmospheric solids analysis probe (ASAP). The precision of all accurate mass measurements was better than 5 ppm.

4.5.3. Synthetic Procedures and Characterization

4.5.3.1. Synthesis of 1,2,3,4,8,9,10,11-Octahydropyrido[1,2-*a*]pyrido[1',2':1,2]imidazo[4,5-*f*]benzimidazole (6)
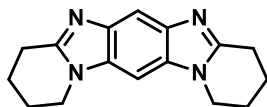
Piperidine (7.50 mL, 75.9 mmol), $NaHCO_3$ (4.210 g, 50.1 mmol) and 1,5-difluoro-2,4-dinitrobenzene (2.042 g, 10.0 mmol) in THF (80 mL) were stirred at room temperature for 1 h. Water (200 mL) was added and the precipitate was collected, washed with water and dried. The yellow solid was stirred with Pd-C (0.206 g) in EtOAc (100 mL) under an atmosphere of H_2 (1 atm; balloon) for 16 h. Upon filtering the solution through Celite and evaporating the filtrate to dryness, Ac_2O (9.45 mL, 0.100 mol) and AcOH (100 mL) were added, and the solution was stirred at 80 °C for 30 min. The mixture was evaporated, $NaHCO_3$ (5% aq, 150 mL) was added, and the mixture was stirred for 1 h. The precipitate was collected, washed with water, and re-dissolved in AcOH (80 mL). Oxone (18.225 g, 59.3 mmol) was added, and the mixture was stirred at 40 °C for 7 h. The solution was evaporated, H_2O (100 mL) was added, neutralized with solid Na_2CO_3, and extracted with CH_2Cl_2 (3 × 100 mL). The organic extracts were dried ($MgSO_4$) and evaporated to dryness to give the **6** (1.358 g, 51%), as an off-white solid; mp (decomp. >264 °C); lit. mp[18] (decomp. 266–270 °C); spectral data was consistent with the literature.[18]

4.5.3.2. Synthesis of 6-Nitro-1,2,3,4,8,9,10,11-octahydropyrido[1,2-a]pyrido[1',2':1,2]imidazo[4,5-f]benzimidazole (7)
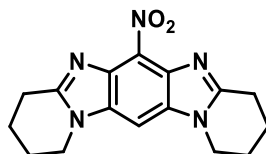
Imidazo[4,5-*f*]benzimidazole **6** (0.963 g, 3.6 mmol), HNO_3 (40 mL) and H_2SO_4 (40 mL) were stirred at 80 °C for 3 h. The mixture was diluted with H_2O (300 mL), neutralized with solid Na_2CO_3, and extracted with CH_2Cl_2 (4 × 100 mL). The organic extracts were dried ($MgSO_4$), evaporated, and purified by column chromatography using gradient elution of EtOAc/MeOH to give **7** (0.608 g, 54%) as a yellow solid; R_f 0.29 (9:1 EtOAc/MeOH); mp (decomp. >238 °C); lit. mp[17] (decomp. 230–232 °C); spectral data was consistent with the literature.[17]

4.5.3.3. Synthesis of 1,2,3,4,8,9,10,11-Octahydropyrido[1,2-a]pyrido[1',2':1,2]imidazo[4,5-f]benzimidazol-6-amine (8)
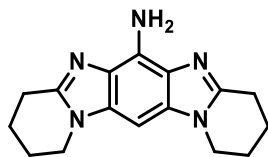
6-Nitroimidazo[4,5-f]benzimidazole **7** (0.502 g, 1.6 mmol), and Pd-C (50 mg) in MeOH (100 mL) were stirred under H_2 at room temperature for 16 h. The mixture was filtered through Celite and evaporated to dryness to give the title compound **8** (0.432 g, 96%) as an off-white solid; mp (decomp. > 215 °C); ν_{max} (neat, cm^{-1}) 3421, 3308 (both NH_2), 3237, 3205, 2951, 2936, 2877, 2864, 2831, 1694, 1683, 1630, 1596, 1532, 1513, 1484, 1456, 1439, 1426, 1385, 1345, 1324, 1283, 1255, 1218, 1164; ^{1}H NMR (400 MHz, CDCl$_3$) δ: 6.40 (s, 1H), 5.04–4.56 (br.s, disappears with D$_2$O, 2H, NH$_2$), 4.00 (t, J = 6.1 Hz, 4H, 1,11-CH$_2$), 3.06 (t, J = 6.4 Hz, 4H, 4,8-CH$_2$), 2.16–2.07 (m, 4H), 2.04–1.95 (m, 4H); ^{13}C NMR (100 MHz, CDCl$_3$) δ: 148.9, 133.0, 127.7, 126.4 (all C), 76.1 (CH), 42.6, 25.6, 22.8, 20.9 (all CH$_2$); HRMS (ASAP) m/z [M + H]$^+$ found 282.1717, C$_{16}$H$_{20}$N$_5$ requires 282.1719.

4.5.3.4. Frémy Oxidation of 8 to Give Iminoquinone 5
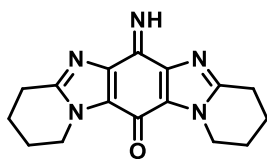
Potassium nitrosodisulfonate (1.012 g, 3.77 mmol) in phosphate buffer (0.2 M, pH 7, 80 mL) was added to amine **6** (0.352 g, 1.25 mmol) in the same buffer (40 mL), and stirred at room temperature for 1 h. The mixture was extracted with CH_2Cl_2 (4 x 90 mL), and the organic extracts were dried ($MgSO_4$), evaporated, and purified by column chromatography using a gradient elution of EtOAc/MeOH/Et_3N.

1,2,3,4,8,9,10,11-Octahydropyrido[1,2-*a*]pyrido[1′,2′:1,2]imidazo[4,5-*f*]benzimidazol-6,13-dione (1). (22 mg, 6%); orange solid; R_f 0.32 (9:1 EtOAc/MeOH); spectral data and melting point were consistent with the literature.[18]

6-Imino-1,2,3,4,8,9,10,11-octahydropyrido[1,2-*a*]pyrido[1′,2′:1,2]imidazo[4,5-*f*]benzimidazole-13-one (5). (0.248 g, 67%); yellow solid; R_f 0.21 (9:1 EtOAc/MeOH); mp (decomp. >225 °C); ν_{max} (neat, cm^{-1}) 2946, 1637 (C=O), 1482, 1422, 1304, 1264, 1166, 1021; ^{1}H NMR (400 MHz, CDCl$_3$) δ: 11.32–10.60 (br.s, disappears with D$_2$O, 1H, NH), 4.34 (t, *J* = 5.9 Hz, 4H, 1,11-CH$_2$), 2.99 (t, *J* = 6.3 Hz, 4H, 4,8-CH$_2$), 2.10–1.92 (m, 8H); ^{13}C NMR (100 MHz, CDCl$_3$) δ: 169.4 (C=O), 157.1 (C=N), 150.7, 142.3, 127.0 (all C), 45.3, 25.0, 22.4, 19.8 (all CH$_2$); HRMS (ESI) *m/z* [M + H]$^+$ found 296.1506, $C_{16}H_{18}N_5O$ requires 296.1511.

4.6. Chapter 4 References

(1)   Perry, N. B.; Blunt, J. W.; McCombs, J. D.; Munro, M. H. G. Discorhabdin C, a Highly Cytotoxic Pigment from a Sponge of the Genus *Latrunculia*. *J. Org. Chem.* **1986**, *51*, 5476–5478. https://doi.org/10.1021/jo00376a096.

(2)   Sun, H. H.; Sakemi, S.; Burres, N.; McCarthy, P. Isobatzellines A, B, C, and D. Cytotoxic and Antifungal Pyrroloquinoline Alkaloids from the Marine Sponge *Batzella sp*. *J. Org. Chem.* **1990**, *55*, 4964–4966. https://doi.org/10.1021/jo00303a043.

(3)   Reyes, F.; Martín, R.; Rueda, A.; Fernández, R.; Montalvo, D.; Gómez, C.; Sánchez-Puelles, J. M. Discorhabdins I and L, Cytotoxic Alkaloids from the Sponge *Latrunculia brevis*. *J. Nat. Prod.* **2004**, *67*, 463–465. https://doi.org/10.1021/np0303761.

(4)   Davis, R. A.; Buchanan, M. S.; Duffy, S.; Avery, V. M.; Charman, S. A.; Charman, W. N.; White, K. L.; Shackleford, D. M.; Edstein, M. D.; Andrews, K. T.; *et al*. Antimalarial Activity of Pyrroloiminoquinones from the Australian Marine Sponge *Zyzzya sp*. *J. Med. Chem.* **2012**, *55*, 5851–5858. https://doi.org/10.1021/jm3002795.

(5)   Zlotkowski, K.; Hewitt, W. M.; Yan, P.; Bokesch, H. R.; Peach, M. L.; Nicklaus, M. C.; O'Keefe, B. R.; McMahon, J. B.; Gustafson, K. R.; Schneekloth, J. S. Macrophilone A: Structure Elucidation, Total Synthesis, and Functional Evaluation of a Biologically Active Iminoquinone from the Marine Hydroid Macrorhynchia Philippina. *Org. Lett.* **2017**, *19*, 1726–1729. https://doi.org/10.1021/acs.orglett.7b00496.

(6)   Copp, B. R.; Ireland, C. M.; Barrows, L. R. Wakayin: A Novel Cytotoxic Pyrroloiminoquinone Alkaloid from the *Ascidian clavelina* Species. *J. Org. Chem.* **1991**, *56*, 4596–4597. https://doi.org/10.1021/jo00015a005.

(7)   Radisky, D. C.; Radisky, E. S.; Copp, B. R.; Ireland, C. M.; Barrows, L. R.; Kramer, R. A. Novel Cytotoxic Topoisomerase II Inhibiting Pyrroloiminoquinones from Fijian Sponges of the Genus *Zyzzya*. *J. Am. Chem. Soc.* **1993**, *115*, 1632–1638. https://doi.org/10.1021/ja00058a003.

(8)   D'Ambrosio, M.; Guerriero, A.; Chiasera, G.; Pietra, F.; Tatò, M. Epinardins A-D, New Pyrroloiminoquinone Alkaloids of Undetermined Deep-Water Green Demosponges from Pre-Antarctic Indian Ocean. *Tetrahedron* **1996**, *52*, 8899–8906. https://doi.org/10.1016/0040-4020(96)00438-3.

(9) Venables, D. A.; Concepción, G. P.; Matsumoto, S. S.; Barrows, L. R.; Ireland, C. M. Makaluvamine N: A New Pyrroloiminoquinone from *Zyzzya fuliginosa*. *J. Nat. Prod.* **1997**, *60*, 408–410. https://doi.org/10.1021/np9607262.

(10) Venables, D. A.; Barrows, L. R.; Lassota, P.; Ireland, C. M. Veiutamine. A New Alkaloid from the Fijian Sponge *Zyzzya fuliginosa*. *Tetrahedron Lett.* **1997**, *38*, 721–722. https://doi.org/https://doi.org/10.1016/S0040-4039(96)02424-0.

(11) Gunasekera, S. P.; McCarthy, P. J.; Longley, R. E.; Pomponi, S. A.; Wright, A. E.; Lobkovsky, E.; Clardy, J. Discorhabdin P, a New Enzyme Inhibitor from a Deep-Water Caribbean Sponge of the Genus *Batzella*. *J. Nat. Prod.* **1999**, *62*, 173–175. https://doi.org/10.1021/np980293y.

(12) Gunasekera, S. P.; McCarthy, P. J.; Longley, R. E.; Pomponi, S. A.; Wright, A. E. Secobatzellines A and B, Two New Enzyme Inhibitors from a Deep-Water Caribbean Sponge of the Genus *Batzella*. *J. Nat. Prod.* **1999**, *62*, 1208–1211. https://doi.org/10.1021/np990177a.

(13) Ford, J.; Capon, R. J. Discorhabdin R: A New Antibacterial Pyrroloiminoquinone from Two *Latrunculiid* Marine Sponges, *Latrunculia sp.* and *Negombata sp. J. Nat. Prod.* **2000**, *63*, 1527–1528. https://doi.org/10.1021/np000220q.

(14) Islam, I.; Skibo, E. B. Synthesis and Physical Studies of Azamitosene and Iminoazamitosene Reductive Alkylating Agents. Iminoquinone Hydrolytic Stability, Syn/Anti Isomerization, and Electrochemistry. *J. Org. Chem.* **1990**, *55*, 3195–3205. https://doi.org/10.1021/jo00297a040.

(15) Tong, G. L.; Henry, D. W.; Acton, E. M. 5-Iminodaunorubicin. Reduced Cardiotoxic Properties in an Antitumor Anthracycline. *J. Med. Chem.* **1979**, *22*, 36–39. https://doi.org/10.1021/jm00187a009.

(16) Schulz, W. G.; Skibo, E. B. Inhibitors of Topoisomerase II Based on the Benzodiimidazole and Dipyrroloimidazobenzimidazole Ring Systems: Controlling DT-Diaphorase Reductive Inactivation with Steric Bulk. *J. Med. Chem.* **2000**, *43*, 629–638. https://doi.org/10.1021/jm990210q.

(17)   Suleman, A.; Skibo, E. B. A Comprehensive Study of the Active Site Residues of DT-Diaphorase: Rational Design of Benzimidazolediones as DT-Diaphorase Substrates. *J. Med. Chem.* **2002**, *45*, 1211–1220. https://doi.org/10.1021/jm0104365.

(18)   Fagan, V.; Bonham, S.; Carty, M. P.; Aldabbagh, F. One-Pot Double Intramolecular Homolytic Aromatic Substitution Routes to Dialicyclic Ring Fused Imidazobenzimidazolequinones and Preliminary Analysis of Anticancer Activity. *Org. Biomol. Chem.* **2010**, *8*, 3149–3156. https://doi.org/10.1039/c003511d.

(19)   Fagan, V.; Bonham, S.; McArdle, P.; Carty, M. P.; Aldabbagh, F. Synthesis and Toxicity of New Ring-Fused Imidazo[5,4-*f*]benzimidazolequinones and Mechanism Using Amine *N*-Oxide Cyclizations. *Eur. J. Org. Chem.* **2012**, 1967–1975. https://doi.org/10.1002/ejoc.201101687.

(20)   Fagan, V.; Bonham, S.; Carty, M. P.; Saenz-Méndez, P.; Eriksson, L. A.; Aldabbagh, F. COMPARE Analysis of the Toxicity of an Iminoquinone Derivative of the Imidazo[5,4-*f*]benzimidazoles with NAD(P)H:Quinone Oxidoreductase 1 (NQO1) Activity and Computational Docking of Quinones as NQO1 Substrates. *Bioorg. Med. Chem.* **2012**, *20*, 3223–3232. https://doi.org/10.1016/j.bmc.2012.03.063.

(21)   Paull, K. D.; Shoemaker, R. H.; Hodes, L.; Monks, A.; Scudiero, D. A.; Rubinstein, L.; Plowman, J.; Boyd, M. R. Display and Analysis of Patterns of Differential Activity of Drugs Against Human Tumor Cell Lines: Development of Mean Graph and COMPARE Algorithm. *J. Natl. Cancer Inst.* **1989**, *81*, 1088–1092. https://doi.org/10.1093/jnci/81.14.1088.

(22)   Shoemaker, R. H. The NCI60 Human Tumour Cell Line Anticancer Drug Screen. *Nat. Rev. Cancer* **2006**, *6*, 813–823. https://doi.org/10.1038/nrc1951.

(23)   Sweeney, M.; Coyle, R.; Kavanagh, P.; Berezin, A. A.; Lo Re, D.; Zissimou, G. A.; Koutentis, P. A.; Carty, M. P.; Aldabbagh, F. Discovery of Anti-Cancer Activity for Benzo[1,2,4]triazin-7-ones: Very Strong Correlation to Pleurotin and Thioredoxin Reductase Inhibition. *Bioorganic Med. Chem.* **2016**, *24*, 3565–3570. https://doi.org/10.1016/j.bmc.2016.05.066.

(24) Wipf, P.; Hopkins, T. D.; Jung, J.-K.; Rodriguez, S.; Birmingham, A.; Southwick, E. C.; Lazo, J. S.; Powis, G. New Inhibitors of the Thioredoxin–Thioredoxin Reductase System Based on a Naphthoquinone Spiroketal Natural Product Lead. *Bioorg. Med. Chem. Lett.* **2001**, *11*, 2637–2641. https://doi.org/https://doi.org/10.1016/S0960-894X(01)00525-X.

(25) Cha, M.-K.; Suh, K.-H.; Kim, I.-H. Overexpression of Peroxiredoxin I and Thioredoxin1 in Human Breast Carcinoma. *J. Exp. Clin. Cancer Res.* **2009**, *28*, 93. https://doi.org/10.1186/1756-9966-28-93.

Chapter 5

Synthesis of Selectively Halogenated Ring-Fused Bis-*p*-Benzimidazolequinones *via* Dimethoxybenzimidazole-Benzimidazolequinones
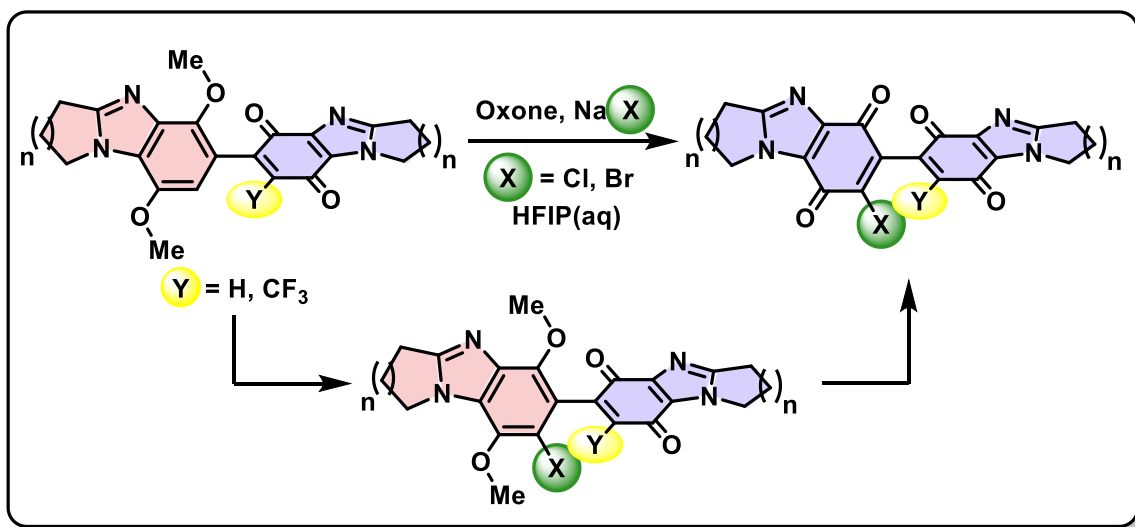
5.1. Introduction

5.1.1. The Use of NaX/Oxone in Organic Synthesis

In nature, halogens are incorporated into organic molecules *via* electrophilic halogenating species, generated *in situ* using enzymatic oxidation of halides (X^-; $X = Cl$, Br) often with H_2O_2 and O_2.[1,2] In Chapter 2 of this thesis, the use of H_2O_2 with HX was discussed as a green mimic of nature for the formation of the electrophilic hypohalous acids (HOX) and molecular halogens (X_2).[3,4] However, higher than ambient temperatures and an excess of acid were necessary to mediate the desired oxidative halogenations. A milder alternative to the H_2O_2/HX system is the combination of Oxone with metal halides (NaX, KX), which has mediated electrophilic aromatic halogenations at room temperature (*vide infra*).[5,6] Oxone ($2KHSO_5 \cdot KHSO_4 \cdot K_2SO_4$) is a non-toxic, stable, cheap, and crystalline oxidant,[6] while metal halides are similarly benign and user-friendly.[7] The reaction of the halide with Oxone generates the hypohalous acid (HOX),[7] which in the presence of excess halide, favours the formation of X_2 (Scheme 5.1).[8]
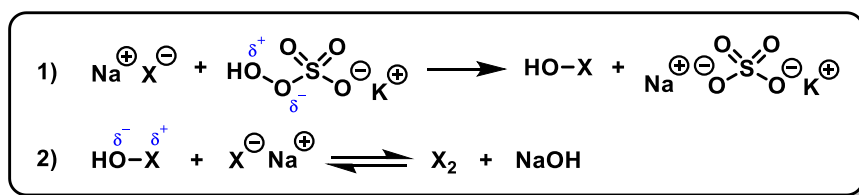

Scheme 5.1. Oxone-mediated halide oxidation.

Dieter and co-workers first exploited the Oxone/NaX system for the halogenation of α,β-enones and alkenes with moderate to quantitative yields of regioselectively α-halogenated enones isolated in biphasic CCl_4/H_2O solvent system (Scheme 5.2).[9] The reaction initially proceeded *via* formation of the α,β-dihalogenated product, which readily underwent dehydrohalogenation upon basic work-up. In the main, yields for chlorinations were moderately higher than the analogous brominations. Subjecting cyclohexene and nonan-1-ene to the Oxone/NaX reaction yielded vicinally-dihalogenated products.[9]
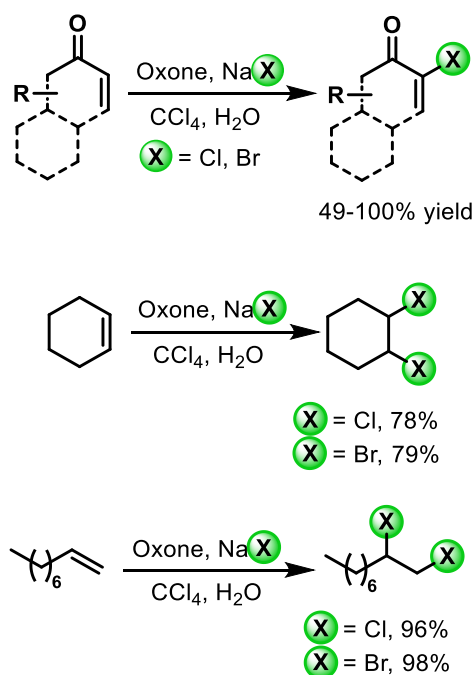
Scheme 5.2. Oxone/NaX-mediated aliphatic halogenation.[9]

The first report of Oxone/MX-mediated aromatic halogenation detailed the *para*-selective chlorination and bromination of a narrow range of electron-rich arenes with potassium chloride or bromide as the halide source (Scheme 5.3).[10] No reaction occurred upon introducing an electron-withdrawing nitro- or chloro-substituent. The scope of halogenation was later expanded to include phenols and alkyl arenes.[11,12] Crucially only aromatic chlorination occurred on toluene.[11] The lack of benzylic chlorination indicated an ionic (S_EAr) rather than radical mechanism. Furthermore, polar organic solvents were necessary for successful halogenation, as switching from MeCN to CCl_4 in the chlorination of anisole resulted in a drop in conversion from 98% to 0%.
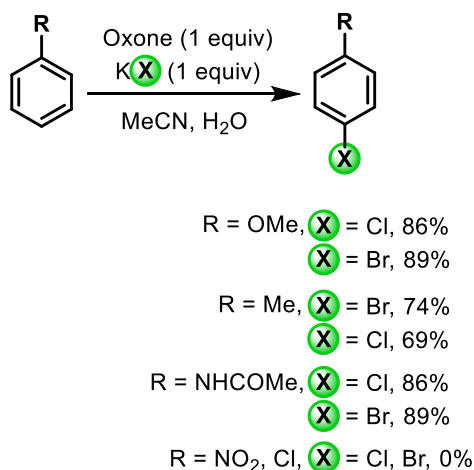

Scheme 5.3. Aromatic halogenation with Oxone/KCl.[10,11]

The necessity for polar solvents in the aromatic chlorination of toluene was more recently highlighted, where NaCl with Oxone in a trifluoroethanol (TFE)/water mixture under visible light irradiation mediated conversion to the aryl chloride, with a mixture of *ortho-* and *para-* chlorinated isomers obtained.[13] Switching the organic solvent to benzene resulted in benzylic chlorination, indicating the occurrence of a radical mechanism in non-polar solvents (Scheme 5.4).
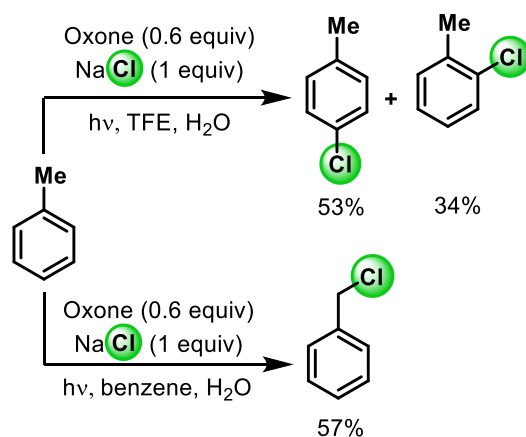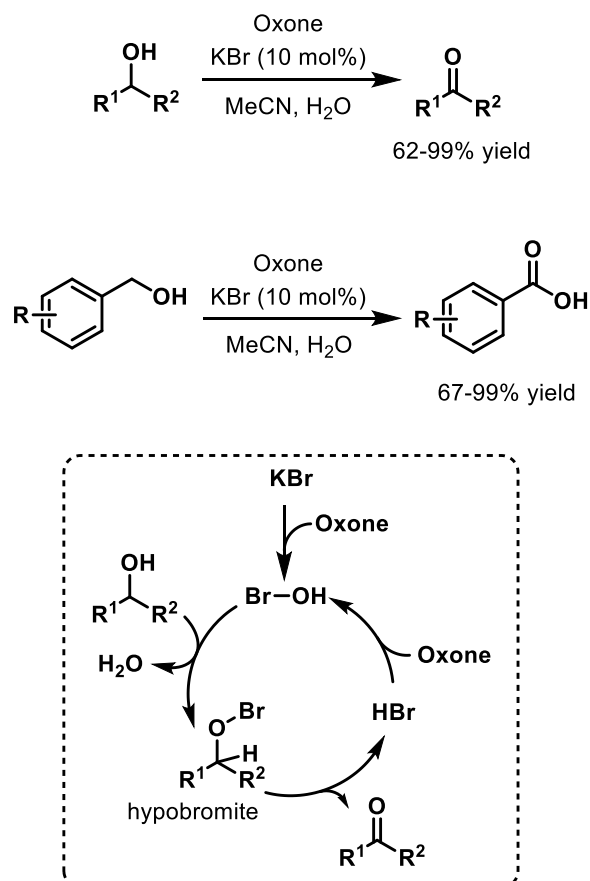

Scheme 5.4. Effect of solvent on regioselectivity of chlorination.[13]

Shown in Scheme 5.5 are some examples of the Oxone/MX halogenation scope.[5,6] Raju and co-workers reported the high-yielding *ortho*-selective chlorination and bromination of anilides and sulfonamides.[14] The same group demonstrated the regioselective halogenation of heterocycles, including indoles and amine-substituted pyridines.[14] The Cl_2 generated *in situ* from the Oxone/NaCl combination was reported to add to alkenes to yield *trans*-dichlorinated diastereomers,[15] while non-activated alkanes underwent visible light-induced chlorination in near-quantitative yields.[13]
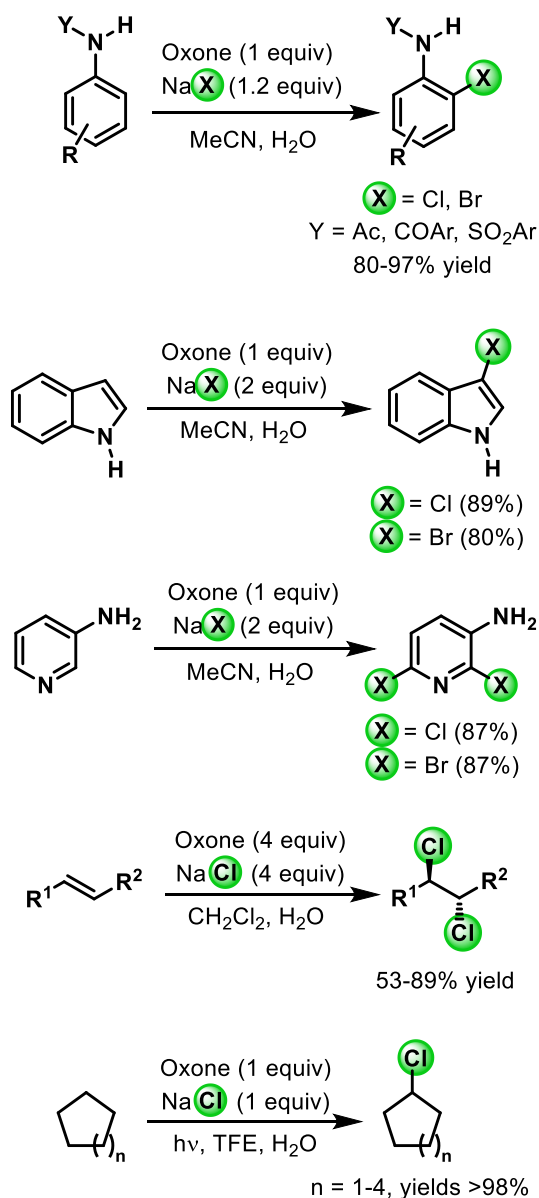
Scheme 5.5. Scope of Oxone/MX-mediated halogenations.[13–15]

Stoichiometric or greater equivalents of both Oxone and the halide are required to mediate the halogenations.[5,6,10–15] Using catalytic quantities of the halide with Oxone has mediated some interesting oxidative transformations.[6] The oxidation of secondary alcohols to the corresponding ketones was achieved using Oxone with 10 mol% of KBr, and primary benzylic alcohols were fully oxidized to the carboxylic acids (Scheme 5.6).[7] Given the low concentrations of KBr, the most likely oxidant according to Scheme 5.1 is hypobromous acid (HOBr). Reaction of HOBr with the alcohol forms an unstable hypobromite intermediate, which undergoes oxidation to the ketone *via* loss of HBr.[7] The latter is reoxidized to HOBr by a further mole of Oxone.[7]

160

Oxone

KBr (10 mol%)

MeCN, H$_2$O

62-99% yield

Oxone

KBr (10 mol%)

MeCN, H$_2$O

67-99% yield

KBr

Oxone

OH

R^1 R^2

Br−OH

H$_2$O

Oxone

O   Br

H

R^1 R^2

HBr

hypobromite

O

R^1 R^2

Scheme 5.6. Oxone/KBr-mediated oxidation of secondary and primary benzylic alcohols.[7]

Benzylic oxidation of alkylarenes to the corresponding ketones was catalyzed by the Oxone/KBr system (Scheme 5.7).[16] The latter reaction proceeded thermally using polar MeNO$_2$ as solvent with excellent yields obtained for substrates with both electron-donating and electron-withdrawing substituents. Switching to a CH$_2$Cl$_2$/H$_2$O mixture allowed the reaction to be done photochemically, although electron-withdrawing aryl substituents were necessary to prevent aromatic bromination. The reaction is postulated to proceed *via* oxidation of KBr to Br•, which abstracts a benzylic hydrogen atom from the substrate (Scheme 5.7). Further oxidation of the benzylic radical yielded the ketone.[16]
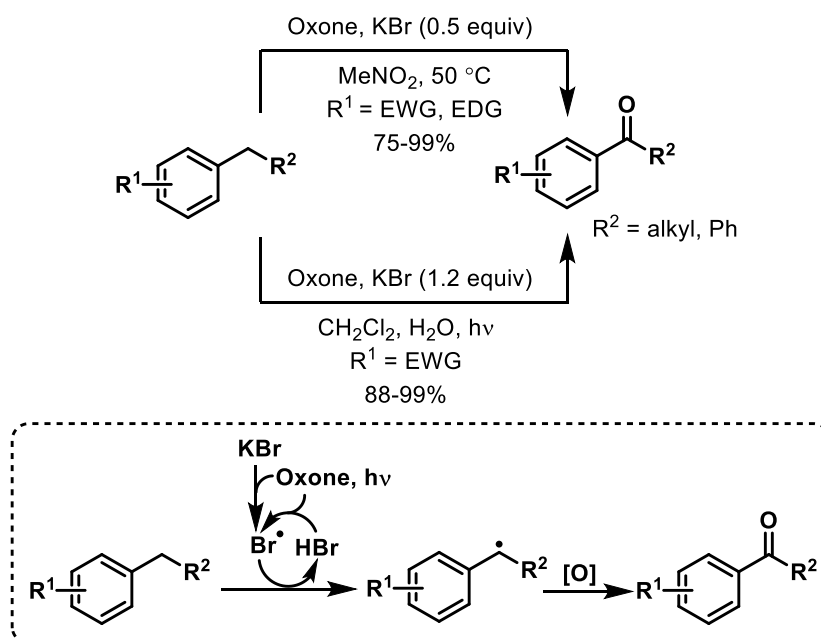
Scheme 5.7. Oxone/KBr-mediated oxidation of alkylarenes.[16]

Tong and co-workers comprehensively studied the reactivity of the Oxone/KX (cat.) combination towards indoles (Scheme 5.8).[17] Tetrahydro-β-carbolines (THCs) underwent oxidative rearrangement in the presence of 5 mol% KBr with Oxone to furnish spirooxindoles. Yields were generally better than the less benign traditional t-BuOCl-AcOH or NBS-AcOH methods. Oxone with KBr (10 mol%) oxidized C-3 substituted indoles to the 2-oxindoles.[17] Oxidative C-2 – C-3 cleavage (Witkop oxidation) occurred using Oxone and KCl (10 mol%) with a mixture of hexafluoroisopropanol (HFIP) and H_2O as solvents.[17] Furthermore, indoles bearing a pendant amine (tryptamine) or alcohol (tryptophol) underwent one-pot halogenation and oxidative cyclization using stoichiometric equivalents of Oxone and KCl or KBr (Scheme 5.8).[18]
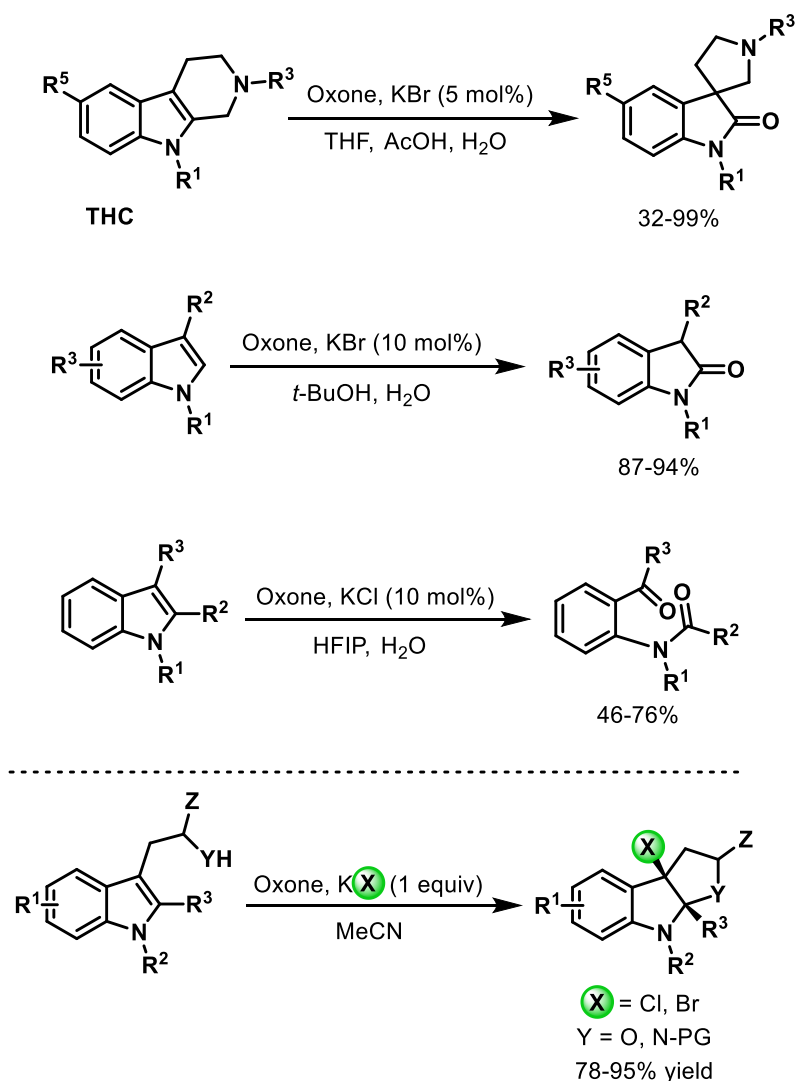
Scheme 5.8. Oxidative transformations of indoles with Oxone and KX.[17,18]

A further one-pot halogenation and oxidation was achieved by Ishihara and co-workers, who reacted naphthols with NaCl and Oxone resulting in dearomative chlorination to give regioselectively *o*-chlorinated naphthalenones (Scheme 5.9).[19] Phenols exhibited similar reactivity towards Oxone/NaCl with the regioselectivity of the chlorination depending on the steric demands of the substituents. Sterically encumbered *t*-Bu groups *ortho* to the alcohol resulted in *para*-chlorination, while the *para*-acylated derivative underwent *o*-chlorination to give cyclohexadienone derivatives.
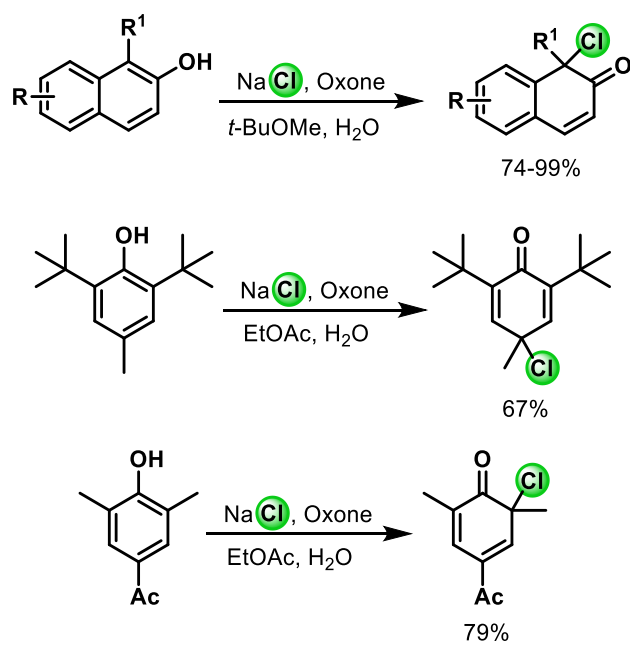
Scheme 5.9. Oxidative chlorination of naphthols and phenols.[19]

5.1.2. Trifluoromethylation of Quinones

Despite its absence from biological systems, fluorine has found extensive application in the agrochemical and pharmaceutical sectors.[20–22] Currently over half of all blockbuster drugs possess at least one fluorine atom, with 17 newly approved drugs in 2018 alone incorporating fluorine.[23] The inductively withdrawing trifluoromethyl group is present on a significant subset of these,[22] eliciting a good balance between increasing polar hydrophobicity (polarity and hydrophobicity), and therefore membrane permeability of drugs, and a low likelihood of accumulation of the drug in lipidic systems such as the nervous system.[20,24]

As nature has not evolved to manipulate fluorine, the development of synthetic methods to incorporate the trifluoromethyl group into organic molecules has been an area of intense research interest.[25] Traditionally, organofluorine chemistry was synonymous with hazards, with aromatic trifluoromethylation generally involving radical chlorination followed by fluorination with the extremely corrosive and toxic anhydrous HF or SbF_3.[26] Furthermore these methods were exclusive to aromatic systems.[24] The advent of trifluoromethylating reagents facilitated a larger scope for trifluoromethylation.[24,25] There are three different types trifluoromethylating reagent, nucleophilic (source of $^-CF_3$), electrophilic (source of $^+CF_3$), and radical (source of $^\bullet CF_3$).[24] Among them, the latter was the most extensively utilized due to the relative stability of the trifluoromethyl radical ($^\bullet CF_3$).[24,27]

The chemistry of $^\bullet CF_3$ is reflected in its geometry. ESR has shown the radical adopts a pyramidal, verging on tetrahedral conformation, with a deviation of 17.8° from planarity (Figure 5.1).[27,28] The pyrimidization is primarily a consequence of fluorine being a π-donor.[29] In contrast, carbon-centered radicals possessing an adjacent π-acceptor, such as the cyanomethyl radical are planar.[30,31]

pyrimidal trifluoromethyl radical
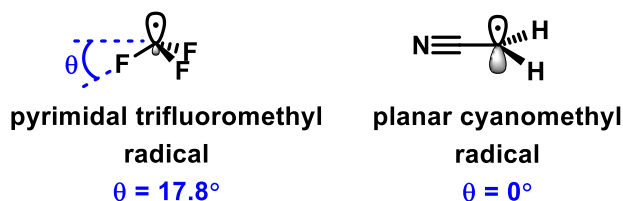θ = 17.8°

planar cyanomethyl radical
θ = 0°

Figure 5.1. Geometry of trifluoromethyl and cyanomethyl radicals.

These observations can be rationalized by resonance structures and frontier orbital diagrams (Figure 5.2). The mesomeric donation of a lone pair of electrons from a fluorine atom in $^\bullet CF_3$ into the C-F bond yields a carbon-centred radical anion canonical form with a lone electron in

an anti-bonding orbital,[30] which violates the octet rule. From a frontier orbital perspective, this is a SOMO-HOMO interaction resulting in the formation of a higher energy destabilized SOMO, which accounts for the nucleophilic character (Figure 5.2).[31] This orbital mixing increases the s-character of the SOMO leading to deviation from the planarity associated with π-type radicals.[32] In contrast, cyanomethyl is a π-type radical due to delocalization with the electron-withdrawing nitrile to give a keteniminyl radical canonical form. From a frontier orbital perspective, the SOMO decreases in energy as a result of SOMO-LUMO interaction, with favorable orbital overlap to elicit planar geometry and electrophilic character.[31,32] Additionally, it is thermodynamically favorable for fluorine's lone pairs in $^{\bullet}CF_3$ to exist in orbitals high in s-character (i.e.) close to the nucleus, so inducing pyrimidization.[33] The destabilizing SOMO-HOMO interaction in $^{\bullet}CF_3$ is counteracted somewhat by the reduction in SOMO energy due to orbital mixing between the SOMO and low-energy LUMO of the electronegative fluorine atoms.[33] However De Proft and co-workers computationally determined $^{\bullet}CF_3$ to be a "moderate nucleophile".[34]
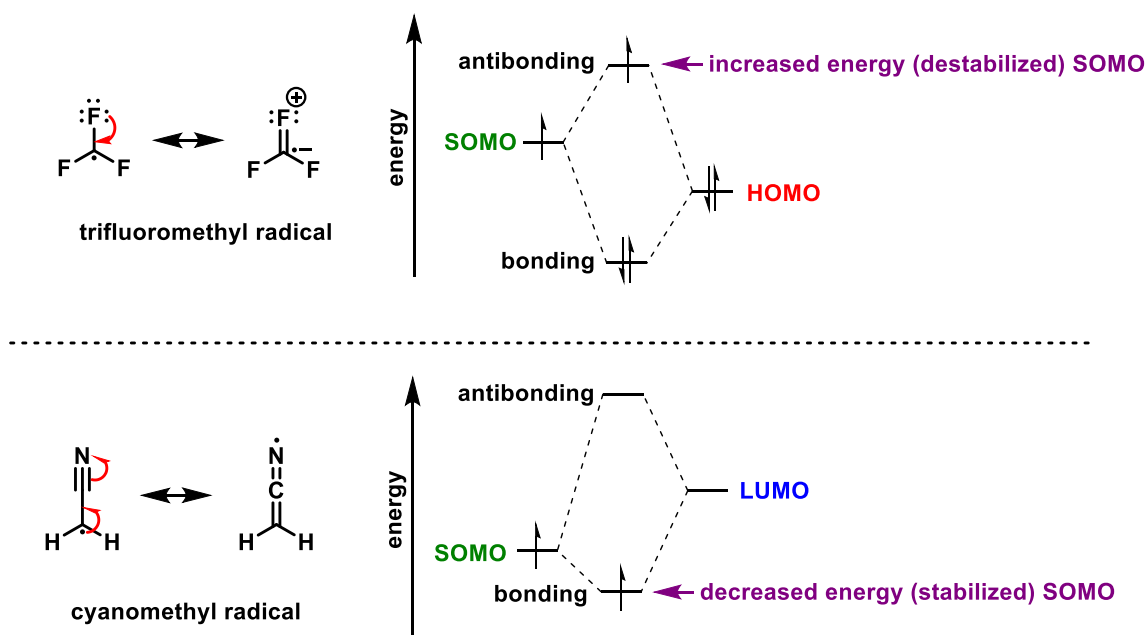

**Figure 5.2.** Resonance structures of trifluoromethyl and AIBN-derived radicals with associated MO diagrams.[32]

Introducing an electron-withdrawing group (such as CF_3) onto quinones gives increased $2e^-/2H^+$ reduction potential, facilitating more facile reduction to the hydroquinone.[35] Earlier syntheses of trifluoromethylated quinones utilized sodium trifluoroacetate (CF_3COONa) with copper(I) iodide for the trifluoromethylation of p-dimethoxyaryl iodides or bromides (Scheme

5.10).[36,37] The mechanism is reported to proceed *via* the decarboxylation of CF_3COONa followed by transmetalation with CuI to generate (trifluoromethyl)copper ($CuCF_3$), which undergoes oxidative insertion into the aryl halide.[38,39] Reductive elimination yields the trifluoromethylated product.[38,39] This method of trifluoromethylation thus required high temperatures, initial regioselective aryl halogenation, and late-stage CAN-mediated oxidative demethylation to yield the quinone.[36,37]
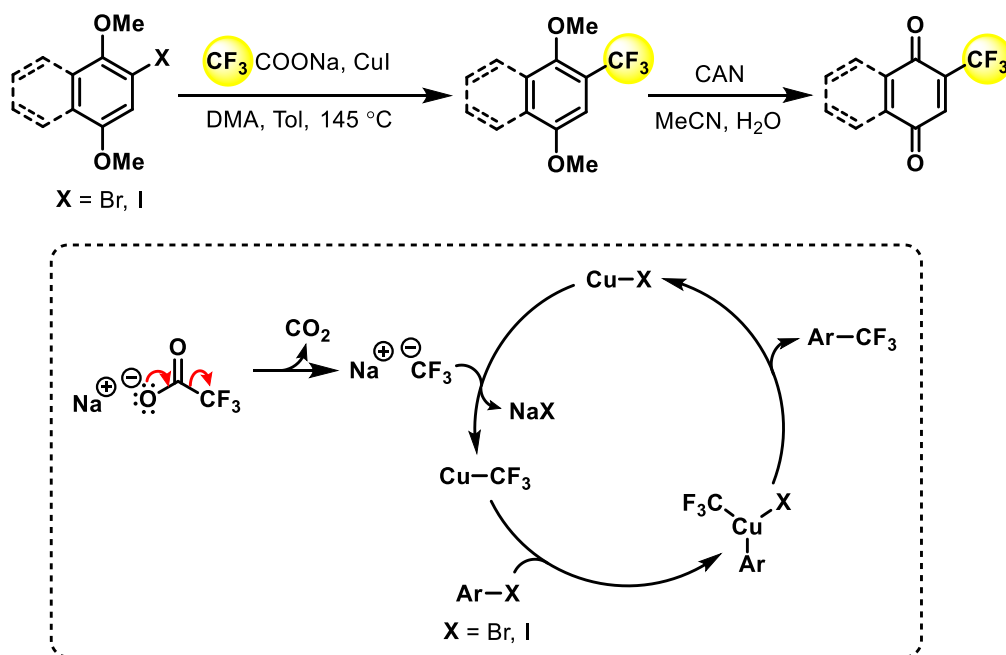

Scheme 5.10. Stepwise formation of trifluoromethylated (naphtho)quinones.[36,37]

In 2013 the first direct radical trifluoromethylation of quinones was reported. The groups of Wang[40] and Szabó[41] independently utilized the Togni reagent to trifluoromethylate (naphtho)quinones in moderate to excellent yields (Scheme 5.11). Although the Togni reagent is traditionally an electrophilic trifluoromethylating reagent,[25] adding a Cu(I) catalyst facilitates single-electron transfer (SET) reduction to yield a radical anion, which undergoes heterolytic cleavage prior to liberation of $^{\bullet}CF_3$ (Scheme 5.11).[40] Wang utilized catalytic CuI,[40] while Szabó opted for stoichiometric quantities of CuCN, with bis(pinacolato)diboron (B_2pin_2) reportedly improving both the rate and reproducibility of the trifluoromethylation.[41] The latter authors did not provide a mechanism, but speculated that B_2pin_2 acted as a radical activator.[41]
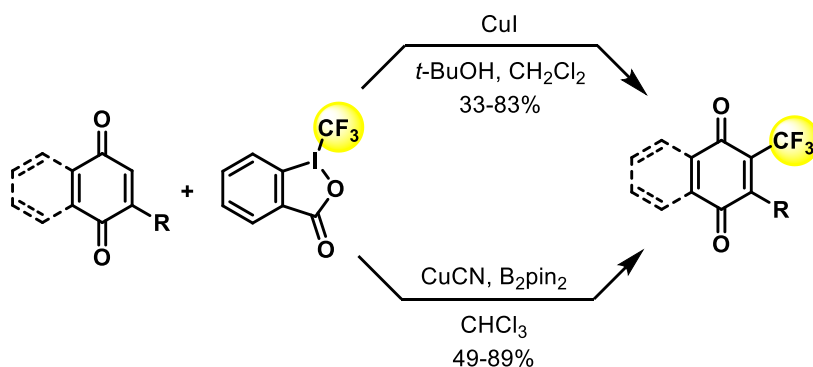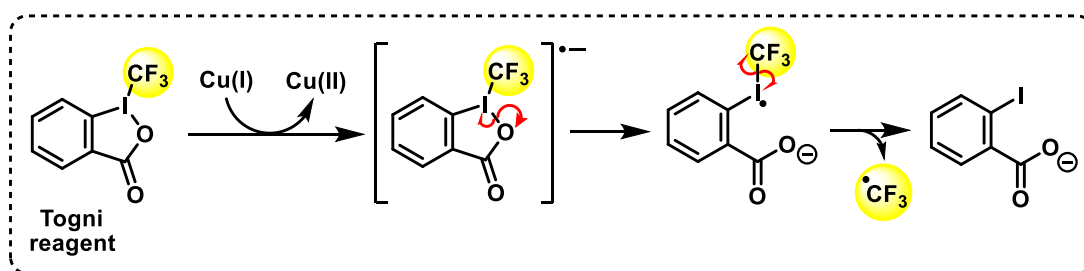
Scheme 5.11. Direct (naphtho)quinone trifluoromethylation.[40,41]

Despite the efficiency with which the Togni reagent mediates trifluoromethylation, its major downfall is its explosive nature.[42] In recent years, Baran has popularized the use of sodium triflinate with *t*-BuOOH and trace metal catalyst as a safer alternative for radical trifluoromethylation of both electron-rich and electron-deficient (hetero)arenes lacking pre-functionalization.[43] He termed sodium triflinate the "Langlois reagent," after the group that discovered its utility in the early 1990s to mediate radical trifluoromethylations.[24,44] Kielty and Aldabbagh elegantly demonstrated the regioselectivity of the Langlois reaction, as only quinone trifluoromethylation occurred on the dimethoxybenzimidazole-benzimidazolequinone **1** (Scheme 5.12).[45]
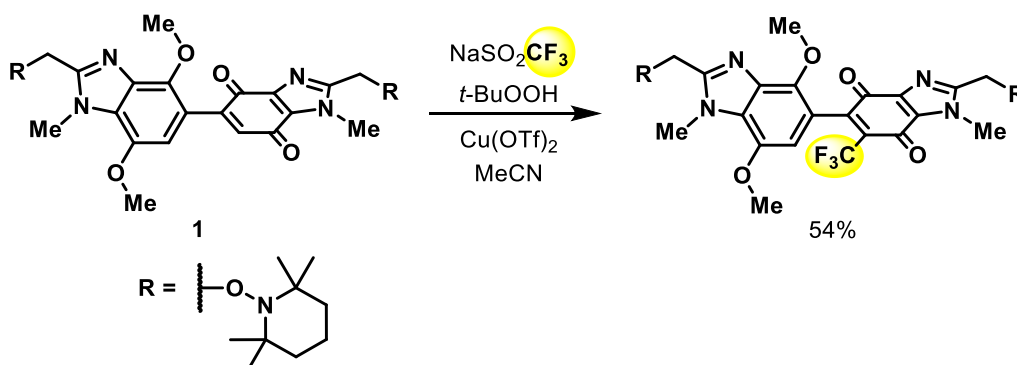

Scheme 5.12. Regioselective Langlois trifluoromethylation.[45]

Similar regioselectivity for radical trifluoromethylation was reported by Nevado and co-workers, whose cascade aryl migration, desulfonylation and C(sp2)−N bond formation was initiated by a radical trifluoromethylation using the Togni reagent with copper(I) oxide (Scheme 5.13).[46] The trifluoromethyl radical added selectively to the electron-deficient acrylamide, rather than the electron-rich aromatic ring.
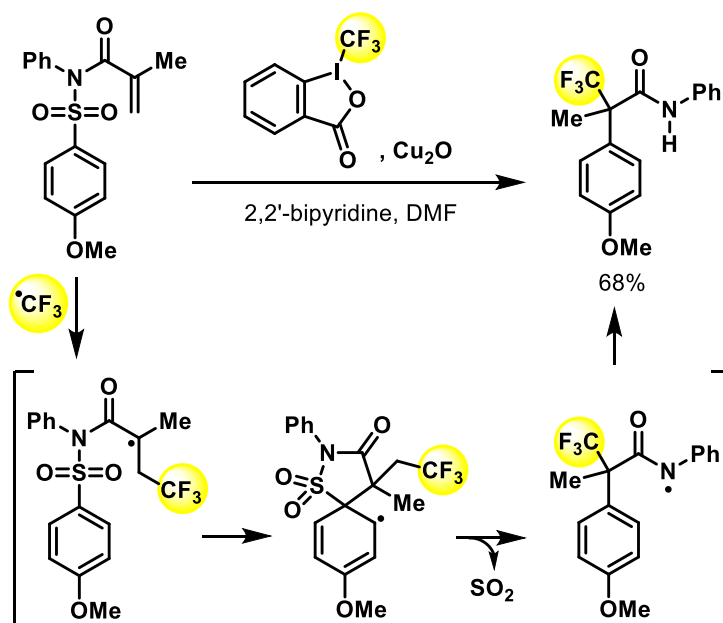

Scheme 5.13. Cascade transformation initiated by regioselective radical trifluoromethylation.

Since Baran's publication in 2012, other triflinate salts have mediated radical trifluoromethylation with equal or greater efficiency than $NaSO_2CF_3$, including $Zn(SO_2CF_3)_2$, which Yang and co-workers used to directly trifluoromethylate amine-substituted quinones in moderate to excellent yields (Scheme 5.14).[47] The addition of $FeSO_4 \cdot 7H_2O$ reportedly made the reaction more repeatable and stable,[47] with Baxter and Blackmond observing an acceleration in the rate of $Zn(SO_2CF_3)_2$-mediated trifluoromethylation of caffeine upon adding $FeSO_4$.[48] Although a comprehensive mechanistic rationale was not provided, the latter authors speculated that the Fe(II) reagent aided in the activation of $Zn(SO_2CF_3)_2$ to yield the $SO_2CF_3^\bullet$, and also reacted with partly decomposed, less reactive Zn species to yield a further mole of $SO_2CF_3^\bullet$ as the reaction progressed.[48]
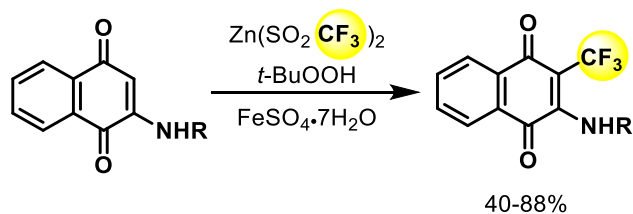
Scheme 5.14. Quinone trifluoromethylation with $Zn(SO_2CF_3)_2$.[47]

Initiation of Langlois trifluoromethylation involves SET oxidation of sodium triflinate by *t*-BuOOH, giving the unstable $CF_3SO_2^•$ which collapses to generate $^•CF_3$ *via* elimination of SO_2 (Scheme 5.15).[24,27] The *tert*-butoxyl radical generated in the initial SET oxidation oxidizes a further mole of $NaSO_2CF_3$, with concurrent formation of sodium *tert*-butoxide. Addition of $^•CF_3$ to the quinone substrate yields a carbon-centered radical, which is oxidized by the Cu(II) catalyst. Reoxidation of Cu(I) to Cu(II) is mediated by *t*-BuOOH. Deprotonation of the trifluoromethylated cyclohexenyl cation yields the quinone.
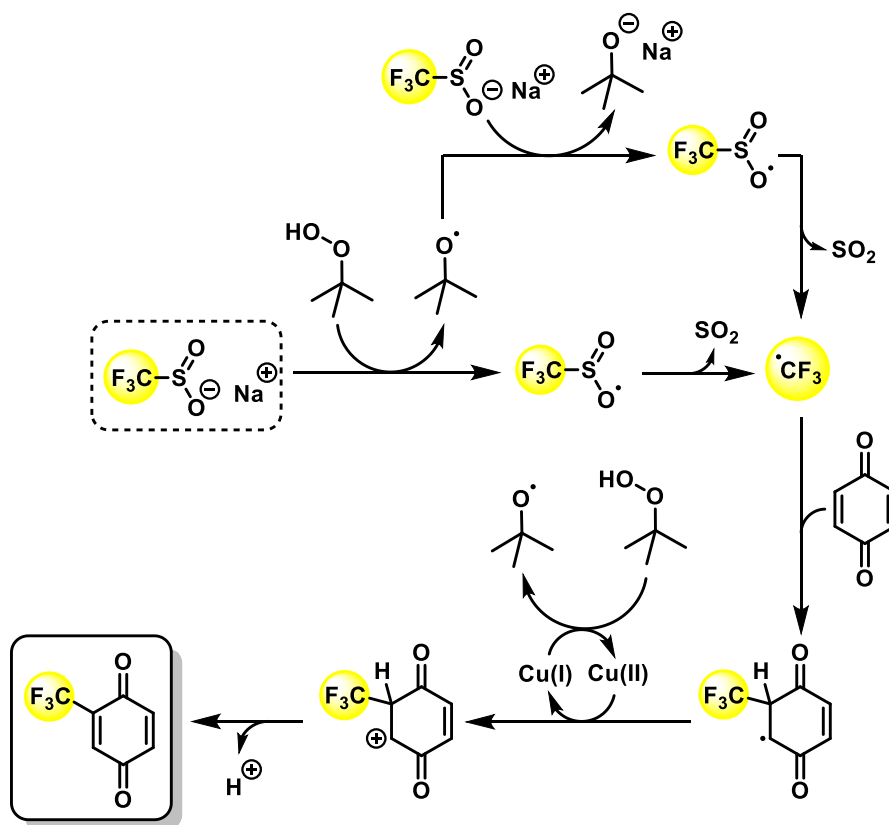
Scheme 5.15. Plausible mechanism for Langlois quinone trifluoromethylation.[24,27]

5.1.3. Bis-*p*-quinones

In Chapter 2, the antitumour activity of benzimidazolequinones was introduced. Dimeric quinones too, possess tumour cell cytotoxicity. Aziridinyl-substituted bis-naphthoquinone exhibited nanomolar cytotoxicity against myeloid leukemia cells,[49] while a derivative of the natural product gossypol was found to induce apoptosis of CT26 colon cancer cells with significantly reduced toxicity to the small intestine compared to the natural product on which it is based (Figure 5.3).[50] Non symmetrical bis-naphthoquinones impaired the growth of MDA-453 breast carcinoma cells with a mechanism of cytotoxicity reportedly related to the generation of reactive oxygen species (ROS).[51]
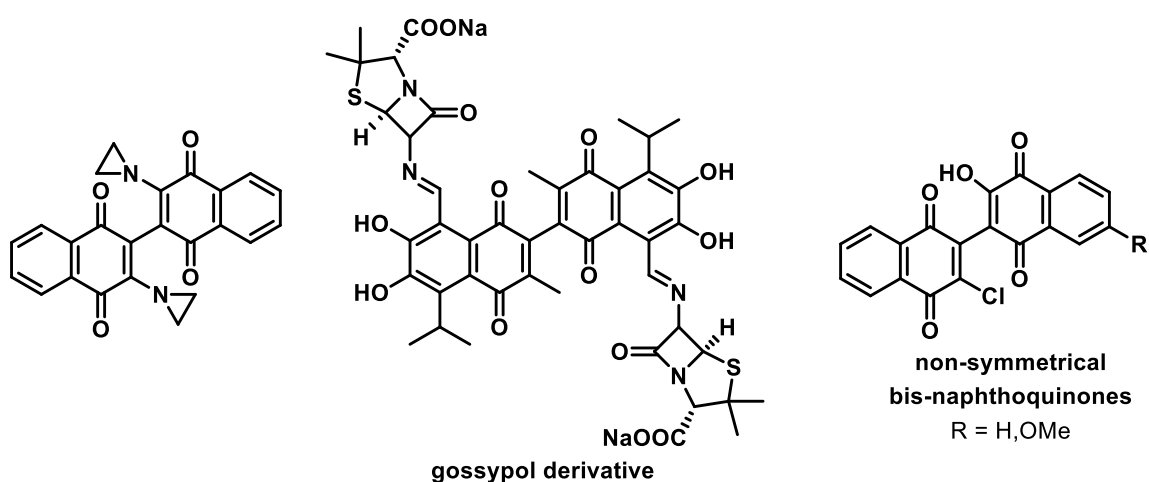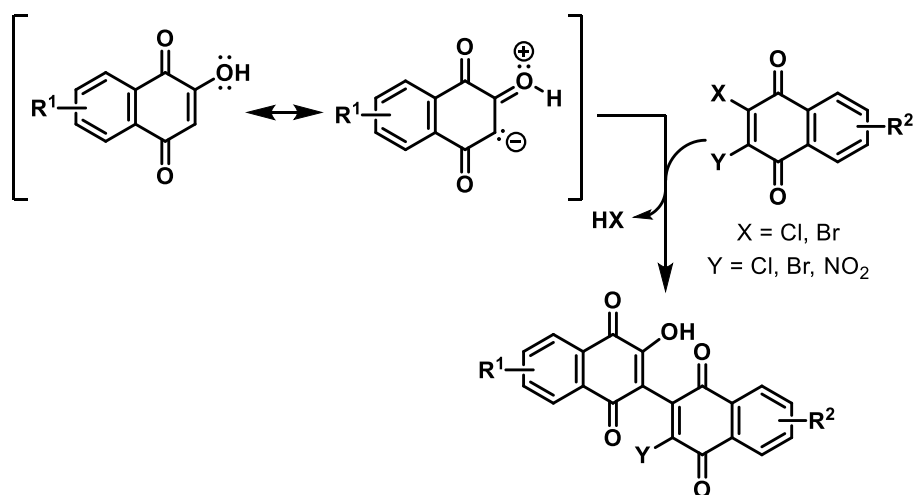

Figure 5.3. Cytotoxic bis-naphthoquinones.[49–51]

The key synthetic transformation in the preparation of dimeric naphthoquinones is the regioselective electrophilic substitution at the quinone, achieved through resonance activation by an adjacent hydroxy-substituent (Scheme 5.16).[52–54]

Scheme 5.16. Synthetic strategy towards bis-naphthoquinones.[52–54]

Dimeric heterocyclic quinones are rare, with the only naturally occurring example being the carbazole alkaloid bismurrayaquinone A, which was isolated from the roots of *Murraya koenigii* (the "curry tree") in the outer Himalayas (Figure 5.4).[55–57]
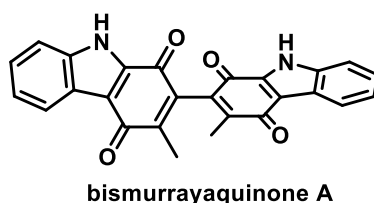

bismurrayaquinone A

Figure 5.4. Naturally occurring bis-heterocyclic quinone.

Synthetic examples of bis-heterocyclic quinones include bis-chloromethylbenzimidazolequinone **2**, which Vanelle and co-workers synthesized in 38% yield from CAN-oxidation of the 4,7-dimethoxybenzimidazole (Scheme 5.17). Dimer **2** exhibited a 30-fold increase in cytotoxicity against solid tumor cell lines compared to the monomeric benzimidazolequinones.[58]
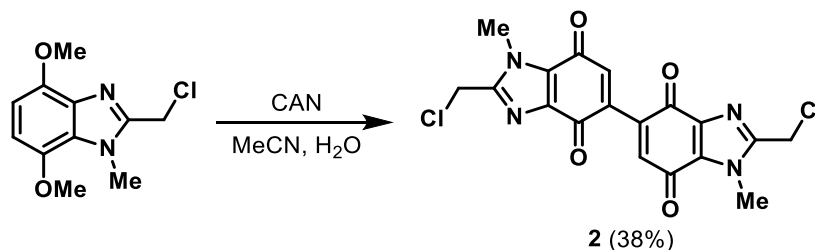
Scheme 5.17. Dimeric bis-*p*-benzimidazolequinone.

Most recently the CAN oxidation of 4,7-dimethoxybenzimidazole **3** was used to give visible-light active alkoxyamines of bis-*p*-benzimidazolequinones,[45] including **Bis-TEMPO-Vis** in 82% yield (Scheme 5.18). Dimethoxybenzimidazole-benzimidazolequinone **1** was obtained in high yield (86%) when using less CAN, and in contrast to **Bis-TEMPO-Vis**, **1** was stable to visible-light.
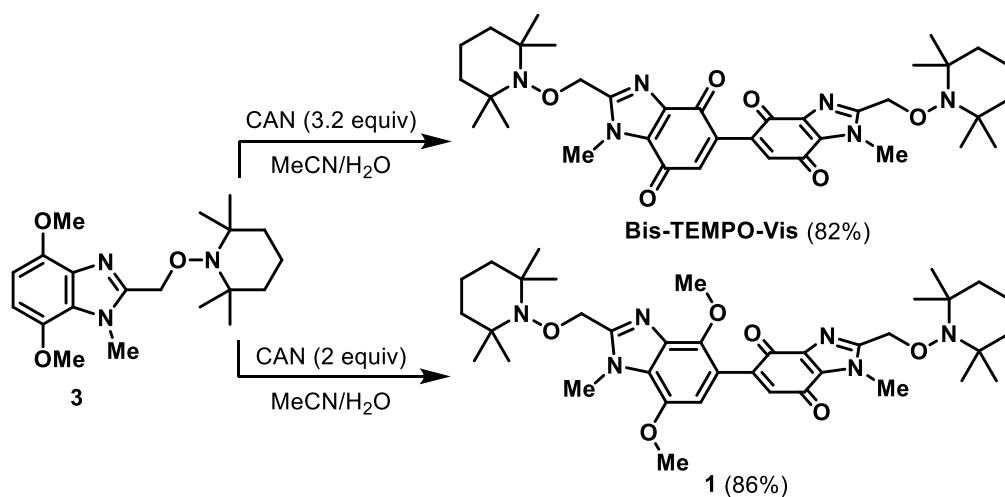

Scheme 5.18. Tunable CAN-mediated oxidative dimerization.[45]

5.2. Chapter Aims and Objectives

The Chapter objectives are outlined in Scheme 5.19.

- To use CAN to give alicyclic ring-fused *p*-dimethoxybenzimidazole-benzimidazolequinone dimers from *p*-dimethoxybenzimidazoles.

- To investigate the reactivity of electrophilic halogen generated from NaX with Oxone towards *p*-dimethoxybenzimidazole-benzimidazolequinone dimers.

- To investigate the potential of the Oxone/NaX combination to mediate one pot halogenation and oxidative demethylation for the synthesis of mono-halogenated bis-*p*-benzimidazolequinones.

- To establish the ambiphilic reactivity of the *p*-dimethoxybenzimidazole-benzimidazolequinone dimer by performing radical trifluoromethylation at the quinone followed by halogenation at the aromatic ring.
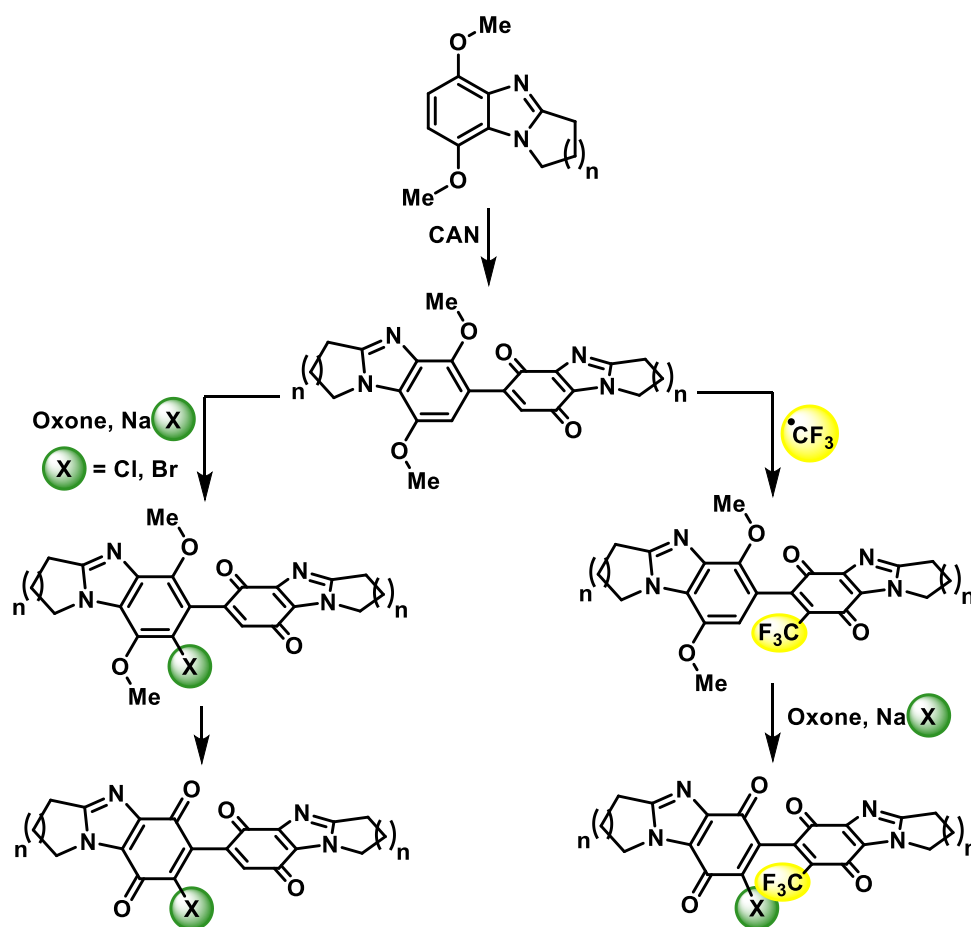

Scheme 5.19. The proposed transformations.

5.3. Results and Discussion

5.3.1. Dimerization of Alicyclic Ring-Fused Benzimidazoles

Pyrrolo-, pyrido- and azepino[1,2-*a*]-fused *p*-dimethoxybenzimidazoles were prepared using the H_2O_2/HI oxidative cyclization conditions described in Chapter 2.[59] Addition of an aqueous CAN (2 equiv) solution to 5,8-dimethoxy-2,3-dihydro-1*H*-pyrrolo[1,2-*a*]benzimidazole (**4a**) in MeCN at 0 °C gave the desired 5',8'-dimethoxy-2,2',3,3'-tetrahydro-1*H*,1'*H*-[6,6'-bipyrrolo[1,2-*a*]benzimidazole]-5,8-dione (**5a**) and mono-quinone **6** in 73 and 19% respective yields (Scheme 5.20).
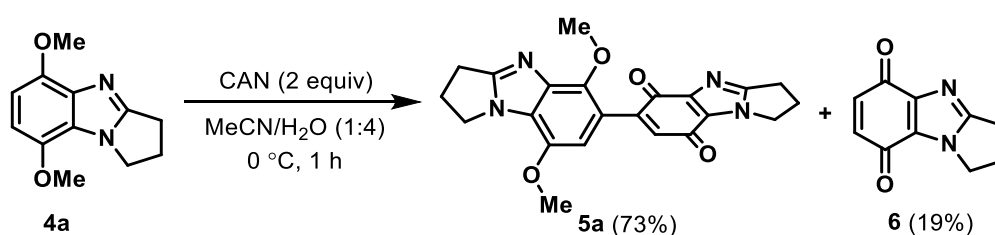
**Scheme 5.20.** Initially attempted CAN-mediated oxidative dimerization.

A plausible mechanism for the conversion of **4a** to **5a** and **6** is shown in Scheme 5.21. Isotopic labelling studies have shown that the CAN-mediated quinone formation occurs *via* oxidative demethylation by the incorporation of water, rather than by demethylation to the hydroquinone and subsequent oxidation.[60] Formation of the mono-quinone is shown to proceed *via* nucleophilic addition of water on the initially-formed radical cation (Scheme 5.21). Dimerization is known to occur before oxidative demethylation.[61] Although CAN is used 4 times in the mechanism for formation of *p*-dimethoxybenzimidazole-*p*-benzimidazolequinone dimer, the reaction requires a stoichiometric ratio of CAN:benzimidazole of 2:1 given the dimerization process. It follows that one equivalent of CAN is used for oxidative dimerization and one equivalent of CAN is necessary for oxidative demethylation of the dimerized *p*-dimethoxybenzimidazole. The regioselectivity of the dimerization is dictated by the initial oxidation step, which is most likely to occur at the more electron-rich methoxy group furthest away from the more inductively-electron withdrawing (basic) imidazole nitrogen atom.[62]
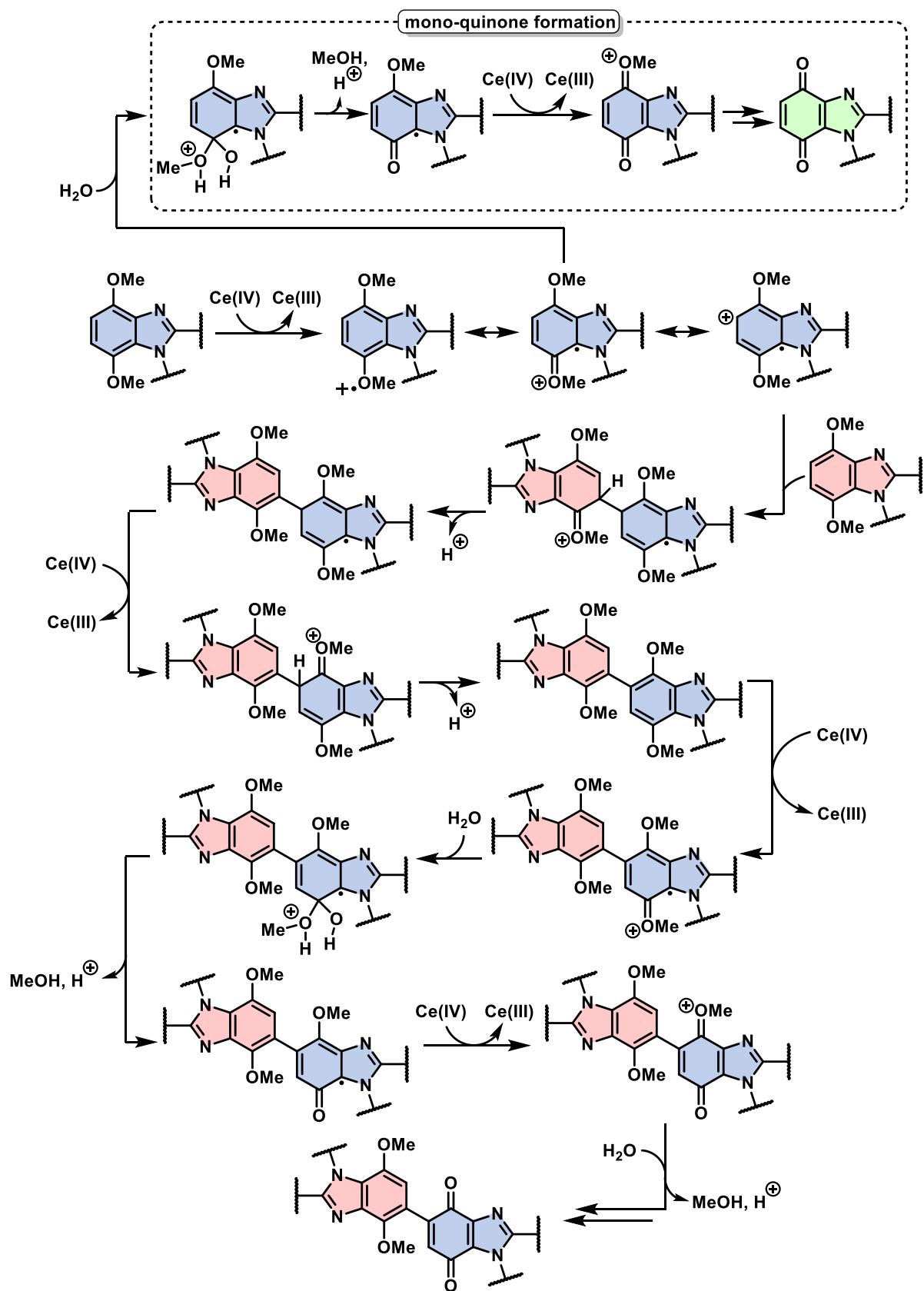
Scheme 5.21. Mechanism of CAN-mediated oxidative dimerization and demethylation.

We proposed that switching the organic solvent from MeCN to hexafluoroisopropanol (HFIP) would favor the oxidative dimerization of benzimidazole over mono-quinone formation:

1. According to the mechanism depicted in Scheme 5.21, dimerization proceeds *via* radical cationic intermediates.[63] HFIP and other fluorinated alcohols are highly polar solvents with low nucleophilicity, and are known to stabilize radical cationic intermediates,[64,65] a characteristic exploited to improve the efficiency of oxidative coupling reactions.[66] A drastic example was the iron-catalyzed coupling of naphthol, which proceeds *via* a radical cation intermediate (Scheme 5.22).[67] In DCE, the maximum conversion to the coupled BINOL product was 9% after 24 h.[67] In stark contrast, the starting naphthol was completely consumed within 1 h when HFIP was used as the reaction solvent.[67] Experimental evidence for the rate enhancement was obtained *via* cyclic voltammetry, which determined the oxidation potential of the naphthol to be lower in HFIP than in other organic solvents, supporting the argument that HFIP stabilizes the intermediate radical cation.[67]


solvent = **DCE**: 9% conversion (after 24 h)
solvent = **HFIP**: 100% conversion (after 1 h)
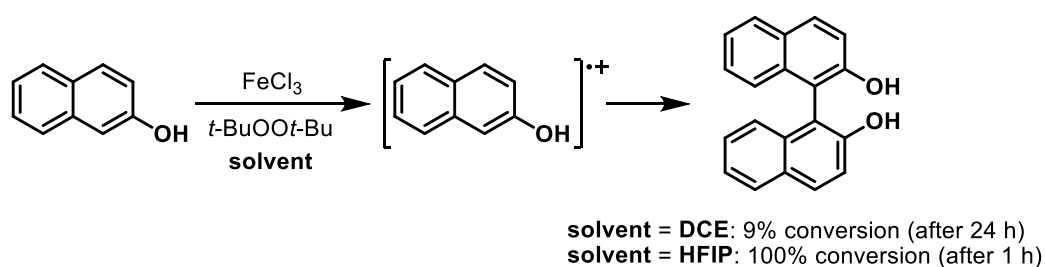
Scheme 5.22. Effect of HFIP on the oxidative coupling of naphthol.[67]

Stabilizing the radical cation intermediate in the CAN reaction would increase the likelihood of dimerization over the reaction with water to give the mono-quinone.

2. Although HFIP macroscopically appears to be fully miscible with H_2O, analysis of HFIP/H_2O mixtures by NMR, FTIR and small-angle X-ray scattering (SAXS) indicated the formation of HFIP microheterogeneous clusters in aqueous solutions.[68,69] The microheterogeneity was rationalized by the tendency of hydrophobic CF_3 groups to cluster to minimize contact with water, alongside the formation of a network of hydrogen bonds between HFIP molecules.[68,69] These HFIP clusters would likely localize a high concentration of benzimidazole in the "fluorous phase" of the CAN dimerization, and reduce the likelihood of reaction with H_2O. A similar effect facilitated Adams and Du Bois' C-H hydroxylation catalyzed by oxaziridine **A** (Scheme 5.23).[70] Oxone was used as terminal oxidant, which necessitated the use of H_2O. But water was found to decompose

the oxaziridine catalyst. Decomposition did not occur when HFIP was added, due to the localization of **A** in the fluorous phase, which effectively shielded the H_2O.[70] Furthermore the overall rate of reaction was accelerated as a result of concentrating the substrate and oxidant in the same phase.[70]
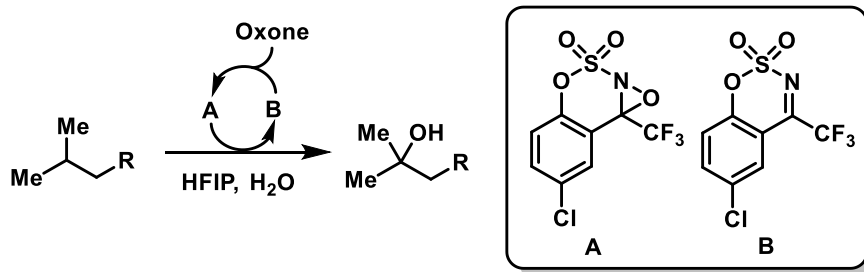
**Scheme 5.23.** Hydroxylation enabled by HFIP.[70]

Switching from MeCN to HFIP in the reaction of benzimidazole **4a** with CAN gave dimer **5a** in an improved yield of 88% without monoquinone formation (Scheme 5.24). The same conditions furnished piperido- and azepino[1,2-*a*]-fused dimers **5b** and **5c** as exclusive products in respective yields of 87% and 83% yield. To the best of our knowledge, this is the first reported enhancement for CAN-mediated oxidative reactions by use of fluorinated solvents.

4a: n = 1
4b: n = 2
4c: n = 3

5a (88%)
5b (87%)
5c (83%)
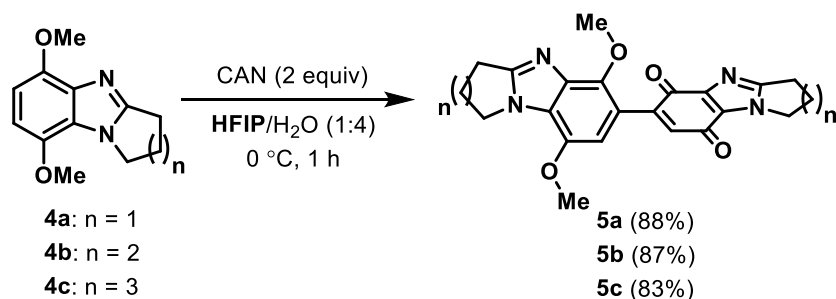
Scheme 5.24. Chemoselective CAN-mediated oxidative dimerization in HFIP/H_2O.

5.3.2. Regioselective Electrophilic Halogenation and Oxidative Demethylation

Resonance structures of the dimers suggest methoxy-group activation is possible at both available substitution positions to give canonical forms **A** and **B** (Scheme 5.25).
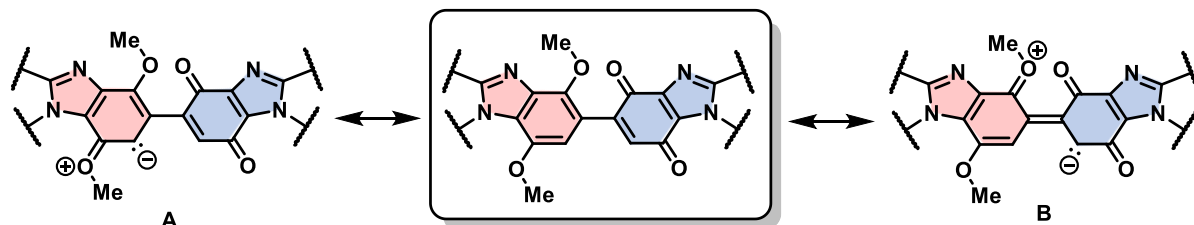
Scheme 5.25. Resonance structures of dimers.

Kielty and Aldabbagh's X-ray crystal structure of bis(chloromethyl)-substituted dimer **7** indicated that the aromatic and quinone rings adopt an out-of-plane conformation with respect to each other, possessing a dihedral angle (θ) of 60.7° (Figure 5.5).[71] The out-of-plane conformation prevents effective orbital overlap over both rings ruling out canonical form **B** (Scheme 5.25). Furthermore, cyclic voltammetry deduced localization of the HOMO of dimer **1** at the *p*-dimethoxybenzimidazole, while the LUMO was localized at the quinone, and time-dependent density functional theory (TD-DFT) showed limited orbital overlap.[45] Electrophilic halogenation of ring-fused dimers **5a**-**5c** would thus be expected to occur regioselectively at the *p*-dimethoxybenzimidazole-CH.
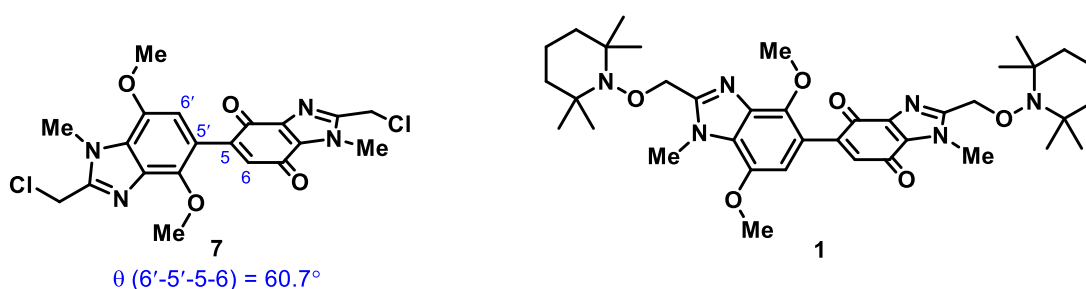

**Figure 5.5.** Dimethoxybenzimidazole-benzimidazolequinone dimers.[45,71]

In chapter 2, H_2O_2 (20 equiv) with HCl (1 equiv) in EtOAc mediated the regioselective chlorination of 3,6-dimethoxy-2-(morpholin-4-yl)aniline in 76% yield (Scheme 5.26),[59] and initially these conditions were evaluated for chlorination of pyrrolo-fused dimer **5a**. Given the lack of solubility of **5a** in EtOAc, the solvent for the reaction was changed to MeCN. Reaction monitoring by TLC indicated complete consumption of dimer **5a**, after heating at reflux for 1 h. Purification by column chromatography led to the isolation of the regioselectively chlorinated adduct, 7'-chloro-5',8'-dimethoxy-2,2',3,3'-tetrahydro-1*H*,1'*H*-[6,6'-bipyrrolo[1,2-

a]benzimidazole]-5,8-dione (**8a**) in 21% yield, accompanied by intractable baseline degradation products, which indicated a requirement for milder oxidizing conditions (Scheme 5.26 and entry 1, Table 5.1).
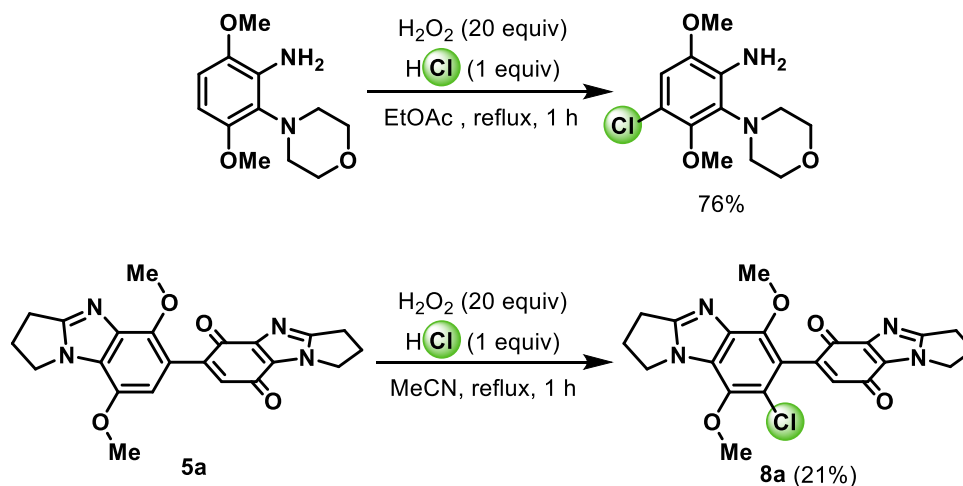
Scheme 5.26. H_2O_2/HCl-mediated chlorination.

This led us to investigate the room-temperature Oxone/NaCl reaction. Reacting dimer **5a** with NaCl (1 equiv) and Oxone (0.6 equiv ≡ 1.2 equiv of the active oxidant, $KHSO_5$) in 5% aqueous MeCN gave after 5 h, chlorinated dimer **8a** in 39% yield alongside 52% unreacted **5a** (entry 2, Table 5.1). The addition of water was necessary in order to solubilize the Oxone. Polyfluorinated alcohols have been shown to improve the yield of Oxone/NaCl-mediated aliphatic and aromatic chlorination,[13] and are known to accelerate aromatic chlorination in systems that generate *in situ* Cl_2.[72] By changing the reaction solvent from MeCN to HFIP, an improved yield of 51% of dimer **8a** was isolated after 5 h with a 43% yield of unreacted **5a** remaining (entry 3, Table 5.1). Increasing the amount of NaCl to 2 equiv led to a complete consumption of **5a** and a yield of 79% for chlorinated dimer **8a** due to the greater amount of *in situ* generated Cl_2 (entry 4, Table 5.1). Separation of 12% of accompanying bis-*p*-quinone chlorinated dimer **9a** was possible by column chromatography using gradient elution due the differences in R_f between chlorinated dimers **8a** (R_f = 0.41; 19:1 CH_2Cl_2/MeOH) and **9a** (R_f = 0.35; 19:1 CH_2Cl_2/MeOH).

Table 5.1. Optimization[a]
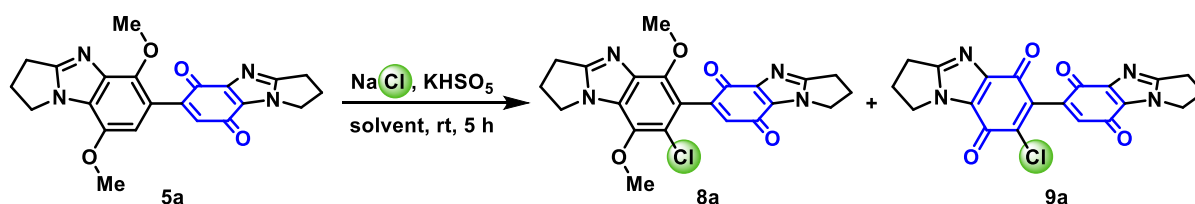
Entry	Solvent	NaCl (mmol)	KHSO₅[b] (mmol)	Yield of 8a (%)[c]	Yield of 9a (%)[c]
1	MeCN	–[d]	–[d]	21	–[e]
2	MeCN(aq)	0.20	0.24	39 (52)	–
3	HFIP(aq)	0.20	0.24	51 (43)	–
4	**HFIP(aq)**	**0.40**	**0.24**	**79**	12
5	HFIP(aq)[f]	0.40	0.80	36	52
6	HFIP(aq)[f]	0.80	0.80	15	71
7	**HFIP(aq)[g]**	**0.80**	**0.80**	–	**89**

[a]Conditions: Dimer (0.20 mmol), MeCN or HFIP (2 mL), H₂O (0.1 mL). [b]Used as Oxone (2KHSO₅·KHSO₄·K₂SO₄). [c]Isolated yields after column chromatography with gradient elution. Values in parentheses refer to recovered **5a**. [d]H₂O₂ (4 mmol), HCl (0.20 mmol), MeCN (2 mL), reflux. [e]Intractable mixture. [f]16 h. [g]HFIP (2 mL), H₂O (0.2 mL), 9 h.

The one-pot chlorination and oxidative demethylation to give **9a** is likely to be mediated by Cl₂, and the mechanism would be analogous to that proposed by Sweeney and Aldabbagh for the synthesis of halogenated ring-fused benzimidazolequinones.[4] Increasing the amount of Oxone and NaCl relative to the substrate would lead to a greater probability of HOCl reacting with Cl⁻, rather than HOCl reacting with the substrate to drive the equilibrium towards Cl₂ formation (reaction 2, Scheme 5.1). It follows that increasing the amount of KHSO₅ (4 equiv) with NaCl (2 equiv), and using a longer reaction time of 16 h (entry 5, Table 5.1), led to an improved yield of 52% bis-*p*-quinone **9a** with **8a** now a minor product at 36% yield. The longer reaction time was required to facilitate the oxidative demethylation of **8a** to give **9a**. Cl₂ generation can be further increased with additional NaCl, and using 4 equiv of both NaCl and KHSO₅ further elevated the yield of **9a** relative to **8a** to 71 and 15% yield respectively (entry

6, Table 5.1). Bis-*p*-quinone **9a** was isolated as the sole product in an optimal yield of 89% after 9 h using NaCl (4 equiv) with KHSO$_5$ (4 equiv) by increasing the amount of water in the solvent system from 5% to 10% relative to HFIP (entry 7, Table 5.1). This is in line with previous isotopic labelling studies, which demonstrated that Cl$_2$ (and Br$_2$) mediated oxidative demethylations proceeded *via* the incorporation of water.[4] A transition was visible during the reaction, from the highly conjugated maroon-coloured *p*-dimethoxybenzimidazole-*p*-benzimidazolequinone dimer **5a**, *via* the orange halogenated dimer **8a**, to the yellow bis-*p*-quinone **9a**. This reaction represents the first reported oxidative demethylation of *p*-dimethoxyarenes to quinones using benign Oxone-based systems.

In order to favour formation of the intermediate chlorinated *p*-dimethoxybenzimidazole-*p*-benzimidazolequinone dimers **8b** and **8c**, entry 4, Table 5.1 conditions were applied to the ring-expanded alicyclic [1,2-*a*] ring-fused dimers **5b** and **5c** (Scheme 5.27). 8'-Chloro-6',9'-dimethoxy-1,1',2,2',3,3',4,4'-octahydro[7,7'-bipyrido[1,2-*a*]benzimidazole]-6,9-dione (**8b**) (R_f = 0.39; 19:1 CH$_2$Cl$_2$/MeOH) and 2'-chloro-1',4'-dimethoxy-7,7',8,8',9,9',10,10'-octahydro-6*H*,6'*H*-[3,3'-biazepino[1,2-*a*]benzimidazole]-1,4-dione (**8c**) (R_f = 0.43; 19:1 CH$_2$Cl$_2$/MeOH) were separated in respective yields of 75 and 72% using column chromatography from inseparable mixtures (due to their identical R_f values) of **5b** and **9b** (R_f = 0.34; 19:1 CH$_2$Cl$_2$/MeOH), and **5c** and **9c** (R_f = 0.40; 19:1 CH$_2$Cl$_2$/MeOH) respectively.

NaCl was replaced with NaBr in an attempt to facilitate regioselective bromination of **5a-5c** using the same optimized conditions (entry 4, Table 5.1), which favored chlorination over quinone formation (Scheme 5.27). There was no observed significant difference in bromination compared to chlorination, with complete consumption of **5a** occurring, and the difference in R_f values allowing separation of 7'-bromo-5',8'-dimethoxy-2,2',3,3'-tetrahydro-1*H*,1'*H*-[6,6'-bipyrrolo[1,2-*a*]benzimidazole]-5,8-dione (**10a**) (R_f = 0.38; 19:1 CH$_2$Cl$_2$/MeOH) and 7-bromo-2,2',3,3'-tetrahydro-1*H*,1'*H*-[6,6'-bipyrrolo[1,2-*a*]benzimidazole]-5,5',8,8'-tetrone (**11a**) (R_f = 0.33; 19:1 CH$_2$Cl$_2$/MeOH) in respective yields of 76% and 10%. Under the same conditions the pyrido- and azepino[1,2-*a*]-fused dimers **5b** and **5c** gave 8'-bromo-6',9'-dimethoxy-1,1',2,2',3,3',4,4'-octahydro[7,7'-bipyrido[1,2-*a*]benzimidazole]-6,9-dione (**10b**), and 2'-bromo-1',4'-dimethoxy-7,7',8,8',9,9',10,10'-octahydro-6*H*,6'*H*-[3,3'-biazepino[1,2-*a*]benzimidazole]-1,4-dione (**10c**) in respective yields of 68% and 71%. Similar to the chlorination reactions, **5b** and **5c** were less reactive towards bromination than the pyrrolo[1,2-*a*]–fused dimer **5a** with unreacted material detected after column chromatography. In this case, the marginally lower yields were due to isolation of desired compounds **10b** (R_f = 0.37; 19:1

CH$_2$Cl$_2$/MeOH) and **10c** (R_f = 0.42; 19:1 CH$_2$Cl$_2$/MeOH) from the inseparable mixture of **5b** and **11b** (R_f = 0.33-0.34; 19:1 CH$_2$Cl$_2$/MeOH), and **5c** and **11c** (R_f = 0.39-0.40; 19:1 CH$_2$Cl$_2$/MeOH).

The optimized conditions necessary for one-pot chlorination and quinone formation (entry 7, Table 5.1) were applied to **5b** and **5c** (Scheme 5.27). 8-Chloro-1,1',2,2',3,3',4,4'-octahydro[7,7'-bipyrido[1,2-*a*]benzimidazole]-6,6',9,9'-tetrone (**9b**) was obtained as the sole product in 88% yield, while 2-chloro-7,7',8,8',9,9',10,10'-octahydro-6*H*,6'*H*-[3,3'-biazepino[1,2-*a*]benzimidazole]-1,1',4,4'-tetrone (**9c**) was isolated in a lower yield of 74% due to a separable amount of intermediate **8c** in 12% yield. Replacing NaCl with NaBr allowed the transformation of **5a**, **5b** and **5c** to 7-bromo-2,2',3,3'-tetrahydro-1*H*,1'*H*-[6,6'-bipyrrolo[1,2-*a*]benzimidazole]-5,5',8,8'-tetrone (**11a**), 8-bromo-1,1',2,2',3,3',4,4'-octahydro[7,7'-bipyrido[1,2-*a*]benzimidazole]-6,6',9,9'-tetrone (**11b**) and 2-bromo-7,7',8,8',9,9',10,10'-octahydro-6*H*,6'*H*-[3,3'-biazepino[1,2-*a*]benzimidazole]-1,1',4,4'-tetrone (**11c**) in yields of 75%, 72% and 69% respectively. The formation of brominated bis-*p*-quinones **11a**-**11c** was accompanied by minor, but significant amounts of the intermediate dimers **10a-10c** in yields of 13%-22%. Presumably, the yields for the one-pot bromination and oxidative demethylation were inferior due to the greater oxidizing ability of Cl$_2$ compared with Br$_2$.[73] The R_f differences between the bis-*p*-quinones **11a-11c** and the brominated *p*-dimethoxybenzimidazole-*p*-benzimidazolequinone intermediates **10a-10c** allowing facile separation by column chromatography. The presence of a red-brown vapor in the Oxone/NaBr-mediated oxidative brominations is evidence for the *in situ* formation of Br$_2$ (Figure 5.6).
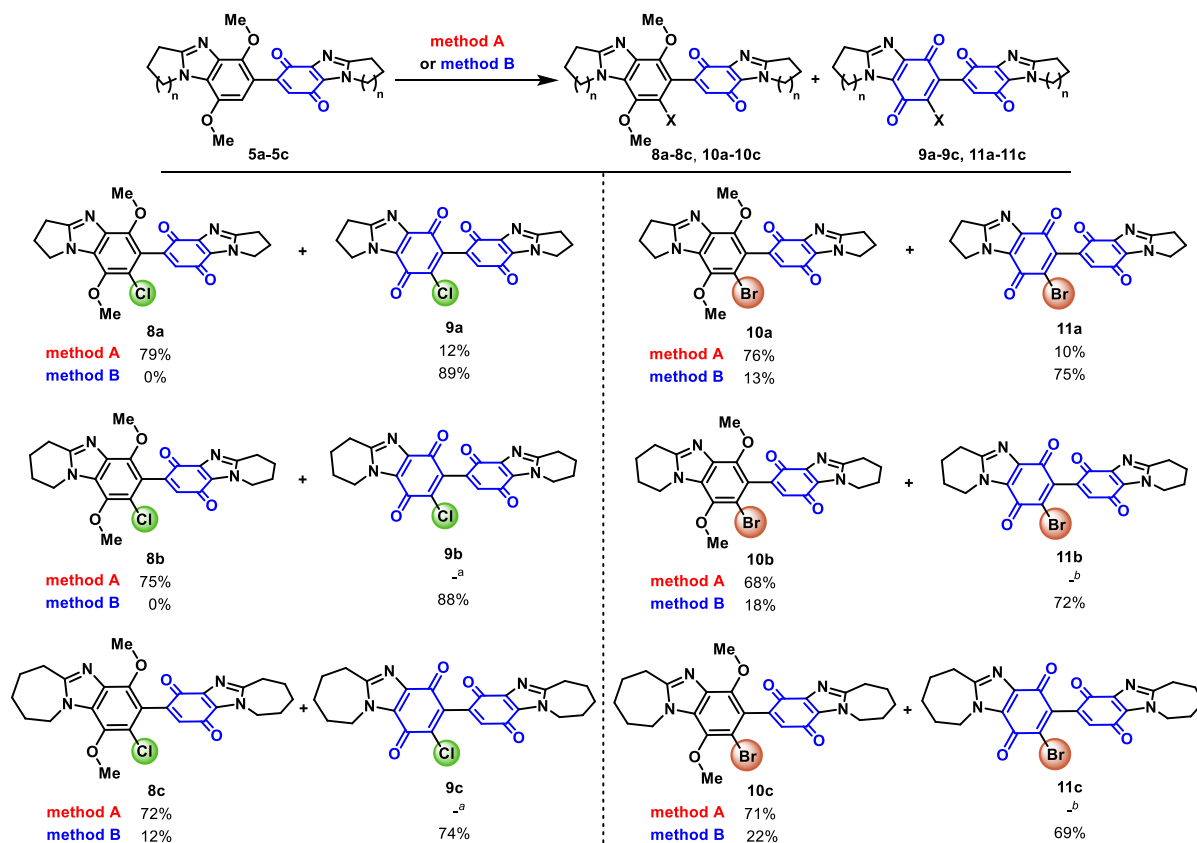
Scheme 5.27. Reaction scope with isolated yields given after column chromatography using gradient elution. **Method A:** Entry 4, Table 5.1 conditions. **Method B:** Entry 7, Table 5.1 conditions. [a]Inseparable mixtures (~10% yield) of unreacted **5b** and **5c** and bis-*p*-quinones **9b** and **9c** respectively. [b]Inseparable mixtures (~15% yield) of unreacted **5b** and **5c** and bis-*p*-quinones **11b** and **11c**.
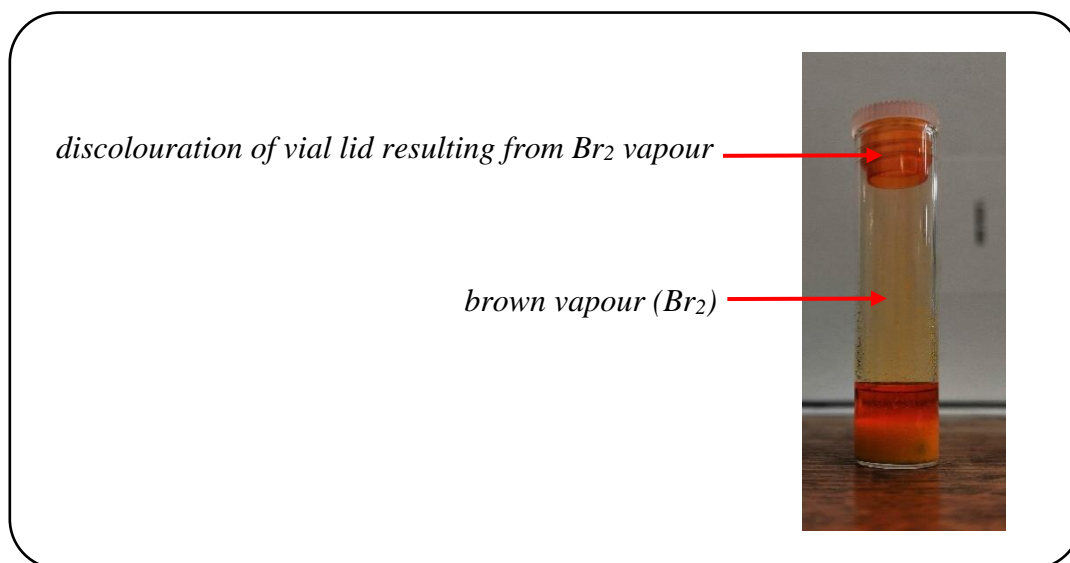
Figure 5.6. Evidence for *in situ* Br$_2$ evolution from a sample of the reaction of dimer **5a** with NaBr (4 equiv) and KHSO$_5$ (4 equiv) at rt after 2 h.

In all cases, the expected fragmentation patterns were observed in the high-resolution mass spectra (HRMS) confirming the incorporation of the halogens. For example, in the HRMS spectrum [M+H$^+$] peaks of chloride dimer **8a** are at *m/z* = 439 (100%) and *m/z* = 441 (36%), a ratio which fits the inclusion of one chlorine atom in the molecule with isotopic abundance of ^{35}Cl and ^{37}Cl of 3:1 (Figure 5.7). Peaks at *m/z* = 440 (25%) and 442 (9%) in both the theoretical and observed spectra are primarily due to contribution of the ^{13}C isotope, whose natural abundance is 1.1% (thus 22 carbon atoms = 24.2% relative abundance).[74] The HRMS spectrum of brominated dimer **10a** also matched the theoretical isotope pattern, with peaks at 483 (^{79}Br) and 485 (^{81}Br) having relative abundances of 97% and 100%, respectively.

Evidence for the regioselectivity of chlorination and bromination was observed in the ^{13}C NMR spectra, which indicated the disappearance of the aromatic CH peak at ~105 ppm upon halogenations, rather than the quinone CH peak at ~134 ppm in *p*-dimethoxybenzimidazole-benzimidazolequinone dimers **5a-5c**.

KINALD-74Y4E-WG-A (0.037) Is (1.00,0.01) C22H19N4O4ClH
1: TOF MS ASAP+
5.82e12

Theoretical Isotope Pattern (M+H)

439.1173
441.1153
440.1203
442.1178
443.1203
444.1227

Me
O
O
O
O
Cl
Me
8a

KINALD-74Y4E-WG-A 348 (3.230) AM (Cen,1, 80.00, Ar,10000.0,0.00,0.00); Cm (348:360)
1: TOF MS ASAP+
2.10e7

Observed Data

439.1171
441.1159
440.1201
442.1186
438.1093
439.1743
440.1766
441.1727
443.1247
444.1295

KINALD-74YCA-WG-A (0.037) Is (1.00,0.01) C22H19N4O4BrH
1: TOF MS ASAP+
3.94e12

Theoretical Isotope Pattern (M+H)

483.0668
485.0651
484.0698
486.0679
487.0705
488.0730

Me
O
N
N
O
O
N
N
O
Br
Me
10a

KINALD-74YCA-WG-A 238 (2.218) AM (Cen,1, 80.00, Ar,10000.0,0.00,0.00); Cm (238:257)
1: TOF MS ASAP+
5.00e6

Observed Data

483.0670
485.0655
484.0704
486.0686
481.4981 482.0577
483.1259
485.1247
486.0686
487.0735
488.0784

Figure 5.7. Theoretical and observed HRMS spectra of **8a** and **10a**.

186

5.3.3. Radical Trifluoromethylation and Demonstrating Ambiphilicity

Having established regioselective electrophilic substitution at the aromatic part, ambiphilicity of the *p*-dimethoxybenzimidazole-benzimidazolequinone scaffold was confirmed through substitution of the nucleophilic •CF₃ at the quinone part. Radical trifluoromethylation of the alkoxyamine-substituted dimer **1** using the Langlois reaction previously proceeded in moderate yield at the quinone,[45] and an analogous outcome was achieved with piperido-fused dimer **5b** giving 6',9'-dimethoxy-8-(trifluoromethyl)-1,1',2,2',3,3',4,4'-octahydro[7,7'-bipyrido[1,2-*a*]benzimidazole]-6,9-dione (**12**) in 51% yield (Scheme 5.28). Comparison of the DEPT spectrum of **12** with chlorinated dimer **8b** and unsubstituted dimer **5b** highlights the differences in regioselectivity for the radical trifluoromethylation compared to the electrophilic halogenation (Figure 5.8). While chlorination resulted in disappearance of the aromatic 8'-CH peak at 105 ppm, the quinone 8-CH peak at 134 ppm was absent from trifluoromethylated dimer **12**. Furthermore, one of the methoxy CH₃ peaks at 56 ppm in the unsubstituted dimer was shifted downfield upon chlorination, while the same peak was not affected upon trifluoromethylation, indicating a change in electron density only at the *p*-dimethoxybenzimidazole part after chlorination.
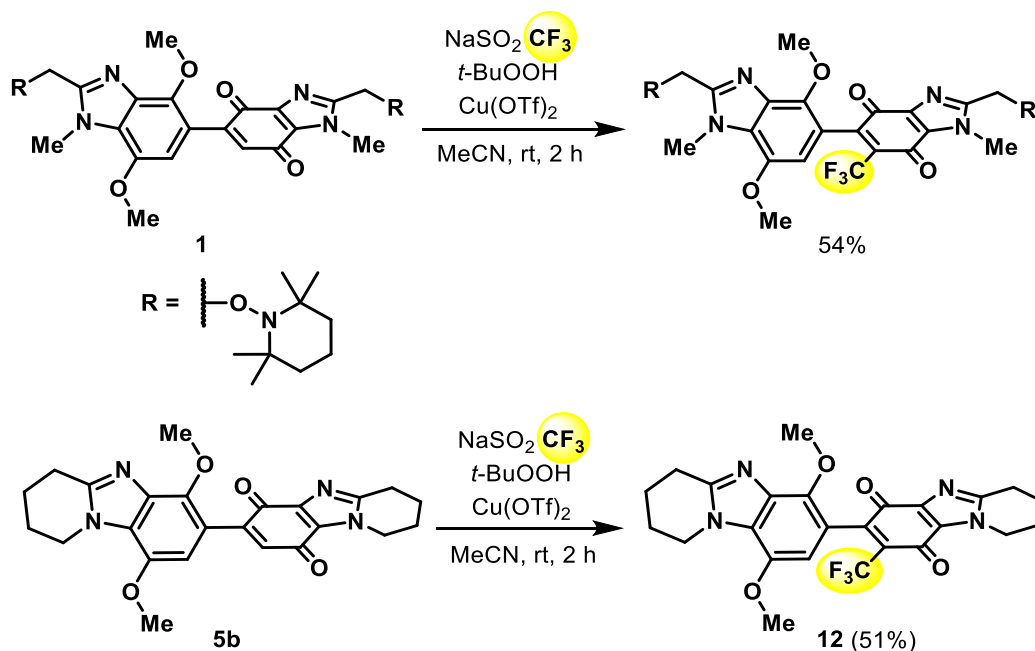
Scheme 5.28. Langlois trifluoromethylation.

187
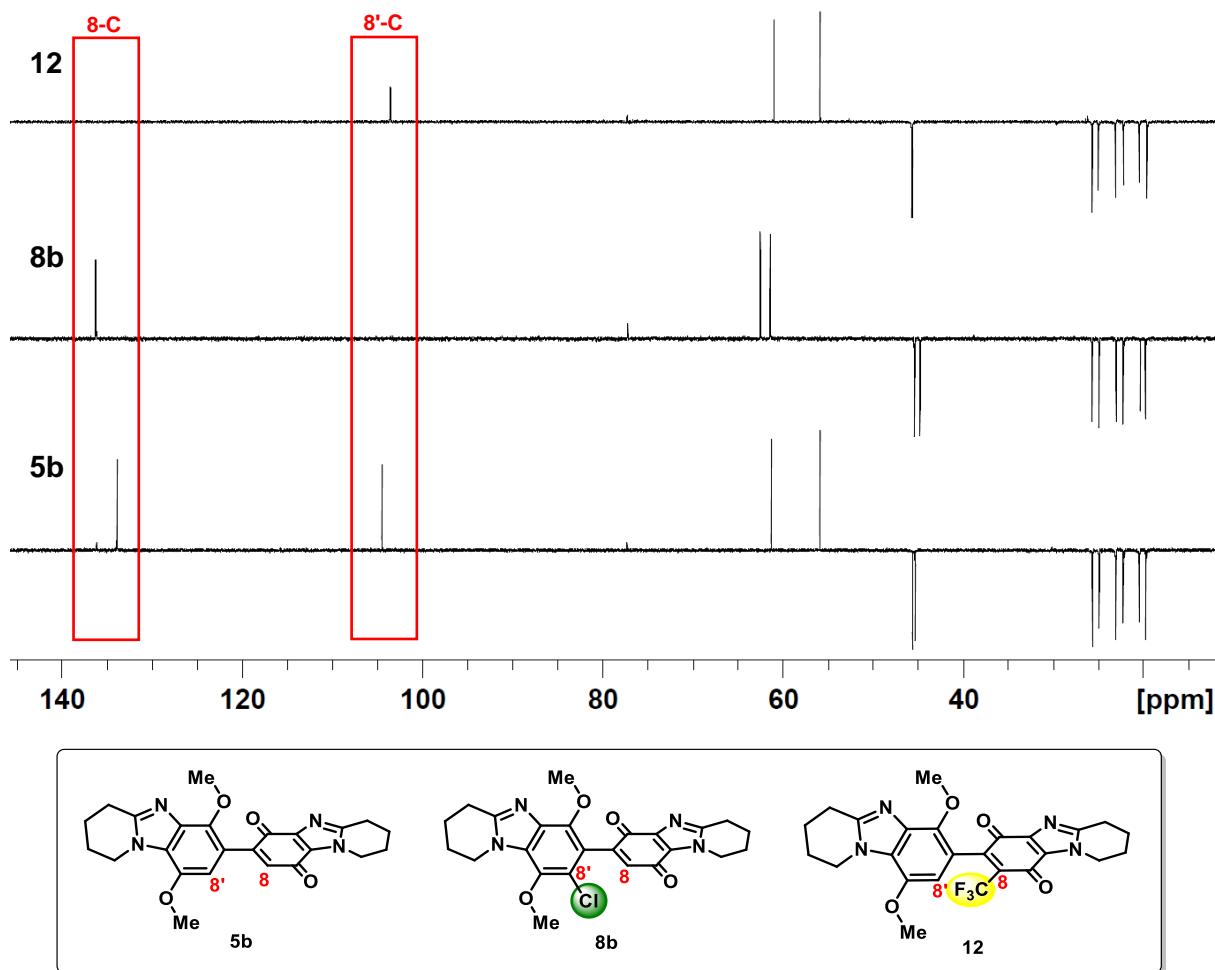
Figure 5.8. DEPT-135 spectra (CDCl$_3$) of dimers **5b**, **12** and **8b** indicating location of substitution.

Chlorination at the available aromatic position of trifluoromethylated dimer **12** was carried out using NaCl (2 equiv) and KHSO$_5$ (1.2 equiv) (entry 4, Table 5.1 conditions) giving 8'-chloro-6',9'-dimethoxy-8-(trifluoromethyl)-1,1',2,2',3,3',4,4'-octahydro[7,7'-bipyrido[1,2-*a*]benzimidazole]-6,9-dione (**13**) in 73% yield, accompanied by unreacted dimer **12** in 17% yield (Scheme 5.29). Compounds **12** and **13** were separable by column chromatography given differences in R_f values of 0.39 and 0.44 (both 19:1 CH$_2$Cl$_2$/MeOH) respectively. The bis-*p*-quinone bearing both a trifluoromethyl- and chloro-substituent (**14**) was accessed in a 68% yield starting from **12** using a greater amount of NaCl (4 equiv) and KHSO$_5$ (4 equiv), alongside 19% of the intermediate dimer **13** (entry 7, Table 5.1 conditions). Compounds **13** and **14** were separable by column chromatography given their different respective R_f values of 0.44 and 0.49 (both 19:1 CH$_2$Cl$_2$/MeOH). The lower yield for chlorination of trifluoromethylated dimer **12** compared with the unsubstituted dimer **5b** may be due to inductive and steric effects associated with the CF$_3$ group.[3] As an alternative to the direct

chlorination and oxidative demethylation, isolated **13** was oxidized to bis-*p*-quinone **14** in 85% yield, when using NaCl (2 equiv) and KHSO$_5$ (2 equiv) (Scheme 5.30).

	13	**14**
method A	73%	0%[a]
method B	19%	68%

[a]Plus unreacted **12** (17%)
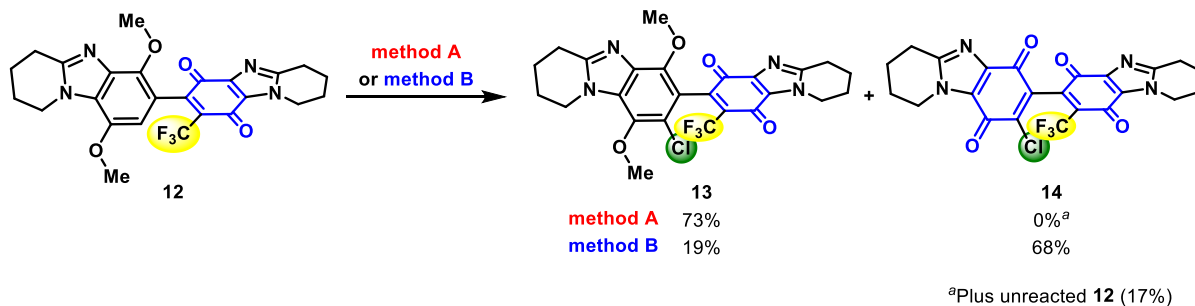
Scheme 5.29. Oxidative chlorination of the trifluoromethylated dimer **12**. **Method A:** Entry 4, Table 5.1 conditions. **Method B:** Entry 7, Table 5.1 conditions.
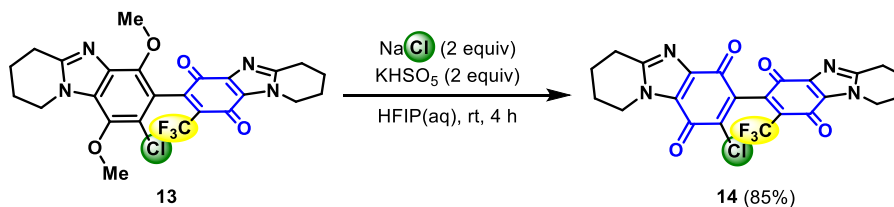
Scheme 5.30. Oxidative demethylation of disubstituted dimer **13**.

5.4. Conclusions

This chapter has demonstrated the ambiphilic character of the *p*-dimethoxybenzimidazole-*p*-benzimidazolequinone dimer through regioselective electrophilic chlorination and bromination at the aromatic ring and nucleophilic radical trifluoromethylation at the quinone. HFIP as reaction solvent improved yields of all described new reactions, including the CAN-mediated oxidative coupling of *p*-dimethoxybenzimidazoles to give the *p*-dimethoxybenzimidazole-*p*-benzimidazolequinone dimers. The mild and benign $KHSO_5$ (Oxone)/NaX system is shown to be tunable with increased equivalents of reagents allowing the halogenation to be combined with the one-pot oxidative demethylation to give halogenated bis-*p*-benzimidazolequinones in high yields.

5.5. Future Work

The cytotoxicity of the bis-*p*-benzimidazolequinones will be evaluated. Vanelle reported a 30-fold increase in cytotoxicity when comparing bis-benzimidazolequinone to the mono-quinone derivatives.[58] Given the nanomolar cytotoxicity of pyrido-fused benzimidazolequinone,[75] the dimers prepared in this Chapter have potential as potent antitumour cytotoxins.

Fluorinated quinones are rare. The *p*-dimethoxybenzimidazole-benzimidazolequinone is a potential scaffold on which to attempt fluorination using electrophilic reagents such as Selectfluor (Scheme 5.31).[76,77] One of the main issues encountered thus far with aromatic fluorinations has been a lack of regioselectivity.[78] As there is only one position available for electrophilic substitution, regioselectivity will not be an issue. Furthermore, Selectfluor has been shown to oxidize aromatic ethers,[79] thus offering potential for mediating one-pot fluorination and oxidative demethylation.
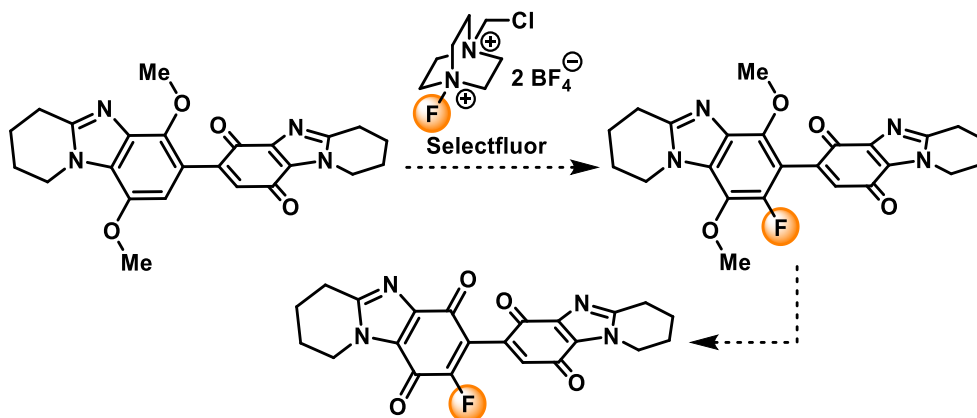
Scheme 5.31. Proposed Selectfluor-mediated functionalization of dimers.

Significant advances have been made in recent years with the direct functionalization of quinones. Baran has developed a method for directly coupling a wide variety of aryl and alkyl boronic acids to quinones (the so-called borono-Minisci reaction).[80] Numerous other Minisci-type reactions have since been developed to functionalize quinones.[81–83] Functionalizing the dimethoxybenzimidazole-benzimidazolequinones in this manner prior to oxidative demethylation would facilitate the synthesis of a library of alkylated and arylated dimers, thus allowing structure-activity relationships to be established (Scheme 5.32).
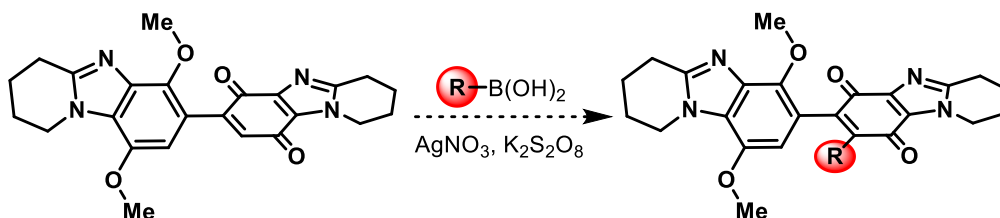
Scheme 5.32. Direct quinone functionalization *via* the borono-Minisci reaction.

5.6. Experimental Section

5.6.1. Materials

Pyrrolo-, piperido-, and azepino-fused *p*-dimethoxybenzimidazoles (**4a-4c**) were prepared according to the procedure described by our group,[59] starting from 1,4-dimethoxybenzene. CAN (Fluorochem, 99%), MeCN (Fisher Scientific, HPLC grade), CH_2Cl_2 (Fisher Scientific, 99.8%), $MgSO_4$ (Anhydrous, Fisher Scientific, Extra Pure, SLR, Dried), MeOH (Alfa Aesar, HPLC Grade, >99.8%), Oxone ($2KHSO_5.KHSO_4.K_2SO_4$, Alfa Aesar), NaCl (Fisher Scientific, Certified AR for Analysis), NaBr (ACROS Organics, 99+%), HFIP (Fluorochem, 99%), *t*-BuOOH (Alfa Aesar, 70% aq. soln.), $NaSO_2CF_3$ (Apollo Scientific, 98%) $Cu(OTf)_2$ (Alfa Aesar, 98%) and $CDCl_3$ (Goss Scientific, 99.8% over molecular sieves + 0.05% TMS) were used as received. Thin layer chromatography (TLC) was performed on TLC silica gel 60 F_{254} plates. Flash column chromatography was carried out on silica gel (Apollo Scientific 60/40−63 μm).

5.6.2. Measurements

Melting points were measured on a Stuart Scientific melting point apparatus SMP1. IR spectra were recorded using a PerkinElmer Spec 1 with ATR attached. NMR spectra were recorded using a Bruker Avance III 400 MHz spectrometer equipped with a 5mm BBFO+, broadband autotune probe and controlled with TopSpin 3.5.7 acquisition software and IconNMR 5.0.7 automation software Copyright © 2017 Bruker BioSpin GmbH. The chemical shifts are in ppm relative to tetramethylsilane. ^{13}C NMR spectra at 100 MHz are with complete proton decoupling. NMR assignments are supported by DEPT-135, ^1H−^1H DQF COSY and ^1H−^{13}C edited HSCQ correlation. ^{19}F NMR spectra were obtained at 376 MHz using automatic digital lock correction in the absence of an internal standard. HRMS spectra were obtained at the National Mass Spectrometry Facility at Swansea University using a Waters Xevo G2-S or Thermo Scientific LTQ Orbitrap XL 1 mass spectrometer with an Atmospheric Solids Analysis Probe (ASAP). The precision of all accurate mass measurements was better than 5 ppm.

5.6.3. Synthetic Procedures and Characterization

5.6.3.1. Synthesis of *p*-Dimethoxybenzimidazole-Benzimidazolequinone Dimers
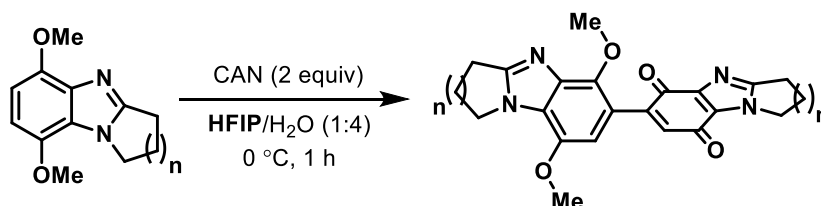
Cerium (IV) ammonium nitrate (8.793 g, 16.04 mmol) in H_2O (80 mL) was added over 30 min to ring-fused benzimidazoles **4a**-**4c** (8.00 mmol) in HFIP (20 mL) at 0 °C. The solution was stirred for a further 30 min and evaporated to dryness. H_2O (200 mL) was added, and the mixture extracted with CH_2Cl_2 (4 x 150 mL). The organic extracts were dried (MgSO$_4$), evaporated, and purified by column chromatography using gradient elution of CH_2Cl_2/MeOH.
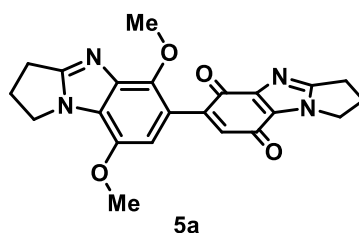
5',8'-Dimethoxy-2,2',3,3'-tetrahydro-1*H*,1'*H*-[6,6'-bipyrrolo[1,2-*a*]benzimidazole]-5,8-dione (5a). (1.423 g, 88%); maroon solid; R_f 0.33 (19:1 CH_2Cl_2/MeOH); mp 189-191 °C; ν_{max} (neat, cm^{-1}) 2944, 2925, 2849, 1674 (C=O), 1650 (C=O), 1620, 1581, 1514, 1489, 1461, 1445, 1393, 1364, 1293, 1276, 1257, 1224, 1140, 1116, 1068; ^{1}H NMR (400 MHz, CDCl$_3$) δ: 6.64 (s, 1H, 7-H), 6.42 (s, 1H, 7'-H), 4.33-4.25 (m, 4H), 4.16 (s, 3H, Me), 3.88 (s, 3H, Me), 3.07-2.97 (m, 4H), 2.80-2.65 (m, 4H); ^{13}C{^{1}H} NMR (100 MHz, CDCl$_3$) δ: 180.0, 177.9 (both C=O), 160.7, 160.3, 147.6, 146.4, 143.5, 141.7, 141.6 (all C), 133.0 (7-CH), 129.5, 125.7, 117.2 (all C), 104.3 (7'-CH), 61.2, 55.9 (both Me), 45.1, 45.0, 26.54, 26.51, 23.4, 22.9 (all CH$_2$); HRMS (ASAP) *m/z* [M + H]$^+$ found 405.1557, $C_{22}H_{21}N_4O_4$ requires 405.1563; *m/z* 407 (4%), 406 (27), 405 ($C_{22}H_{21}N_4O_4$, 100).

193
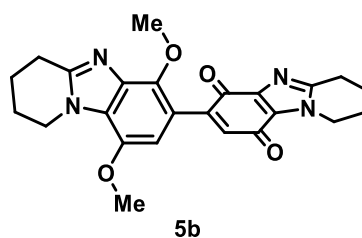
6',9'-Dimethoxy-1,1',2,2',3,3',4,4'-octahydro[7,7'-bipyrido[1,2-*a*]benzimidazole]-6,9-dione (5b). (1.502 g, 87%); maroon solid; R_f 0.34 (19:1 CH$_2$Cl$_2$/MeOH); mp 176-177 °C; ν_{max} (neat, cm^{-1}) 2946, 2869, 1675 (C=O), 1645 (C=O), 1607, 1586, 1531, 1515, 1494, 1484, 1463, 1443, 1394, 1358, 1342, 1326, 1306, 1278, 1244, 1221, 1150, 1129, 1067; ^{1}H NMR (400 MHz, CDCl$_3$) δ: 6.64 (s, 1H, 8-H), 6.41 (s, 1H, 8'-H), 4.44 (t, J = 5.1 Hz, 2H), 4.39-4.32 (m, 2H), 4.13 (s, 3H, Me), 3.86 (s, 3H, Me), 3.10-2.99 (m, 4H), 2.11-1.92 (m, 8H); ^{13}C{^{1}H} NMR (100 MHz, CDCl$_3$) δ: 180.3, 178.4 (both C=O), 151.7, 150.9, 146.7, 143.3, 142.7, 141.7, 136.5 (all C), 133.9 (8-CH), 130.0, 127.3, 117.3 (all C), 104.5 (8'-CH), 61.3, 55.9 (both Me), 45.6, 45.4, 25.7, 24.9, 23.1, 22.3, 20.5, 19.8 (all CH$_2$); HRMS (ASAP) m/z [M + H]$^+$ found 433.1871, C$_{24}$H$_{25}$N$_4$O$_4$ requires 433.1876; m/z 435 (5%), 434 (27), 433 (C$_{24}$H$_{25}$N$_4$O$_4$, 100).
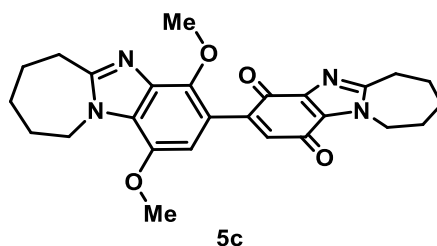
1',4'-Dimethoxy-7,7',8,8',9,9',10,10'-octahydro-6*H*,6'*H*-[3,3'-biazepino[1,2-*a*]benzimidazole]-1,4-dione (5c). (1.529 g, 83%); maroon solid; R_f 0.40 (19:1 CH$_2$Cl$_2$/MeOH); mp 169-171 °C; ν_{max} (neat, cm^{-1}) 2927, 2848, 1714, 1674 (C=O), 1650 (C=O), 1610, 1593, 1525, 1495, 1478, 1440, 1357, 1339, 1314, 1270, 1244, 1231, 1198, 1145, 1127, 1088, 1073, 1049; ^{1}H NMR (400 MHz, CDCl$_3$) δ: 6.63 (s, 1H, 2-H), 6.45 (s, 1H, 2'-H), 4.70-4.55 (m, 4H), 4.16 (s, 3H, Me), 3.88 (s, 3H, Me), 3.12-3.01 (m, 4H), 1.98-1.72 (m, 12H); ^{13}C{^{1}H} NMR (100 MHz, CDCl$_3$) δ: 180.4, 179.0 (both C=O), 158.1, 157.4, 146.3, 143.7, 142.0, 141.1, 136.2 (all C), 134.2 (2-CH), 130.4, 127.8, 116.6 (all C), 105.1 (2'-CH), 61.4, 55.9 (both Me), 46.1, 45.8, 30.9, 30.8, 29.8, 29.3, 28.9, 28.3, 25.6, 25.0 (all CH$_2$); HRMS (ASAP) m/z [M + H]$^+$ found 461.2187, C$_{26}$H$_{29}$N$_4$O$_4$ requires 461.2189; m/z 463 (5%), 462 (29), 461 (C$_{26}$H$_{29}$N$_4$O$_4$), 431 (5).

5.6.3.2. NaX/Oxone-Mediated Halogenation (Method A) or Halogenation with Oxidative Demethylation (Method B)

Method A

Oxone (74 mg, 0.12 mmol ≡ 0.24 mmol $KHSO_5$) and NaCl (23 mg, 0.40 mmol) or NaBr (41 mg, 0.40 mmol) in H_2O (0.1 mL) were added over the course of 5 min to a stirred solution of *p*-dimethoxybenzimidazole-*p*-benzimidazolequinone dimers **5a**-**5c** (0.20 mmol) in HFIP (2 mL) at room temperature, and stirred for 5 h.

Method B

Oxone (0.246 g, 0.40 mmol ≡ 0.80 mmol $KHSO_5$) and NaCl (47 mg, 0.80 mmol) or NaBr (82 mg, 0.80 mmol) in H_2O (0.2 mL) were added over the course of 5 min to a stirred solution of *p*-dimethoxybenzimidazole-*p*-benzimidazolequinone dimers **5a**-**5c** (0.20 mmol) in HFIP (2 mL) at room temperature, and stirred for 9 h.

General Work-Up and Purification

H_2O (5 mL) was added, and the mixture extracted with CH_2Cl_2 (3 x 5 mL). The organic extracts were dried ($MgSO_4$), evaporated to dryness, and purified by column chromatography using gradient elution of CH_2Cl_2/MeOH.
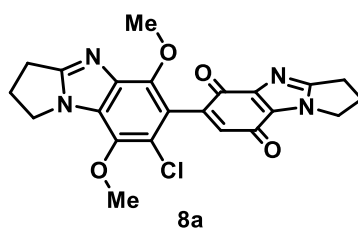
7'-Chloro-5',8'-dimethoxy-2,2',3,3'-tetrahydro-1*H*,1'*H*-[6,6'-bipyrrolo[1,2-*a*]benzimidazole]-5,8-dione (8a). (Method A: 69 mg, 79%); (Method B: 0%); orange solid; R_f 0.41 (19:1 CH$_2$Cl$_2$/MeOH); mp (decomp >206 °C); ν_{max} (neat, cm^{-1}) 2937, 2841, 1674 (C=O), 1653 (C=O), 1614, 1515, 1478, 1434, 1383, 1349, 1294, 1274, 1239, 1139, 1124, 1058, 1013; ^{1}H NMR (400 MHz, CDCl$_3$) δ: 6.58 (s, 1H, 7-H), 4.30 (t, J = 7.2 Hz, 4H), 4.17 (s, 3H, Me), 3.94 (s, 3H, Me), 3.09-2.97 (m, 4H), 2.80-2.70 (m, 4H); ^{13}C{^{1}H} NMR (100 MHz, CDCl$_3$) δ: 179.4, 177.7 (both C=O), 160.84, 160.75, 146.3, 145.7, 144.5, 140.1, 137.2 (all C), 135.5 (7-CH), 129.7, 128.8, 119.2, 117.3 (all C), 62.6, 61.3 (both Me), 45.1, 44.5, 26.6, 26.5, 23.3, 22.9 (all CH$_2$); HRMS (ASAP) m/z [M + H]$^+$ found 439.1171, C$_{22}$H$_{20}$N$_4$O$_4$^{35}Cl requires 439.1173; m/z 442 (9%), 441 (C$_{22}$H$_{20}$N$_4$O$_4$^{37}Cl, 36), 440 (25), 439 (C$_{22}$H$_{20}$N$_4$O$_4$^{35}Cl, 100).
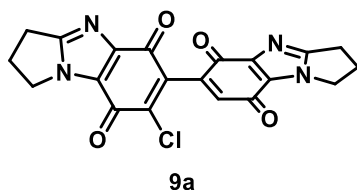
7-Chloro-2,2',3,3'-tetrahydro-1*H*,1'*H*-[6,6'-bipyrrolo[1,2-*a*]benzimidazole]-5,5',8,8'-tetrone (9a). (Method A: 10 mg, 12%); (Method B: 73 mg, 89%); yellow solid; R_f 0.35 (19:1 CH$_2$Cl$_2$/MeOH); mp (decomp >207 °C); ν_{max} (neat, cm^{-1}) 2961, 2924, 2872, 2854, 1659 (C=O), 1529, 1510, 1483, 1465, 1445, 1418, 1336, 1294, 1252, 1238, 1109, 1054, 1011; ^{1}H NMR (400 MHz, CDCl$_3$) δ: 6.55 (s, 1H, 7'-H), 4.31 (q, J = 7.6 Hz, 4H), 3.06-2.98 (m, 4H), 2.83-2.73 (m, 4H); ^{13}C{^{1}H} NMR (100 MHz, CDCl$_3$) δ: 177.2, 176.3, 176.2, 168.9 (all C=O), 162.2, 161.3, 146.4, 145.8, 141.6, 140.6, 138.1 (all C), 135.3 (7'-CH), 129.6, 128.7 (both C), 45.5, 45.2, 26.5, 26.4, 23.1, 22.9 (all CH$_2$); HRMS (ASAP) m/z [M + H]$^+$ found 409.0703, C$_{20}$H$_{14}$N$_4$O$_4$^{35}Cl requires 409.0703; m/z 412 (8%), 411 (C$_{20}$H$_{14}$N$_4$O$_4$^{37}Cl, 35), 410 (23), 409 (C$_{20}$H$_{14}$N$_4$O$_4$^{35}Cl, 100).
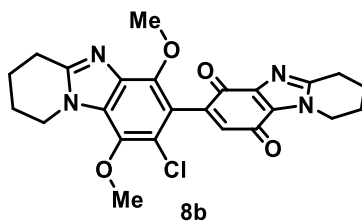
8'-Chloro-6',9'-dimethoxy-1,1',2,2',3,3',4,4'-octahydro[7,7'-bipyrido[1,2-

a]benzimidazole]-6,9-dione (8b). (Method A: 70 mg, 75%); (Method B: 0%); orange solid; R_f 0.39 (19:1 CH_2Cl_2/MeOH); mp (decomp >197°C); ν_{max} (neat, cm^{-1}) 3048, 2948, 2868, 2840, 1676 (C=O), 1653 (C=O), 1607, 1535, 1512, 1476, 1430, 1384, 1353, 1306, 1288, 1245, 1145, 1134, 1086, 1068, 1014; ^{1}H NMR (400 MHz, CDCl$_3$) δ: 6.56 (s, 1H, 8-H), 4.46-4.32 (m, 4H), 4.13 (s, 3H, Me), 3.94 (s, 3H, Me), 3.11-3.01 (m, 4H), 2.16-1.95 (m, 8H); ^{13}C{^{1}H} NMR (100 MHz, CDCl$_3$) δ: 179.6, 178.2 (both C=O), 151.7, 151.5, 145.5, 143.8, 141.6, 138.1 (all C), 136.3 (8-CH), 135.1, 130.24, 130.19, 119.6, 117.7 (all C), 62.5, 61.4 (both Me), 45.4, 44.8, 25.7, 25.0, 23.0, 22.3, 20.4, 19.8 (all CH$_2$); HRMS (ASAP) m/z [M + H]$^+$ found 467.1482, $C_{24}H_{24}N_4O_4{}^{35}Cl$ requires 467.1486; m/z 471 (2%), 470 (9), 469 ($C_{24}H_{24}N_4O_4{}^{37}Cl$, 35), 468 (27), 467 ($C_{24}H_{24}N_4O_4{}^{35}Cl$, 100).
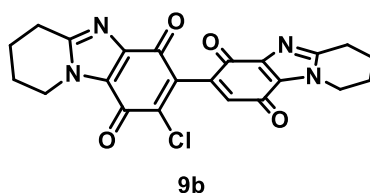
8-Chloro-1,1',2,2',3,3',4,4'-octahydro[7,7'-bipyrido[1,2-a]benzimidazole]-6,6',9,9'-

tetrone (9b). (Method A: isolated as mixture with **5b**); (Method B: 77 mg, 88%); yellow solid; R_f 0.34 (19:1 CH_2Cl_2/MeOH); mp (decomp >212 °C); ν_{max} (neat, cm^{-1}) 3053, 2955, 2869, 1655 (C=O), 1530, 1508, 1483, 1460, 1446, 1429, 1408, 1373, 1321, 1304, 1265, 1243, 1169, 1152, 1118, 1064; ^{1}H NMR (400 MHz, CDCl$_3$) δ: 6.54 (s, 1H, 8'-H), 4.37 (q, J = 5.9 Hz, 4H), 3.04 (t, J = 6.3 Hz, 4H), 2.13-1.96 (m, 8H); ^{13}C{^{1}H} NMR (100 MHz, CDCl$_3$) δ: 177.4, 176.8, 176.4, 169.1 (all C=O), 153.3, 152.3, 142.4, 141.7, 141.2, 139.9, 137.4 (all C), 136.2 (8'-CH), 130.2, 129.3 (both C), 45.8, 45.5, 25.0, 24.9, 22.2, 22.1, 19.7, 19.5 (all CH$_2$); HRMS (ASAP) m/z [M + H]$^+$ found 437.1016, $C_{22}H_{18}N_4O_4{}^{35}Cl$ requires 437.1017; m/z 440 (8%), 439 ($C_{22}H_{18}N_4O_4{}^{37}Cl$, 35), 438 (25), 437 ($C_{22}H_{18}N_4O_4{}^{35}Cl$, 100).
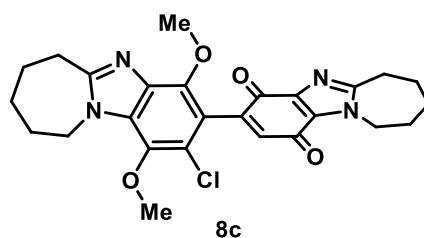
8c

**2'-Chloro-1',4'-dimethoxy-7,7',8,8',9,9',10,10'-octahydro-6H,6'H-[3,3'-biazepino[1,2-a]benzimidazole]-1,4-dione (8c).** (Method A: 71 mg, 72%); (Method B: 12 mg, 12%); orange solid; R_f 0.43 (19:1 CH$_2$Cl$_2$/MeOH); mp (decomp >234 °C); ν_{max} (neat, cm^{-1}) 2930, 2854, 1675 (C=O), 1651 (C=O), 1608, 1516, 1478, 1442, 1388, 1355, 1302, 1268, 1245, 1225, 1149, 1127, 1074, 1054, 1005; ^{1}H NMR (400 MHz, CDCl$_3$) δ: 6.56 (s, 1H, 2-H), 4.73-4.46 (m, 4H), 4.15 (s, 3H, Me), 3.90 (s, 3H, Me), 3.15-3.01 (m, 4H), 1.99-1.74 (m, 12H); ^{13}C{^{1}H} NMR (100 MHz, CDCl$_3$) δ: 179.7, 178.7 (both C=O), 158.2, 157.9, 145.7, 143.4, 140.9, 137.5 (all C), 136.7 (2-CH), 134.7, 130.5, 130.3, 120.1, 117.1 (all C), 61.59, 61.56 (both Me), 45.9, 45.3, 30.9, 30.8, 29.7, 29.3, 28.9, 28.1, 25.5, 24.9 (all CH$_2$); HRMS (ASAP) m/z [M + H]$^+$ found 495.1801, C$_{26}$H$_{28}$N$_4$O$_4$^{35}Cl requires 495.1799; m/z 499 (2%), 498 (10), 497 (C$_{26}$H$_{28}$N$_4$O$_4$^{37}Cl, 36), 496 (29), 495 (C$_{26}$H$_{28}$N$_4$O$_4$^{35}Cl, 100).

9c
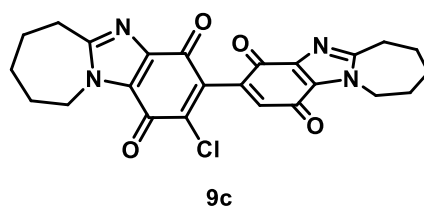
2-Chloro-7,7',8,8',9,9',10,10'-octahydro-6H,6'H-[3,3'-biazepino[1,2-a]benzimidazole]-1,1',4,4'-tetrone (9c). (Method A: isolated as mixture with **5c**); (Method B: 69 mg, 74%); R_f 0.40 (19:1 CH$_2$Cl$_2$/MeOH); mp (decomp >237 °C); ν_{max} (neat, cm^{-1}) 2929, 2855, 1659 (C=O), 1583, 1514, 1476, 1442, 1410, 1373, 1358, 1336, 1318, 1294, 1266, 1240, 1225, 1194, 1116, 1055; ^{1}H NMR (400 MHz, CDCl$_3$) δ: 6.50 (s, 1H, 2'-H), 4.75-4.61 (m, 2H), 4.61-4.51 (m, 2H), 3.16-2.99 (m, 4H), 2.03-1.69 (m, 12H); ^{13}C{^{1}H} NMR (100 MHz, CDCl$_3$) δ: 177.4, 177.3, 176.3, 169.7 (all C=O), 159.7, 158.8, 142.6, 141.1, 140.5, 139.5, 137.0 (all C), 136.5 (2'-CH), 130.5, 129.7 (both C), 46.3, 46.0, 30.73, 30.65 (all CH$_2$), 29.3 (2 x CH$_2$), 28.1, 28.0, 24.8, 24.7 (all CH$_2$); HRMS (ASAP) m/z [M + H]$^+$ found 465.1326, C$_{24}$H$_{22}$N$_4$O$_4$^{35}Cl requires 465.1330; m/z 468 (9%), 467 (C$_{24}$H$_{22}$N$_4$O$_4$^{37}Cl, 36), 466 (27), 465 (C$_{24}$H$_{22}$N$_4$O$_4$^{35}Cl, 100).

10a
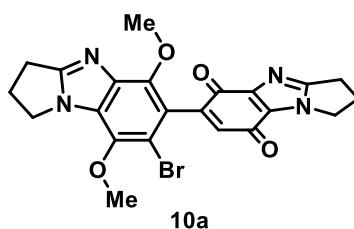
**7'-Bromo-5',8'-dimethoxy-2,2',3,3'-tetrahydro-1H,1'H-[6,6'-bipyrrolo[1,2-
a]benzimidazole]-5,8-dione (10a).** (Method A: 73 mg, 76%); (Method B: 12 mg, 13%);
orange solid; R_f 0.38 (19:1 CH$_2$Cl$_2$/MeOH); mp (decomp >209°C); ν_{max} (neat, cm^{-1}) 3047,
2936, 2840, 1674 (C=O), 1652 (C=O), 1610, 1515, 1473, 1433, 1381, 1344, 1296, 1272, 1237,
1123, 1057, 1007; ^{1}H NMR (400 MHz, CDCl$_3$) δ: 6.55 (s, 1H, 7-H), 4.31 (t, J = 7.2 Hz, 4H),
4.16 (s, 3H, Me), 3.93 (s, 3H, Me), 3.09-2.99 (m, 4H), 2.81-2.71 (m, 4H); ^{13}C{^{1}H} NMR (100
MHz, CDCl$_3$) δ: 179.3, 177.8 (both C=O), 160.81, 160.79, 146.3, 146.1, 145.9, 140.8, 138.2
(all C), 135.4 (7-CH), 129.7, 128.9, 118.9, 109.6 (all C), 62.8, 61.4 (both Me), 45.1, 44.5, 26.6,
26.5, 23.3, 22.9 (all CH$_2$); HRMS (ASAP) m/z [M + H]$^+$ found 483.0670, C$_{22}$H$_{20}$N$_4$O$_4$^{79}Br
requires 483.0668; m/z 487 (5%), 486 (24), 485 (C$_{22}$H$_{20}$N$_4$O$_4$^{81}Br, 100), 484 (24), 483
(C$_{22}$H$_{20}$N$_4$O$_4$^{79}Br, 97).

11a
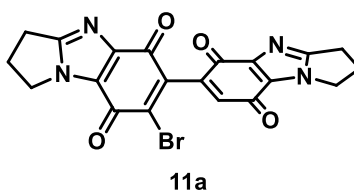
**7-Bromo-2,2',3,3'-tetrahydro-1H,1'H-[6,6'-bipyrrolo[1,2-*a*]benzimidazole]-5,5',8,8'-
tetrone (11a).** (Method A: 9 mg, 10%); (Method B: 68 mg, 75%); R_f 0.33 (19:1
CH$_2$Cl$_2$/MeOH); mp (decomp >209 °C); ν_{max} (neat, cm^{-1}) 2964, 2927, 2856, 1662 (C=O), 1574,
1513, 1483, 1466, 1446, 1409, 1353, 1293, 1251, 1235, 1106, 1054; ^{1}H NMR (400 MHz,
CDCl$_3$) δ: 6.53 (s, 1H, 7'-H), 4.31 (q, J = 6.6 Hz, 4H), 3.07-2.97 (m, 4H), 2.83-2.71 (m, 4H);
^{13}C{^{1}H} NMR (100 MHz, CDCl$_3$) δ: 177.1, 176.4, 175.7, 169.0 (all C=O), 162.0, 161.3, 146.2,
145.8, 142.5, 141.9, 136.8 (all C), 134.8 (7'-CH), 129.7, 128.4 (both C), 45.4, 45.2, 26.5, 26.4,
23.1, 22.9 (all CH$_2$); HRMS (ASAP) m/z [M + H]$^+$ found 453.0180, C$_{20}$H$_{14}$O$_4$N$_4$^{79}Br requires
453.0193; m/z 456 (22%), 455 (C$_{20}$H$_{14}$O$_4$N$_4$^{81}Br, 97), 454 (22), 453 (C$_{20}$H$_{14}$O$_4$N$_4$^{79}Br, 100).
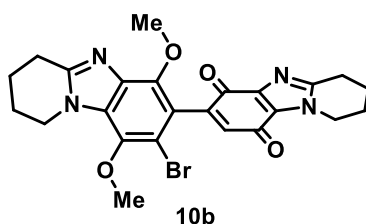
8'-Bromo-6',9'-dimethoxy-1,1',2,2',3,3',4,4'-octahydro[7,7'-bipyrido[1,2-a]benzimidazole]-6,9-dione (10b). (Method A: 69 mg, 68%); (Method B: 18 mg, 18%); orange solid; R_f 0.37 (19:1 CH_2Cl_2/MeOH); mp (decomp >186 °C); ν_{max} (neat, cm^{-1}) 3049, 2947, 2868, 1675 (C=O), 1652 (C=O), 1605, 1534, 1512, 1474, 1445, 1382, 1345, 1322, 1307, 1283, 1245, 1143, 1132, 1085, 1065, 1008; ^{1}H NMR (400 MHz, CDCl$_3$) δ: 6.54 (s, 1H, 8-H), 4.47-4.34 (m, 4H), 4.11 (s, 3H, Me), 3.93 (s, 3H, Me), 3.11-3.02 (m, 4H), 2.16-1.96 (m, 8H); ^{13}C{^{1}H} NMR (100 MHz, CDCl$_3$) δ: 179.6, 178.2 (both C=O), 151.8, 151.5, 145.6, 145.4, 141.6, 139.1 (all C), 136.2 (8-CH), 135.8, 130.4, 130.2, 119.4, 110.1 (all C), 62.7, 61.5 (both Me), 45.4, 44.8, 25.7, 25.0, 23.1, 22.3, 20.4, 19.8 (all CH$_2$); HRMS (ASAP) *m/z* [M + H]$^+$ found 511.0984, $C_{24}H_{24}N_4O_4{}^{79}$Br requires 511.0981; *m/z* 515 (6%), 514 (26), 513 ($C_{24}H_{24}N_4O_4{}^{81}$Br, 100), 512 (26), 511 ($C_{24}H_{24}N_4O_4{}^{79}$Br, 97).
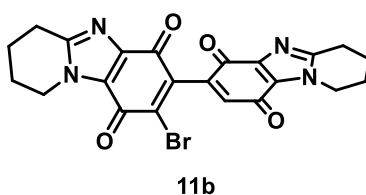
8-Bromo-1,1',2,2',3,3',4,4'-octahydro[7,7'-bipyrido[1,2-a]benzimidazole]-6,6',9,9'-tetrone (11b). (Method A: isolated as mixture with **5b**); (Method B: 69 mg, 72%); R_f 0.33 (19:1 CH_2Cl_2/MeOH); mp (decomp >220 °C); ν_{max} (neat, cm^{-1}) 3050, 2953, 2869, 1655 (C=O), 1520, 1507, 1483, 1460, 1445, 1428, 1408, 1372, 1321, 1303, 1242, 1227, 1169, 1116, 1063; ^{1}H NMR (400 MHz, CDCl$_3$) δ: 6.51 (s, 1H, 8'-H), 4.37 (t, *J* = 5.6 Hz, 4H), 3.05 (t, *J* = 6.3 Hz, 4H), 2.14-1.96 (m, 8H); ^{13}C{^{1}H} NMR (100 MHz, CDCl$_3$) δ: 177.3, 176.9, 175.9, 169.3 (all C=O), 153.2, 152.3, 141.7, 141.6, 141.19, 141.17, 137.9 (all C), 135.6 (8'-CH), 130.2, 129.0 (both C), 45.7, 45.5, 25.0, 24.9, 22.2, 22.1, 19.7, 19.5 (all CH$_2$); HRMS (ASAP) *m/z* [M + H]$^+$ found 481.0512, $C_{22}H_{18}N_4O_4{}^{79}$Br requires 481.0511; *m/z* 485 (3%), 484 (24), 483 ($C_{22}H_{18}N_4O_4{}^{81}$Br, 97), 482 (26), 481 ($C_{22}H_{18}N_4O_4{}^{79}$Br, 100).
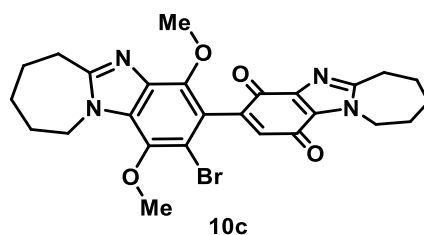
2'-Bromo-1',4'-dimethoxy-7,7',8,8',9,9',10,10'-octahydro-6H,6'H-[3,3'-biazepino[1,2-a]benzimidazole]-1,4-dione (10c). (Method A: 76 mg, 71%); (Method B: 24 mg, 22%); orange solid; R_f 0.42 (19:1 CH$_2$Cl$_2$/MeOH); mp (decomp >243 °C); ν_{max} (neat, cm^{-1}) 3049, 2930, 2854, 1675 (C=O), 1651 (C=O), 1607, 1516, 1475, 1442, 1434, 1386, 1353, 1319, 1299, 1268, 1242, 1224, 1199, 1148, 1086, 1053; ^{1}H NMR (400 MHz, CDCl$_3$) δ: 6.53 (s, 1H, 2-H), 4.73-4.45 (m, 4H), 4.14 (s, 3H, Me), 3.89 (s, 3H, Me), 3.15-3.00 (m, 4H), 1.99-1.69 (m, 12H); ^{13}C{^{1}H} NMR (100 MHz, CDCl$_3$) δ: 179.7, 178.8 (both C=O), 158.3, 157.9, 145.9, 145.0, 140.9, 138.4 (all C), 136.6 (2-CH), 135.5, 130.5, 130.4, 118.8, 110.8 (all C), 61.7, 61.6 (both Me), 45.9, 45.3, 30.89, 30.85, 29.7, 29.4, 28.9, 28.2, 25.5, 24.9 (all CH$_2$); HRMS (ASAP) *m/z* [M + H]$^+$ found 539.1297, C$_{26}$H$_{28}$N$_4$O$_4$^{79}Br requires 539.1294; *m/z* 543 (5%), 542 (27), 541 (C$_{26}$H$_{28}$N$_4$O$_4$^{81}Br, 100), 540 (28), 539 (C$_{26}$H$_{28}$N$_4$O$_4$^{79}Br, 97).
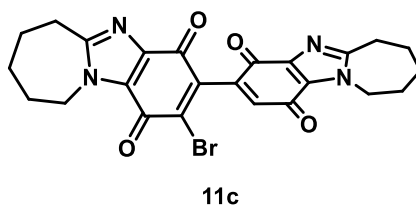
2-Bromo-7,7',8,8',9,9',10,10'-octahydro-6H,6'H-[3,3'-biazepino[1,2-a]benzimidazole]-1,1',4,4'-tetrone (11c). (Method A: isolated as mixture with **5c**); (Method B: 70 mg, 69%); R_f 0.39 (19:1 CH$_2$Cl$_2$/MeOH); mp (decomp >232 °C); ν_{max} (neat, cm^{-1}) 3051, 2929, 2855, 1659 (C=O), 1515, 1475, 1441, 1411, 1372, 1359, 1337, 1318, 1294, 1265, 1235, 1194, 1113, 1050; ^{1}H NMR (400 MHz, CDCl$_3$) δ: 6.49 (s, 1H, 2'-H), 4.78-4.64 (m, 2H), 4.62-4.48 (m, 2H), 3.16-2.99 (m, 4H), 2.05-1.68 (m, 12H); ^{13}C{^{1}H} NMR (100 MHz, CDCl$_3$) δ: 177.4, 177.3, 175.9, 169.8 (all C=O), 159.6, 158.7, 141.3, 141.0, 140.8, 140.5, 138.2 (all C), 135.9 (2'-CH), 130.5, 129.3 (both C), 46.2, 46.0, 30.74, 30.66, 29.3, 28.1, 28.0, 24.8, 24.7 (all CH$_2$); HRMS (ASAP) *m/z* [M + H]$^+$ found 509.0826, C$_{24}$H$_{22}$N$_4$O$_4$^{79}Br requires 509.0824; *m/z* 513 (4%), 512 (26), 511 (C$_{24}$H$_{22}$N$_4$O$_4$^{81}Br, 100), 510 (26), 509 (C$_{24}$H$_{22}$N$_4$O$_4$^{79}Br, 97).

5.6.3.3. Synthesis of 6',9'-dimethoxy-8-(trifluoromethyl)-1,1',2,2',3,3',4,4'-octahydro[7,7'-bipyrido[1,2-*a*]benzimidazole]-6,9-dione (12)
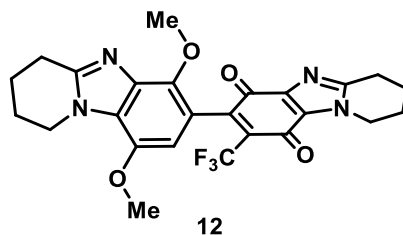
t-BuOOH (0.288 mL, 3.03 mmol) was added over the course of 10 min to a stirred solution of 6',9'-dimethoxy-1,1',2,2',3,3',4,4'-octahydro[7,7'-bipyrido[1,2-*a*]benzimidazole]-6,9-dione (0.181 g, 0.42 mmol), $NaSO_2CF_3$ (0.197 g, 1.26 mmol) and $Cu(OTf)_2$ (15 mg, 0.04 mmol) in MeCN (5 mL) at room temperature, and the mixture was stirred for 2 h. H_2O (20 mL) was added, and the mixture was extracted with CH_2Cl_2 (3 x 15 mL). The combined organic extracts were dried ($MgSO_4$), evaporated to dryness and purified by column chromatography using gradient elution of CH_2Cl_2/MeOH to give the *title compound* **12** (0.107 g, 51%) as a brown solid; R_f 0.39 (19:1 CH_2Cl_2/MeOH); mp 177-179 °C; ν_{max} (neat, cm^{-1}) 2950, 1682, 1663 (C=O), 1610, 1545, 1518, 1500, 1484, 1462, 1432, 1392, 1357, 1346, 1312, 1288, 1238, 1175, 1155, 1144, 1127; ^{1}H NMR (400 MHz, CDCl$_3$) δ: 6.24 (s, 1H, 8'-H), 4.52-4.32 (m, 4H), 4.12 (s, 3H, Me), 3.84 (s, 3H, Me), 3.06 (q, J = 6.5 Hz, 4H), 2.13-1.92 (m, 8H); ^{13}C{^{1}H} NMR (100 MHz, CDCl$_3$) δ: 178.5, 174.1 (both C=O), 153.1, 150.8, 147.73, 147.70, 142.3, 141.0, 135.6 (all C), 130.2 (q, $^2J_{C-F}$ = 27.2 Hz, 8-C), 129.9, 127.4 (C), 121.8 (q, $^1J_{C-F}$ = 276.6 Hz, CF$_3$), 114.4 (C), 103.6 (d, J = 2.1 Hz, 8'-CH), 61.0, 55.9 (both Me), 45.7, 45.6, 25.7, 25.0, 23.1, 22.2, 20.5, 19.6 (all CH$_2$); ^{19}F NMR (376 MHz, CDCl$_3$) δ: -56.48; HRMS (ASAP) *m/z* [M + H]$^+$ found 501.1752, $C_{25}H_{24}N_4O_4F_3$ requires 501.1750; *m/z* 503 (5%), 502 (28), 501 ($C_{25}H_{24}N_4O_4F_3$, 100).

5.6.3.4. NaCl/Oxone-Mediated Halogenation (Method A) or Halogenation with Oxidative Demethylation (Method B) of Trifluoromethyl Dimer 12

Following Procedure 5.6.3.2, trifluoromethyl-substituted dimer **12** (50 mg, 0.10 mmol), Oxone (Method A: 37 mg, 0.06 mmol ≡ 0.12 mmol KHSO$_5$; Method B: 0.123 g, 0.20 mmol ≡ 0.40 mmol KHSO$_5$) and NaCl (Method A: 12 mg, 0.20 mmol; Method B: 23 mg, 0.40 mmol) in HFIP(aq) (Method A: 1 mL HFIP, 0.05 mL H$_2$O; Method B: 1 mL HFIP, 0.1 mL H$_2$O) gave:
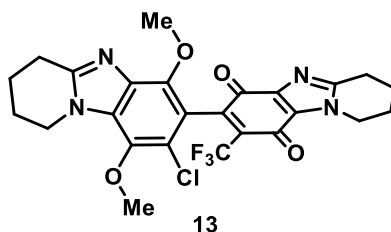
13

8'-Chloro-6',9'-dimethoxy-8-(trifluoromethyl)-1,1',2,2',3,3',4,4'-octahydro[7,7'-bipyrido[1,2-*a*]benzimidazole]-6,9-dione (13). (Method A: 39 mg, 73%); (Method B: 10 mg, 19%); brown solid; R_f 0.44 (19:1 CH$_2$Cl$_2$/MeOH); mp 163-166 °C; ν_{max} (neat, cm^{-1}) 2950, 2871, 2841, 1683 (C=O), 1668 (C=O), 1605, 1548, 1515, 1482, 1460, 1447, 1431, 1386, 1357, 1326, 1311, 1286, 1267, 1235, 1176, 1155, 1132, 1094, 1075, 1019; ^{1}H NMR (400 MHz, CDCl$_3$) δ: 4.48-4.36 (m, 4H), 4.15 (s, 3H, Me), 3.93 (s, 3H, Me), 3.07 (q, *J* = 6.6 Hz, 4H), 2.15-2.06 (m, 4H), 2.09-1.96 (m, 4H); ^{13}C{^{1}H} NMR (100 MHz, CDCl$_3$) δ: 177.7, 173.7 (both C=O), 153.1, 151.4 (both C), 144.29-144.17 (m, C), 144.1, 141.0, 137.7, 134.3 (all C), 131.7 (q, $^2J_{C-F}$ = 27.5 Hz, 8-C), 130.4, 130.1 (both C), 121.5 (q, $^1J_{C-F}$ = 276.4 Hz, CF$_3$), 118.5, 115.2 (both C), 62.6, 61.1 (both Me), 45.7, 44.8, 25.7, 25.0, 23.0, 22.2, 20.4, 19.6 (all CH$_2$); ^{19}F NMR (376 MHz, CDCl$_3$) δ: -58.95; HRMS (ASAP) *m/z* [M + H]$^+$ found 535.1357, C$_{25}$H$_{23}$N$_4$O$_4$F$_3$^{35}Cl requires 535.1360; *m/z* 539 (2%), 538 (9), 537 (C$_{25}$H$_{23}$N$_4$O$_4$F$_3$^{37}Cl, 35), 536 (27), 535 (C$_{25}$H$_{23}$N$_4$O$_4$F$_3$^{35}Cl, 100).
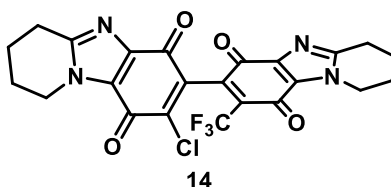
14

8-Chloro-8'-(trifluoromethyl)-1,1',2,2',3,3',4,4'-octahydro[7,7'-bipyrido[1,2-*a*]benzimidazole]-6,6',9,9'-tetrone (14). (Method A: 0%); (Method B: 34 mg, 68%); orange solid; R_f 0.49 (19:1 CH$_2$Cl$_2$/MeOH); mp (decomp. >239 °C); ν_{max} (neat, cm^{-1}) 2960, 2870, 1669 (C=O), 1589, 1534, 1510, 1483, 1461, 1445, 1431, 1411, 1376, 1345, 1332, 1315, 1304, 1249,

1217, 1181, 1152, 1120, 1080; ^{1}H NMR (400 MHz, CDCl$_3$) δ: 4.39 (t, J = 5.9 Hz, 4H), 3.05 (t, J = 6.3 Hz, 4H), 2.15-2.06 (m, 4H), 2.06-1.96 (m, 4H); ^{13}C{^{1}H} NMR (100 MHz, CDCl$_3$) δ: 175.7, 175.5, 172.1, 168.6 (all C=O), 153.7, 153.4, 141.6, 140.7, 140.5, 139.8, 137.1 (all C), 132.0 (q, $^2J_{C-F}$ = 28.3 Hz, 8'-C), 130.2, 129.5 (both C), 121.0 (q, $^1J_{C-F}$ = 276.6 Hz, CF$_3$), 45.9, 45.8, 25.00, 24.99 (all CH$_2$), 22.1 (2 x C), 19.51, 19.48 (both CH$_2$); ^{19}F NMR (376 MHz, CDCl$_3$) δ: -59.03; HRMS (ASAP) m/z [M + H]$^+$ found 505.0889, C$_{23}$H$_{17}$N$_4$O$_4$F$_3$^{35}Cl requires 505.0891; m/z 508 (12%), 507 (C$_{23}$H$_{17}$N$_4$O$_4$F$_3$^{37}Cl, 34), 506 (25), 505 (C$_{23}$H$_{17}$N$_4$O$_4$F$_3$^{35}Cl, 100).

5.7.   Chapter 5 References

(1)   Vaillancourt, F. H.; Yeh, E.; Vosburg, D. A.; Garneau-Tsodikova, S.; Walsh, C. T. Nature's Inventory of Halogenation Catalysts: Oxidative Strategies Predominate. *Chem. Rev.* **2006**, *106*, 3364–3378. https://doi.org/10.1021/cr050313i.

(2)   Podgoršek, A.; Zupan, M.; Iskra, J. Oxidative Halogenation with "Green" Oxidants: Oxygen and Hydrogen Peroxide. *Angew. Chem. Int. Ed.* **2009**, *48*, 8424–8450. https://doi.org/10.1002/anie.200901223.

(3)   Gurry, M.; Sweeney, M.; McArdle, P.; Aldabbagh, F. One-Pot Hydrogen Peroxide and Hydrohalic Acid Induced Ring Closure and Selective Aromatic Halogenation to Give New Ring-Fused Benzimidazoles. *Org. Lett.* **2015**, *17*, 2856–2859. https://doi.org/10.1021/acs.orglett.5b01317.

(4)   Sweeney, M.; Keane, L. A. J.; Gurry, M.; McArdle, P.; Aldabbagh, F. One-Pot Synthesis of Dihalogenated Ring-Fused Benzimidazolequinones from 3,6-Dimethoxy-2-(Cycloamino)anilines Using Hydrogen Peroxide and Hydrohalic Acid. *Org. Lett.* **2018**, *20*, 6970–6974. https://doi.org/10.1021/acs.orglett.8b03135.

(5)   Mohan Kandepi, V. V. K.; Narender, N. Ecofriendly Oxidative Nuclear Halogenation of Aromatic Compounds Using Potassium and Ammonium Halides. *Synthesis* **2012**, *44*, 15–26. https://doi.org/10.1055/s-0031-1289620.

(6)   Hussain, H.; Green, I. R.; Ahmed, I. Journey Describing Applications of Oxone in Synthetic Chemistry. *Chem. Rev.* **2013**, *113*, 3329–3371. https://doi.org/10.1021/cr3004373.

(7)   Moriyama, K.; Takemura, M.; Togo, H. Selective Oxidation of Alcohols with Alkali Metal Bromides as Bromide Catalysts: Experimental Study of the Reaction Mechanism. *J. Org. Chem.* **2014**, *79*, 6094–6104. https://doi.org/10.1021/jo5008064.

(8)   Anbar, M.; Guttmann, S.; Rein, R. The Isotopic Exchange between Hypohalites and Halide Ions. II. The Exchange between Hypochlorous Acid and Chloride Ions. *J. Am. Chem. Soc.* **1959**, *81*, 1816–1821. https://doi.org/10.1021/ja01517a011.

(9)   Dieter, R. K.; Nice, L. E.; Velu, S. E. Oxidation of α,β-Enones and Alkenes with Oxone and Sodium Halides: A Convenient Laboratory Preparation of Chlorine and Bromine. *Tetrahedron Lett.* **1996**, *37*, 2377–2380. https://doi.org/10.1016/0040-4039(96)00295-X.

(10)   Tamhankar, B. V; Desai, U. V; Mane, R. B.; Wadgaonkar, P. P.; Bedekar, A. V. A Simple and Practical Halogenation of Activated Arenes Using Potassium Halide and Oxone® in Water-Acetonitrile Medium. *Synth. Commun.* **2001**, *31*, 2021–2027. https://doi.org/10.1081/SCC-100104419.

(11)   Narender, N.; Srinivasu, P.; Kulkarni, S. J.; Raghavan, K. V. Highly Efficient, Para-Selective Oxychlorination of Aromatic Compounds Using Potassium Chloride and Oxone. *Synth. Commun.* **2002**, *32*, 279–286. https://doi.org/10.1081/SCC-120002013.

(12)   Narender, N.; Srinivasu, P.; Ramakrishna Prasad, M.; Kulkarni, S. J.; Raghavan, K. V. An Efficient and Regioselective Oxybromination of Aromatic Compounds Using Potassium Bromide and Oxone®. *Synth. Commun.* **2002**, *32*, 2313–2318. https://doi.org/10.1081/SCC-120006001.

(13)   Zhao, M.; Lu, W. Visible Light-Induced Oxidative Chlorination of Alkyl sp^3 C–H Bonds with NaCl/Oxone at Room Temperature. *Org. Lett.* **2017**, *19*, 4560–4563. https://doi.org/10.1021/acs.orglett.7b02153.

(14)   Lakshmireddy, V. M.; Naga Veera, Y.; Reddy, T. J.; Rao, V. J.; China Raju, B. A Green and Sustainable Approach for Selective Halogenation of Anilides, Benzanilides, Sulphonamides and Heterocycles. *Asian J. Org. Chem.* **2019**, *8*, 1380–1384. https://doi.org/10.1002/ajoc.201900296.

(15)   Ren, J.; Tong, R. Convenient in Situ Generation of Various Dichlorinating Agents from Oxone and Chloride: Diastereoselective Dichlorination of Allylic and Homoallylic Alcohol Derivatives. *Org. Biomol. Chem.* **2013**, *11*, 4312–4315. https://doi.org/10.1039/c3ob40670a.

(16)   Moriyama, K.; Takemura, M.; Togo, H. Direct and Selective Benzylic Oxidation of Alkylarenes *via* C-H Abstraction Using Alkali Metal Bromides. *Org. Lett.* **2012**, *14*, 2414–2417. https://doi.org/10.1021/ol300853z.

(17) Xu, J.; Liang, L.; Zheng, H.; Chi, Y. R.; Tong, R. Green Oxidation of Indoles Using Halide Catalysis. *Nat. Commun.* **2019**, *10*, 4754. https://doi.org/10.1038/s41467-019-12768-4.

(18) Xu, J.; Tong, R. An Environmentally Friendly Protocol for Oxidative Halocyclization of Tryptamine and Tryptophol Derivatives. *Green Chem.* **2017**, *19*, 2952–2956. https://doi.org/10.1039/c7gc01341h.

(19) Uyanik, M.; Sahara, N.; Ishihara, K. Regioselective Oxidative Chlorination of Arenols Using NaCl and Oxone. *Eur. J. Org. Chem.* **2019**, 27–31. https://doi.org/10.1002/ejoc.201801063.

(20) Purser, S.; Moore, P. R.; Swallow, S.; Gouverneur, V. Fluorine in Medicinal Chemistry. *Chem. Soc. Rev.* **2008**, *37*, 320–330. https://doi.org/10.1039/b610213c.

(21) Gillis, E. P.; Eastman, K. J.; Hill, M. D.; Donnelly, D. J.; Meanwell, N. A. Applications of Fluorine in Medicinal Chemistry. *J. Med. Chem.* **2015**, *58*, 8315–8359. https://doi.org/10.1021/acs.jmedchem.5b00258.

(22) Zhou, Y.; Wang, J.; Gu, Z.; Wang, S.; Zhu, W.; Acenã, J. L.; Soloshonok, V. A.; Izawa, K.; Liu, H. Next Generation of Fluorine-Containing Pharmaceuticals, Compounds Currently in Phase II-III Clinical Trials of Major Pharmaceutical Companies: New Structural Trends and Therapeutic Areas. *Chem. Rev.* **2016**, *116*, 422–518. https://doi.org/10.1021/acs.chemrev.5b00392.

(23) Mei, H.; Han, J.; Fustero, S.; Medio-Simon, M.; Sedgwick, D. M.; Santi, C.; Ruzziconi, R.; Soloshonok, V. A. Fluorine-Containing Drugs Approved by the FDA in 2018. *Chem. Eur. J.* **2019**, *25*, 11797–11819. https://doi.org/10.1002/chem.201901840.

(24) Langlois, B. R. Once Upon a Time Was the Langlois' Reagent: A "Sleeping Beauty." In *Modern Synthesis Processes and Reactivity of Fluorinated Compounds*; Groult, H., Leroux, F. R., Tressaud, A., Eds.; Elsevier: 2017; pp 125–140. https://doi.org/10.1016/B978-0-12-803740-9.00005-6.

(25) Liang, T.; Neumann, C. N.; Ritter, T. Introduction of Fluorine and Fluorine-Containing Functional Groups. *Angew. Chem. Int. Ed.* **2013**, *52*, 8214–8264. https://doi.org/10.1002/anie.201206566.

(26)   McClinton, M. A.; McClinton, D. A. Trifluoromethylations and Related Reactions in Organic Chemistry. *Tetrahedron* **1992**, *48*, 6555–6666. https://doi.org/https://doi.org/10.1016/S0040-4020(01)80011-9.

(27)   Studer, A. A "Renaissance" in Radical Trifluoromethylation. *Angew. Chem. Int. Ed.* **2012**, *51*, 8950–8958. https://doi.org/10.1002/anie.201202624.

(28)   Fessenden, R. W.; Schdxer, R. H. ESR Spectra and Structure of the Fluorinated Methyl Radicals. *J. Chem. Phys.* **1965**, *43*, 2704–2712. https://doi.org/10.1063/1.1697199.

(29)   Krusic, P. J.; Bingham, R. C. An Electron Spin Resonance Study of the Substituent Effects Causing Nonplanarity in Alkyl Radicals. Electronegativity vs. π-Conjugative Destabilization. *J. Am. Chem. Soc.* **1976**, *98*, 230–232. https://doi.org/10.1021/ja00417a037.

(30)   Bernardi, F.; Cherry, W.; Epiotis, N. D.; Cherry, W.; Schlegel, H. B.; Whangbo, M. H.; Wolfe, S. A Molecular Orbital Interpretation of the Static, Dynamic, and Chemical Properties of CH_2X Radicals. *J. Am. Chem. Soc.* **1976**, *98*, 469–478. https://doi.org/10.1021/ja00418a024.

(31)   Henry, D. J.; Parkinson, C. J.; Mayer, P. M.; Radom, L. Bond Dissociation Energies and Radical Stabilization Energies Associated with Substituted Methyl Radicals. *J. Phys. Chem. A* **2001**, *105*, 6750–6756. https://doi.org/10.1021/jp010442c.

(32)   Fossey, J.; Lefort, D.; Sorba, J.; Davies, A. G.; Lomas, J.; Ourisson, G. *Free Radicals in Organic Chemistry*; Wiley, 1995.

(33)   Dolbier, W. R. Structure, Reactivity, and Chemistry of Fluoroalkyl Radicals. *Chem. Rev.* **1996**, *96*, 1557–1584. https://doi.org/10.1021/cr941142c.

(34)   De Vleeschouwer, F.; Van Speybroeck, V.; Waroquier, M.; Geerlings, P.; De Proft, F. Electrophilicity and Nucleophilicity Index for Radicals. *Org. Lett.* **2007**, *9*, 2720–2724. https://doi.org/10.1021/ol071038k.

(35)   Huynh, M. T.; Anson, C. W.; Cavell, A. C.; Stahl, S. S.; Hammes-Schiffer, S. Quinone 1 e$^-$ and 2 e$^-$/2 H$^+$ Reduction Potentials: Identification and Analysis of Deviations from Systematic Scaling Relationships. *J. Am. Chem. Soc.* **2016**, *138*, 15903–15910. https://doi.org/10.1021/jacs.6b05797.

(36) Hünig, S.; Bau, R.; Kemmer, M.; Meixner, H.; Metzenthin, T.; Peters, K.; Sinzger, K.; Gulbis, J. 2,5-Disubstituted *N,N′*-Dicyanoquinone Diimines (DCNQIs) - Syntheses, and Redox Properties. *Eur. J. Org. Chem.* **1998**, 335–348. https://doi.org/10.1002/(SICI)1099-0690(199802)1998:2<335::AID-EJOC335>3.0.CO;2-A.

(37) Lanfranchi, D. A.; Belorgey, D.; Müller, T.; Vezin, H.; Lanzer, M.; Davioud-Charvet, E. Exploring the Trifluoromenadione Core as a Template to Design Antimalarial Redox-Active Agents Interacting with Glutathione Reductase. *Org. Biomol. Chem.* **2012**, *10*, 4795–4806. https://doi.org/10.1039/c2ob25229e.

(38) Schareina, T.; Wu, X. F.; Zapf, A.; Cotté, A.; Gotta, M.; Beller, M. Towards a Practical and Efficient Copper-Catalyzed Trifluoromethylation of Aryl Halides. *Top. Catal.* **2012**, *55*, 426–431. https://doi.org/10.1007/s11244-012-9824-0.

(39) Johansen, M. B.; Lindhardt, A. T. Copper-Catalyzed and Additive Free Decarboxylative Trifluoromethylation of Aromatic and Heteroaromatic Iodides. *Org. Biomol. Chem.* **2020**, *18*, 1417–1425. https://doi.org/10.1039/c9ob02635e.

(40) Wang, X.; Ye, Y.; Ji, G.; Xu, Y.; Zhang, S.; Feng, J.; Zhang, Y.; Wang, J. Copper-Catalyzed Direct C-H Trifluoromethylation of Quinones. *Org. Lett.* **2013**, *15*, 3730–3733. https://doi.org/10.1021/ol4016095.

(41) Ilchenko, N. O.; Janson, P. G.; Szabó, K. J. Copper-Mediated C-H Trifluoromethylation of Quinones. *Chem. Commun.* **2013**, *49*, 6614–6616. https://doi.org/10.1039/c3cc43357a.

(42) Fiederling, N.; Haller, J.; Schramm, H. Notification about the Explosive Properties of Togni's Reagent II and One of Its Precursors. *Org. Process Res. Dev.* **2013**, *17*, 318–319. https://doi.org/10.1021/op400035b.

(43) Ji, Y.; Brueckl, T.; Baxter, R. D.; Fujiwara, Y.; Seiple, I. B.; Su, S.; Blackmond, D. G.; Baran, P. S. Innate C-H Trifluoromethylation of Heterocycles. *Proc. Natl. Acad. Sci. U. S. A.* **2011**, *108*, 14411–14415. https://doi.org/10.1073/pnas.1109059108.

(44) Langlois, B. R.; Laurent, E.; Roidot, N. Trifluoromethylation of Aromatic Compounds with Sodium Trifluoromethanesulfinate under Oxidative Conditions. *Tetrahedron Lett.* **1991**, *32*, 7525–7528. https://doi.org/10.1016/0040-4039(91)80524-A.

(45) Kielty, P.; Farràs, P.; McArdle, P.; Smith, D. A.; Aldabbagh, F. Visible-Light Unmasking of Heterocyclic Quinone Methide Radicals from Alkoxyamines. *Chem. Commun.* **2019**, *55*, 14665–14668. https://doi.org/10.1039/C9CC08261A.

(46) Kong, W.; Casimiro, M.; Merino, E.; Nevado, C. Copper-Catalyzed One-Pot Trifluoromethylation/Aryl Migration/ Desulfonylation and $C(sp^2)$-N Bond Formation of Conjugated Tosyl Amides. *J. Am. Chem. Soc.* **2013**, *135*, 14480–14483. https://doi.org/10.1021/ja403954g.

(47) Li, J.; Zhang, X.; Xiang, H.; Tong, L.; Feng, F.; Xie, H.; Ding, J.; Yang, C. C-H Trifluoromethylation of 2-Substituted/Unsubstituted Aminonaphthoquinones at Room Temperature with Bench-Stable $(CF_3SO_2)_2Zn$: Synthesis and Antiproliferative Evaluation. *J. Org. Chem.* **2017**, *82*, 6795–6800. https://doi.org/10.1021/acs.joc.7b00940.

(48) Baxter, R. D.; Blackmond, D. G. In Situ Kinetic Studies of the Trifluoromethylation of Caffeine with $Zn(SO_2CF_3)_2$. *Tetrahedron* **2013**, *69*, 5604–5608. https://doi.org/10.1016/j.tet.2013.04.007.

(49) Carter-Cooper, B. A.; Fletcher, S.; Ferraris, D.; Choi, E. Y.; Kronfli, D.; Dash, S.; Truong, P.; Sausville, E. A.; Lapidus, R. G.; Emadi, A. Synthesis, Characterization and Antineoplastic Activity of Bis-Aziridinyl Dimeric Naphthoquinone – A Novel Class of Compounds with Potent Activity against Acute Myeloid Leukemia Cells. *Bioorg. Med. Chem. Lett.* **2017**, *27*, 6–10. https://doi.org/10.1016/j.bmcl.2016.11.045.

(50) Yan, F.; Cao, X. X.; Jiang, H. X.; Zhao, X. L.; Wang, J. Y.; Lin, Y. H.; Liu, Q. L.; Zhang, C.; Jiang, B.; Guo, F. A Novel Water-Soluble Gossypol Derivative Increases Chemotherapeutic Sensitivity and Promotes Growth Inhibition in Colon Cancer. *J. Med. Chem.* **2010**, *53*, 5502–5510. https://doi.org/10.1021/jm1001698.

(51) Emadi, A.; Le, A.; Harwood, C. J.; Stagliano, K. W.; Kamangar, F.; Ross, A. E.; Cooper, C. R.; Dang, C. V.; Karp, J. E.; Vuica-Ross, M. Metabolic and Electrochemical Mechanisms of Dimeric Naphthoquinones Cytotoxicity in Breast Cancer Cells. *Bioorg. Med. Chem.* **2011**, *19*, 7057–7062. https://doi.org/10.1016/j.bmc.2011.10.005.

(52) Emadi, A.; Harwood, J. S.; Kohanim, S.; Stagliano, K. W. Regiocontrolled Synthesis of the Trimeric Quinone Framework of Conocurvone. *Org. Lett.* **2002**, *4*, 521–524. https://doi.org/10.1021/ol010272m.

(53) Yu, M.; Malinakova, H. C.; Stagliano, K. W. A New Method for the Synthesis of 2-Hydroxy-3-Nitro-1,4-Naphthoquinones: Application to Regiospecific Preparation of Unsymmetrical Nitrobiquinones. *J. Org. Chem.* **2006**, *71*, 6648–6651. https://doi.org/10.1021/jo060825c.

(54) Dai, F.; Yan, W. J.; Fu, X.; Zheng, Y. L.; Du, Y. T.; Bao, X. Z.; Kang, Y. F.; Jin, X. L.; Zhou, B. Designing Dichlorobinaphthoquinone as a Prooxidative Anticancer Agent Based on Hydrogen Peroxide-Responsive in Situ Production of Hydroxyl Radicals. *Eur. J. Med. Chem.* **2018**, *159*, 317–323. https://doi.org/10.1016/j.ejmech.2018.09.075.

(55) Bringmann, G.; Ledermann, A.; Stahl, M.; Gulden, K. P. Bismurrayaquinone A: Synthesis, Chromatographic Enantiomer Resolution, and Stereoanalysis by Computational and Experimental CD Investigations. *Tetrahedron* **1995**, *51*, 9353–9360. https://doi.org/10.1016/0040-4020(95)00528-G.

(56) Murphy, W. S.; Bertrand, M. Bromoquinone – Enaminone Annulations: Syntheses of Murrayaquinone-A and (±)-Bismurrayaquinone-A. *J. Chem. Soc., Perkin Trans. 1* **1998**, 4115–4120.

(57) Konkol, L. C.; Guo, F.; Sarjeant, A. A.; Thomson, R. J. Enantioselective Total Synthesis and Studies into the Configurational Stability of Bismurrayaquinone A. *Angew. Chem. Int. Ed.* **2011**, *50*, 9931–9934. https://doi.org/10.1002/anie.201104726.

(58) Gellis, A.; Kovacic, H.; Boufatah, N.; Vanelle, P. Synthesis and Cytotoxicity Evaluation of Some Benzimidazole-4,7-diones as Bioreductive Anticancer Agents. *Eur. J. Med. Chem.* **2008**, *43*, 1858–1864. https://doi.org/10.1016/j.ejmech.2007.11.020.

(59) Conboy, D.; Mirallai, S. I.; Craig, A.; McArdle, P.; Al-Kinani, A. A.; Barton, S.; Aldabbagh, F. Incorporating Morpholine and Oxetane into Benzimidazolequinone Antitumor Agents: The Discovery of 1,4,6,9-Tetramethoxyphenazine from Hydrogen Peroxide and Hydroiodic Acid-Mediated Oxidative Cyclizations. *J. Org. Chem.* **2019**, *84*, 9811–9818. https://doi.org/10.1021/acs.joc.9b01427.

(60) Love, B.; Bonner-Stewart, J.; Forrest, L. Improved Synthesis of Diquinones. *Synlett* **2009**, 813–817. https://doi.org/10.1055/s-0028-1087937.

(61) Jacob, P.; Callery, P. S.; Shulgin, A. T.; Castagnoli, N. A Convenient Synthesis of Quinones from Hydroquinone Dimethyl Ethers. Oxidative Demethylation with Ceric Ammonium Nitrate. *J. Org. Chem.* **1976**, *41*, 3627–3629. https://doi.org/10.1021/jo00884a035.

(62) Ji Ram, V.; Sethi, A.; Nath, M.; Pratap, R. *The Chemistry of Heterocycles*; Elsevier, 2019; pp 149-478. https://doi.org/10.1016/b978-0-08-101033-4.00005-x.

(63) Love, B. E.; Simmons, A. L. Substituent Effects in the Oxidation of 2-Alkyl-1,4-Dialkoxybenzenes with Ceric Ammonium Nitrate. *Tetrahedron Lett.* **2016**, *57*, 5712–5715. https://doi.org/10.1016/j.tetlet.2016.11.042.

(64) Eberson, L.; Hartshorn, M. P.; Persson, O. 1,1,1,3,3,3-Hexafluoropropan-2-ol as a Solvent for the Generation of Highly Persistent Radical Cations. *J. Chem. Soc. Perkin Trans. 2* **1995**, 1735–1744. https://doi.org/10.1039/p29950001735.

(65) Colomer, I.; Chamberlain, A. E. R.; Haughey, M. B.; Donohoe, T. J. Hexafluoroisopropanol as a Highly Versatile Solvent. *Nat. Rev. Chem.* **2017**, *1*, 0088. https://doi.org/10.1038/s41570-017-0088.

(66) Shalit, H.; Dyadyuk, A.; Pappo, D. Selective Oxidative Phenol Coupling by Iron Catalysis. *J. Org. Chem.* **2019**, *84*, 1677–1686. https://doi.org/10.1021/acs.joc.8b03084.

(67) Gaster, E.; Vainer, Y.; Regev, A.; Narute, S.; Sudheendran, K.; Werbeloff, A.; Shalit, H.; Pappo, D. Significant Enhancement in the Efficiency and Selectivity of Iron-Catalyzed Oxidative Cross-Coupling of Phenols by Fluoroalcohols. *Angew. Chem. Int. Ed.* **2015**, *54*, 4198–4202. https://doi.org/10.1002/anie.201409694.

(68) Hong, D. P.; Hoshino, M.; Kuboi, R.; Goto, Y. Clustering of Fluorine-Substituted Alcohols as a Factor Responsible for Their Marked Effects on Proteins and Peptides. *J. Am. Chem. Soc.* **1999**, *121*, 8427–8433. https://doi.org/10.1021/ja990833t.

(69) Fioroni, M.; Burger, K.; Mark, A. E.; Roccatano, D. Model of 1,1,1,3,3,3-Hexafluoro-Propan-2-ol for Molecular Dynamics Simulations. *J. Phys. Chem. B* **2001**, *105*, 10967–10975. https://doi.org/10.1021/jp012476q.

(70) Adams, A. M.; Du Bois, J. Organocatalytic C-H Hydroxylation with Oxone® Enabled by an Aqueous Fluoroalcohol Solvent System. *Chem. Sci.* **2014**, *5*, 656–659. https://doi.org/10.1039/c3sc52649f.

(71) Kielty, P. Heterocyclic Chemistry: Controlled Unmasking of Nitric Oxide and Nitroxides. PhD Thesis, National University of Ireland Galway, 2020.

(72) Ben-Daniel, R.; De Visser, S. P.; Shaik, S.; Neumann, R. Electrophilic Aromatic Chlorination and Haloperoxidation of Chloride Catalyzed by Polyfluorinated Alcohols: A New Manifestation of Template Catalysis. *J. Am. Chem. Soc.* **2003**, *125*, 12116–12117. https://doi.org/10.1021/ja0364524.

(73) Isse, A. A.; Lin, C. Y.; Coote, M. L.; Gennaro, A. Estimation of Standard Reduction Potentials of Halogen Atoms and Alkyl Halides. *J. Phys. Chem. B* **2011**, *115*, 678–684. https://doi.org/10.1021/jp109613t.

(74) Wagner, T.; Magill, C. R.; Herrle, J. O. Carbon Isotopes. In *Encyclopedia of Geochemistry. Encyclopedia of Earth Sciences Series*; White, W. M., Ed.; Springer, Cham, 2018; pp 194–204. https://doi.org/10.1007/978-3-319-39312-4_176.

(75) Lynch, M.; Hehir, S.; Kavanagh, P.; Leech, D.; O'Shaughnessy, J.; Carty, M. P.; Aldabbagh, F. Synthesis by Radical Cyclization and Cytotoxicity of Highly Potent Bioreductive Alicyclic Ring Fused [1,2-*a*]Benzimidazolequinones. *Chem. Eur. J.* **2007**, *13*, 3218–3226. https://doi.org/10.1002/chem.200601450.

(76) Nyffeler, P. T.; Durón, S. G.; Burkart, M. D.; Vincent, S. P.; Wong, C. H. Selectfluor: Mechanistic Insight and Applications. *Angew. Chem. Int. Ed.* **2004**, *44*, 192–212. https://doi.org/10.1002/anie.200400648.

(77) Stavber, S. Recent Advances in the Application of Selectfluor™ F-TEDA-BF$_4$ as a Versatile Mediator or Catalyst in Organic Synthesis. *Molecules* **2011**, *16*, 6432–6464. https://doi.org/10.3390/molecules16086432.

(78) Campbell, M. G.; Ritter, T. Modern Carbon-Fluorine Bond Forming Reactions for Aryl Fluoride Synthesis. *Chem. Rev.* **2015**, *115*, 612–633. https://doi.org/10.1021/cr500366b.

(79) Stavber, G.; Zupan, M.; Jereb, M.; Stavber, S. Selective and Effective Fluorination of Organic Compounds in Water Using Selectfluor F-TEDA-BF$_4$. *Org. Lett.* **2004**, *6*, 4973–4976. https://doi.org/10.1021/ol047867c.

(80) Fujiwara, Y.; Domingo, V.; Seiple, I. B.; Gianatassio, R.; Del Bel, M.; Baran, P. S. Practical C-H Functionalization of Quinones with Boronic Acids. *J. Am. Chem. Soc.* **2011**, *133*, 3292–3295. https://doi.org/10.1021/ja111152z.

(81)   Galloway, J. D.; Mai, D. N.; Baxter, R. D. Silver-Catalyzed Minisci Reactions Using Selectfluor as a Mild Oxidant. *Org. Lett.* **2017**, *19*, 5772–5775. https://doi.org/10.1021/acs.orglett.7b02706.

(82)   Sutherland, D. R.; Veguillas, M.; Oates, C. L.; Lee, A. L. Metal-, Photocatalyst-, and Light-Free, Late-Stage C-H Alkylation of Heteroarenes and 1,4-Quinones Using Carboxylic Acids. *Org. Lett.* **2018**, *20*, 6863–6867. https://doi.org/10.1021/acs.orglett.8b02988.

(83)   Wang, Y.; Zhu, S.; Zou, L. H. Recent Advances in Direct Functionalization of Quinones. *Eur. J. Org. Chem.* **2019**, 2179–2201. https://doi.org/10.1002/ejoc.201900028.

Appendix

^{1}H NMR (400 MHz) of 5',8'-Dimethoxy-2,2',3,3'-tetrahydro-1*H*,1'*H*-[6,6'-bipyrrolo[1,2-*a*]benzimidazole]-5,8-dione (5a) in CDCl$_3$
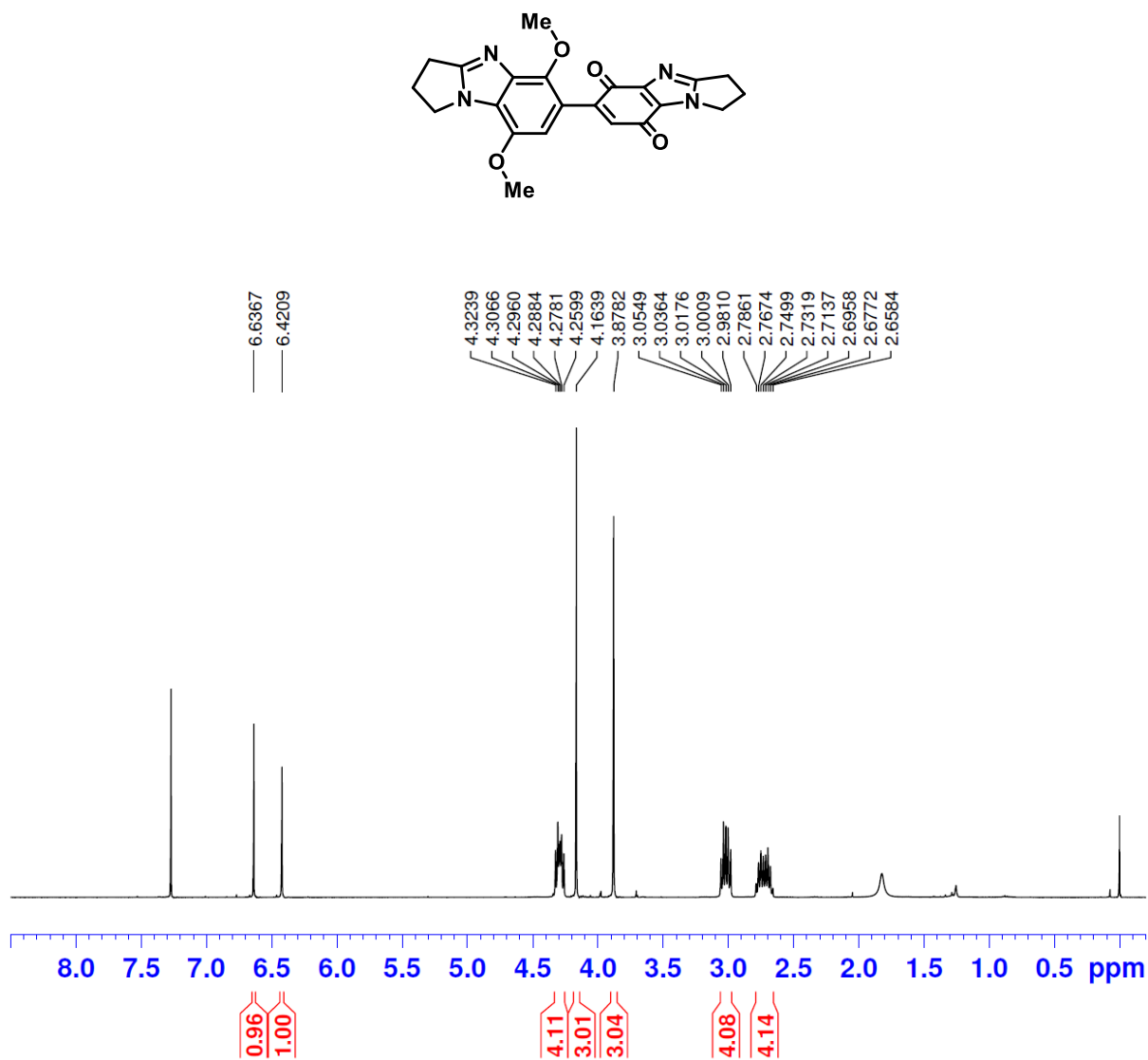
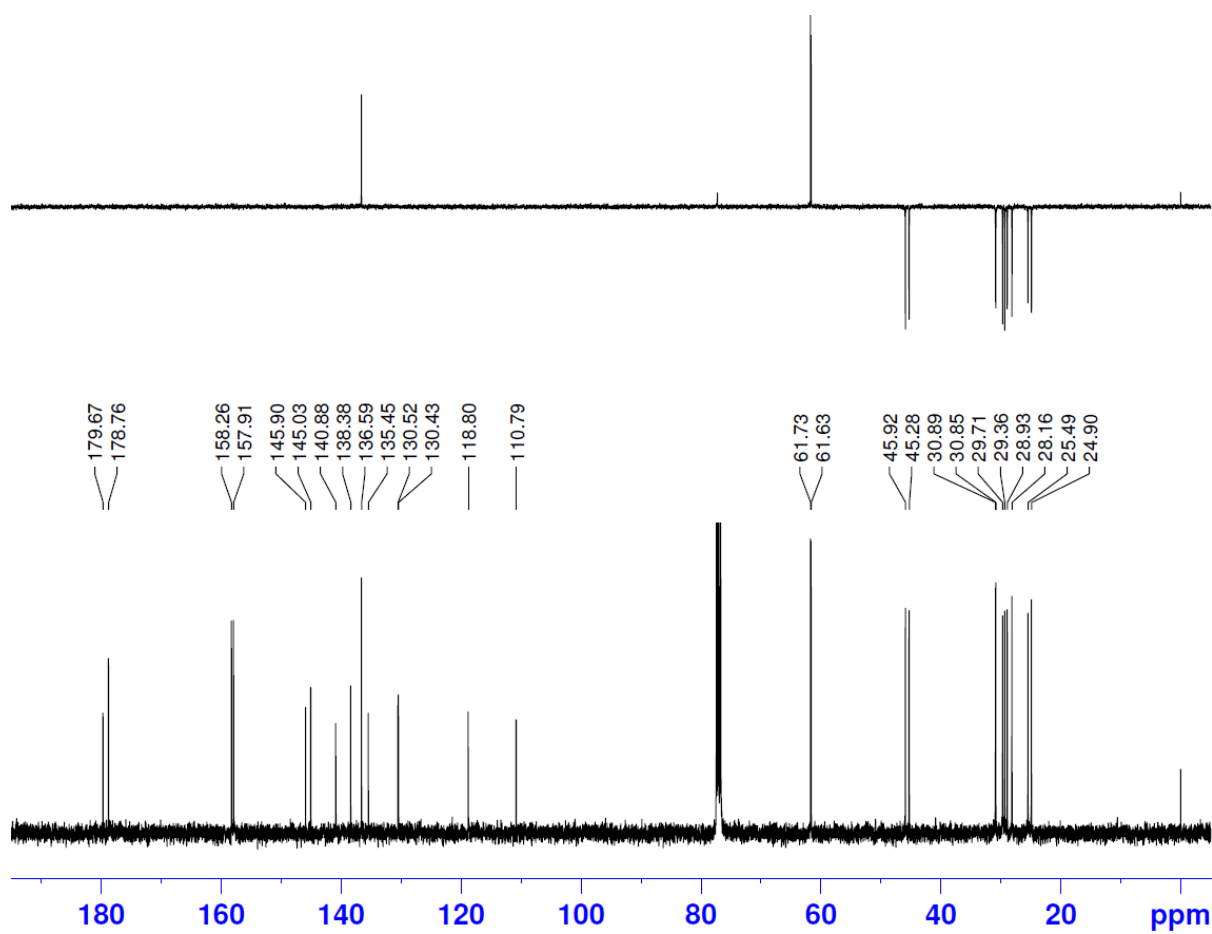# ¹³C NMR (100 MHz) of 5',8'-Dimethoxy-2,2',3,3'-tetrahydro-1*H*,1'*H*-[6,6'-bipyrrolo[1,2-*a*]benzimidazole]-5,8-dione (5a) in CDCl₃
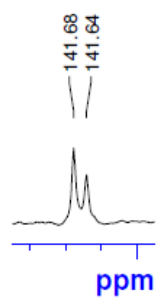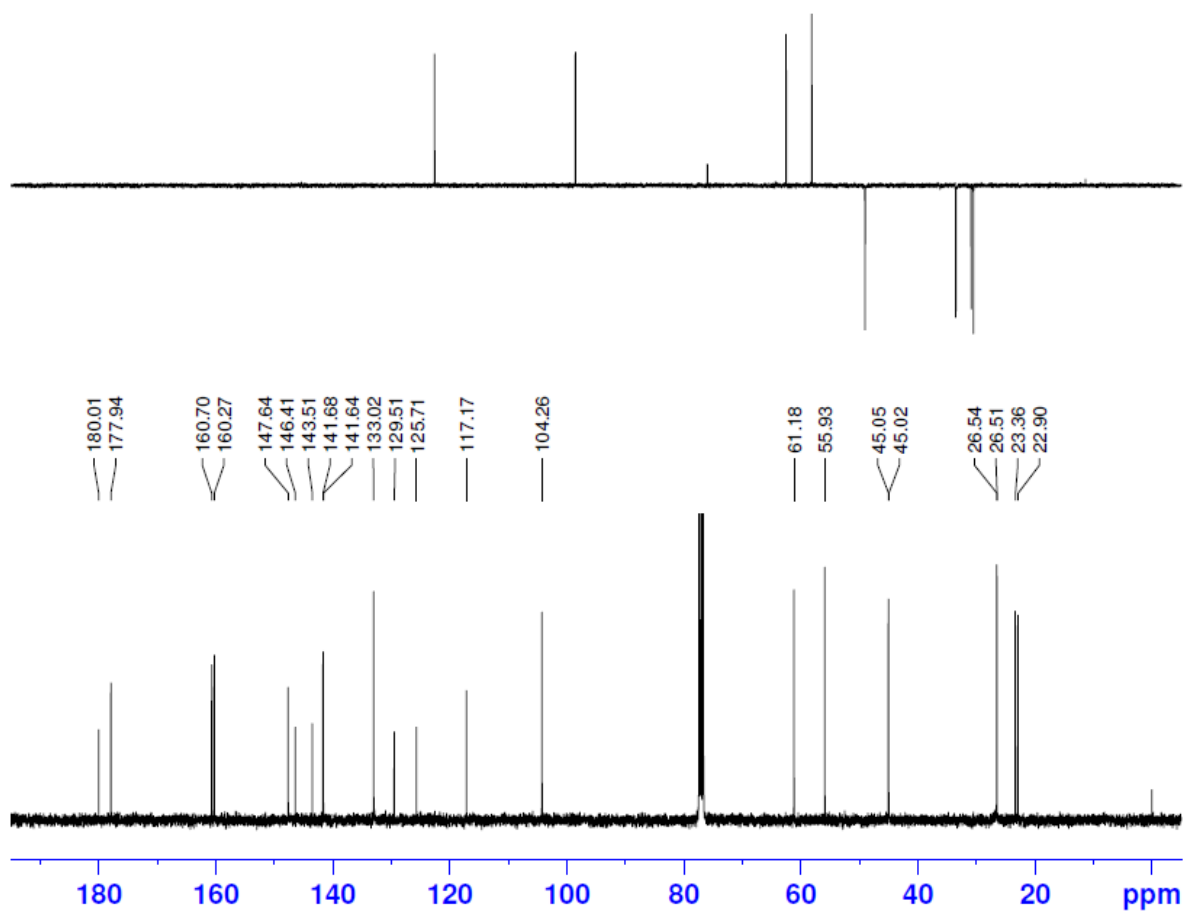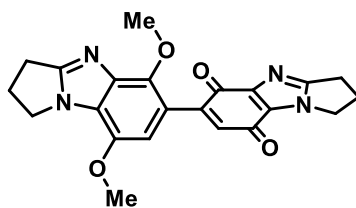
¹H NMR (400 MHz) of 6',9'-Dimethoxy-1,1',2,2',3,3',4,4'-octahydro[7,7'-bipyrido[1,2-a]benzimidazole]-6,9-dione (5b) in CDCl₃
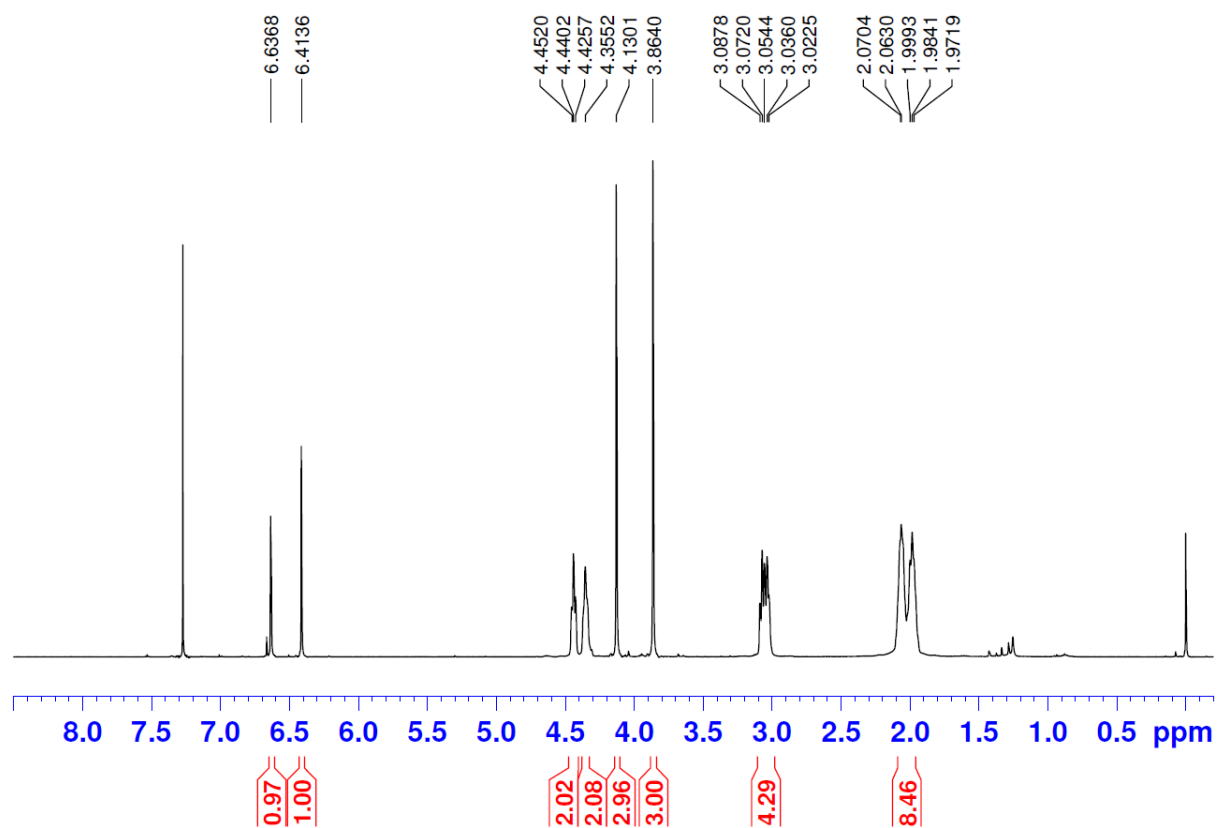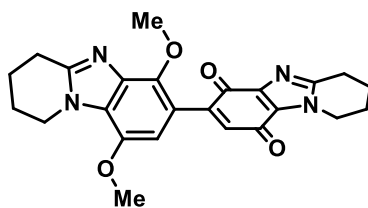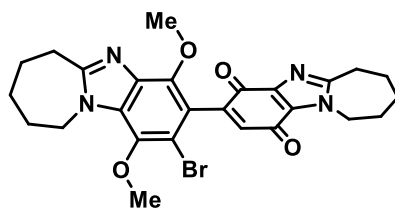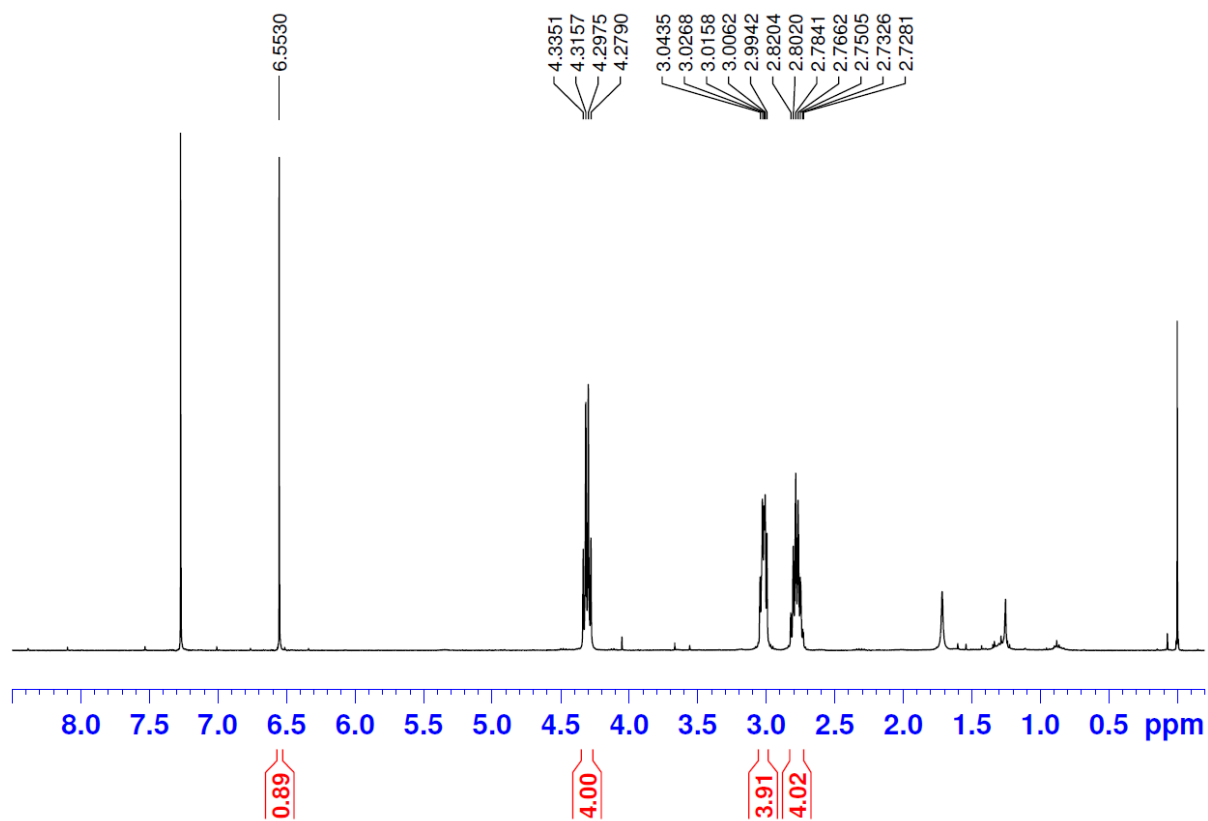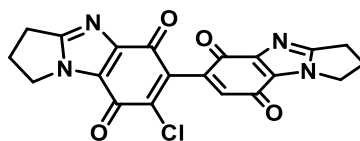
13C NMR (100 MHz) of 6',9'-Dimethoxy-1,1',2,2',3,3',4,4'-octahydro[7,7'-bipyrido[1,2-*a*]benzimidazole]-6,9-dione (5b) in CDCl₃
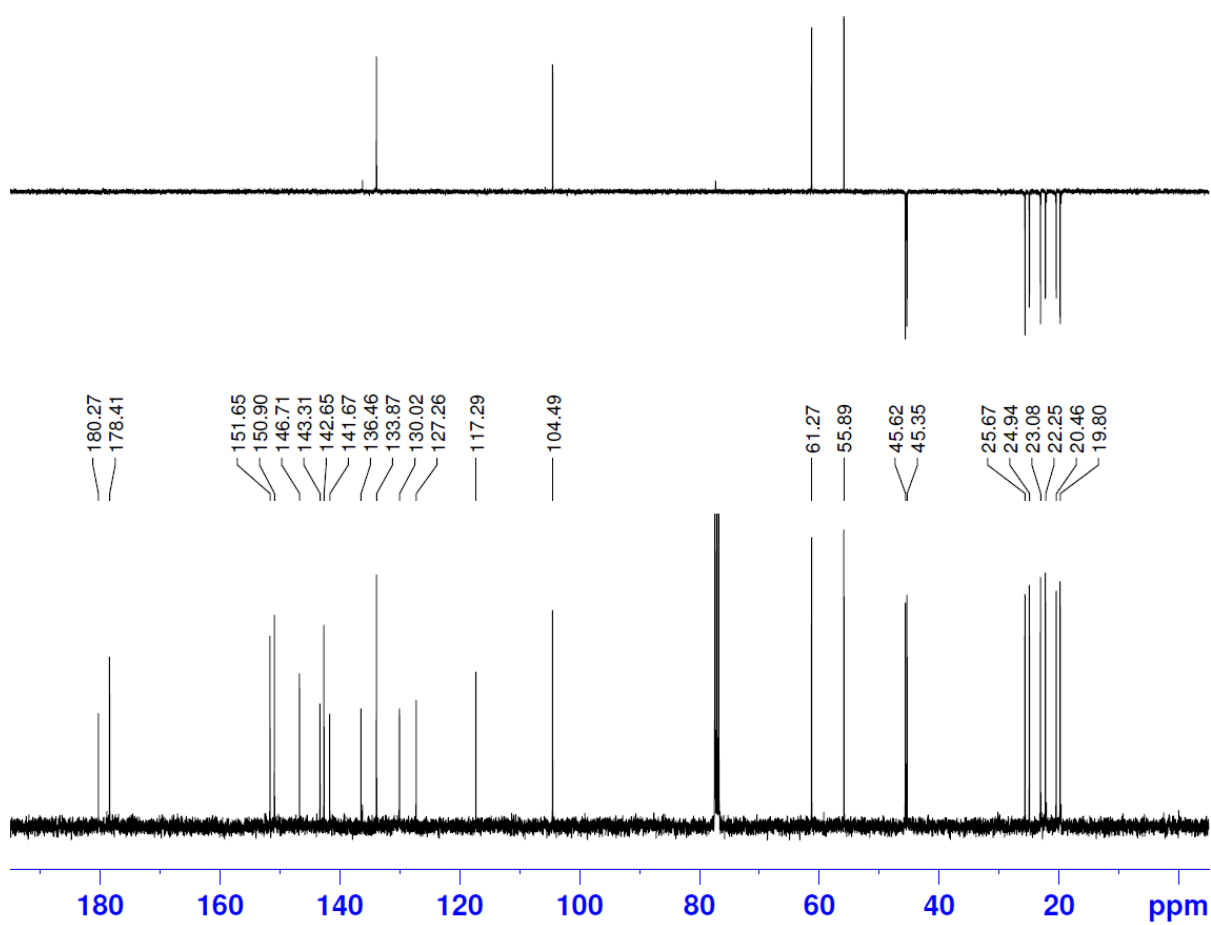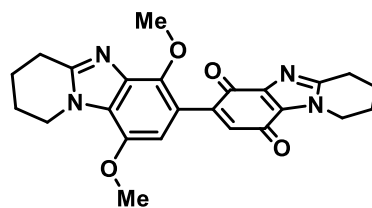
¹H NMR (400 MHz) of 1',4'-Dimethoxy-7,7',8,8',9,9',10,10'-octahydro-4*H*,6'*H*-[3,3'-biazepino[1,2-*a*]benzimidazole]-1,4(6*H*)-dione (5c) in CDCl₃
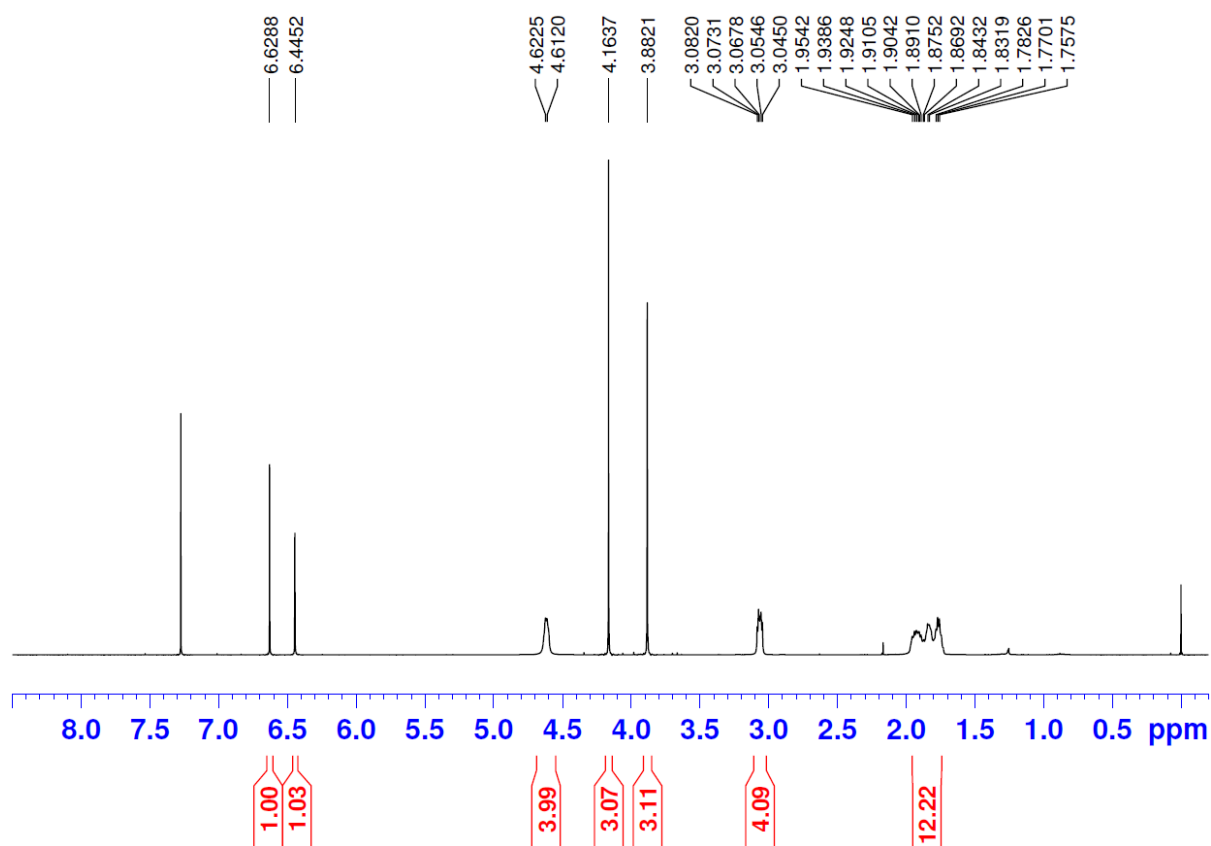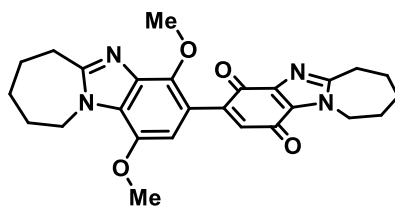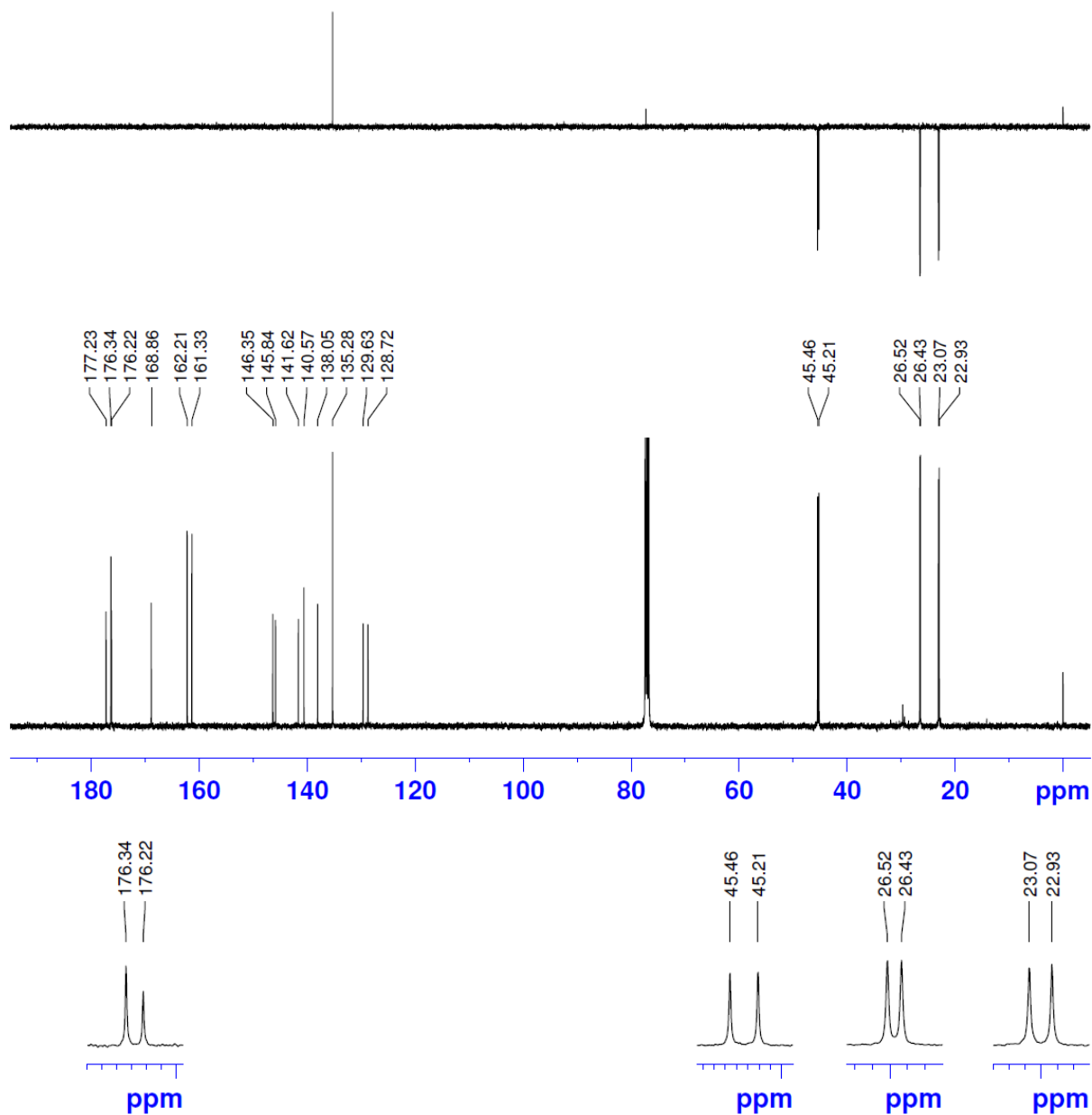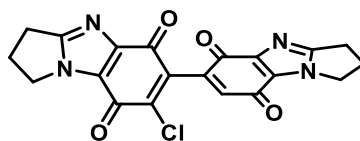
¹³C NMR (100 MHz) of 1',4'-Dimethoxy-7,7',8,8',9,9',10,10'-octahydro-4*H*,6'*H*-[3,3'-biazepino[1,2-*a*]benzimidazole]-1,4(6*H*)-dione (5c) in CDCl₃

180.35
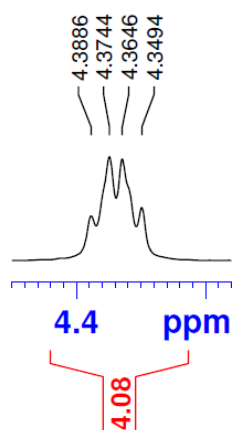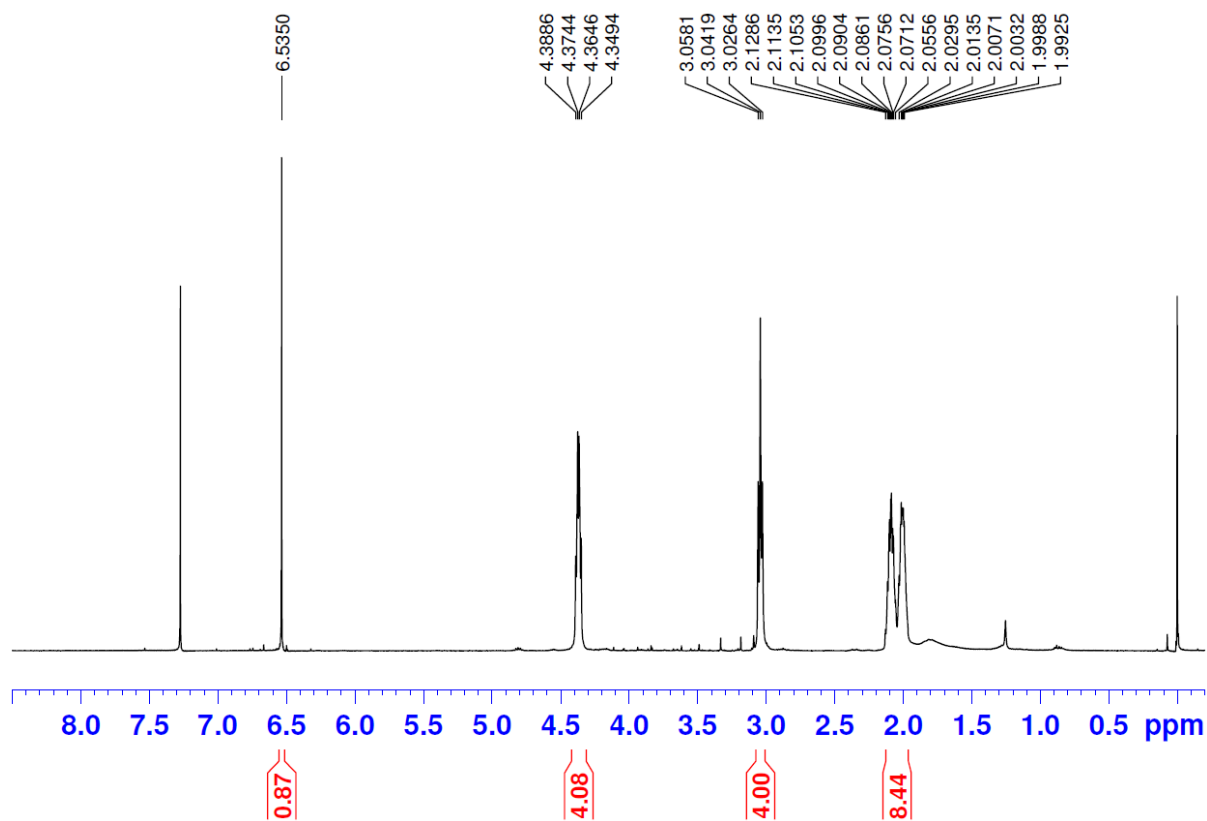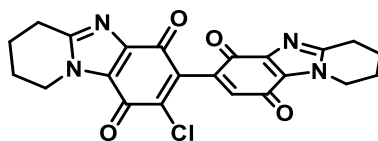178.99
158.09
157.39
146.32
143.69
142.02
141.05
136.19
134.18
130.37
127.84
116.61
105.07
61.42
55.88
46.09
45.82
30.93
30.82
29.77
29.32
28.90
28.25
25.60
24.97

30.93
30.82
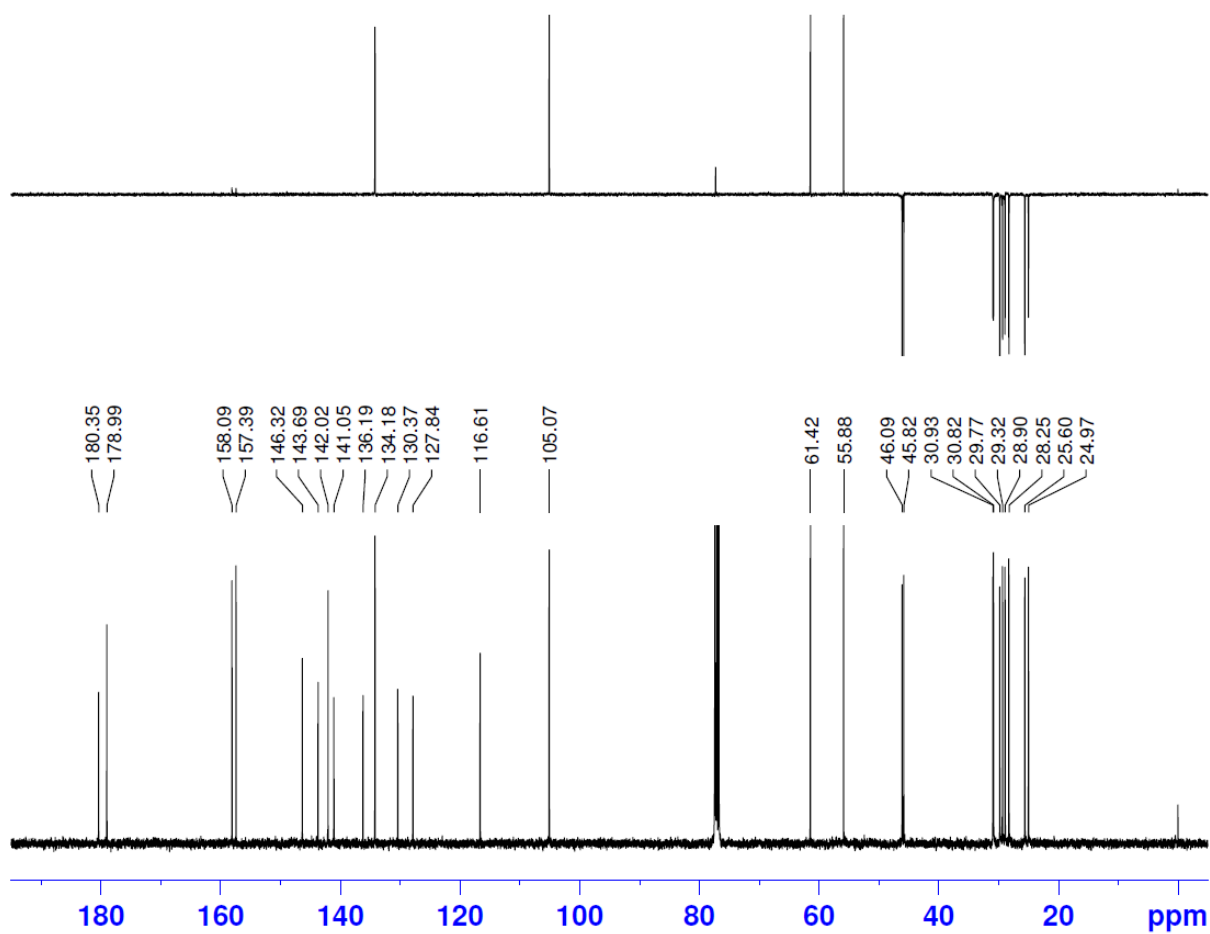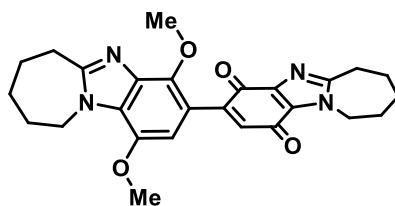
¹H NMR (400 MHz) of 7'-Chloro-5',8'-dimethoxy-2,2',3,3'-tetrahydro-1*H*,1'*H*-[6,6'-bipyrrolo[1,2-*a*]benzimidazole]-5,8-dione (8a) in CDCl₃
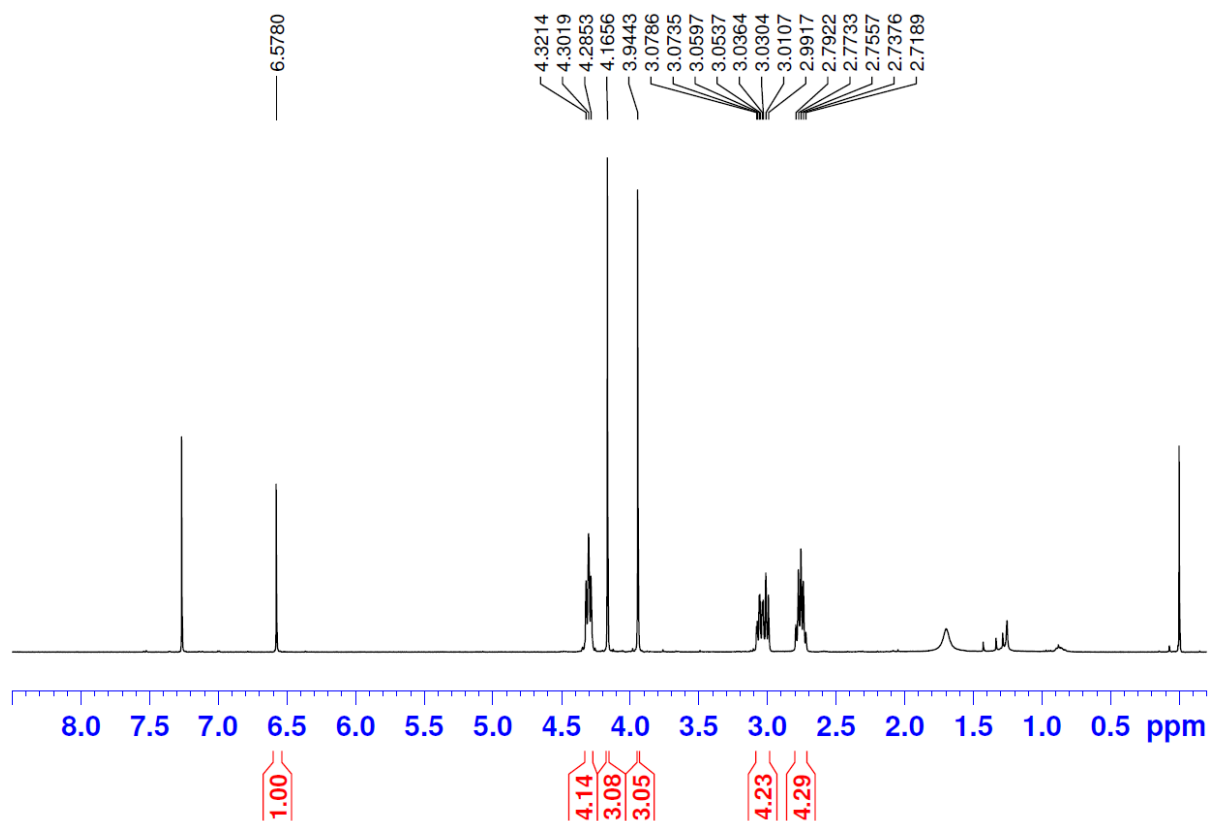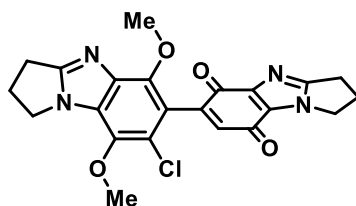
^{13}**C NMR (100 MHz) of 7'-Chloro-5',8'-dimethoxy-2,2',3,3'-tetrahydro-1***H***,1'***H***-[6,6'-bipyrrolo[1,2-***a***]benzimidazole]-5,8-dione (8a) in CDCl₃**
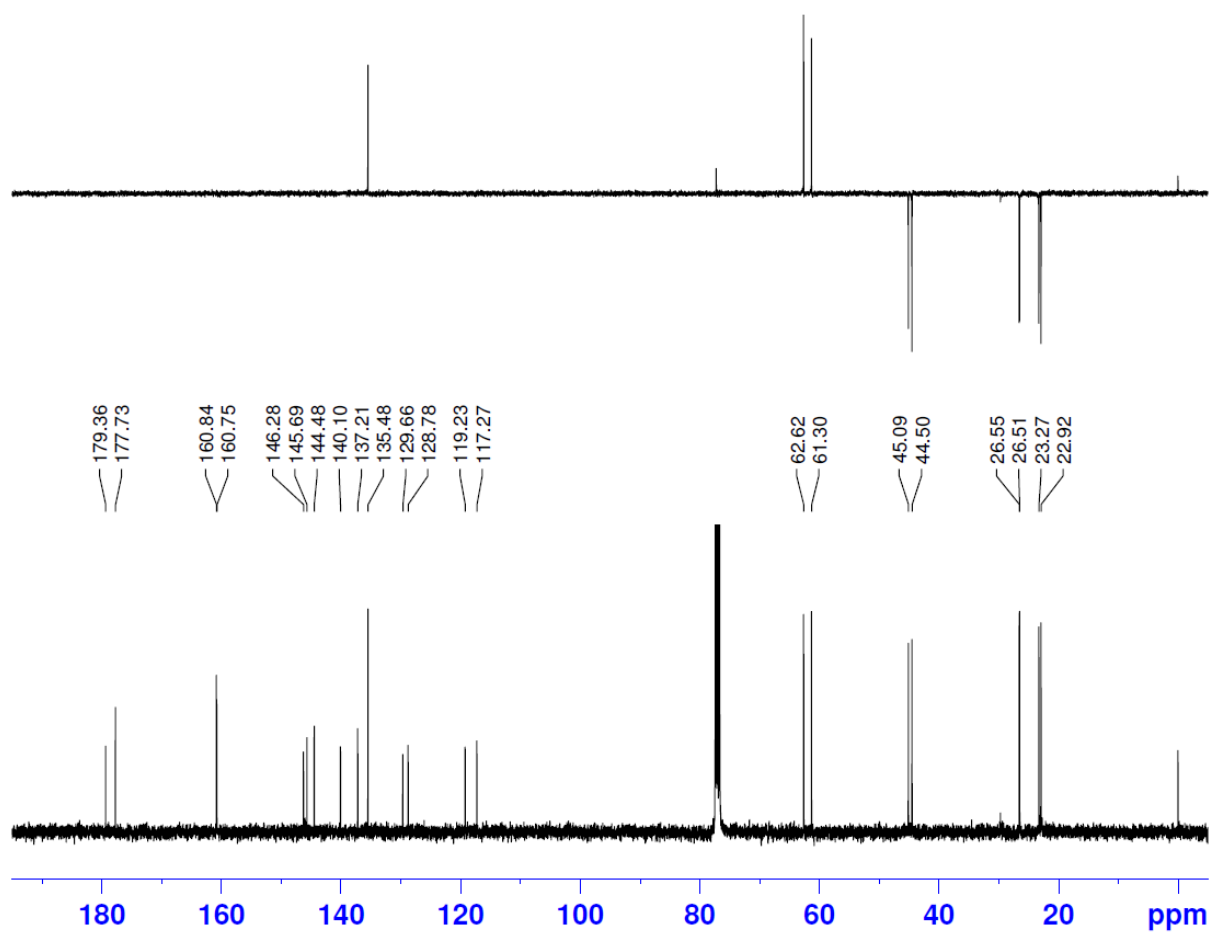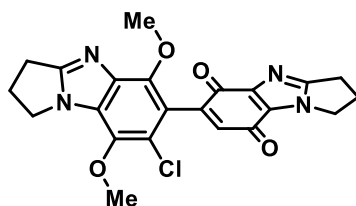
^{1}H NMR (400 MHz) of 8'-Chloro-6',9'-dimethoxy-1,1',2,2',3,3',4,4'-octahydro[7,7'-bipyrido[1,2-a]benzimidazole]-6,9-dione (8b) in CDCl₃

^{13}C NMR (100 MHz) of 8'-Chloro-6',9'-dimethoxy-1,1',2,2',3,3',4,4'-octahydro[7,7'-bipyrido[1,2-*a*]benzimidazole]-6,9-dione (8b) in CDCl$_3$

179.60
178.19
151.73
151.53
145.47
143.79
141.57
138.11
136.29
135.05
130.24
130.19
119.57
117.68
62.50
61.44
45.41
44.81
25.71
24.95
23.04
22.26
20.38
19.81

151.73
151.53
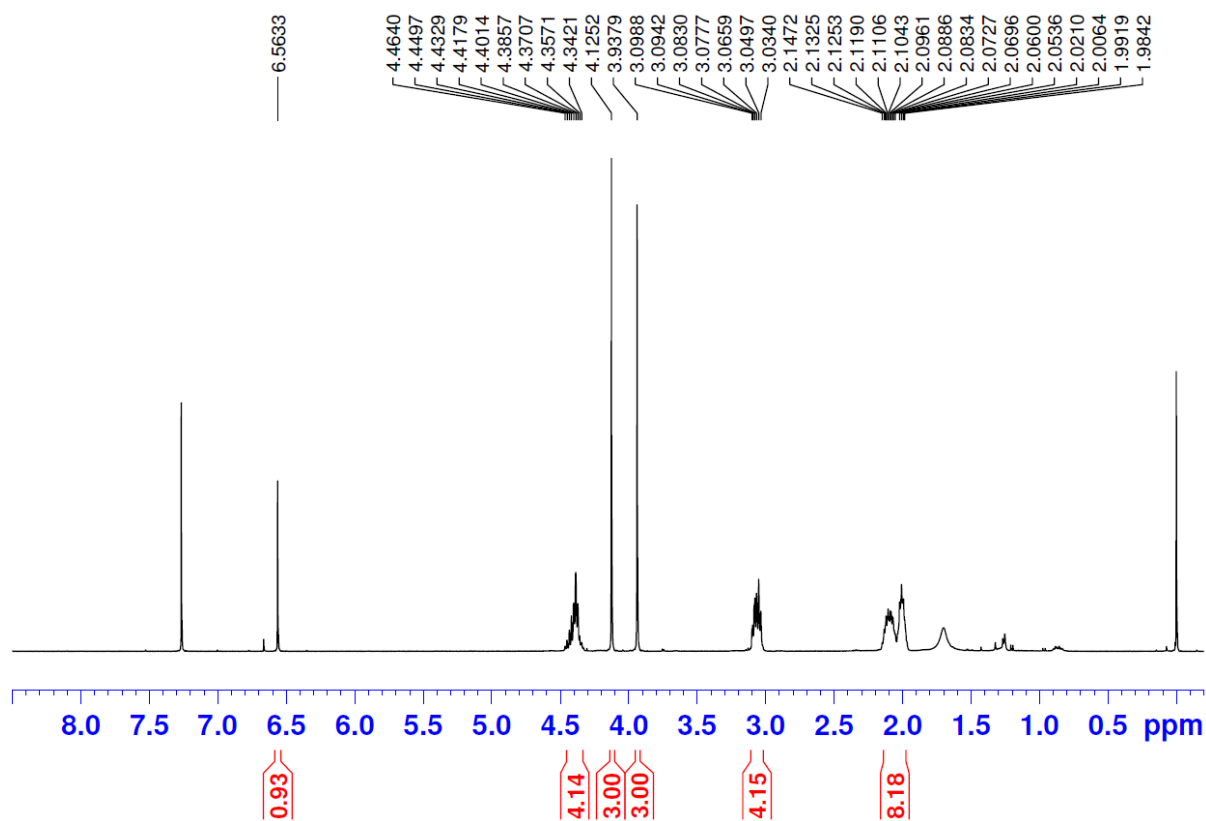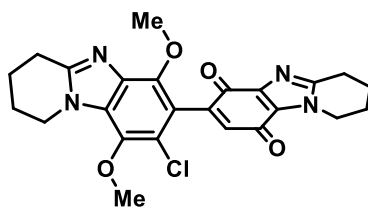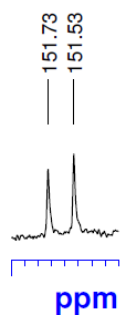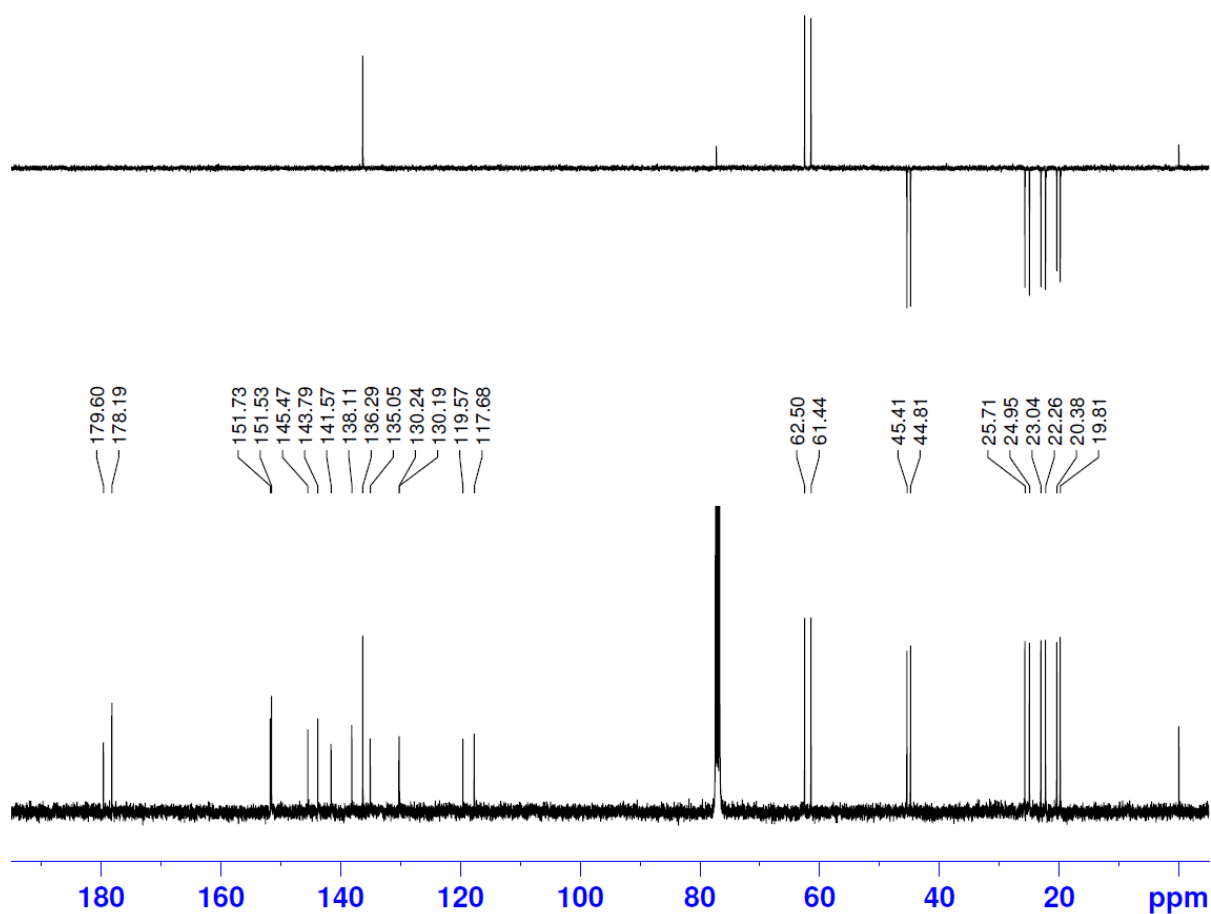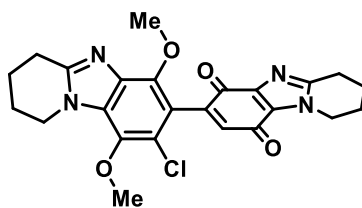
¹H NMR (400 MHz) of 2'-Chloro-1',4'-dimethoxy-7,7',8,8',9,9',10,10'-octahydro-4H,6'H-[3,3'-biazepino[1,2-a]benzimidazole]-1,4(6H)-dione (8c) in CDCl₃
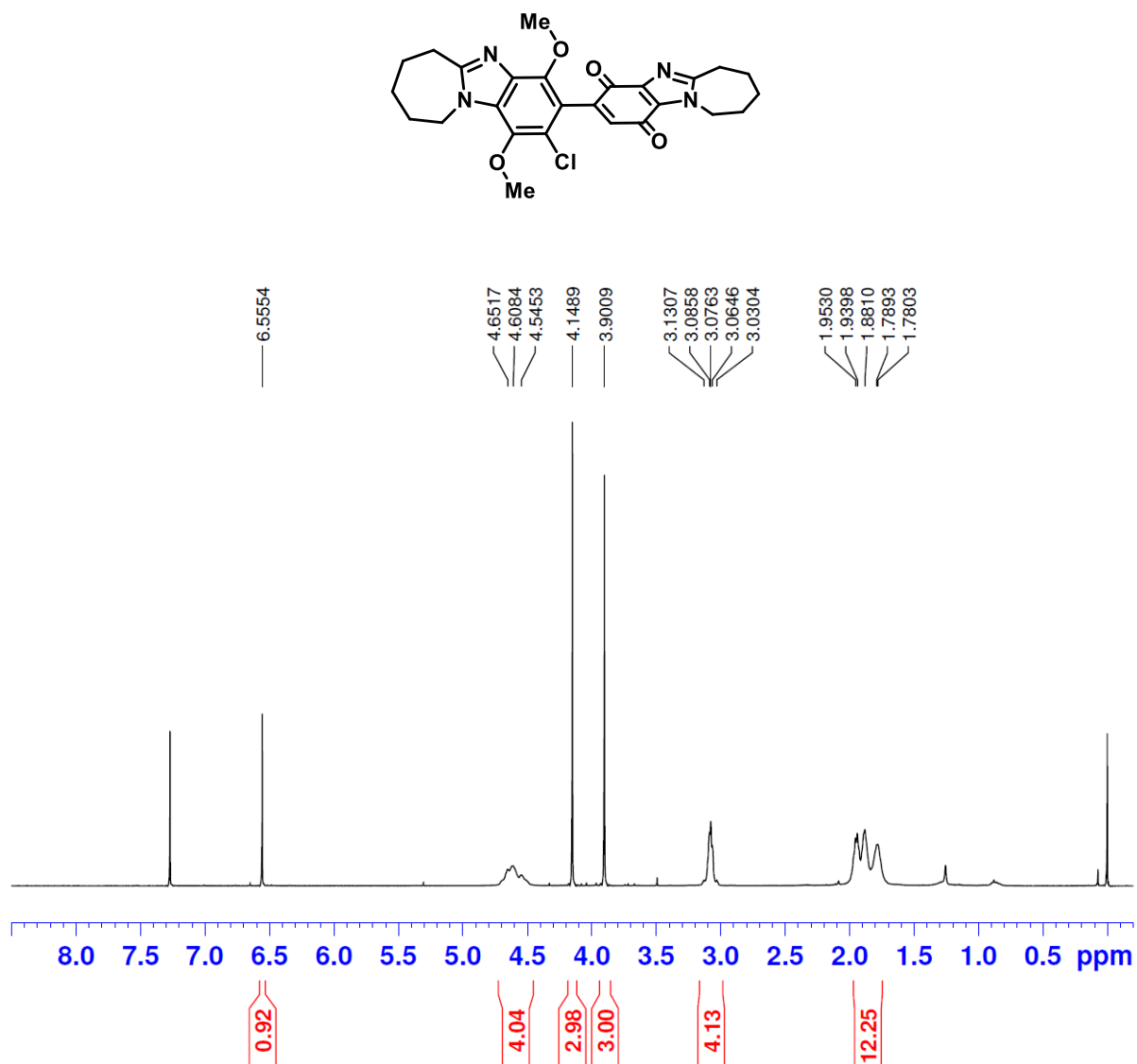
¹³C NMR (100 MHz) of 2'-Chloro-1',4'-dimethoxy-7,7',8,8',9,9',10,10'-octahydro-4*H*,6'*H*-[3,3'-biazepino[1,2-*a*]benzimidazole]-1,4(6*H*)-dione (8c) in CDCl₃

¹H NMR (400 MHz) of 7'-Bromo-5',8'-dimethoxy-2,2',3,3'-tetrahydro-1*H*,1'*H*-[6,6'-bipyrrolo[1,2-*a*]benzimidazole]-5,8-dione (10a) in CDCl₃
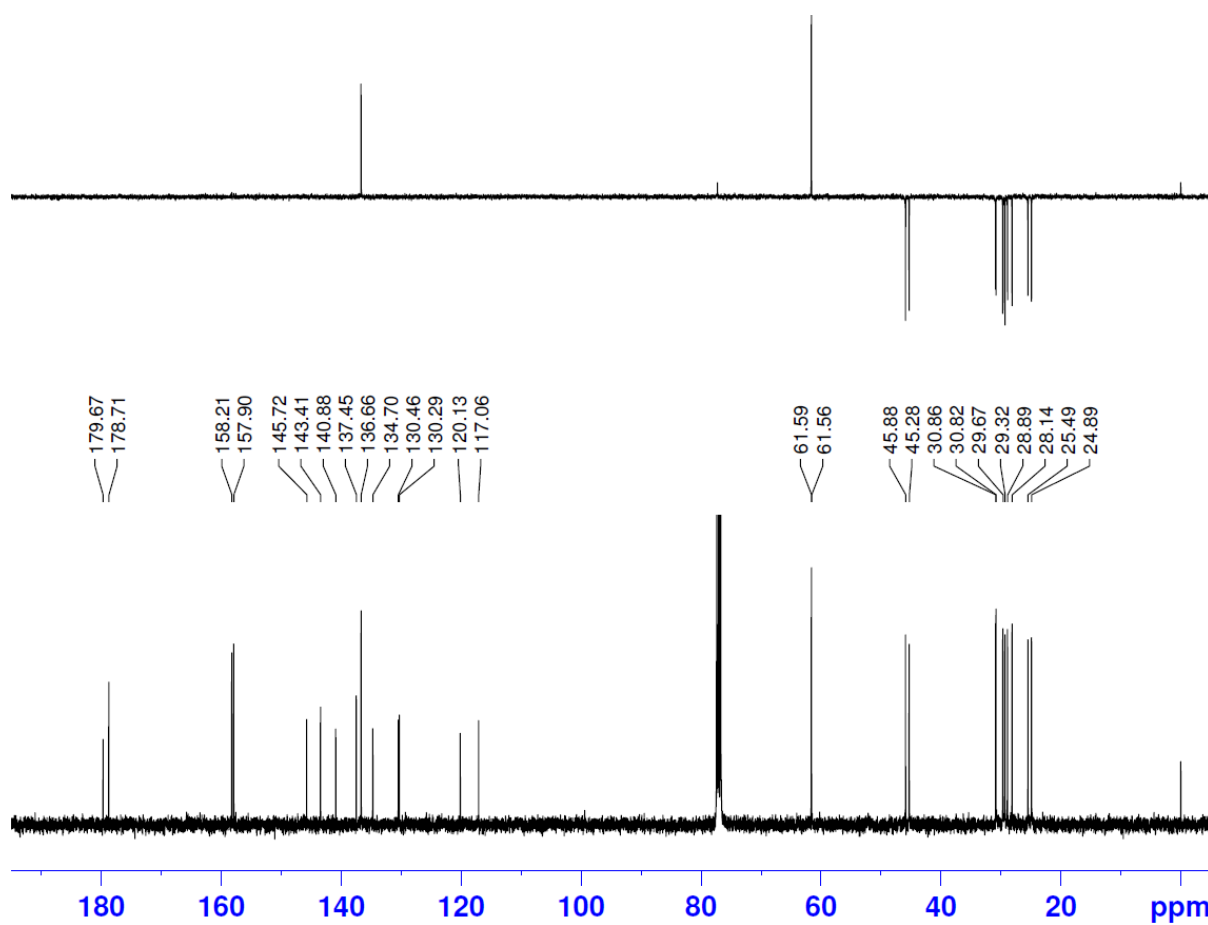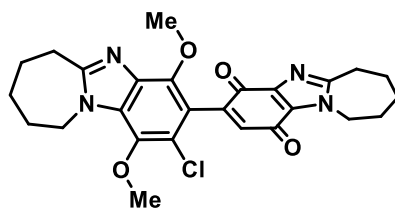
13C NMR (100 MHz) of 7'-Bromo-5',8'-dimethoxy-2,2',3,3'-tetrahydro-1*H*,1'*H*-[6,6'-bipyrrolo[1,2-*a*]benzimidazole]-5,8-dione (10a) in CDCl₃
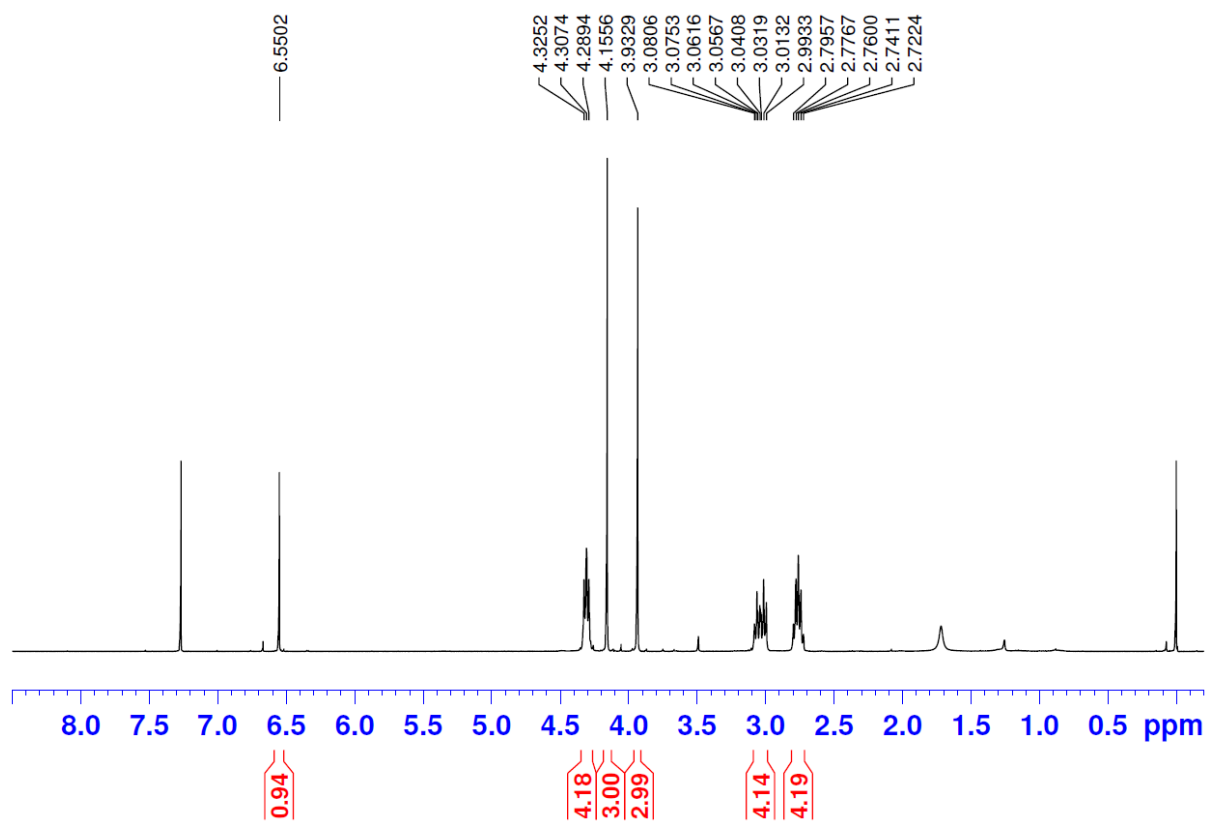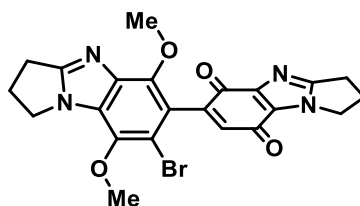
^{13}C NMR (100 MHz) of 7'-Bromo-5',8'-dimethoxy-2,2',3,3'-tetrahydro-1*H*,1'*H*-[6,6'-bipyrrolo[1,2-*a*]benzimidazole]-5,8-dione (10a) in CDCl₃
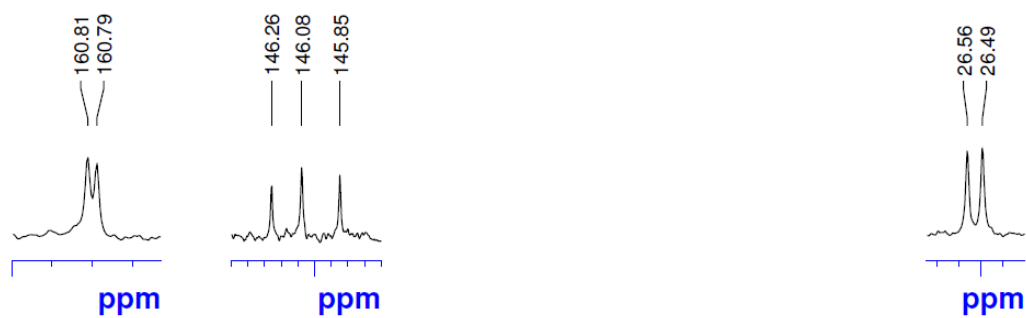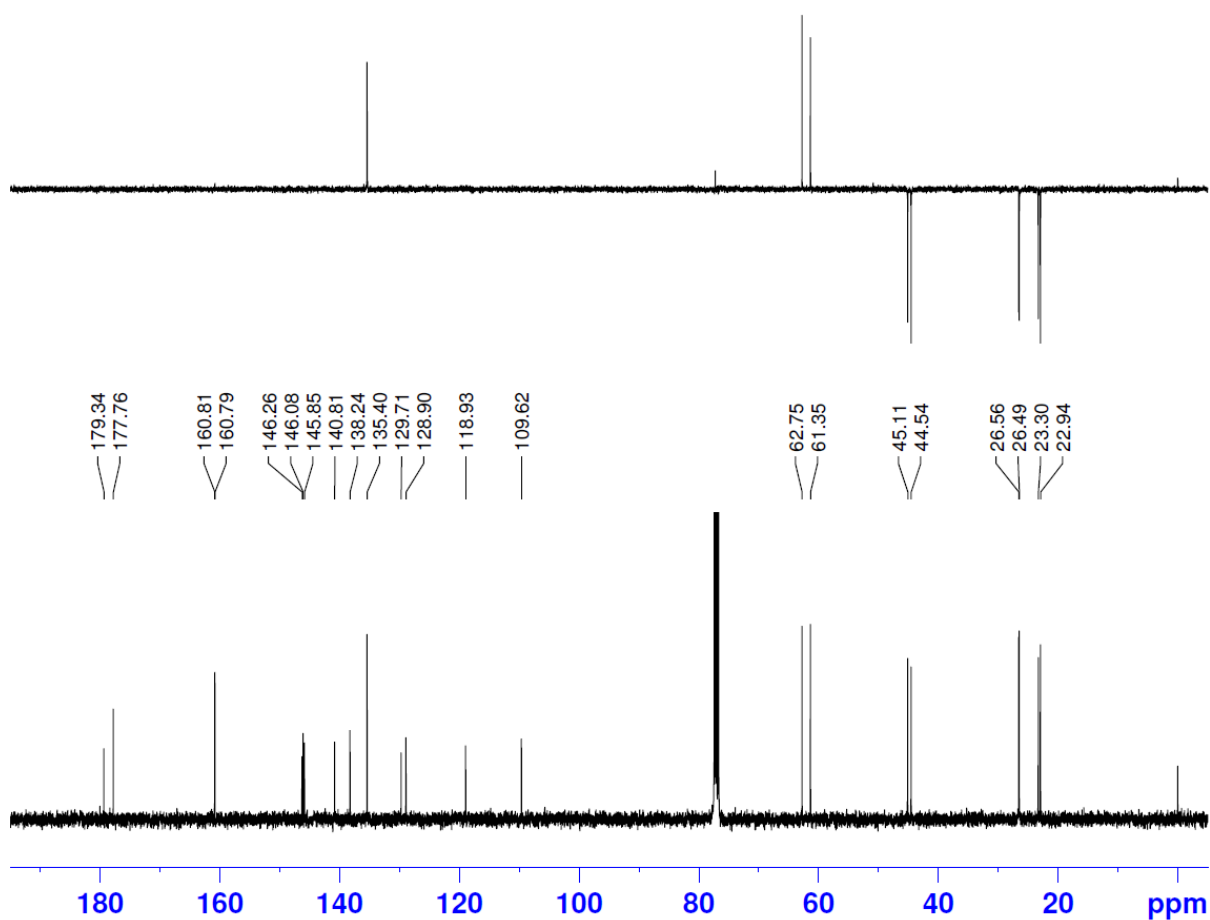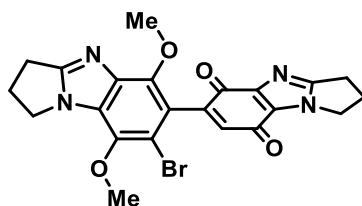
¹H NMR (400 MHz) of 8'-Bromo-6',9'-dimethoxy-1,1',2,2',3,3',4,4'-octahydro[7,7'-bipyrido[1,2-*a*]benzimidazole]-6,9-dione (10b) in CDCl₃
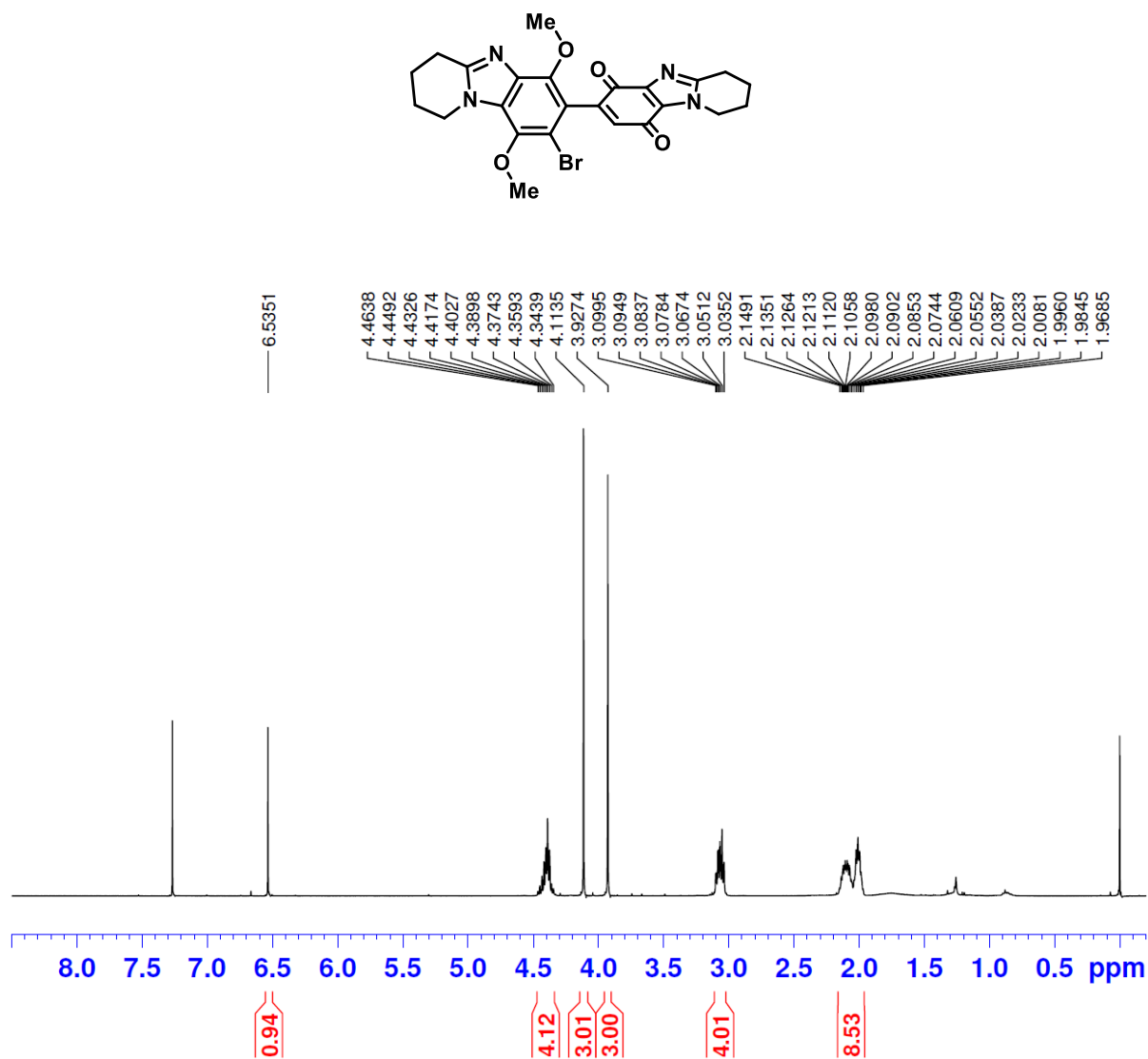
¹³C NMR (100 MHz) of 8'-Bromo-6',9'-dimethoxy-1,1',2,2',3,3',4,4'-octahydro[7,7'-bipyrido[1,2-*a*]benzimidazole]-6,9-dione (10b) in CDCl₃

¹H NMR (400 MHz) of 2'-Bromo-1',4'-dimethoxy-7,7',8,8',9,9',10,10'-octahydro-4*H*,6'*H*-[3,3'-biazepino[1,2-*a*]benzimidazole]-1,4(6*H*)-dione (10c) in CDCl₃

6.5275

4.6597
4.6165
4.6037
4.5345
4.1370
3.8875
3.1327
3.1250
3.0790
3.0275
1.9518
1.9395
1.8843
1.8422
1.7956
1.7841

8.0 7.5 7.0 6.5 6.0 5.5 5.0 4.5 4.0 3.5 3.0 2.5 2.0 1.5 1.0 0.5 ppm

0.92   4.06   3.02 3.00   4.15   12.25

¹³C NMR (100 MHz) of 2'-Bromo-1',4'-dimethoxy-7,7',8,8',9,9',10,10'-octahydro-4*H*,6'*H*-[3,3'-biazepino[1,2-*a*]benzimidazole]-1,4(6*H*)-dione (10c) in CDCl₃

179.67
178.76
158.26
157.91
145.90
145.03
140.88
138.38
136.59
135.45
130.52
130.43
118.80
110.79
61.73
61.63
45.92
45.28
30.89
30.85
29.71
29.36
28.93
28.16
25.49
24.90

180   160   140   120   100   80   60   40   20   ppm

130.52
130.43

61.73
61.63

30.89
30.85

ppm   ppm   ppm
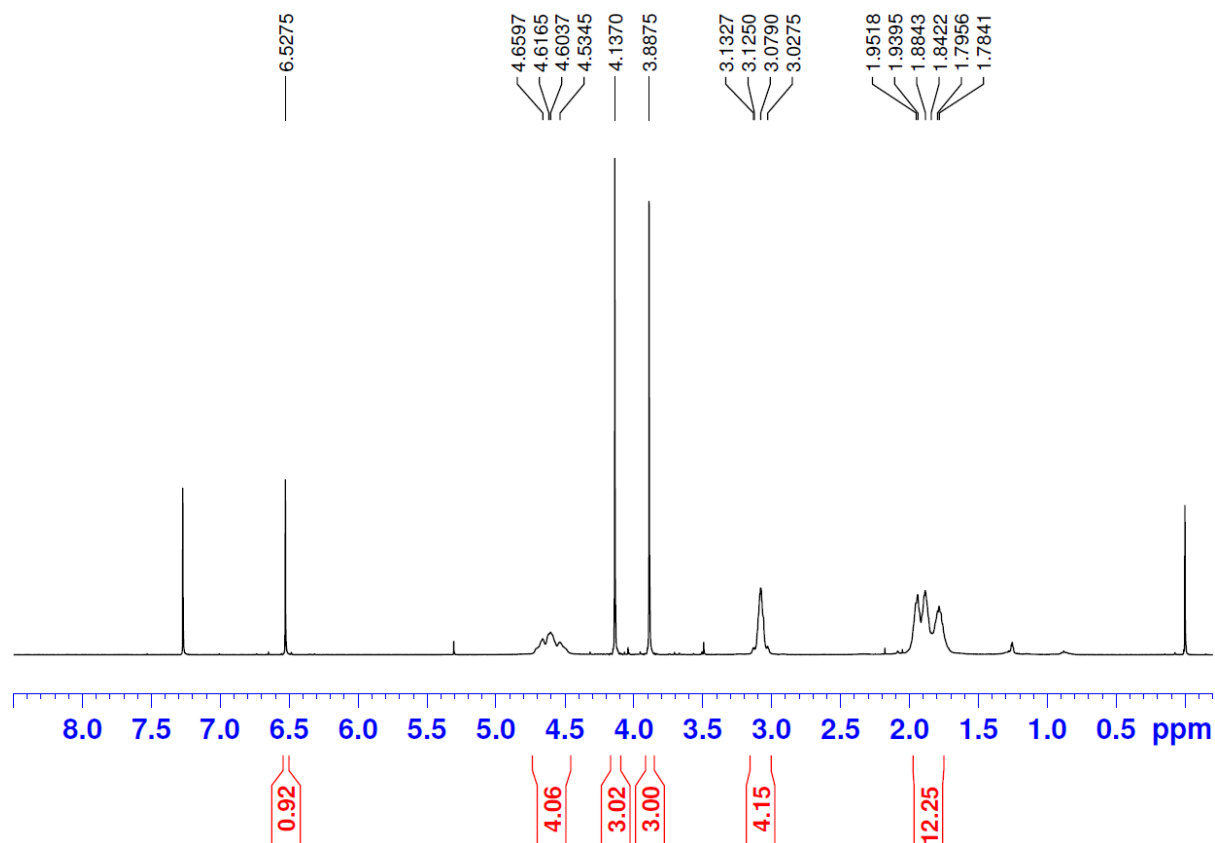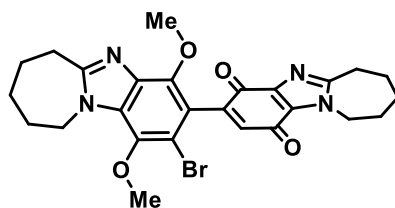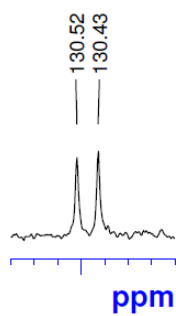
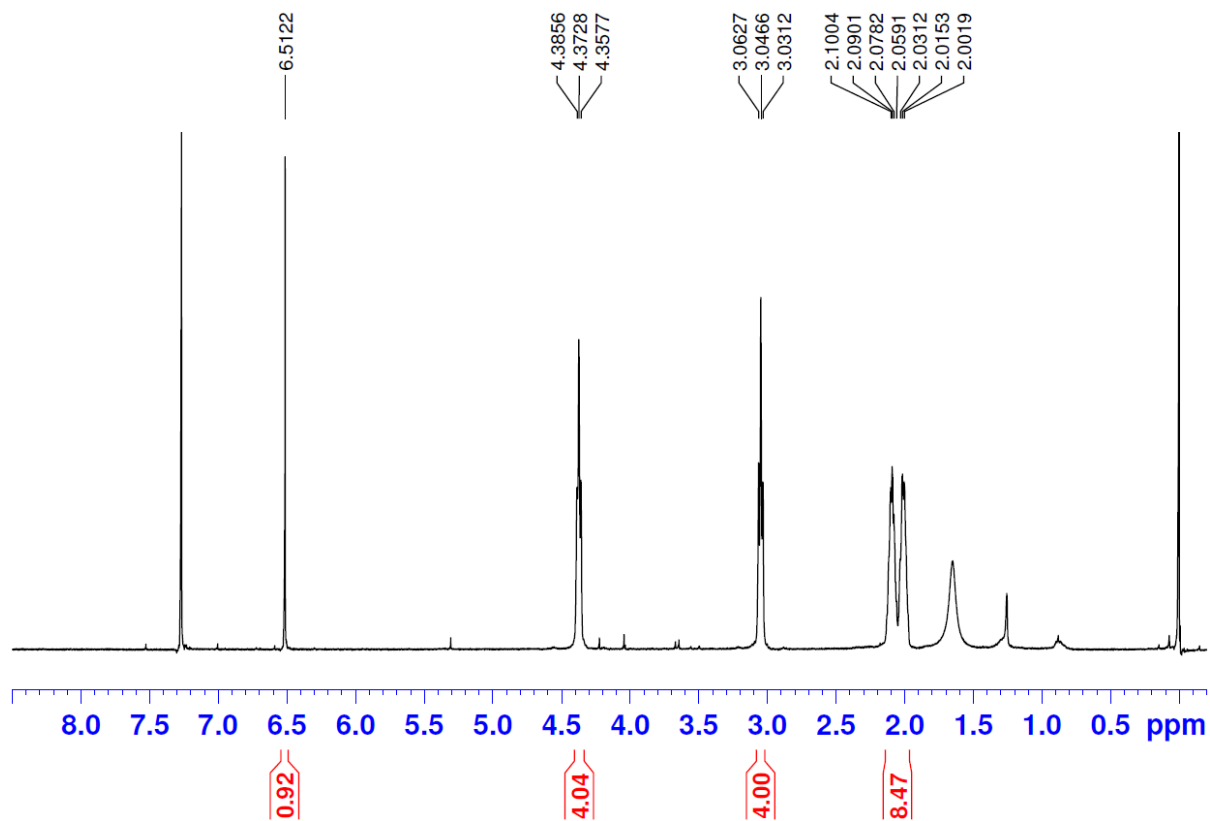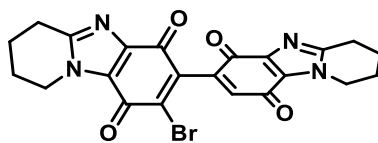**¹H NMR (400 MHz) of 7-Chloro-2,2',3,3'-tetrahydro-1*H*,1'*H*-[6,6'-bipyrrolo[1,2-*a*]benzimidazole]-5,5',8,8'-tetrone (9a) in CDCl₃**

¹³C NMR (100 MHz) of 7-Chloro-2,2',3,3'-tetrahydro-1*H*,1'*H*-[6,6'-bipyrrolo[1,2-*a*]benzimidazole]-5,5',8,8'-tetrone (9a) in CDCl₃

^{13}C NMR (100 MHz) of 8-Chloro-1,1',2,2',3,3',4,4'-octahydro[7,7'-bipyrido[1,2-a]benzimidazole]-6,6',9,9'-tetrone (9b) in CDCl₃
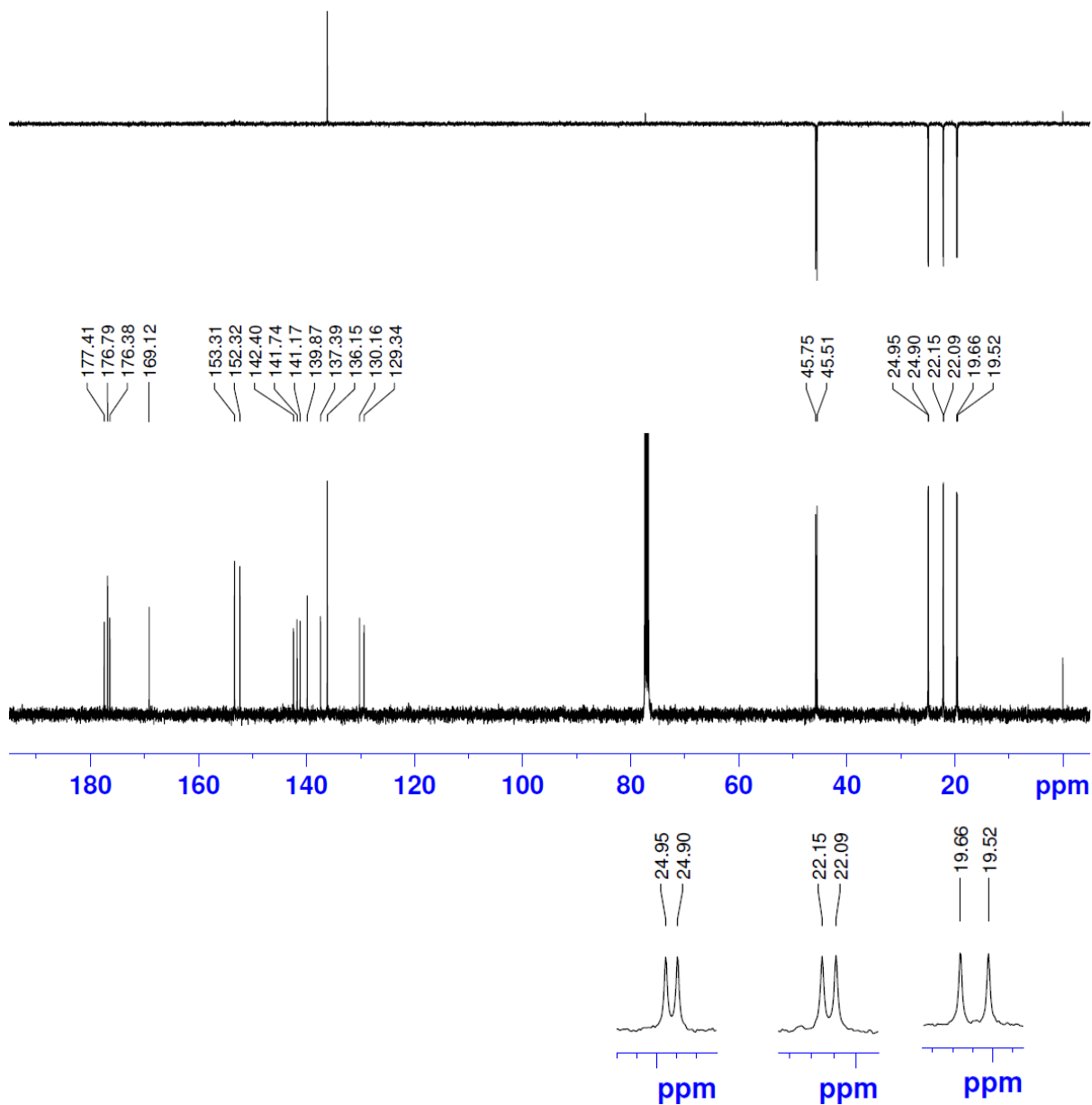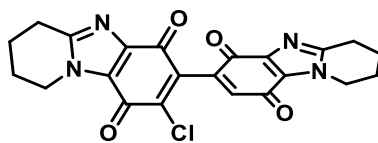
¹H NMR (400 MHz) of 2-Chloro-7,7',8,8',9,9',10,10'-octahydro-4*H*,4'*H*-[3,3'-biazepino[1,2-*a*]benzimidazole]-1,1',4,4'(6*H*,6'*H*)-tetrone (9c) in CDCl₃
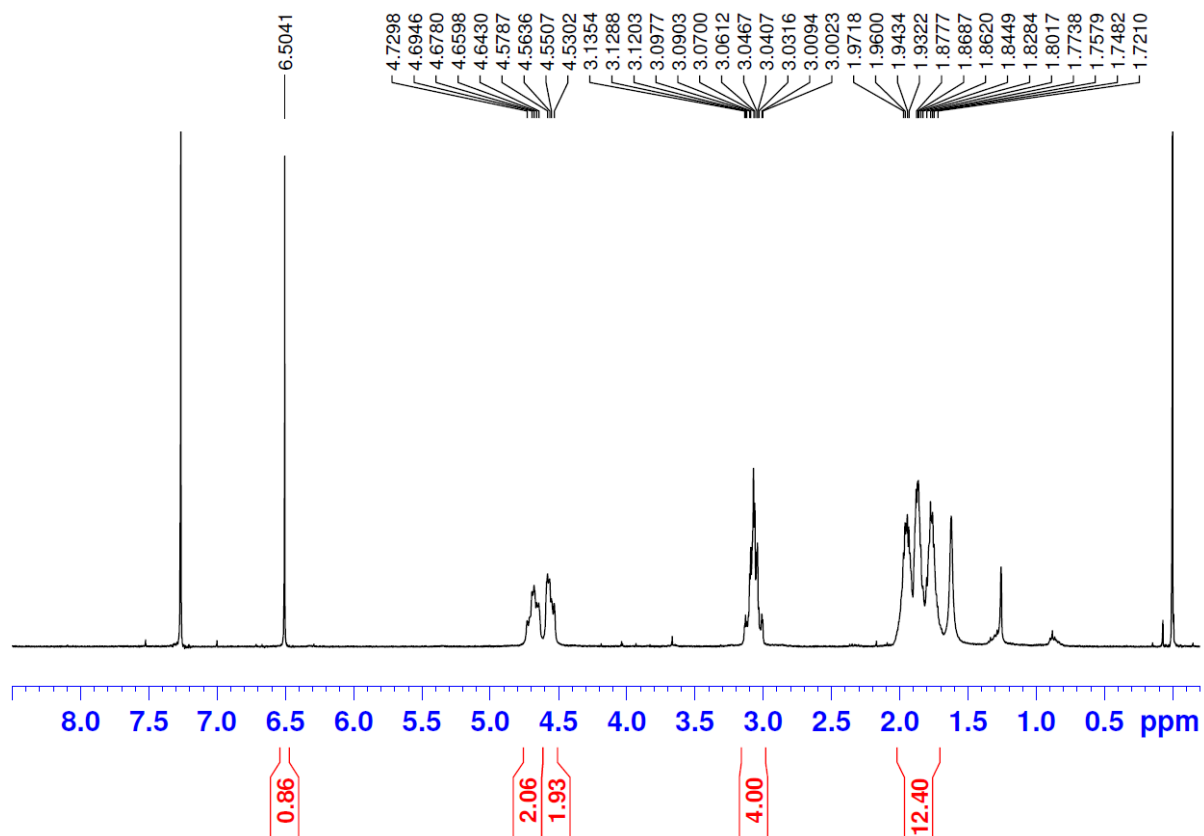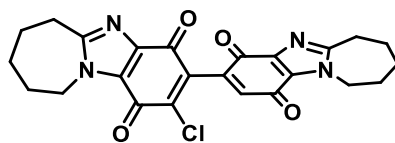
¹³C NMR (100 MHz) of 2-Chloro-7,7',8,8',9,9',10,10'-octahydro-4*H*,4'*H*-[3,3'-biazepino[1,2-*a*]benzimidazole]-1,1',4,4'(6*H*,6'*H*)-tetrone (9c) in CDCl₃
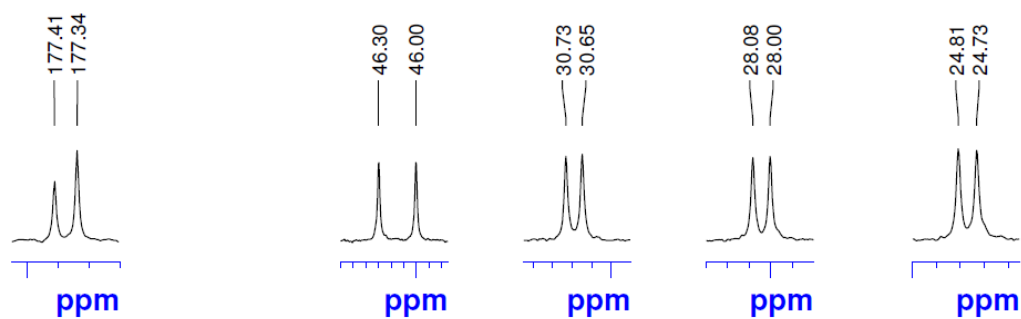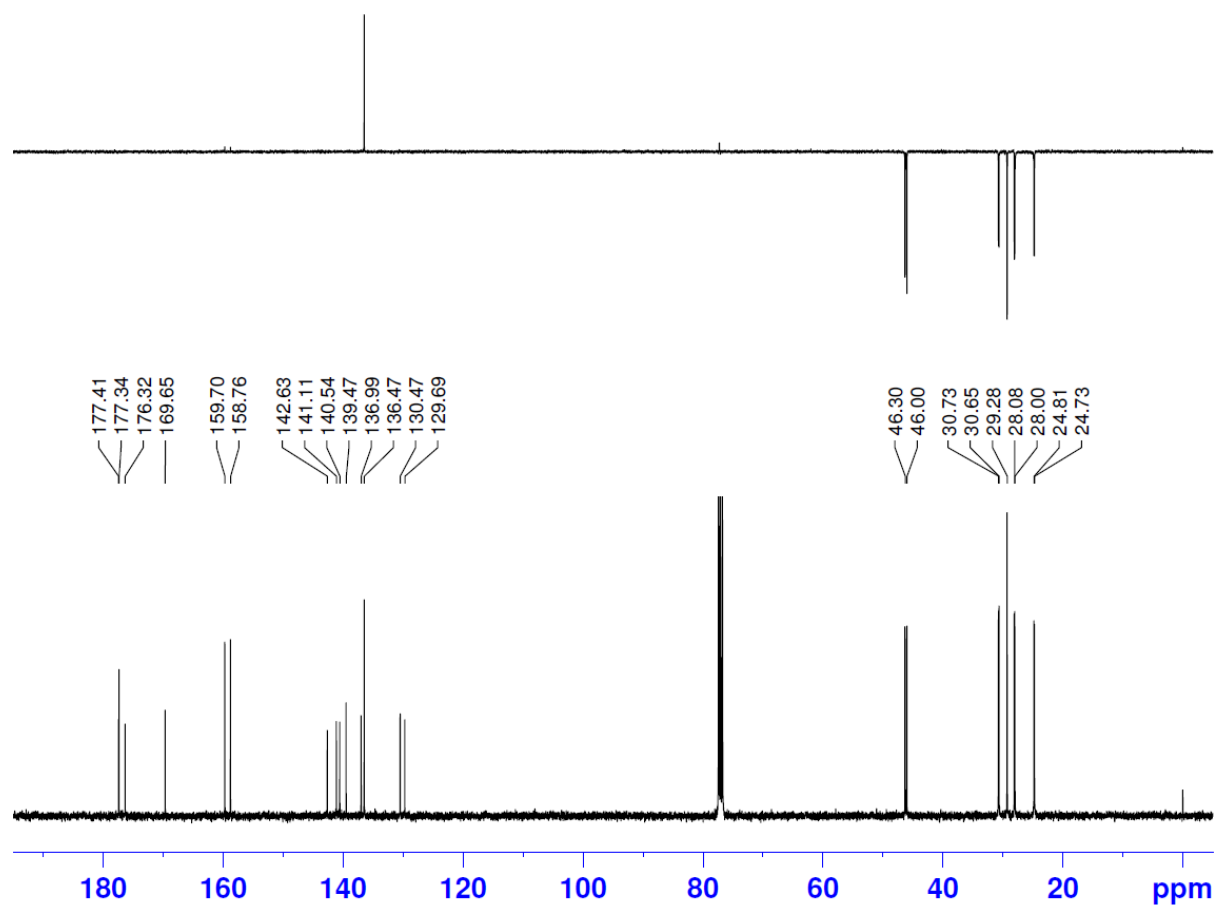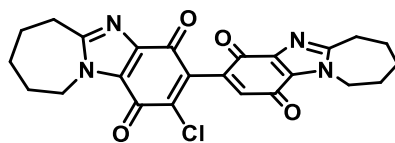
^{1}H NMR (400 MHz) of 7-Bromo-2,2',3,3'-tetrahydro-1*H*,1'*H*-[6,6'-bipyrrolo[1,2-*a*]benzimidazole]-5,5',8,8'-tetrone (11a) in CDCl₃
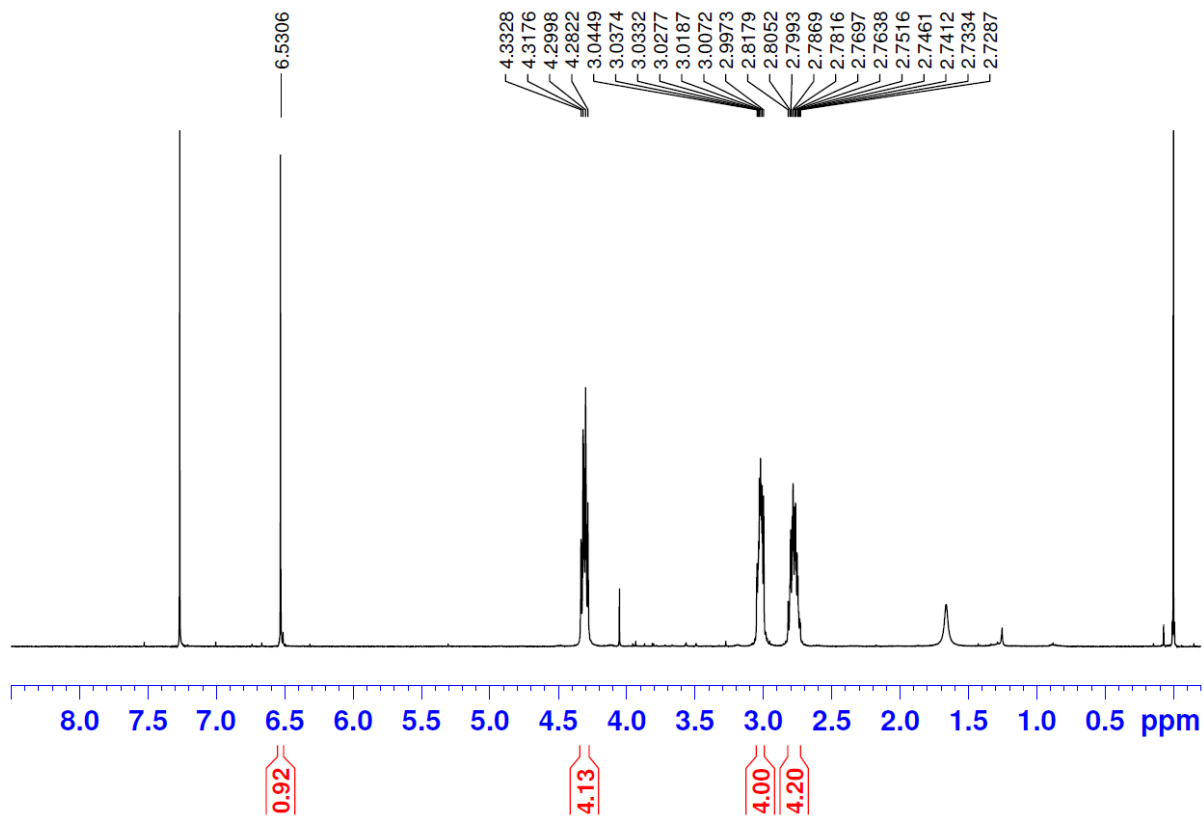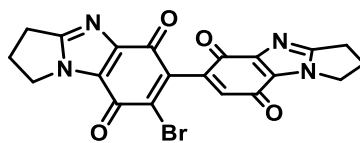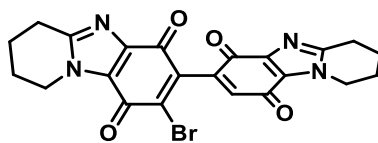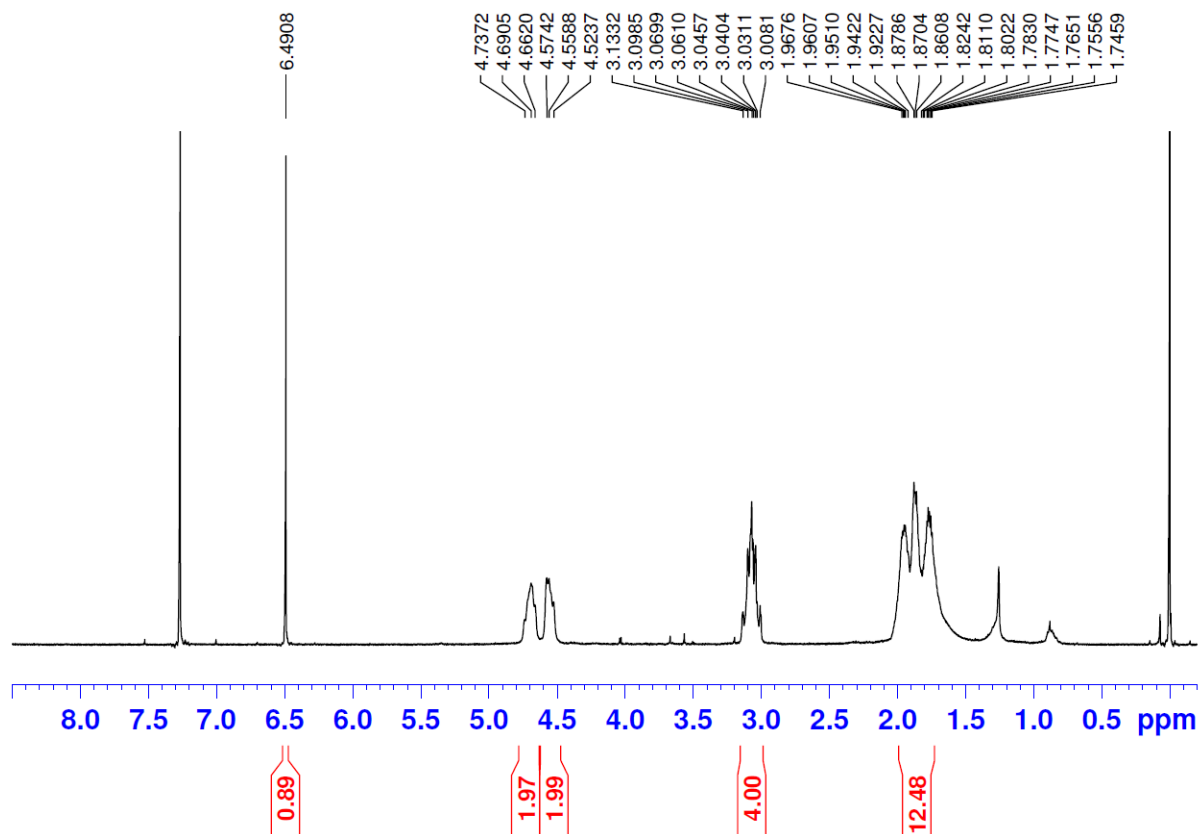
¹³C NMR (100 MHz) of 7-Bromo-2,2',3,3'-tetrahydro-1*H*,1'*H*-[6,6'-bipyrrolo[1,2-*a*]benzimidazole]-5,5',8,8'-tetrone (11a) in CDCl₃
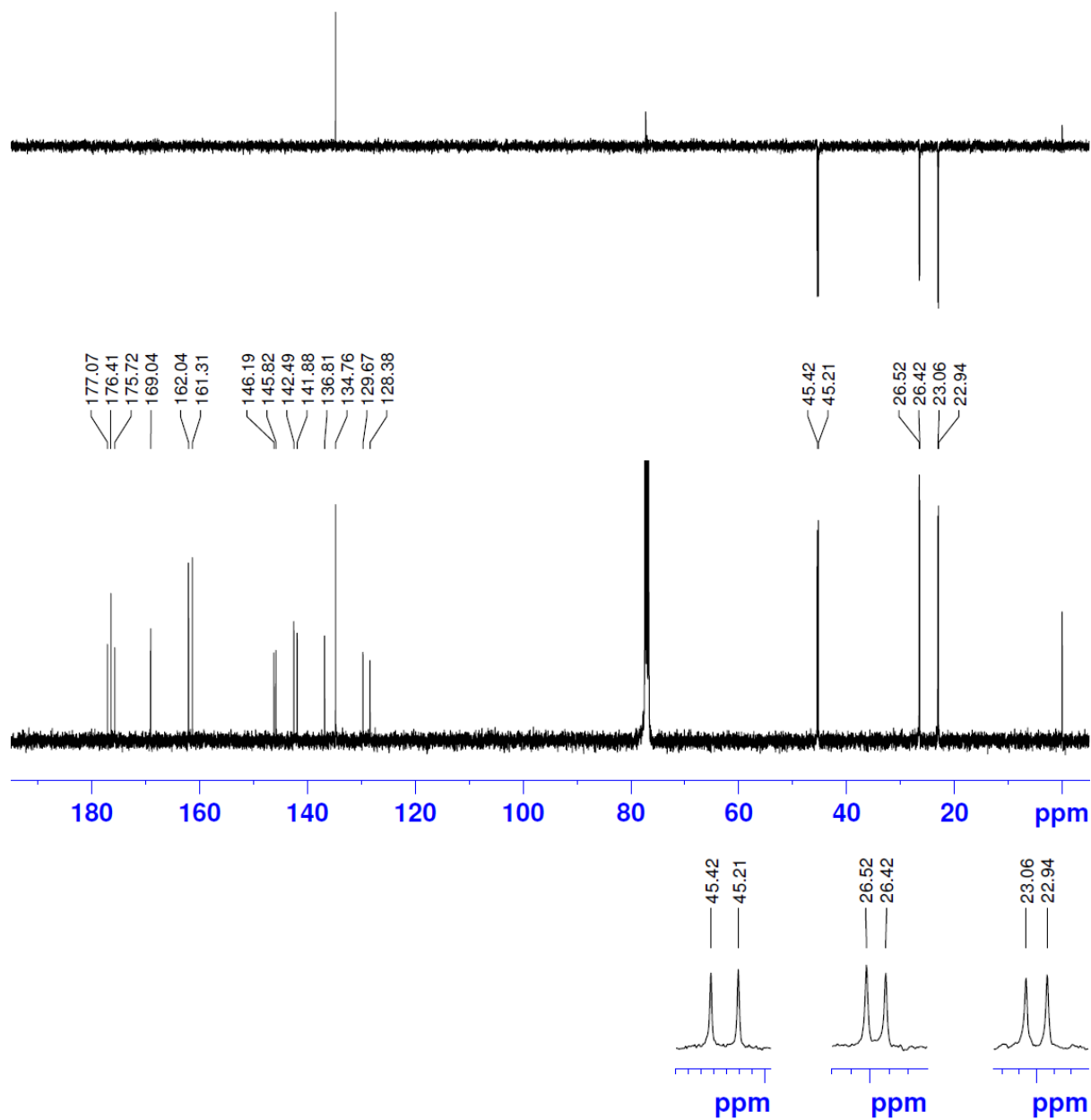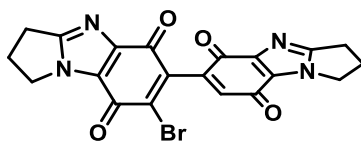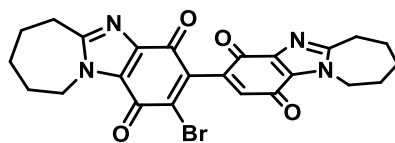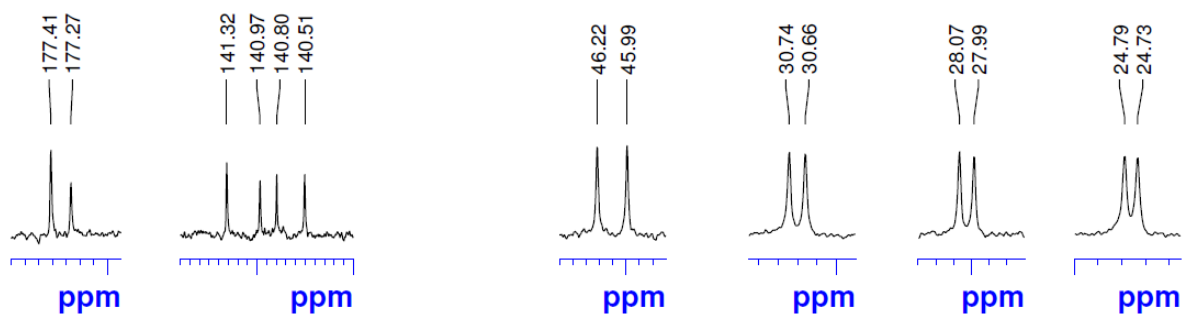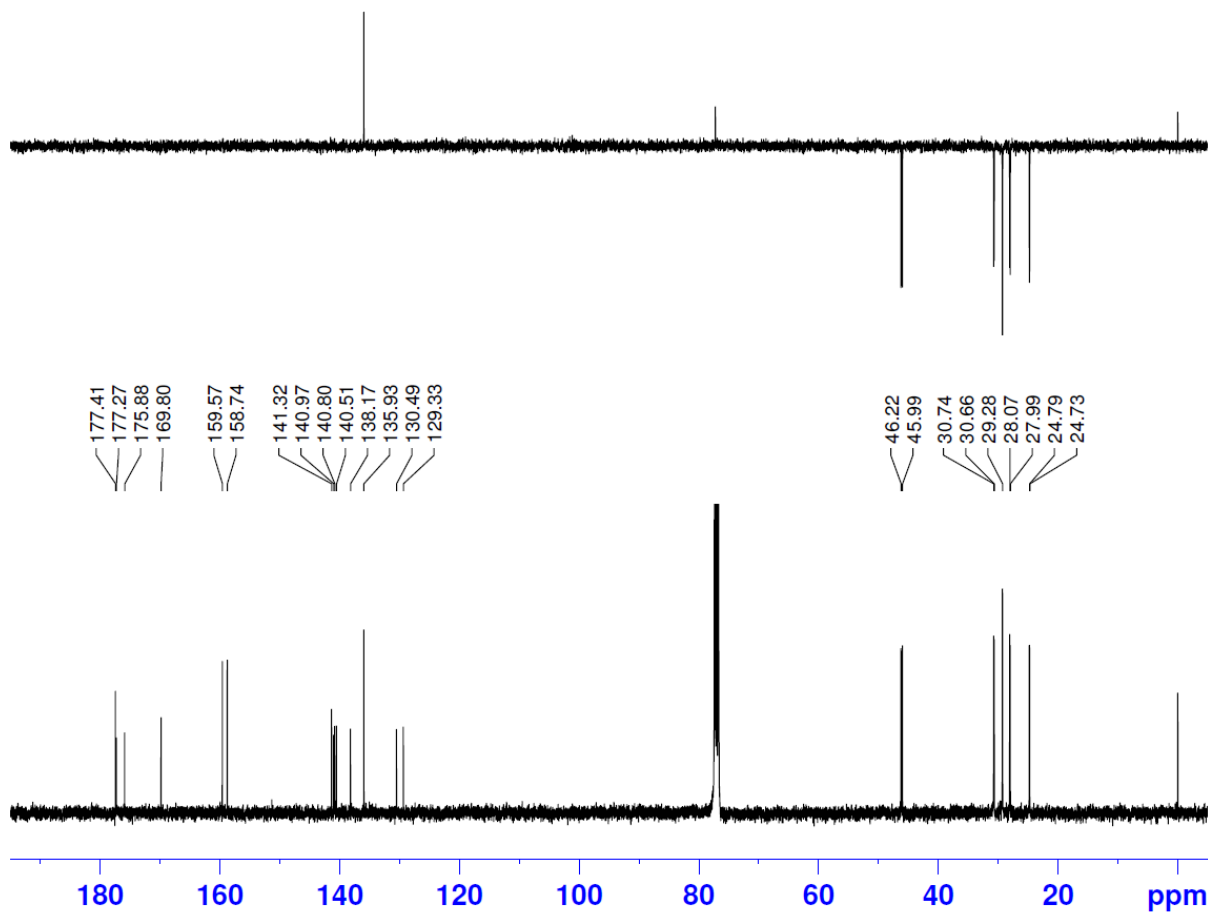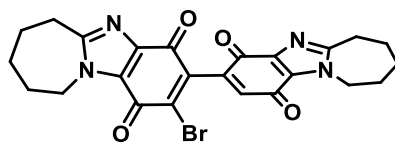
13C NMR (100 MHz) of 8-Bromo-1,1',2,2',3,3',4,4'-octahydro[7,7'-bipyrido[1,2-a]benzimidazole]-6,6',9,9'-tetrone (11b) in CDCl₃
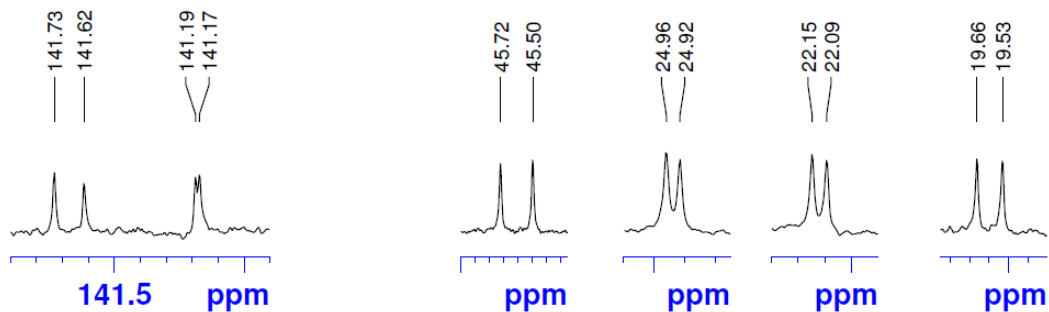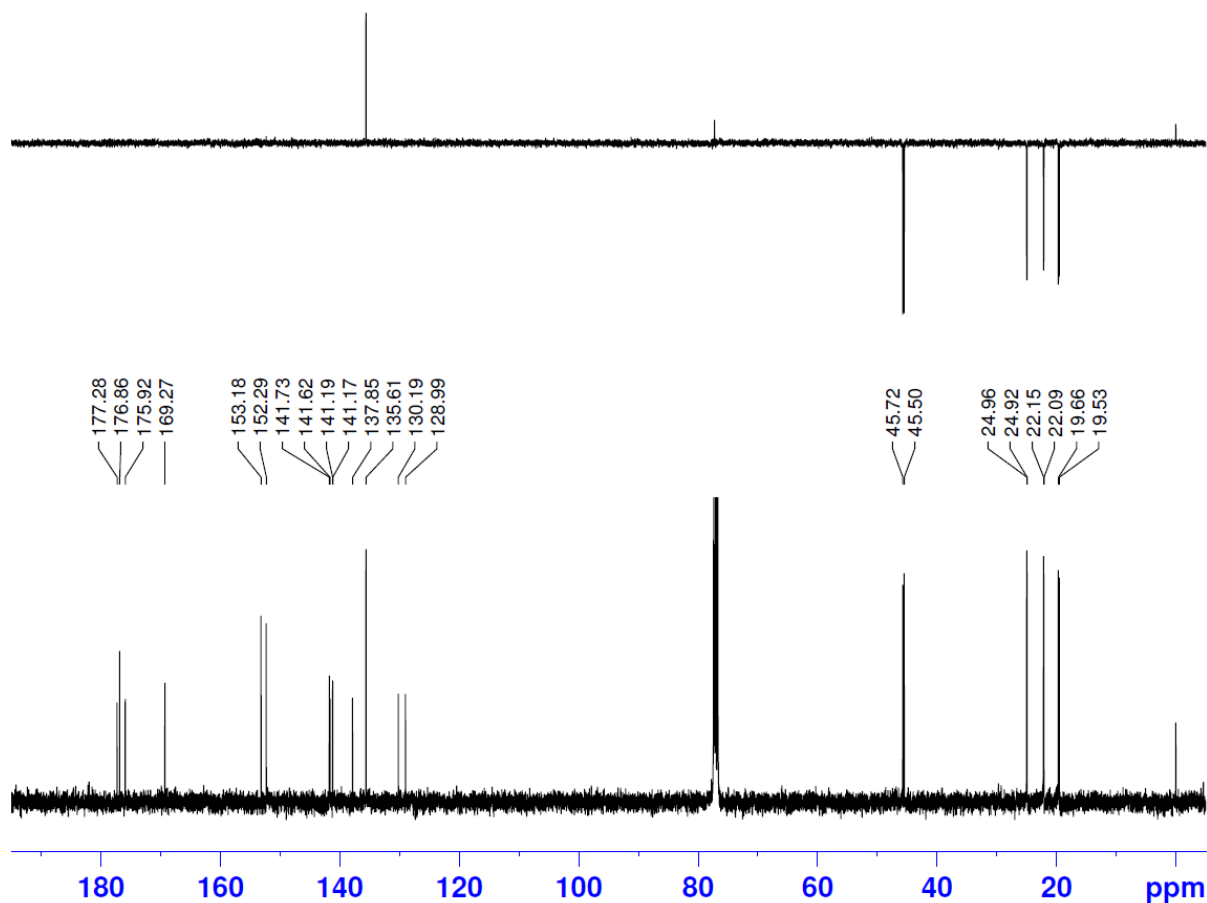
¹H NMR (400 MHz) of 2-Bromo-7,7',8,8',9,9',10,10'-octahydro-4*H*,4'*H*-[3,3'-biazepino[1,2-*a*]benzimidazole]-1,1',4,4'(6*H*,6'*H*)-tetrone (11c) in CDCl₃

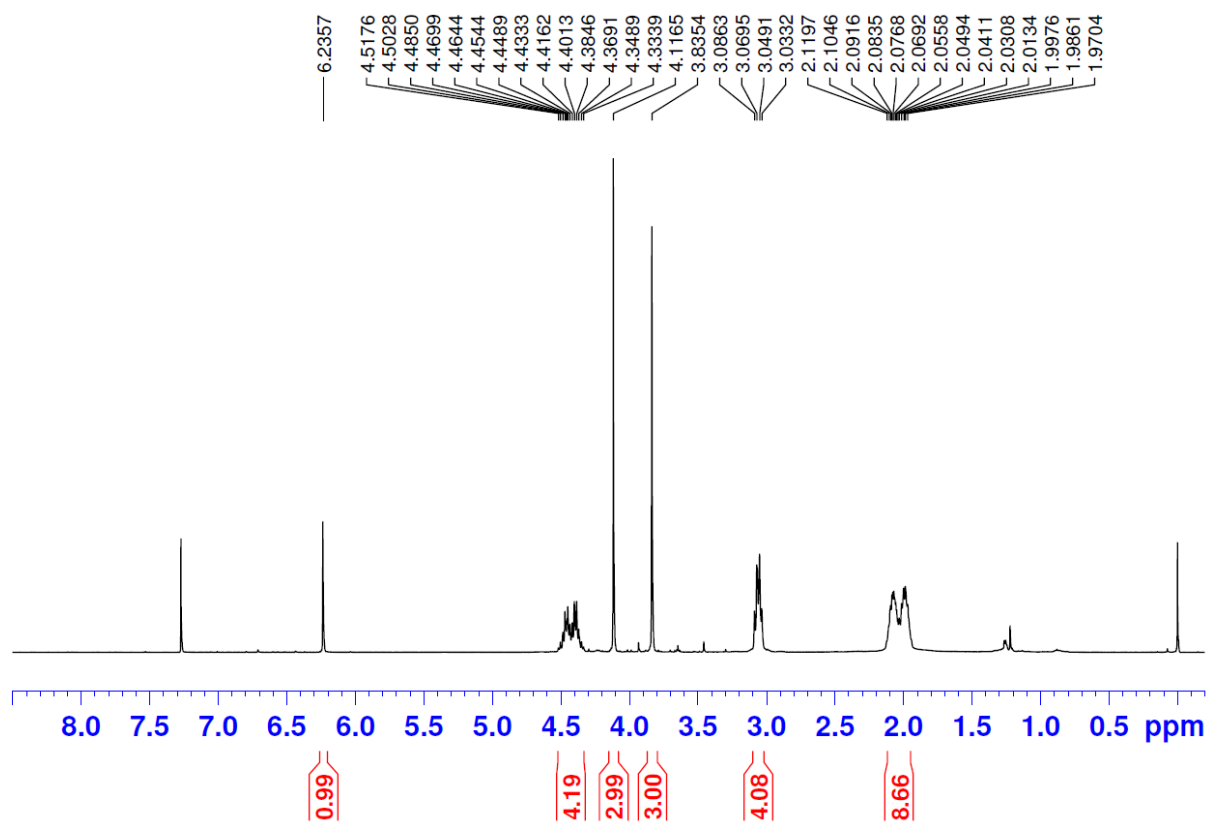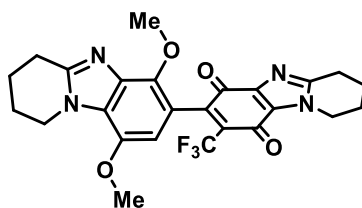¹³C NMR (100 MHz) of 2-Bromo-7,7',8,8',9,9',10,10'-octahydro-4*H*,4'*H*-[3,3'-biazepino[1,2-*a*]benzimidazole]-1,1',4,4'(6*H*,6'*H*)-tetrone (11c) in CDCl₃
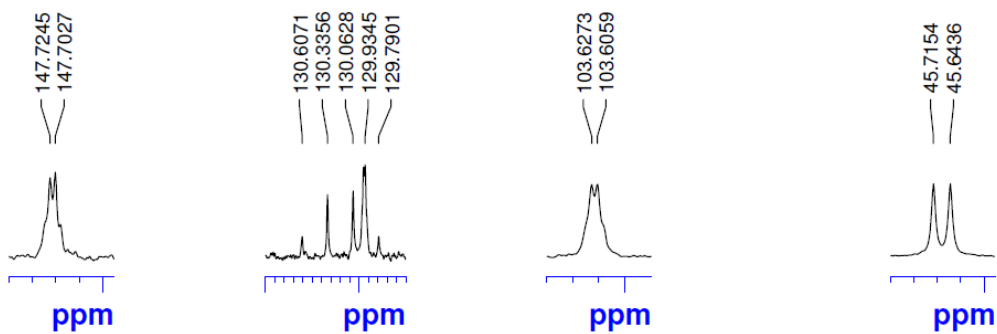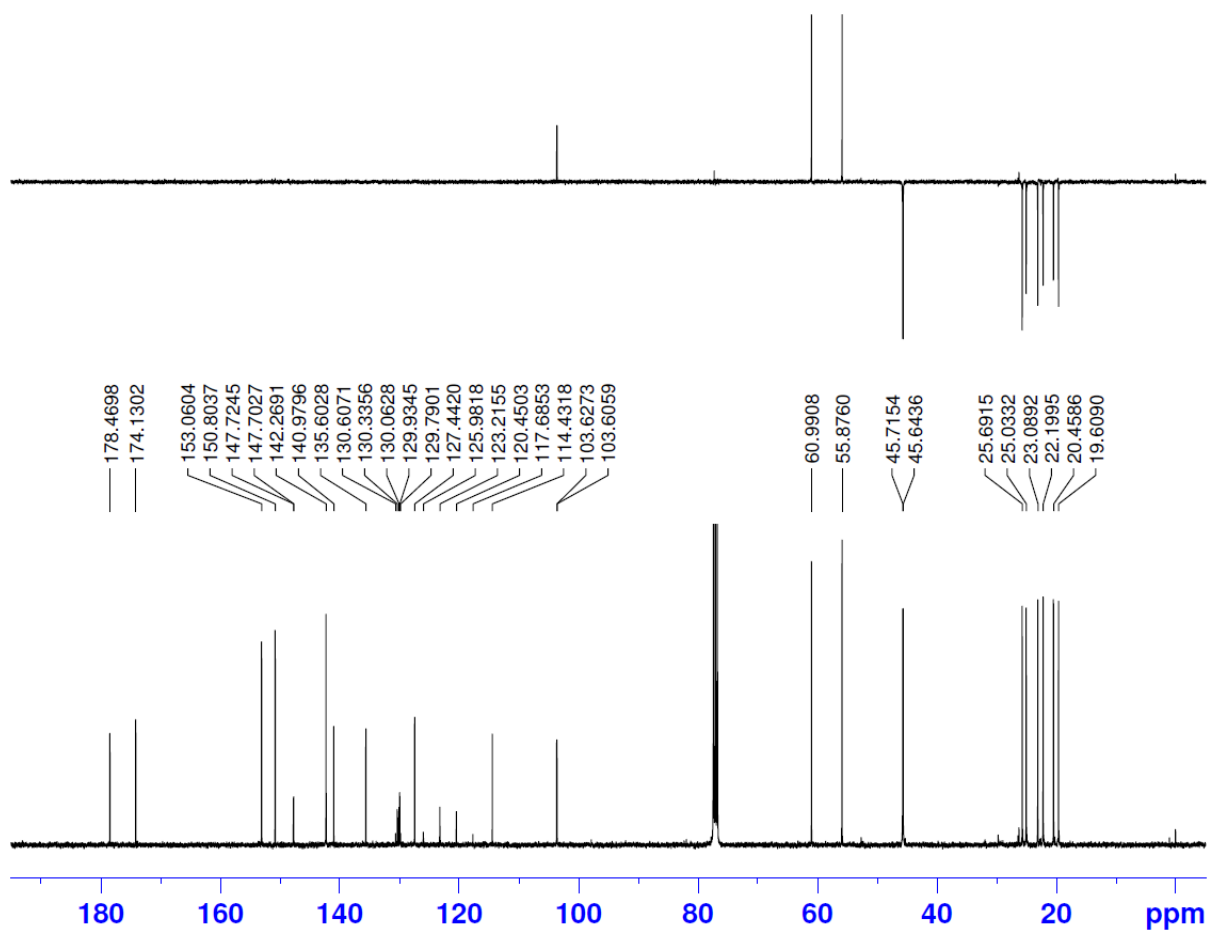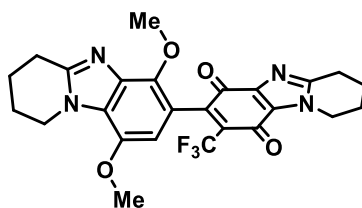
¹H NMR (400 MHz) of 6',9'-Dimethoxy-8-(trifluoromethyl)-1,1',2,2',3,3',4,4'-octahydro[7,7'-bipyrido[1,2-*a*]benzimidazole]-6,9-dione (12) in CDCl₃

¹³C NMR (100 MHz) of 6',9'-Dimethoxy-8-(trifluoromethyl)-1,1',2,2',3,3',4,4'-octahydro[7,7'-bipyrido[1,2-*a*]benzimidazole]-6,9-dione (12) in CDCl₃

Peak labels (top listing):
178.4698, 174.1302, 153.0604, 150.8037, 147.7245, 147.7027, 142.2691, 140.9796, 135.6028, 130.6071, 130.3356, 130.0628, 129.9345, 129.7901, 127.4420, 125.9818, 123.2155, 120.4503, 117.6853, 114.4318, 103.6273, 103.6059, 60.9908, 55.8760, 45.7154, 45.6436, 25.6915, 25.0332, 23.0892, 22.1995, 20.4586, 19.6090

Expansions:
- 147.7245, 147.7027
- 130.6071, 130.3356, 130.0628, 129.9345, 129.7901
- 103.6273, 103.6059
- 45.7154, 45.6436

247

^{19}F NMR (376 MHz) of 6',9'-Dimethoxy-8-(trifluoromethyl)-1,1',2,2',3,3',4,4'-octahydro[7,7'-bipyrido[1,2-a]benzimidazole]-6,9-dione (12) in CDCl₃

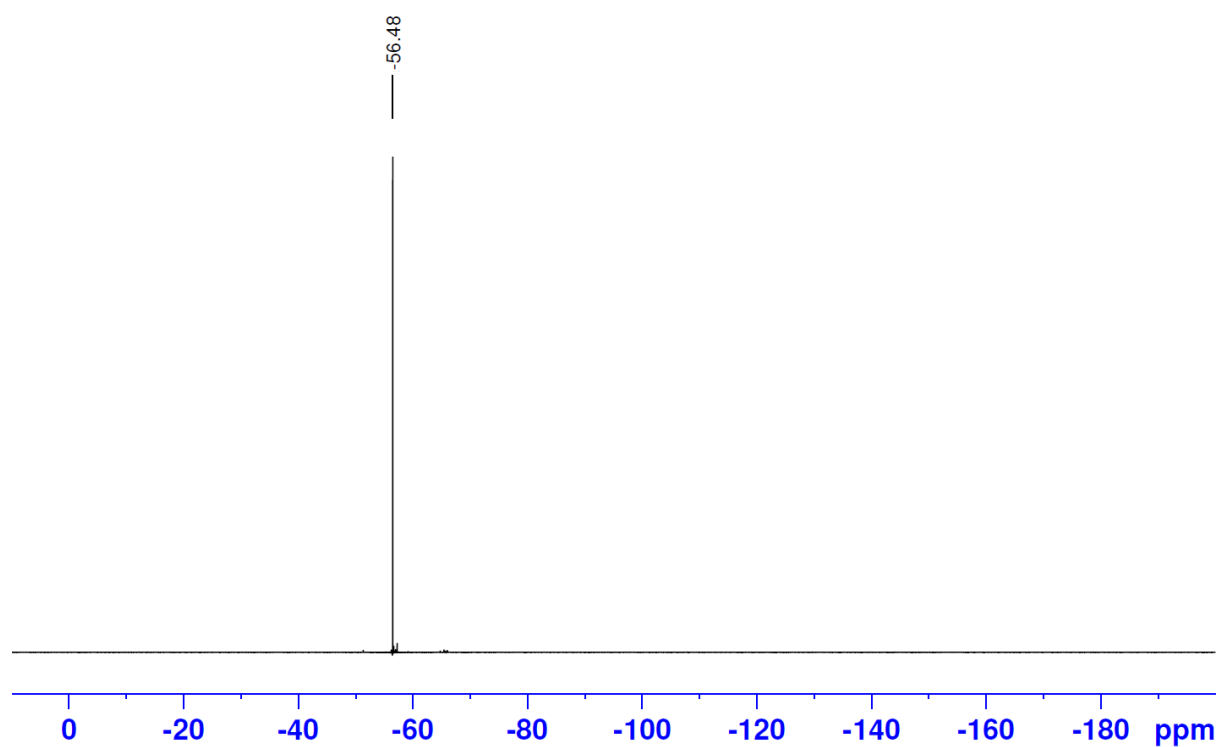**¹H NMR (400 MHz) of 8'-Chloro-6',9'-dimethoxy-8-(trifluoromethyl)-1,1',2,2',3,3',4,4'-octahydro[7,7'-bipyrido[1,2-*a*]benzimidazole]-6,9-dione (13) in CDCl₃**
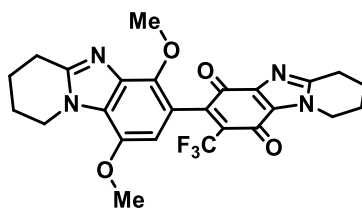
13C NMR (100 MHz) of 8'-Chloro-6',9'-dimethoxy-8-(trifluoromethyl)-1,1',2,2',3,3',4,4'-octahydro[7,7'-bipyrido[1,2-*a*]benzimidazole]-6,9-dione (13) in CDCl₃

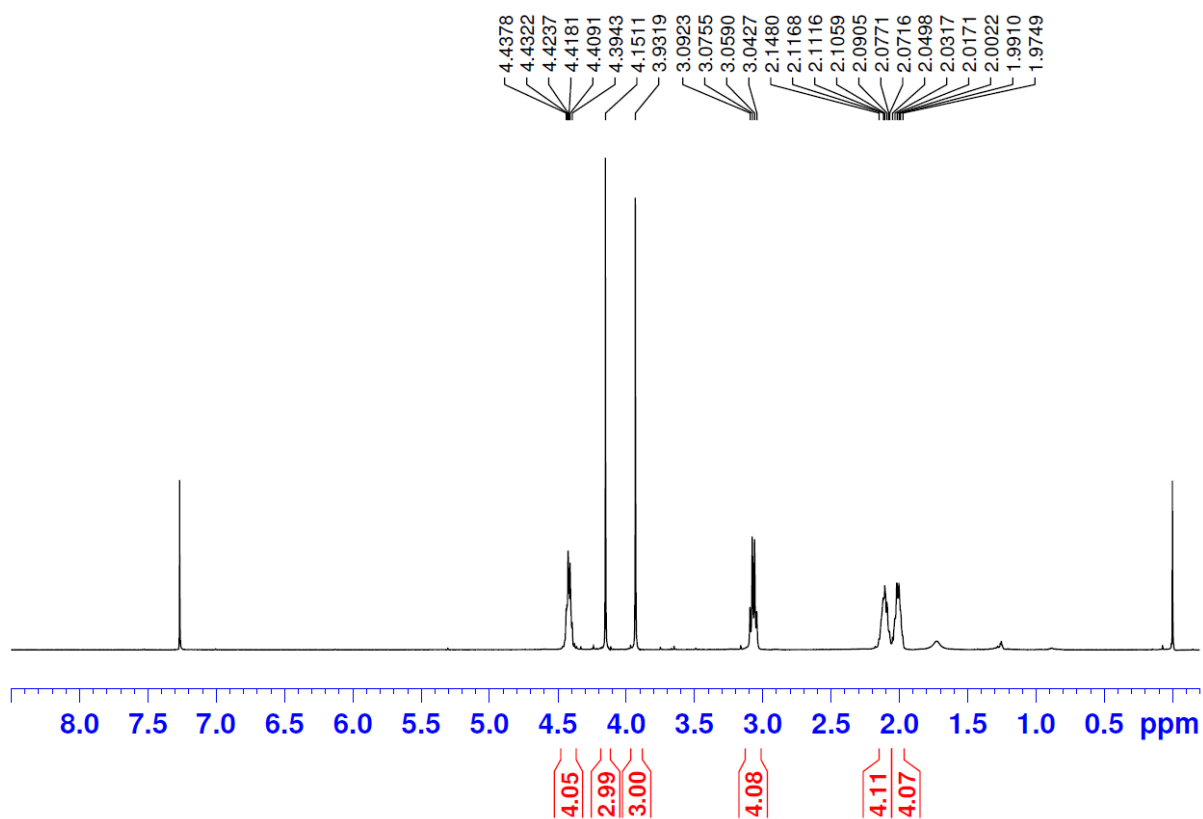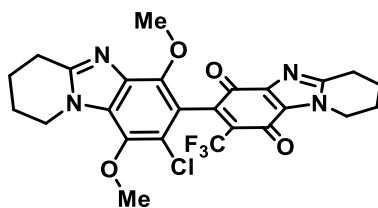**¹⁹F NMR (376 MHz) of 8'-Chloro-6',9'-dimethoxy-8-(trifluoromethyl)-1,1',2,2',3,3',4,4'-octahydro[7,7'-bipyrido[1,2-*a*]benzimidazole]-6,9-dione (13) in CDCl₃**

-58.95

| 0 | -20 | -40 | -60 | -80 | -100 | -120 | -140 | -160 | -180 | ppm |

¹H NMR (400 MHz) of 8-Chloro-8'-(trifluoromethyl)-1,1',2,2',3,3',4,4'-octahydro[7,7'-bipyrido[1,2-*a*]benzimidazole]-6,6',9,9'-tetrone (14) in CDCl₃

13C NMR (100 MHz) of 8-Chloro-8'-(trifluoromethyl)-1,1',2,2',3,3',4,4'-octahydro[7,7'-bipyrido[1,2-a]benzimidazole]-6,6',9,9'-tetrone (14) in CDCl₃
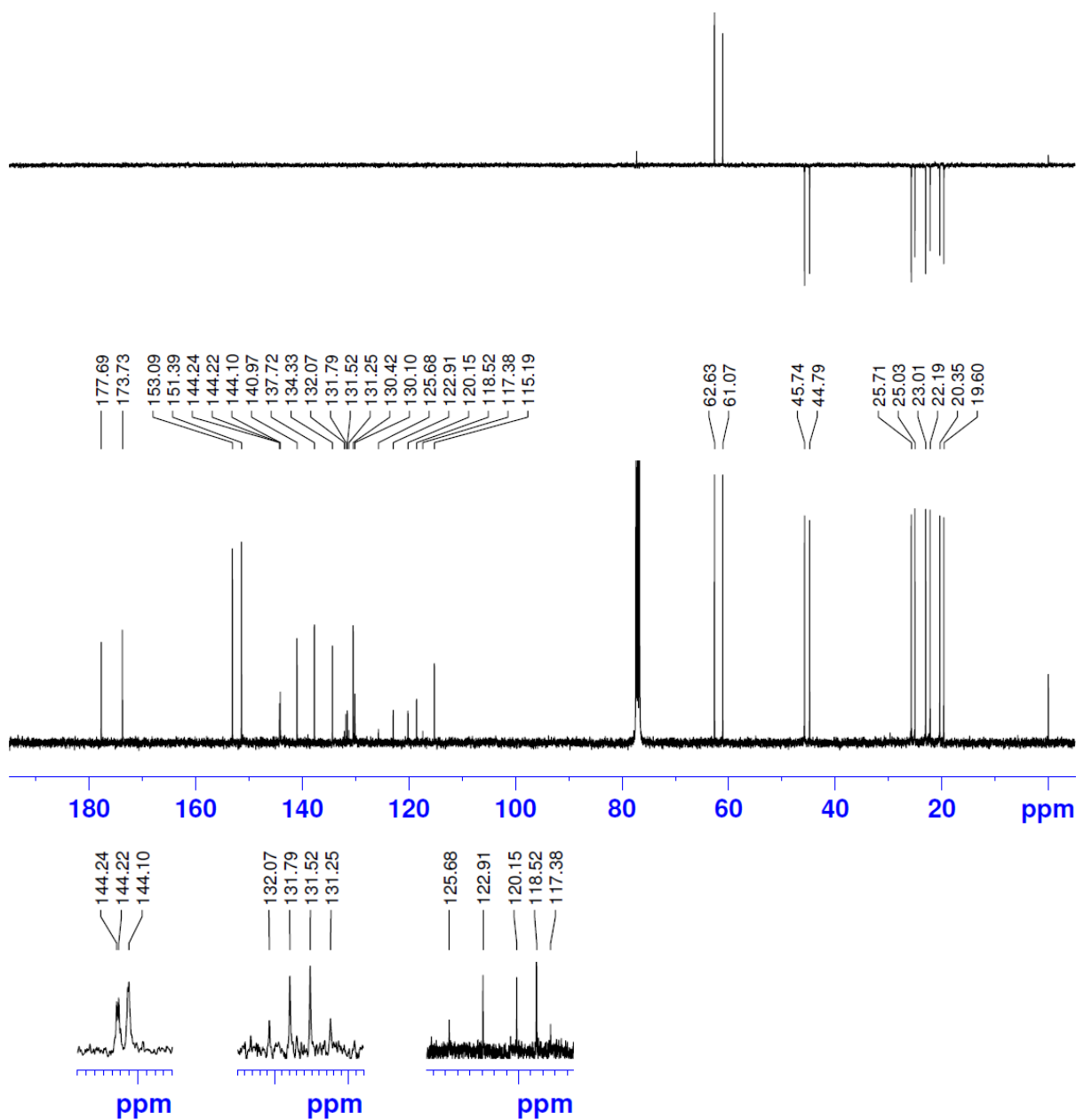
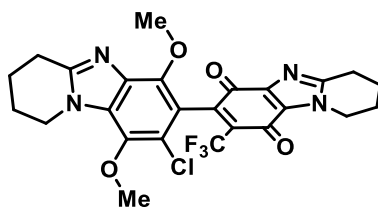**^{19}F NMR (376 MHz) of 8-Chloro-8'-(trifluoromethyl)-1,1',2,2',3,3',4,4'-octahydro[7,7'-bipyrido[1,2-a]benzimidazole]-6,6',9,9'-tetrone (14) in CDCl$_3$**
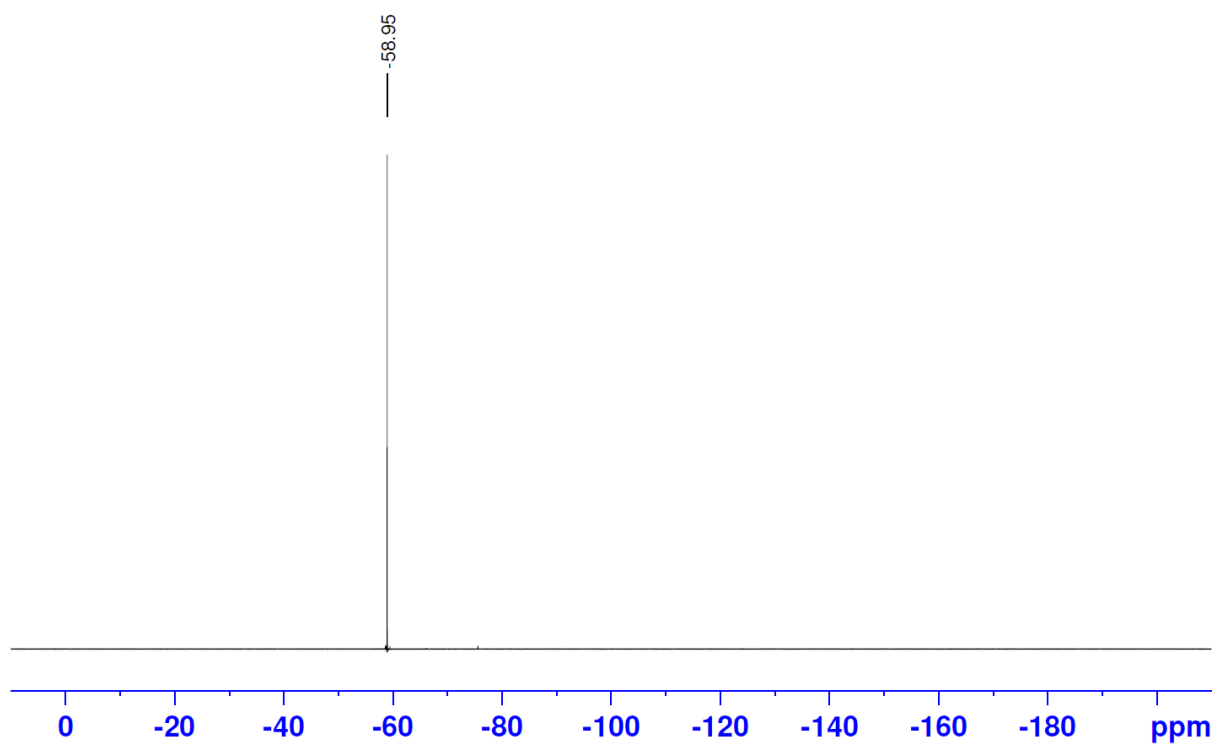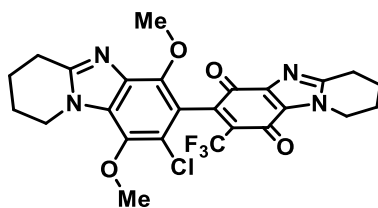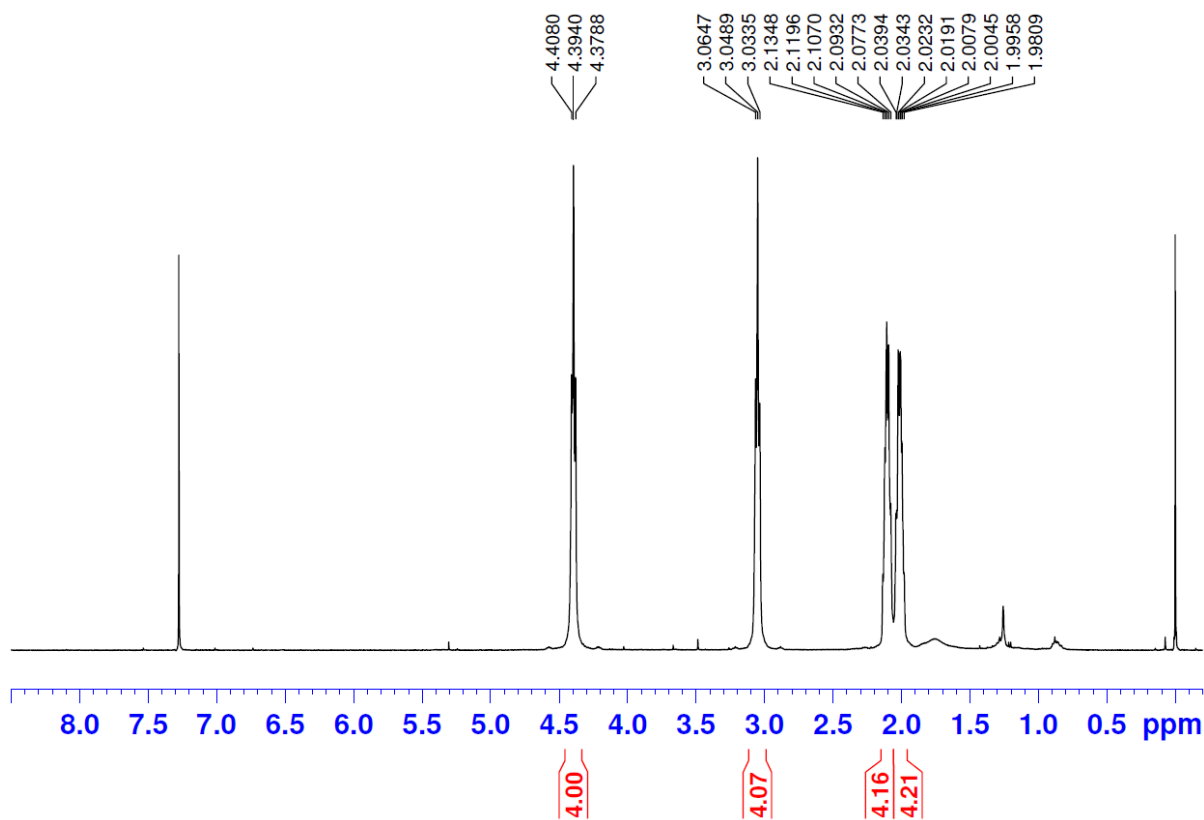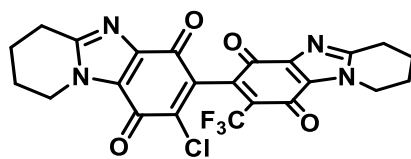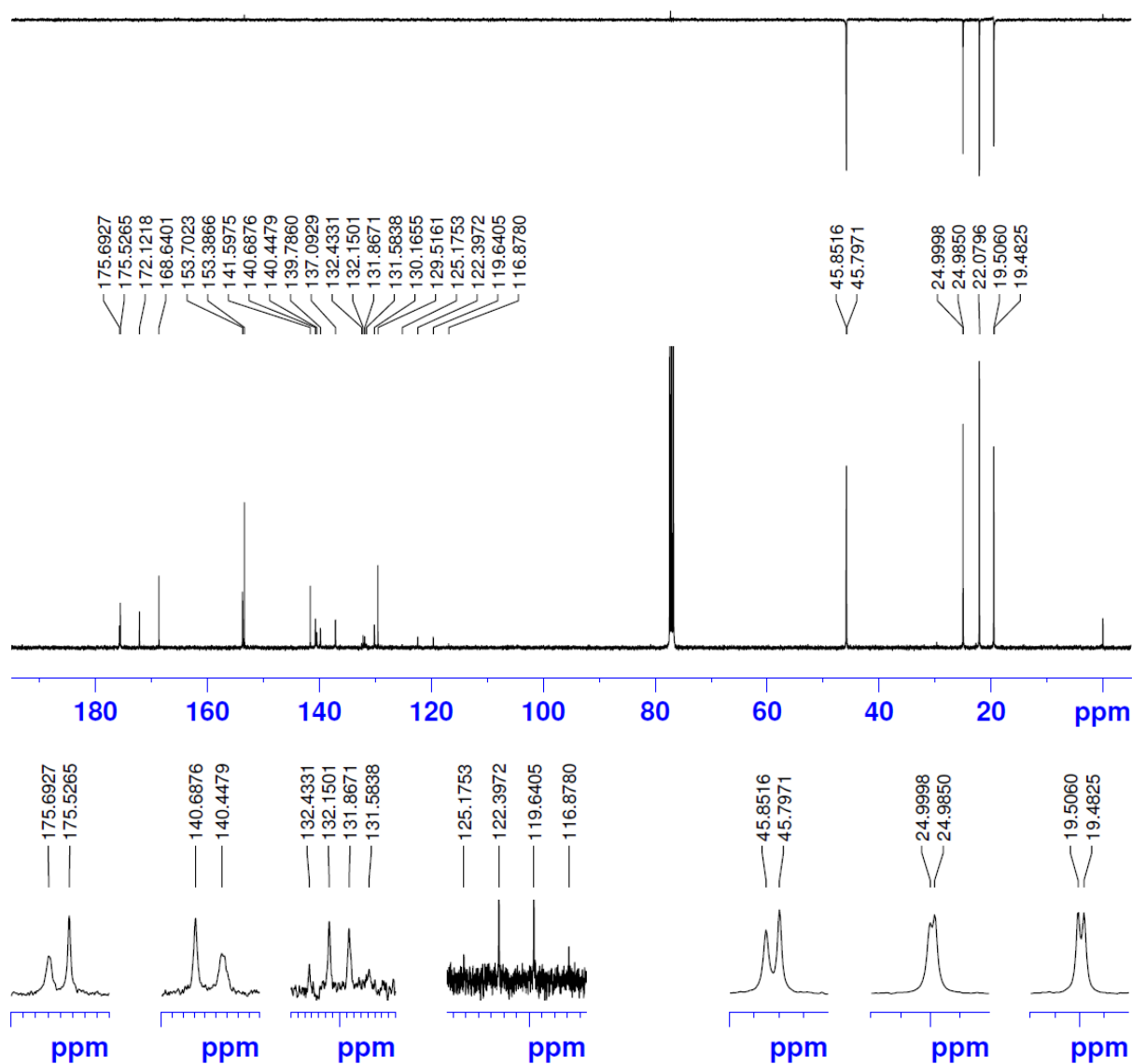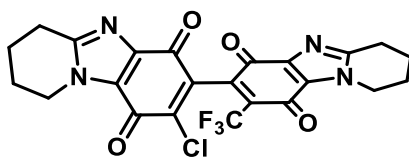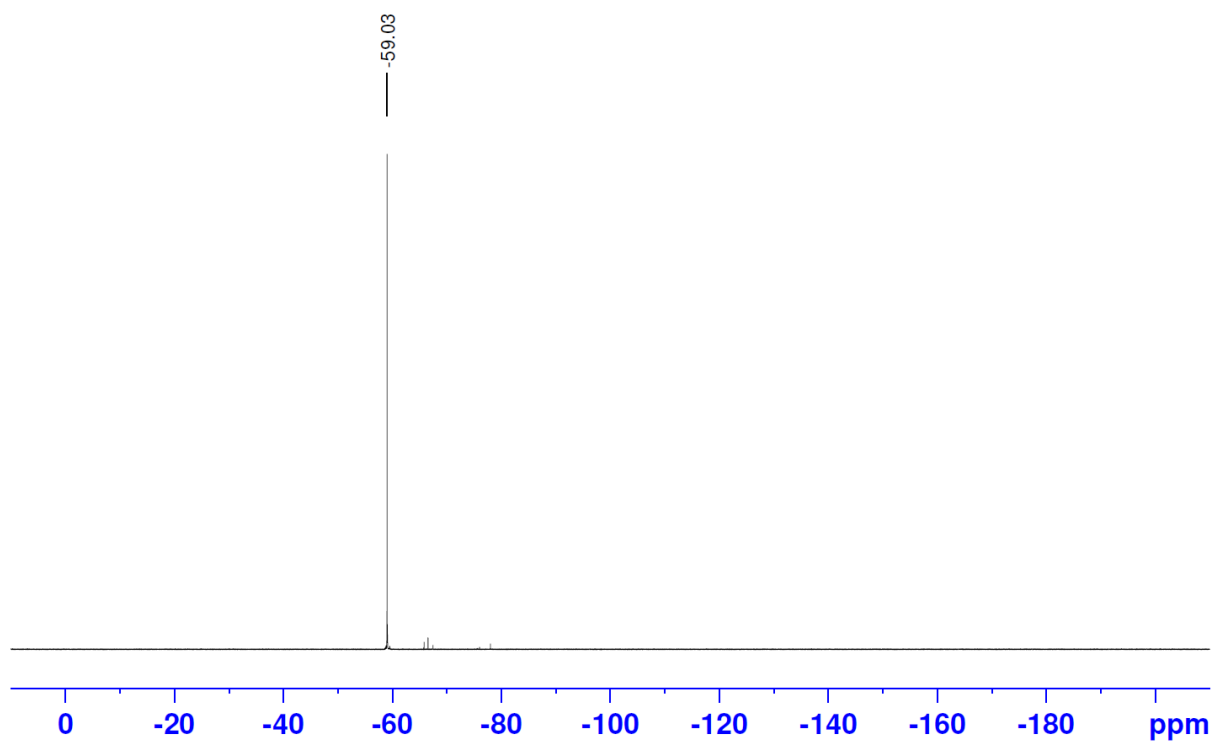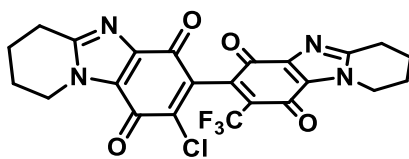
Peer-Reviewed Publications

- **Conboy, Darren;** Aldabbagh, Fawaz. The Reactivity of Oxone towards 4,6-Di(cycloamino)-1,3-phenylenediamines: Synthesis of Spirocyclic Oxetane Ring-Fused Imidazobenzimidazoles. *Arkivoc* **2020**, *2020*, Part (vii), 180-191. DOI: https://doi.org/10.24820/ark.5550190.p011.229

- **Conboy, Darren;** Aldabbagh, Fawaz. Chapter 10.21: Tricyclic Systems: Central Carbocyclic Ring with Fused Five-membered Rings, in *Comprehensive Heterocyclic Chemistry IV*, David Black, Janine Cossy, and Christian Stevens, EIC; Fawaz Aldabbagh, Vol. Ed.; Elsevier; **2020**, Section 10, *in press*.

- **Conboy, Darren;** Aldabbagh, Fawaz. 6-Imino-1,2,3,4,8,9,10,11-octahydropyrido[1,2-*a*]pyrido[1′,2′:1,2]imidazo[4,5-*f*]benzimidazole-13-one: Synthesis and Cytotoxicity Evaluation. *Molbank* **2020**, *2020*, M1118. DOI: https://doi.org/10.3390/M1118

- **Conboy, Darren;** Mirallai, Styliana I.; Craig, Austin; McArdle, Patrick; Al-Kinani, Ali A.; Barton, Stephen; Aldabbagh, Fawaz. Incorporating Morpholine and Oxetane into Benzimidazolequinone Antitumor Agents: The Discovery of 1,4,6,9-Tetramethoxyphenazine from Hydrogen Peroxide and Hydroiodic Acid-Mediated Oxidative Cyclizations. *The Journal of Organic Chemistry* **2019**, *84*, 9811. DOI: https://doi.org/10.1021/acs.joc.9b01427

Conference Proceedings

- "H$_2$O$_2$/HX: A Tuneable Oxidative System for the Synthesis of Halogenated and Non-Halogenated Heterocyclic Scaffolds." D. Conboy, S. I. Mirallai, M. Sweeney, M. Gurry, P. McArdle, A. A. Al-Kinani, S. Barton, F. Aldabbagh. Royal Society of Chemistry London & South East Organic Division Regional Meeting 2020, Kingston University; 13th February 2020. **Poster Communication**.

- "H$_2$O$_2$/HX: A Tuneable Oxidative System for the Synthesis of Halogenated and Non-Halogenated Heterocyclic Scaffolds." D. Conboy, S. I. Mirallai, M. Sweeney, M. Gurry, P. McArdle, A. A. Al-Kinani, S. Barton, F. Aldabbagh. Kingston University First Symposium on Synthesis & Drug Discovery; 1st November 2019. **Poster Communication**.

- "Hydrogen Peroxide and Hydrohalic Acid-Mediated Synthesis of Ring-Fused Benzimidazolequinone Anti-Cancer Agents." D. Conboy, F. Aldabbagh. Bioheterocycles XVIII International Conference on Heterocycles in Bioorganic Chemistry, Ghent, Belgium; 17th-20th June 2019. **Oral Communication: 2nd Runner-Up for Best Oral Communication.**

- "Green Synthesis of Benzimidazolequinone Anticancer Agents." D. Conboy. Faculty of Science, Engineering and Computing Research Conference, Kingston University; 3rd April 2019. **Oral Communication: 1st Prize for Best Oral Communication.**

- "H$_2$O$_2$/HX: A Tuneable Oxidative System for the Synthesis of Halogenated and Non-Halogenated Heterocyclic Scaffolds." D. Conboy, S. I. Mirallai, M. Sweeney, M. Gurry, P. McArdle, A. A. Al-Kinani, S. Barton, F. Aldabbagh. Royal Society of Chemistry London & South East Organic Division Regional Meeting 2019, Greenwich University; 13th February 2019. **Poster Communication.**

- "Incorporating Oxetane into Heterocyclic Quinone Anti-Cancer Agents." D. Conboy, A. Craig, M. Gurry, S. I. Mirallai, P. McArdle, A. A. Al-Kinani, S. Barton, F. Aldabbagh. Royal Society of Chemistry Heterocyclic and Synthesis Group Postgraduate Symposium, GlaxoSmithKline, Stevenage; 20th September 2018. **Poster Communication.**

- "Incorporating Oxetane into Heterocyclic Quinone Anti-Cancer Agents." <u>D. Conboy</u>, A. Craig, M. Gurry, S. I. Mirallai, P. McArdle, F. Aldabbagh. Royal Society of Chemistry Organic Division Midlands Meeting 2018, Loughborough University; 22nd March 2018. **Poster Communication: 1st Prize for Best Poster Communication.**

- "Synthesis of Spirocyclic Oxetane-Fused Benzimidazolequinone." <u>D. Conboy</u>, A. Craig, M. Gurry, S. I. Mirallai, P. McArdle, F. Aldabbagh. Bioheterocycles XVII International Conference on Heterocycles in Bioorganic Chemistry, Galway, Ireland; 28th – 31st May 2017. **Poster Communication.**

H$_2$O$_2$/HX: A Tuneable Oxidative System for the Synthesis of Halogenated and Non-Halogenated Heterocyclic Scaffolds

Kingston University London

Darren Conboy,[a] Styliana I. Mirallai,[b] Martin Sweeney,[b] Michael Gurry,[b] Patrick McArdle,[b] Ali A. Al-Kinani,[a] Stephen Barton,[a] Fawaz Aldabbagh*[a,b]

[a] Department of Pharmacy, School of Life Sciences, Pharmacy and Chemistry, Kingston University, Penrhyn Road, Kingston upon Thames, KT1 2EE, UK.
[b] School of Chemistry, National University of Ireland Galway, University Road, Galway, Ireland.

Introduction

Halogenated benzimidazoles possess wide-ranging biological activities, and are valuable synthetic intermediates. Ring-fused benzimidazolequinones are established substrates of NAD(P)H:quinone oxidoreductase 1 (NQO1), an enzyme overexpressed in several solid tumour cell lines.
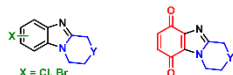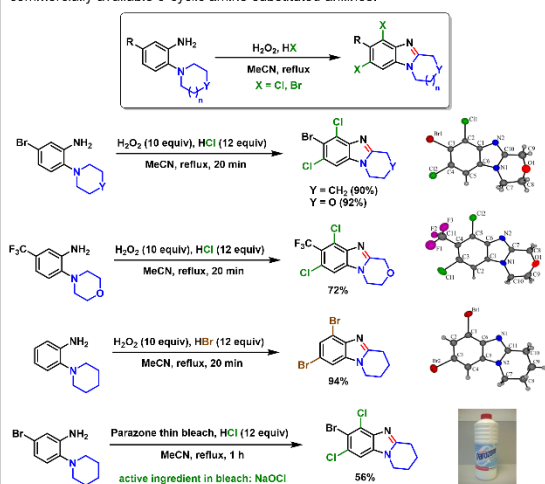
X = Cl, Br

The combination of H$_2$O$_2$/HX (where X = Cl, Br) is a source of electrophilic chlorine and bromine that can be used for facile aromatic halogenation. Furthermore the intermediate hypohalous acids (HOX) are powerful oxidizing agents.

$$H_2O_2 + HX \longrightarrow HOX + H_2O$$
$$HOX + HX \rightleftharpoons X_2 + H_2O$$

Herein we describe the utility and tuneability of the H$_2$O$_2$/HX system in the preparation of halogenated ring-fused benzimidazoles and benzimidazolequinones. Replacing HCl and HBr with HI can mediate cyclization without halogenation.
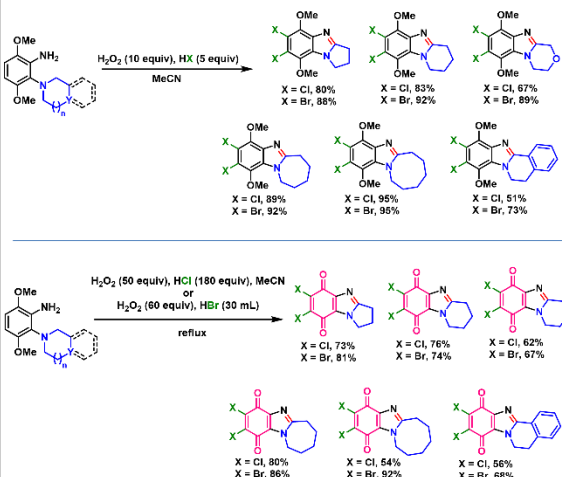
1. Halogenated Ring-Fused Benzimidazoles

A new series of selectively dichlorinated and dibrominated ring fused benzimidazoles were synthesized in mostly high yields of >80% using the reaction of H$_2$O$_2$/HX with commercially available o-cyclic amine substituted anilines.

R–ArNH$_2$ → H$_2$O$_2$, HX, MeCN, reflux, X = Cl, Br

Br–ArNH$_2$ → H$_2$O$_2$ (10 equiv), HCl (12 equiv), MeCN, reflux, 20 min → Y = CH$_2$ (90%), Y = O (92%)

F$_3$C–ArNH$_2$ → H$_2$O$_2$ (10 equiv), HCl (12 equiv), MeCN, reflux, 20 min → 72%

ArNH$_2$ → H$_2$O$_2$ (10 equiv), HBr (12 equiv), MeCN, reflux, 20 min → 94%

Br–ArNH$_2$ → Parazone thin bleach, HCl (12 equiv), MeCN, reflux, 1 h → 56%
active ingredient in bleach: NaOCl

M. Gurry, M. Sweeney, P. McArdle, F. Aldabbagh, *Org. Lett.* **2015**, *17*, 2856-2859.

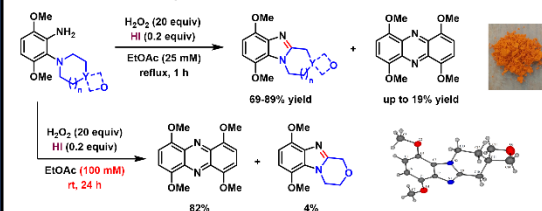## 2. Halogenation, Ring-Closure and Quinone Formation

3,6-Dimethoxy-2-(cycloamino)anilines undergo 4- or 6-electron oxidations to afford novel ring-fused halogenated benzimidazoles or benzimidazolequinones using H$_2$O$_2$/HCl or H$_2$O$_2$/HBr. Elemental Cl$_2$ and Br$_2$ in water are capable of the same oxidative transformation to give the ring-fused benzimidazolequinones.

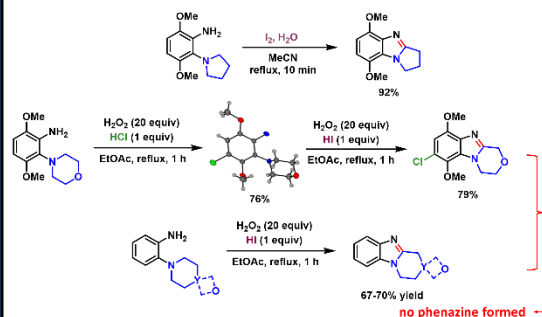H$_2$O$_2$ (10 equiv), HX (5 equiv), MeCN

X = Cl, 80%; X = Br, 88%
X = Cl, 83%; X = Br, 92%
X = Cl, 67%; X = Br, 89%
X = Cl, 89%; X = Br, 92%
X = Cl, 95%; X = Br, 95%
X = Cl, 51%; X = Br, 73%

H$_2$O$_2$ (50 equiv), HCl (180 equiv), MeCN or H$_2$O$_2$ (60 equiv), HBr (30 mL), reflux

X = Cl, 73%; X = Br, 81%
X = Cl, 76%; X = Br, 74%
X = Cl, 62%; X = Br, 67%
X = Cl, 80%; X = Br, 86%
X = Cl, 54%; X = Br, 92%
X = Cl, 56%; X = Br, 68%

M. Sweeney, L.-A. J. Keane, M. Gurry, P. McArdle, F. Aldabbagh, *Org. Lett.* **2018**, *20*, 6970-6974.

## 3. H$_2$O$_2$/HI Oxidative Cyclization & Phenazine Formation

o-Cyclic amine substituted dimethoxyanilines with H$_2$O$_2$ and catalytic HI gave non-halogenated dimethoxybenzimidazoles and an unexpected orange precipitate, determined to be 1,4,6,9-tetramethoxyphenazine. Phenazines are a highly prevalent class of bioactive heterocycles. Increasing the reaction concentration and decreasing the temperature favoured the intermolecular phenazine formation over the intramolecular oxidative cyclization.

H$_2$O$_2$ (20 equiv), HI (0.2 equiv), EtOAc (25 mM), reflux, 1 h → 69-89% yield + up to 19% yield

H$_2$O$_2$ (20 equiv), HI (0.2 equiv), EtOAc (100 mM), rt, 24 h → 82% + 4%

The oxidative cyclization proceeded using a mixture of molecular iodine and water. A stoichiometric equivalent of HCl with H$_2$O$_2$ resulted in aromatic chlorination rather than oxidative cyclization. The inductively-withdrawing Cl-substituent inhibited phenazine formation in the H$_2$O$_2$/HI reaction, while substrates lacking resonance-activating methoxy-substituents gave ring-fused benzimidazoles without phenazine formation.

I$_2$, H$_2$O, MeCN, reflux, 10 min → 92%

H$_2$O$_2$ (20 equiv), HCl (1 equiv), EtOAc, reflux, 1 h → 76%
H$_2$O$_2$ (20 equiv), HI (1 equiv), EtOAc, reflux, 1 h → 79%

H$_2$O$_2$ (20 equiv), HI (1 equiv), EtOAc, reflux, 1 h → 67-70% yield
no phenazine formed

Oxidative demethylation using [bis(trifluoroacetoxy)iodo]benzene (PIFA) gave the target non-halogenated benzimidazolequinones in good yields.

PhI(OCOCF$_3$)$_2$, MeOH, H$_2$O → Y = (cyclobutyl) (78%), Y = O (74%)
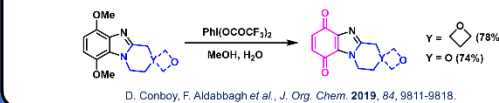
D. Conboy, F. Aldabbagh et al., *J. Org. Chem.* **2019**, *84*, 9811-9818.

Conclusions

- A new series of selectively dichlorinated and dibrominated ring-fused benzimidazoles have been prepared using environmentally benign H$_2$O$_2$ in combination with HCl or HBr.
- When the same system was applied to o-cyclic amine-substituted dimethoxyanilines, the reaction could be tuned to form either dihalogenated ring-fused dimethoxybenzimidazoles or benzimidazolequinones.
- Cl$_2$ and Br$_2$ in H$_2$O can mediate halogenation, cyclization and quinone formation.
- Oxidative cyclization without halogenation was possible using H$_2$O$_2$/HI. Phenazine formation was optimized at lower temperatures and higher concentrations of the aniline.

Incoporating Oxetane into Heterocyclic Quinone Anti-Cancer Agents

Darren Conboy,[a] Austin Craig,[b] Michael Gurry,[b]
Styliana I. Mirallai,[b] Patrick McArdle,[b] Fawaz Aldabbagh*,[a,b]
[a] *Department of Pharmacy, School of Life Sciences, Pharmacy and Chemistry, Kingston University, Penrhyn Road, Kingston upon Thames, KT1 2EE, UK.*
[b] *School of Chemistry, National University of Ireland Galway, University Road, Galway, Ireland.*

Introduction

Elevated levels of the enzyme, NAD(P)H:quinone oxidoreductase 1 (NQO1) are expressed in several solid tumour cell lines. Computational docking into the active site of NQO1 and COMPARE analysis at the National Cancer Institute (USA) has indicated that a polar group four or five bonds away from the reducible (imino)quinone moiety has the potential to increase specificity.[1] Our attention turned to oxetane due to its heralded metabolic robustness in comparison to carbonyl alternatives,[2] while offering the hydrogen bonding capacity necessary for efficient binding to NQO1. The synthesis of the first spirocyclic oxetane-fused benzmidazole **1** and benzimidazolequinone **2** are now detailed. Progress towards formation of imidazo[5,4-*f*]benzimidazolequinone **3** and imidazo[4,5-*f*]benzimidazolequinone **4** is also described.
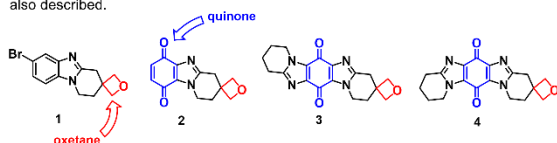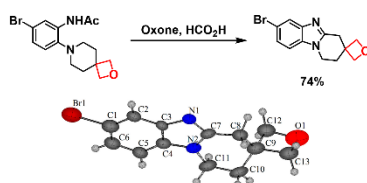

1. Preparation of 2-oxa-7-azaspiro[3.5]nonane oxalate salt
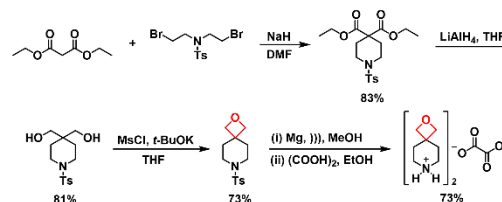
A new efficient synthesis of 2-oxa-7-azaspiro[3.5]nonane oxalate salt has been achieved. This facilitates incorporation of the spirocyclic oxetane motif onto heterocycles.
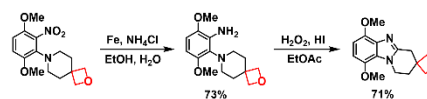
2. Spirocyclic Oxetane-Fused Benzimidazole

Fusion of spirocyclic oxetane onto benzimidazole proceeds *via* oxidative cyclization of o-*tert*-aminoacetanilide mediated by Oxone in formic acid.[3]

3. Benzimidazolequinone Formation

Nucleophilic aromatic substitution (NAS) of 2-oxa-7-azaspiro[3.5]nonane oxalate salt onto 1,4-dimethoxy-2,3-dinitrobenzene provided the basis for formation of spirocyclic oxetane-fused benzimidazolequinone.
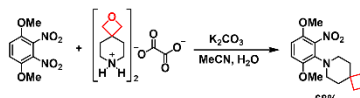
Reduction of the nitro group using iron and ammonium chloride yielded the corresponding aniline. Oxidative cyclization proceeded directly from the latter using hydrogen peroxide in ethyl acetate with small amounts of hydroiodic acid added.


Hypervalent iodine reagent [bis(trifluoroacetoxy)iodo]benzene (PIFA) provided mild conditions necessary to oxidatively demethylate the dimethoxybenzimidazole, forming the quinone in high yield.
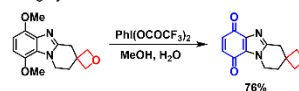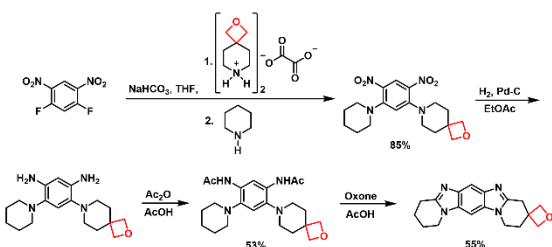

4. Synthesis of Imidazobenzimidazoles

Synthesis of spirocyclic oxetane-fused imidazo[5,4-*f*]benzimidazole proceeded by NAS of 2-oxa-7-azaspiro[3.5]nonane oxalate salt followed by piperidine onto 1,4-difluoro-2,5-dinitrobenzene. Reduction by catalytic hydrogenation and subsequent acetylation yielded the corresponding di-*tert*-aminodiacetanilide. Oxidative cyclization of the latter using Oxone in glacial acetic acid gave the desired imidazo[5,4-*f*]benzimidazole.
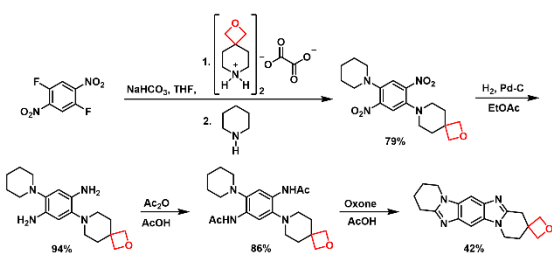

Analogous NAS onto 1,5-difluoro-2,4-dinitrobenzene followed by reduction, acetylation and oxidative cyclization gave the isomeric imidazo[4,5-*f*]benzimidazole.

Conclusions & Future Work

- Spirocyclic oxetane has been fused onto benzimidazole for the first time, utilising a new route to the formation of 2-oxa-7-azaspiro[3.5]nonane that has been established.
- The synthesis of a spirocyclic oxetane-fused benzimidazolequinone will give a potential anti-tumour agent with specificity towards NQO1.
- The synthesis of spirocyclic oxetane-fused imidazo[4,5-*f*] and [5,4-*f*]benzimidazoles has been achieved. These will be converted to their quinone analogues by nitration, reduction and Fremy oxidation.
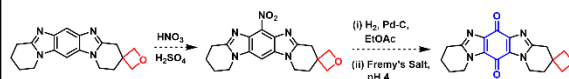
- Cytotoxicity evaluation will be carried out on all novel quinones prepared.

References

[1] V. Fagan, S. Bonham, M. P. Carty, P. Saenz-Méndez, L. A. Eriksson, F. Aldabbagh, *Bioorganic & Medicinal Chemistry* **2012**, *20*, 3223-3232.

[2] G. Wuitschik, E. M. Carreira, B. Wagner, H. Fischer, I. Parrilla, F. Schuler, M. Rogers-Evans, K. Müller, *Journal of Medicinal Chemistry* **2010**, *53*, 3227-3246.

[3] M. Gurry, P. McArdle, F. Aldabbagh, *Molecules (MDPI, Basel)* **2015**, *20*, 13864-13874.

Acknowledgements